Department of Theoretical Medicine and Biosciences,

Faculty of Medicine

Saarland University, Homburg/Saar

MOLECULAR AND FUNCTIONAL CHARACTERIZATION OF RIBEYE AND RIBEYE-INTERACTING PROTEINS

Ph.D. thesis

A dissertation submitted to the Faculty of Medicine
in fulfilment of the requirements for the degree of
Doctor in Natural Sciences at
SAARLAND UNIVERSITY
2008

Submitted by
Venkat Giri Magupalli

Date of Birth: 28 March 1980
Place of Birth: Orissa, India

Supervisor:

Co-supervisor:

Declaration

I hereby declare that the Ph.D thesis entitled "Molecular and functional characterization of RIBEYE and RIBEYE-interacting proteins" has been written independently and with no other sources and aids than quoted.

Venkat Giri Magupalli
Homburg, 22.9.2008

Acknowledgements

I would like to place on record my deep sense of gratitude and indebtedness to Prof. Dr. Frank Schmitz, for his inspiring and expert guidance in carrying out this PhD thesis work. I thank him for bringing best out of me. My thanks also goes to Prof. Dr. Jens Rettig, who immediately agreed to be in my PhD thesis committee. I am grateful for his time and critical suggestions during development of this project.

I wish to express my gratitude to Prof. Dr. Dieter Bruns and all the members of synapse club (AG Dieter Bruns, AG Jens Rettig and AG Schmitz) for their time, insights and enthusiasm. The talks, discussions were of great scientific value and important for my learning it even got back me in orbit when I was fogged in.

Many thanks to all the former and current members of our group for sticking it out with me, for making my stay in lab easier and unforgettable. I thank all the co-authors for their efforts. I thank Dr. Karin Schwarz for her continuous support and constructive suggestions, Dr. Jutta Schmitz-Kraemer for proof reading the thesis and manuscript, Dr. Louise Köblitz for initial help to get start with the experiments. I thank Mr. Kannan Alpadi and Mr. Josif Mirceski for important clones and refreshing coffee breaks. I also thank Mr. Jagadish Kumar Venkatesan and Mr. Sivaraman Natarajan who brightened my laboratory experience with their immunolabellings, humour and friendship.

I want to gratefully acknowledge Sonderforschungsbereichs (SFB 530) TP C-11, Deutsche Forschungsgemeinschaft (DFG), and University of Saarlands (Faculty of Medicine) Grants (HOMFOR) for financially supporting my entire Ph.D thesis work.

I also acknowledge Sylvia Brundaler, Gerlinde Kühnreich, Britta Leiner, Anne Rupp, Franziska Markwart and Tamara Paul for their excellent technical support.

I thank Mrs. Iva Das, Dr. Bernard Fanthome, Dr. Subash Ranjan, Dr. V.P Singh, Mr. D.S.S Hembram, Mr. S.K Mohanty, and all my nearer and dearer ones for their motivation, care and affection, whether in person, by phone, or by e-mail.

I am endlessly grateful for everything to my parents Mr. Papa Rao Magupalli and Mrs. Puspavalli Magupalli, who always supported my interest in scientific research. I thank by brothers Mr. Giri Shankar Magupalli and Mr. Gangadhar Giri Magupalli for all their support which kept me moving on.

I am thankful to almighty god for constant blessings.

To my parents and beloved brothers

Contents

Summary 1

Zusammenfassung 4

1 Introduction 7

1.1 The visual system and the approachable retina 7
1.2 Synaptic organisation of the retina 7
1.3 Synaptic transmission in the retina 8
1.4 Retinal Synapses 9
1.5 Ribbon synapse and the synaptic ribbon 10
1.6 RIBEYE the major component of synaptic ribbons 13
1.7 Tubby-like protein 1 (Tulp 1) 16
1.8 Working hypothesis 20

2 Materials and Methods 21

2.1 Materials 21

2.1.1 Host strains 21

2.1.1.1 Bacterial Strains 21
2.1.1.2 *Saccharomyces cerevisiae* strains 21
2.1.1.3 COS 7 cell line 21
2.1.1.4 R28 cell line 22
2.1.1.5 *Pichia pastoris* strain 22

2.1.2 Plasmid vectors 22

2.1.2.1 *Escherichia coli* cloning vectors 22
2.1.2.2 Yeast two-hybrid vectors 23
2.1.2.3 Eukaryotic expression vectors 24
2.1.2.4 *Pichia pastoris* vector 24

2.1.3 Antibodies 25
2.1.4 Plasmid clones 26
2.1.5 Oligonucleotides 27
2.1.6 PCR products 29
2.1.7 Subcloning products 30
2.1.8 Sequencing primers 30
2.1.9 Enzymes, Proteins and Molecular weight standards 30

2.1.10 Reaction Kits 30
2.1.11 Reagents and Chemicals 31
2.1.12 Buffer and Media 32
2.1.13 Miscellaneous consumables/materials 36
2.1.14 Laboratory hardware equipments 36

2.2 Methods 38

2.2.1 DNA related techniques and Cloning 38

2.2.1.1 PCR amplification of DNA fragments 38
2.2.1.2 Genomic DNA isolation 39
2.2.1.3 Genomic PCR 39
2.2.1.4 DNA Electrophoresis 40
2.2.1.5 Purification of DNA 40
2.2.1.6 Restriction digestion of DNA 41
2.2.1.7 Ligation of DNA fragments 41
2.2.1.8 Precipitation of DNA 41
2.2.1.9 Preparation of electrocompetent cells 41
2.2.1.10 Transformation of electrocompetent cells 43
2.2.1.11 Plasmid DNA preparation (mini preparation & maxi preparation method) 44
2.2.1.12 DNA sequencing 45
2.2.1.13 Glycerol stocks 45

2.2.2 Protein related techniques 46

2.2.2.1 SDS-PAGE 46
2.2.2.2 Western Blotting 46
2.2.2.3 Stripping of nitrocellulose membranes 47
2.2.2.4 Determination of Protein concentrations 47
2.2.2.5 Recombinant Protein Expression 47
2.2.2.6 Purification of Recombinant Proteins 51

2.2.3 Protein-Protein Interaction 52

2.2.3.1 Yeast Two-Hybrid assay 52

2.2.3.1.1 Yeast mating 54
2.2.3.1.2 β-Galactosidase assays 54

2.2.3.2 Protein pull-down assays 56

2.2.3.2.1 Recombinant protein pull-down (expressed in bacteria) 56
2.2.3.2.2 Recombinant protein pull-down (expressed in COS cells) 57
2.2.3.2.3 Recombinant protein pull-down (expressed in *Pichia pastoris*) 57

2.2.3.3 Synaptic ribbons based pull-downs 58
2.2.3.4 Morphological analyses of protein-protein interactions 58

2.2.3.4.1 Light microscopic analyses 58
2.2.3.4.2 Conventional transmission electron microscopy 59
2.2.3.4.3 Postembedding immunogold electron microscopy 59

2.2.3.5 NAD(H) dependence of RIBEYE(A)-RIBEYE(B) interaction 60

3 Results 61

3.1 ANALYSES OF RIBEYE-RIBEYE INTERACTIONS 61

3.1.1 Homo-dimerization of RIBEYE(A)-domain 61
3.1.2 Mapping of RIBEYE(A)-RIBEYE(A) interaction(s) 63
3.1.3 Multiple interactions among RIBEYE(A)-domain interacting modules 65
3.1.4 Homo-dimerization of RIBEYE(B)-domain 68
3.1.5 Hetero-dimerization of RIBEYE(A)-and RIBEYE(B)-domains 70
3.1.6 Mapping of RIBEYE(A)-RIBEYE(B) interaction 71
3.1.7 RIBEYE(A)-RIBEYE(B) interaction mapping using NBD point mutants 74
3.1.8 NAD^+ and NADH inhibit RIBEYE(A) and RIBEYE(B) interaction 77
3.1.9 RIBEYE co-aggregates in transfected cells 78
3.1.10 Synaptic ribbons recruit externally added RIBEYE subunit(s) 82
3.1.11 RIBEYE-induced protein aggregates recruits endogenous bassoon 84
3.1.12 Physiological role of RIBEYE induced protein aggregates 85
3.1.13 Schematic RIBEYE-RIBEYE interaction model 87

3.2 IDENTIFICATION AND FURTHER ANALYSIS OF RIBEYE-TULP1 INTERACTIONS 88

3.2.1 RIBEYE interacts with photoreceptor specific TULP1 in YTH assay 88
3.2.2 RIBEYE interacts with photoreceptor specific TULP1 in pull-down assay 90
3.2.3 TULP1 is a dissociable peripheral component of synaptic ribbons 91
3.2.4 Mapping of RIBEYE-TULP1 interactions 92
3.2.5 Implications of human TULP1 mutants on RIBEYE-TULP1 interactions 95

4 Discussion 97

4.1 RIBEYE-RIBEYE interactions and the making of synaptic ribbons 98

4.2 RIBEYE-TULP1 interaction 103

5 References 107

APPENDICES

List of figures

List of abbreviations

Curriculum Vitae

Parts of thesis work already published

Summary

Ribbon synapses are tonically active, high-performance synapses found e.g. in the retina and inner ear. Ribbon synapses can maintain high rates of synaptic vesicle exocytosis for prolonged periods of time. Morphologically, ribbon synapses are characterized by conspicuous presynaptic structures, the synaptic ribbons. Synaptic ribbons are large presynaptic structures in the active zone complex and, are crucial for the physiological characteristics of ribbon synapses. But, the components and precise role of synaptic ribbons were largely unknown. RIBEYE was identified by our group as a novel and major protein component of synaptic ribbons (Schmitz *et al*., 2000). RIBEYE consists of a unique aminoterminal A-domain with unknown function, and a carboxyterminal B-domain which is identical to the protein CtBP2. The B-domain binds to NAD(H) with high affinity (Schmitz *et al*., 2000). Based on the finding that RIBEYE is the major component of synaptic ribbons, it could be assumed that RIBEYE is important for both the structure and function of synaptic ribbons. In the first part of thesis work, I showed that RIBEYE has the properties of a synaptic scaffold protein that could build the synaptic ribbon. I demonstrate that RIBEYE self-associates using different independent approaches (yeast two-hybrid analyses, protein pull-downs, synaptic ribbon-RIBEYE interaction assays, co-aggregation experiments, transmission- and immunogold electron microscopy). RIBEYE interacts via five distinct sites with other RIBEYE molecules. Three RIBEYE-RIBEYE interaction sites, denoted as “A1”, “A2” and “A3” are located in the A-domain and two RIBEYE-RIBEYE interaction sites, denoted as “B1” and “B2”, are present in the B-domain. The five interacting sites were mapped and characterized with independent approaches. The five distinct sites on A- and B-domain of RIBEYE also mediate interaction in multiple ways with other RIBEYE molecules. The A-domain as well as the B-domains of RIBEYE can homo-dimerize. The homo-dimerization of the A-domain can occur via three-distinct interacting sites (A1, A2 and A3). The homo-dimerization of RIBEYE(B) is accomplished by B1 interacting site. These interactions allow either homotypic domain interactions (interactions between same type of domains; RIBEYE(A)-RIBEYE(A), RIBEYE(B)-RIBEYE(B)) or heterotypic domain interactions (i.e. RIBEYE(A)-RIBEYE(B) interaction). Homotypic domain interactions can be either homotypic or heterotypic with refer to the sub-domain which is involved: RIBEYE(A)-RIBEYE(A) can be mediated either by homotypic sub-domain interactions, e.g. RIBEYE(A1)-RIBEYE(A1), or by heterotypic sub-domain interactions, e.g. RIBEYE(A1)-RIBEYE(A2). In addition to homo-dimerization, hetero-dimerization between the A- and B-domain of

RIBEYE can take place. I mapped the hetero-dimerization sites present on RIBEYE(A)- and RIBEYE(B)-domains using YTH assay and showed that A2 (present on RIBEYE(A)-domain) interacts with NAD(H)-binding sub-domain located on RIBEYE(B)-domain. I further substantiated these findings by mutating crucial amino acids localized on the NADH-binding sub-domain (NBD). It showed that the hetero-dimerization interaction spans over a large extent of NBD sub-domain. The docking site of RIBEYE(A)-domain on RIBEYE(B) is topographically different from RIBEYE(B) homo-dimerization interface. Also, this interaction was found to be regulated by NAD(H). Using protein pull-down assays, I showed that A- and B-domain interaction is inhibited by the physiological levels of NAD(H). Using isolated ribbon fraction I demonstrated that the native ribbons bind externally added RIBEYE domains (i.e., A- and B-domain). Additionally, the binding of A1 and A3 sub-domains but not A2 to purified ribbons suggests that a large portion of RIBEYE(A)-domain is likely buried in the core of synaptic ribbons. Still, part of it is exposed which is accessible for interactions. In cotransfection experiments, RIBEYE proteins interacted with each other and coaggregated into the same protein clusters. Heterologously expressed RIBEYE forms large electron-dense aggregates that are in part physically associated with surrounding vesicles and membrane compartments. These structures resemble spherical synaptic ribbons. These ribbon-like structures coassemble with the active zone protein bassoon, an interacting partner of RIBEYE at the active zone of ribbon synapses emphasizing the physiological relevance of these RIBEYE-containing aggregates. Taken together, these data suggest a structural role of RIBEYE and provide a mechanism how a single protein, RIBEYE can build the three-dimensional structure of the synaptic ribbon. This novel functional property of RIBEYE will help to understand how the synaptic ribbon is built and how the assembly of the ribbon could contribute to its ultrastructural plasticity.

In the next part, I showed that RIBEYE also mediates functional properties. I characterized the phospholipid-binding protein Tulp1 as a RIBEYE interacting protein. These findings were corroborated by yeast two-hybrid, protein pull-downs and synaptic ribbon western blot analyses. Yeast two-hybrid analyses demonstrated that the interaction between Tulp1 and RIBEYE is mediated by the tubby-domain of Tulp1 and both the A- and the B-domain of RIBEYE. In comprehensive mapping analyses, I showed that carboxyterminal region of RIBEYE(A)-domain binds to the tubby-domain. On RIBEYE(B)-domain it maps to NBD sub-domain. I excluded the possible role of a PTNLS motif (present in tubby-domain) in mediation of interaction. Morphologically, TULP 1 is enriched in photoreceptors and contained in purified synaptic ribbons. The association of RIBEYE with TULP1 is

of clinical significance because mutations in TULP 1 lead to an early onset, severe form of Retinitis pigmentosa (RP-14) which finally results in blindness. I tested the implication of tubby mutations on RIBEYE interactions. I found that RIBEYE(B) and TULP1 interactions are disrupted as compared to wild type conditions. On the other hand, RIBEYE(A) and TULP1 interactions are unperturbed. In a cellular level these disruptions may lead to impairment of synaptic transmission and disturbances in vision. My findings emphasize the importance of protein interaction cascade in the generation of the ribbon scaffold, and this scaffold works by interaction with several proteins. One such important protein was found to be photoreceptor-specific TULP1 protein.

Zusammenfassung

Ribbonsynapsen sind tonisch aktive Hochleistungssynapsen, die beispielsweise in der Retina und im Innenohr gefunden werden. Ribbonsynapsen können schnelle Exozytose von synaptischen Vesikeln über lange Zeiträume aufrecht erhalten. Morphologisch sind diese Synapsen durch die Anwesenheit von Synaptic Ribbons charakterisiert. Synaptic Ribbons sind große plattenartige Strukturen in der aktiven Zone dieser Synapsen. Synaptic Ribbons sind für die physiologischen Eigenschaften von Ribbonsynapsen unabdingbar. Der genaue Aufbau und die Wirkungsweise der Synaptic Ribbons ist jedoch noch unbekannt. Unserer Arbeitsgruppe hat RIBEYE wurde von als spezifische Hauptkomponente synaptischer Ribbons identifiziert (Schmitz *et al*., 2000). RIBEYE ist nicht nur maßgeblich am Aufbau synaptischer Ribbons beteiligt, es ist vielmehr auch ein Ribbonsynapsen-spezifisches Protein. RIBEYE besteht aus einer aminoterminalen proteinspezifischen A-Domäne und einer carboxyterminalen B-Domäne, die mit dem Protein CtBP2 identisch ist. Die B-Domäne bindet NAD(H) mit hoher Affinität (Schmitz *et al*., 2000). Basierend auf der Tatsache, dass RIBEYE eine Hauptkomponente der Synaptic Ribbons ist, vermuteten wir, dass sowohl die Struktur als auch die Funktion der Synaptic Ribbons massgeblich durch RIBEYE bestimmt werden. Im ersten Teil meiner Dissertationsarbeit zeige ich, dass RIBEYE die Eigenschaften eines Gerüstproteins besitzt, das die Ribbons aufbauen kann. Ich zeige in mehreren unabhängigen Ansätzen, dass RIBEYE in der Lage ist, mit sich selber zu interagieren . Es gibt 5 unabhängige Interaktionsstellen im RIBEYE-Protein, über die RIBEYE mit anderen RIBEYE Molekülen Proteinen interagieren kann. Von diesen befinden sich drei in der A-Domäne, die wir als A1, A2 und A3 bezeichnen, und zwei in der B-Domäne, die wir dem entsprechend als B1 und B2 bezeichnet haben bezeichnen. Diese fünf unterschiedlichen Interaktionsstellen habe ich mit verschiedenen Methoden kartiert und charakterisiert. Sowohl die A- als auch die B-Domäne von RIBEYE können homo-dimerisieren. Die Homo-Dimerisierung der A-Domäne wird über die drei Interaktionsstellen in der A-Domäne (A1, A2, A3) vermittelt. Die Homo-Dimerisierung der B-Domäne dagegen erfolgt ausschließlich wird über die B1-Interaktionsstelle vermittelt. Homotypische Interaktionen zwischen den Domänen (z.B. RIBEYE(A)-RIBEYE(A)-Interaktionen) können in Bezug auf die beteiligten Subdomänen homotypischer oder heterotypischer Natur sein (homotypisch: z.B. RIBEYE(A1)-RIBEYE(A1)-Interaktionen; hetereotypisch: RIBEYE(A1)-RIBEYE(A2)-Interaktionen). Zusätzlich zur Homo-Dimerisierung kann es auch zur Hetero-Dimerisierung zwischen der A-Domäne und der B-Domäne von RIBEYE kommen. Diese

werden durch die A2-Interaktionsstelle und die NADH-bindende NBD-Subdomäne vermittelt. Ich habe durch ausgedehnte Proteinkartierungsexperimente mit Hilfe des YTH-Systems konnte ich die für die Interaktion wichtigen Aminosäuren kartieren. Dabei ergab sich ein breites Interaktionsareal auf der NBD-Subdomäne, welches für die Interaktion mit der A-Domäne wichtig ist. Diese Interaktion zwischen der A-Domäne und der B-Domäne wird dabei durch NAD(H) reguliert. Sowohl die reduzierte Form (NADH) als auch die oxidierte Form (NAD^+) sind in physiologischen Konzentrationen in der Lage, die Interaktion zwischen RIBEYE(A) und RIBEYE(B) sehr effizient zu inhibieren. NADH inhbiert die Interaktion zwischen RIBEYE(A)- Domäne und RIBEYE(B)-Domäne sehr effizient. Zusammengefasst weisen die Daten auf eine strukturelle Rolle des Proteins RIBEYE hin und zeigen einen Mechanismus auf, wie die Synaptic Ribbons aus einem einzigen Protein, nämlich RIBEYE, aufgebaut werden können. Ultrastrukturelle Untersuchungen weisen ebenfalls darauf hin, daß RIBEYE das Potential besitzt, Synaptic Ribbons aufzubauen. Hetelolog exprimiertes RIBEYE bildet große electronendichte Strukturen, die Ähnlichkeit mil globulären Synaptic Ribbons besitzen. Diese Ribbon-artigen Strukturen sind partiell physisch mit Vesikeln assoziiert und kolokalisieren mit dem physiologischen RIBEYE-Interaktionspartner Bassoon. Bindungsuntersuchungen an isolierten Synaptic Ribbons legen nahe, dass weite Teile der A-Domäne im Inneren der Synaptic Ribbons verborgen vorliegen. Teile der A-Dömane befinden sich aber an der Oberfläche der Ribbons und können dort mit anderen Proteinen interagieren. Diese neuen funktionellen Eigenschaften von RIBEYE helfen zu verstehen, wie der Ribbon aufgebaut wird und wie der Aufbau der Ribbons zur bekannten ultrastrukturellen Plastizität der Ribbons beiträgt.

Im zweiten Teil der Dissertationsarbeit habe ich das Phospholipid-bindende Protein Tulp1 als einen Interaktionspartner von RIBEYE charakterisiert. Diese Interaktionen wurden sowohl mit dem Hefe-Zwei-Hybridsystem als auch mit verschiedenen Pulldown-Assays analysiert gezeigt. Ich konnte zeigen, dass sowohl die A-Domäne als auch die B-Domäne an der Interaktion zwischen Tulp1 und RIBEYE beteiligt sind. In der RIBEYE(B)-Domäne ist die NBD-Subdomäne von RIBEYE ist für die Interaktion mit Tulp1 verantwortlich. Auf Seiten der A-Domäne erfolgt eine Interaktion mit ist Tulp1über die A2-Interaktionsstelle für die Interaktion mit verantwortlich. Die Interaktion mit Tulp1 ist von klinischer Relevanz klinisch interessant, da Mutationen im Tulp1 Gen zu früh beginnenden, schwer verlaufenden Formen der Retinitis pigmentosa führen. Diese krankheitsrelevanten Mutationen im Tulp1-Protein fürhen zu einer Unterbrechung der inhibieren die Interaktion zwischen Tulp1 und der B-Domäne von RIBEYE. Diese Befunde unterstützen die physiologische Bedeutung der

gefundenen Interaktionen. Zusammengefasst betonen meine Untersuchungen die Bedeutung von Proteininteraktionskaskaden beim Aufbau und der Funktion der Synaptic Ribbons. Die erzielten Daten sind wichtig für ein besseres Verständis der retinalen Signalverarbeitung.

1 Introduction

1.1 The visual system and the approachable retina

The eyes are the sophisticated sense organs involved in vision. The perception of light and dark cues from the external environment by the retina and its faithful processing involves a labyrinthine task. This complex processing of visual signals occurs as early as at the retina, the first stage in the visual system. The brain extrapolates the many different signals conveyed by the retina, to build a clear cohesive image of the outer environment. The retina is an intensively studied organ in vision, and anatomically a part of brain (diencephalon). Unlike higher visual centers, the retina offers an excellent source of material for detailed anatomical, physiological, and pharmacological analysis of the neural mechanism underlying elementary information processing by the vertebrate brain.

1.2 Synaptic organization of the retina

All vertebrate retinas are organized according to the similar basic plan: two synaptic layers (outer and inner plexiform layers) are intercalated between three cellular layers (outer and inner nuclear layers and ganglion cell layers). The visual responses in the retina (and elsewhere in the brain) are initiated by the photoreceptors. In addition to the photoreceptors, the retina has five other basic classes of retinal neurons: horizontal, bipolar, amacrine, interplexiform, and ganglion cells.

The perikarya of the photoreceptors are located in the outer nuclear layer (ONL). Except for ganglion cells, the perikarya of the remaining basic classes of retinal neurons are in the inner nuclear layer (INL). Horizontal cells lie along the outer margin of the inner nuclear layer; the bipolar cell perikarya are predominantly located in the middle layer; and amacrine and interplexiform cell perikarya are arranged along the proximal border of the inner nuclear layer.

The perikarya of the ganglion cells make up the most proximal layer, the ganglion cell layer. Müller cells are the predominant type of the glial cell in the vertebrate retina. These cells spans vertically through the retina, from the distal region of the outer nuclear layer to the inner margin of the retina. The nuclei lie usually in the middle of the inner nuclear layer. Amacrine cells, like the horizontal cells in the outer plexiform layer (OPL), extend processes widely in the inner plexiform layer (IPL); their processes are confined to this layer and they mediate interactions within it.

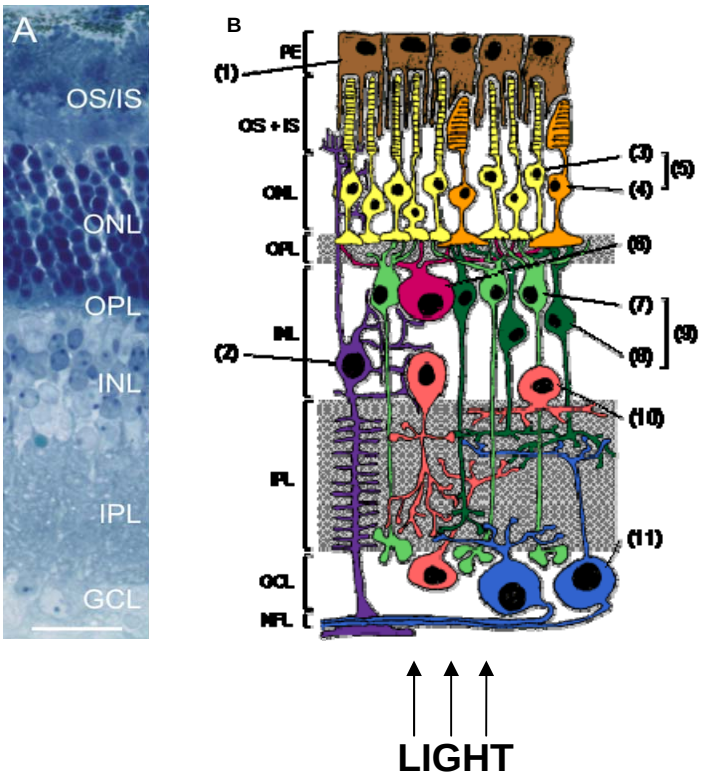

Figure 1. Schematic overview of the mammalian retina.

A) Toluidine blue-stained vertical cryostat section of retina showing the various retinal layers (OS/IS contains the outer and inner segments of the rod and cone photoreceptors; outer nuclear layer (ONL) containing the somata of the photoreceptors, outer plexiform layer (OPL) or first synaptic region, inner nuclear layer (INL) containing the somata of the second order neurons, i.e. horizontal, bipolar and amacrine cells, inner plexiform layer (IPL) or second synaptic region, ganglion cell layer (GCL) containing the somata of the ganglion cells and of displaced amacrine cells) (Tom Dieck *et al*., 2006). **B)** Vertical section through a mammalian retina. (obtained from MPI for Brain research, Frankfurt). The following cell types are shown: retinal pigment epithelium (PE,1), Müller cells (2), photoreceptors (5), rods (3), and cones (4), horizontal cells (6), bipolar cells (9): rod -(7) and cone bipolar cells (8), amacrine cells (10), ganglion cells (11). The arrows show the direction of the light falling into the eye (and through the layer of the retina). Abbreviations. OS, outer segment; IS, inner segment. Scale: 20µm.

1.3 Synaptic transmission in the retina

The receptor cell terminals provide input to the outer plexiform synaptic layer, whereas the bipolar cells are the output neurons, carrying visual information from outer to inner plexiform layers. Horizontal cells extend processes widely in the outer plexiform layer, but these processes are confined to this layer; they mediate lateral interactions within this first synaptic zone. The interplexiform cells appear to be primarily centrifugal neurons, carrying information for the inner to the outer plexiform layers and spreading processes in both layers. In the inner plexiform layer also, the processes of four neuronal classes interact. The bipolar cell terminal provides the input to the layer, and the ganglion cells are the output neurons. Indeed, the ganglion cells are the output neurons for the entire retina;

their axons run along the margin of the retina and collect at the optic disk to form the optic nerve, which carries all visual information from the eye to the higher visual centres.

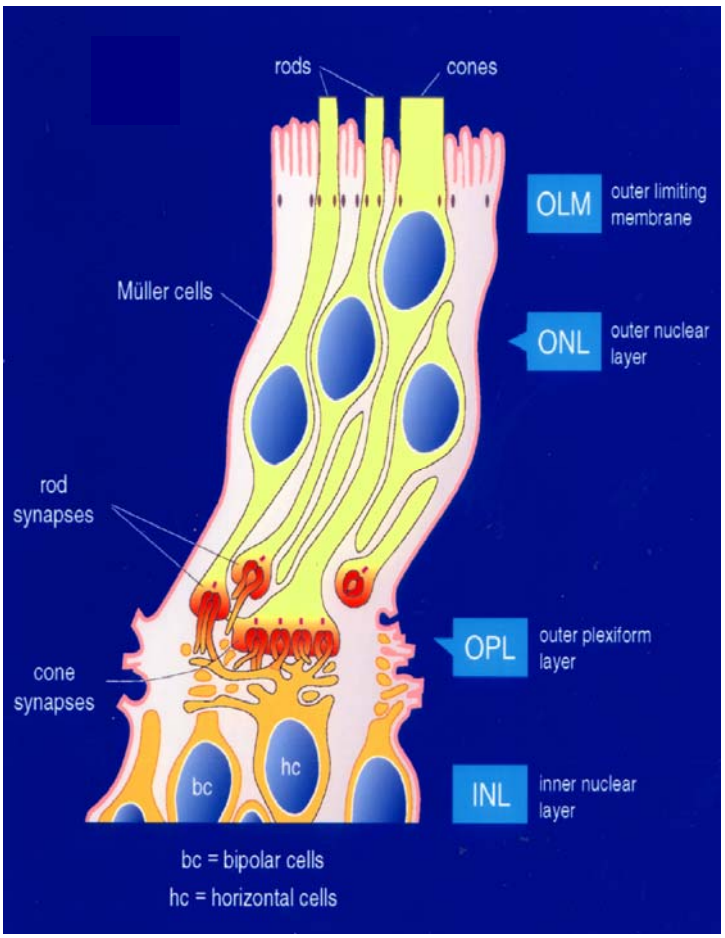

Figure 2. Detailed anatomy of the outer portion of mammalian retina (Schmitz, unpublished).

Schematic representation of the outer retina showing the details of photoreceptors and their synapses. OLM - Outer limiting membrane, ONL - outer nuclear layer containing the somata of the photoreceptors, OPL- outer plexiform layer or first synaptic region, INL inner nuclear layer containing the somata of the second order neurons, i.e. horizontal, bipolar and amacrine cells. Synaptic ribbons are shown as flags (red color) emerging from rod and cone synapses.

1.4 Retinal synapses

In retina, the communication between the two neurons takes place by various synaptic contacts such as Basal junctions, Gap junctions, Conventional synapses and Ribbon synapses. Basal junction is made by terminal receptors of cone cells. Retinal gap junctions are similar to the electrical junctions (Pappas and Waxman, 1972). The two apposing membranes, being separated by a gap of no more than 2-4 nm. Conventional synapse in the retina resembles chemical synapse seen throughout the vertebrate nervous

system (Pappas and Waxman, 1972). It is characterized by an aggregation of synaptic vesicles in the presynaptic terminal clustered close to the presynaptic membrane.

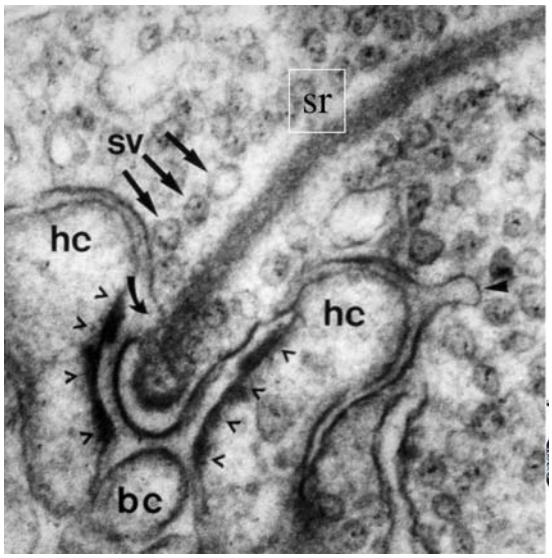

Figure 3. Ultrastructural representation of a retinal ribbon synapse.

Conventional transmission electron micrographs of the photoreceptor synapse from (*Carassius carassius*). Synaptic ribbon (sr), synaptic vesicle (sv), horizontal cell (hc) and bipolar cell (bc). The synaptic vesicles are shown by arrows; the arrowheads denote the site of endocytosis (Schmitz, 1996).

1.5 Ribbon synapse and the synaptic ribbons

Synaptic ribbons are the hallmark of ribbon synapse. These are specialized and tonically active chemical synapse. Retinal photoreceptor and bipolar cells represent ribbon synapses (Dowling, 1987; Sterling. 1998). In addition, hair cells in the cochlea and pinelocytes in the epiphysis have presynaptic dense bodies that resemble ribbons and probably function similarly (Smith and Sjöstrand, 1961; Hopsu and Arstila, 1964; Jastrow *et al*., 1997; Lenzi *et al*., 1999). In invertebrates such as *Drosophila*, T-shaped presynaptic structures that are similar to ribbons are probably function analogously is found in photoreceptor nerve terminals, neuromuscular junctions, and other synapses (Trujillo-Cenoz, 1972; Wan *et al*., 2005). However the invertebrate structures are probably different from vertebrate synaptic ribbons because they have a distinct shape and texture and are directly connected to the active zones, whereas synaptic ribbons are not contiguous with active zones. Physiologically, ribbon synapses are characterized by a high rate of tonic neurotransmitter release mediated by continuous synaptic vesicle exocytosis (for review, see Dowling, 1987; Sterling, 1998; Fuchs, 2005; Heidelberger *et al*., 2005;

Prescott and Zenisek, 2005; Sterling and Matthews, 2005; Nouvian *et al*., 2006; Singer, 2007). At the ribbon-type synapses of the auditory, vestibular, and visual systems, vesicles are docked to a synaptic ribbon. It's a general notion that these ribbon synapses are specialized for the rapid supply of the synaptic vesicle for the release (for review, see tom Dieck and Brandstätter, 2006; Nouvian *et al*., 2006; Sterling and Matthews, 2005). In comparison to the conventional synapse, the high rate of tonic release from ribbon synapse demands much faster vesicle traffic. Being the synaptic ribbons constituting the major difference it's likely that the primary function of the ribbons is to speed up vesicle traffic by serving as a conduit for synaptic vesicles. This is evident from values, that the exocytosis of docked vesicles in ribbon synapse is stimulated by Ca^{+2}, similar to conventional synapse but at a higher rate. Per ribbon, moderate Ca^{+2} levels induce release of ~50 vesicles/sec, whereas maximal calcium concentration causes rates as high as 500 vesicles/sec (Pearson *et al*., 1994, 2003). This high rate of release per ribbon is astounding, considering that a hippocampal synapse exhibits maximal release rates of only ~20 vesicles/sec (Stevens and Tsujimoto, 1995). This high release rate is probably made possible by the function of the ribbons, in providing a reservoir of release ready synaptic vesicles that are immediately available for fusion. At a ribbon synapse, stimulation by high Ca^{+2} triggers release of the entire pool of vesicles tethered to the ribbon on a millisecond timeframe (von Gersdorff *et al*., 1996), suggesting that the sizable ribbon surface allows priming of a large number of vesicles that are than immediately available for exocytosis.

Morphologically, ribbon synapses are characterized by an electron-dense ribbon or lamella in the presynaptic cytoplasm (Vollrath *et al*., 1996). It represents a specialization of the cytomatrix at the active zone (CAZ) present at conventional synapse (tom Dieck *et.* al., 2005). The photoreceptor ribbon is typically a plate, ~ 30nm thick, which extends perpendicular to the plasma membrane. It juts ~ 200 nm into the cytoplasm, and length varies from 200-1000 nm. In EM sections retinal synaptic ribbons usually appear bar-shaped. Synaptic ribbons in the inner ear are usually spherical structures (for review, see Nouvian *et al*., 2006). Also in the retina, the assembly of the bar-shaped ribbon is believed to go through spherical ribbon intermediates, the so called synaptic spheres (Spiwoks-Becker *et al*., 2004; for review, see Vollrath and Spiwoks-Becker, 1996). The dimensions of synaptic ribbons in the retina can vary and are subject to changes e.g. in response to different stimuli (lighting conditions/circadian rhythm) probably reflecting structural adaptations to different degrees of synaptic activity (for review, see Vollrath and Spiwoks-Becker, 1996; Wagner, 1997). Irrespective of their shape synaptic ribbons are associated with large amounts of synaptic vesicles and other membrane

compartments (for review, see Sterling and Matthews, 2005). Between the ribbon and the ridge membrane is a curved dense band, called the arciform density (for review, Wagner, 1997). These are absent in hair cells. Surrounding the synaptic ribbon is a precisely arranged array of synaptic vesicles, and a high resolution electron microscopy often shows thin filaments (~5 nm thick and ~ 40 nm long) extending from the ribbon to the synaptic vesicle. The tethered vesicle densely but do not touch. Vesicles tethered along the base of the ribbon directly contact the presynaptic membrane and thus are considered ´docked': The ratio between the vesicles tethered and docked is roughly 5:1 for the plate like ribbons and 10:1 for spheroidal ones.

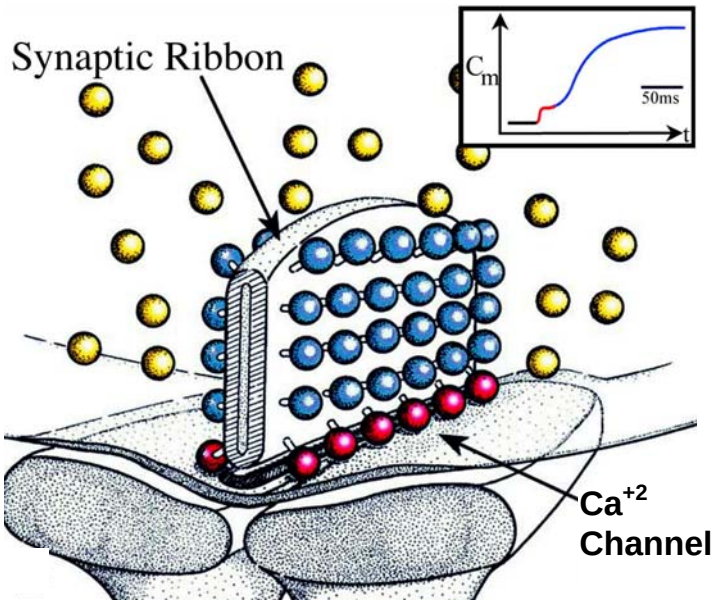

Figure 4. 3D representation of synaptic ribbons. (Von Gersdorff *et al*., 2001).

Vesicles (yellow color) are reserve, vesicles (blue color) bound to synaptic ribbons are considered as tethered, vesicles tethered along the base of synaptic ribbon (red vesicles) are considered as docked (Sterling *et al*., 2005). A typical bipolar contains 5-7 calcium channels (Tachibana, 1999).

In the recent years, the individual protein constituents of the ribbon synapse are started to be revealed. The CAZ proteins are segregated in to two distinct molecular compartments of the ribbon complex: a ribbon and an active zone compartment. The ribbon-associated compartment includes RIBEYE/CtBP2, CtBP1, KIF3A, Piccolo, and RIM1; the active zone compartment includes RIM2, Munc13-1, ERC2/CAST1, and Ca^{+2} channel α 1 subunit (tom Dieck *et.* al., 2005). The physical interaction between Bassoon and RIBEYE seems to be involved in linking the two compartments and the assembly of a functional ribbon complex (tom Dieck *et.* al., 2005). This protein profiling of ribbon synapse is almost similar to conventional synapse (Ullrich and Südhof, 1994; Brandstatter *et al*.,

1996a, 1996b; von Kriegstein *et al*., 1999). In spite of this, ribbon is a unique in composition as till to date no cytoskeletal protein has been localized to ribbons, nor do they have the typical filaments that are characteristic of various types of cytoskeleton. Only few proteins have been localized to ribbons, e.g. the presynaptic active zone protein RIM (Wang *et al*., 1997). This seems to be rather specific, since other active zone proteins such as bassoon and Munc13-1 do not localize to ribbons but only to the active zone (Brandstatter *et al*., 1999). In addition, KIF3A the kinesin motor protein is associated with ribbons as well as other organelle in the presynaptic nerve terminal (Muresan *et al*., 1999). Minor difference lies in the usage of Syntaxin 3, instead of Syntaxin 1 for fusion (Morgans *et al*., 1996) and of L-type Ca^{+2} channels instead of N-, P/Q-, or R type channels for Ca^{+2} influx (Heidelberger and Matthews, 1992; Nachman-Clewner *et al*., 1999). Furthermore, rabphilin and synapsins are absent from ribbon synapses in some but not all species (Mandell *et al*., 1990; von Kriegstein *et al*., 1999). However the absence of rabphilin is unlikely to be a functionally important, since a knockout of *rabphilin* has no measurable phenotype in the conventional synapse (Schlüter *et al*., 1999), and the significance of the absence of the synapsins is similarly uncertain since expression of synapsins 1 in photoreceptor synapses does not alter synaptic transmission (Geppert *et al*., 1994). Together, these results suggest that ribbon are not composed of known components but are assembled from a novel class of proteins specific for the ribbons. However, still to date the exact molecular function and the formation of synaptic ribbon is unclear.

1.6 RIBEYE the major component of synaptic ribbons

RIBEYE is a novel component of the synaptic ribbons. RIBEYE is present in synaptic ribbons of all vertebrate ribbon synapses (Schmitz *et al*., 2000; Zenisek *et al*., 2004; Wan *et al*., 2005; tom Dieck *et al*., 2005; Khimich *et al*., 2005; Schmitz *et al*., 2006, for review, see tom Dieck and Brandstätter, 2006). Previous data indicated that RIBEYE is the major component of synaptic ribbons (Schmitz *et al*., 2000; Zenisek *et al*., 2004; Wan *et al*., 2005) representing up to 67% of the volume of the synaptic ribbon (Zenisek *et al*., 2004). Using peptide binding experiments, Zenisek *et al*., 2004 had showed that the each ribbon in a retinal bipolar cell (in goldfish) contains ~ 4000 molecules of RIBEYE. The authors, emphasized that these experiments underestimates the amount of RIBEYE because 1) its uncertain that peptide concentration in cell reaches the pipette concentration during the time course of experiments; 2) some RIBEYE molecules may have their binding sites obscured by other endogenous

proteins possibly containing the consensus sequence for RIBEYE binding, and 3) confocal serial sections may have caused some photobleaching of ribbon bound peptide. Using RIBEYE specific antibody Schmitz *et al*., 2000 had shown the presence of RIBEYE molecule over the entire length of synaptic ribbon. These experiments suggest that the bulk of ribbon is made up of RIBEYE and its homogenous distribution over the entire ribbon.

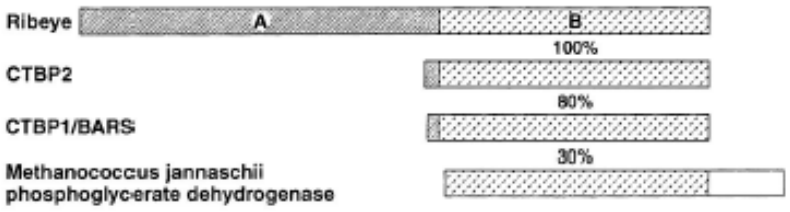

Figure 5. Domain structures of RIBEYE, CtBP2, CtBP1, and phosphoglycerate dehydrogenase.

RIBEYE is composed of a unique N-terminal A domain and a C-terminal B domain that is identical with CtBP2 and homologous to phosphoglycerate dehydrogenase. The percentage sequence identity between the various protein domains is shown between the bar diagrams (Schmitz *et al*., 2000).

RIBEYE as a molecule comprises of a unique A-domain (563 residues) specific for RIBEYE, and a B-domain (420 residues) identical with CtBP2 except for the first 20 amino acids (Schmitz *et al*., 2000). CtBP2 is transcriptional co-repressor that in turn is related to 2-hydroxyacid dehydrogenases.

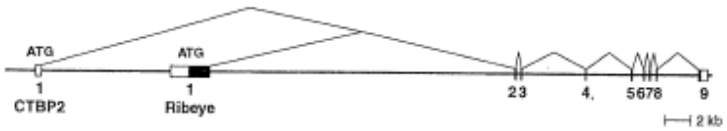

Figure 6. Structure of the Human Gene Encoding RIBEYE and CtBP2.

The genomic organization of the RIBEYE/CtBP2 was deduced from the sequence of clone RP11-114N8 (accession number AC013533). (Schmitz *et al*., 2000).

CtBP2 and RIBEYE are transcribed from independent promoters in the same gene in which the unique N-terminal sequences of each proteins are included in single 5' exon (exon1), while their shared C-terminal sequences are encoded by eight common 3' exons (exon 2-9). Exon 1 of CtBP2 encodes only its N-terminal 20 residues, whereas exon1 of RIBEYE includes the sequence of the entire A-domain of RIBEYE. RIBEYE is exclusively localized to synaptic ribbons, whereas the ubiquitously expressed CtBP2, which lacks completely RIBEYE (A)-domain has a largely nuclear localization (for review, see Chinnadurai, 2003). Recently, Wan *et al*., 2005 identified two teleost homology of *Ribeye* gene,

Ribeye a and *Ribeye b*. Fish deficient in Ribeye a lack an optokinetic response and have shorter synaptic ribbons in photoreceptors and fewer synaptic ribbons in bipolar cells. But, these studies did not address neither the reason behind shorter synaptic ribbons nor the direct role of RIBEYE in ribbon formation. It was suggested that the A-domain of RIBEYE, identical to full length RIBEYE tends to form cellular aggregates (Schmitz *et al*., 2000). What are these aggregates, the underlying mechanism to generate such aggregates, and their precise role is not known so far. The RIBEYE, B-domain binds NAD^+ with high affinity, similar to 2-hydroxyacid dehydrogenases. The structural analysis of these proteins e.g. of CtBP1, revealed the presence of two globular sub-domains, namely a NAD(H) binding sub-domain (NBD) and the substrate-binding sub-domain (SBD) (Kumar *et al*., 2002; Nardini *et al*., 2003; for a review, see Chinnadurai, 2002). On the basis of accumulated evidences and our findings, a model for the synaptic ribbons was proposed considering the domains of the RIBEYE being the major component.

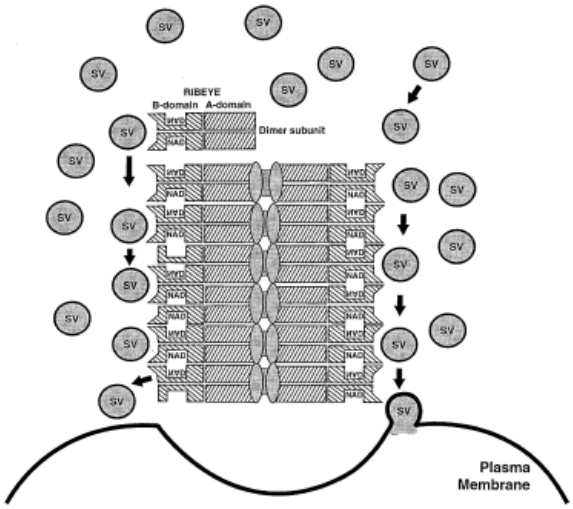

Figure 7. Working Model for the role of RIBEYE in the function of synaptic ribbons.

RIBEYE is displayed in the ribbons as a protein aggregate formed by it's A- domain, with the NAD binding B-domain (which is identical to CtBP2) exposed on the surface to interact with an unknown component of synaptic vesicle (sv), analogous to the function of CtBP2 in the nucleus as binding partner for transcription factors. The B-domain is depicted as a dimmer since CtBP2 is a dimer (Poortinga *et al*., 1998). The model suggests that RIBEYE is a major component of ribbons in addition to other proteins, some of which are schematically indicated as inner-core proteins. This protein may correspond to the second unique protein besides RIBEYE that was found in the biochemically purified ribbon fraction (Schmitz *et al*., 2000).

Understanding the structure of ribbons will be necessary to get insight into the mechanism by which these fascinating synapses prime vesicle for rapid continuous release. In addition, such understanding may provide clues to deciphering genetic diseases, since ribbon component would be prime candidates for disorders that selectively affect vision and hearing, for example in various forms of Usher's

syndrome. I focused on the structure of the synaptic ribbons, and targeted its prime component RIBEYE and analyzed its structural properties. Furthermore, we addressed the functional role of RIBEYE in the ribbon synapse. This was addressed by the identification and characterization of the photoreceptor specific phospholipid binding protein TULP1. This interaction is of particular functional relevance because TULP1 is essential for normal vision and information processing in the retina.

1.7 Tubby - like protein 1 (TULP 1)

TULP 1 (tubby-like protein 1) is a member of a tubby family with includes other three members (TULPs 1-3). These proteins are conserved among different mammalian species and are also found in other multicellular organisms including plants. The biochemical function of the TULPs is currently not fully understood. It functions as transcription factors (Santagata *et al*., 2001), intermediates in insulin signaling (Kapeller *et al*., 1999), or in intracellular transport have been proposed (Hagstrom *et al*., 2001). The *TUB* gene is expressed in multiple human tissues including retina, whereas the TULP1 gene product is found mainly in retina, where it localizes primarily to the inner segments and connecting cilium of photoreceptor cells. TULP 2 is expressed primarily in testis (North *et al*., 1997), and TULP 3 is found in multiple tissues, including the retina (Nishina *et al*., 1998). These proteins feature a characteristic ‘‘tubby-domain’’ of about 260 amino acids at the carboxyterminal that forms that forms a unique helix filled barrel structure. This carboxyterminal also binds avidly to double-stranded DNA via the tubby-domain.

Inositol phospholipids have long been known to have an important regulatory role in cell physiology. They are known to serve as second messengers in signal-transduction cascade. Many cellular processes known to be directly or indirectly controlled by this class of lipids has now dramatically expanded. Phosphoinositides achieve direct signaling effects through the binding of their head groups to cytosolic proteins or cytosolic domains of membrane proteins. Tubby molecule serves as a downstream effector of G_q subclass of G_α proteins. Tubby is anchored to plasma membrane through binding phosphatidylinositol 4,5-bisphosphate [PtdIns $(4,5)P_2$] and the other lipids being [PtdIns $(3,4)P_2$] and [PtdIns $(3,4,5)P_3$]. This association is mediated by β-strands 4, 5 and 6 and helix 6A of the tubby-domain. The hydrolysis of [PtdIns $(4,5)P_2$] by phospholipase C-β mediates the release of tubby from plasma membrane and translocates it to nucleus where it binds to DNA. The amino

terminal region of tubby proteins, in their primary sequence, resemble activation domain from known transcription factors (Boggon *et al*., 1999) and also contains a functional nuclear localization signal. Therefore, tubby proteins represent the family for which the dynamic nuclear translocation is clearly regulated by [PtdIns (4,5)P_2] hydrolysis.

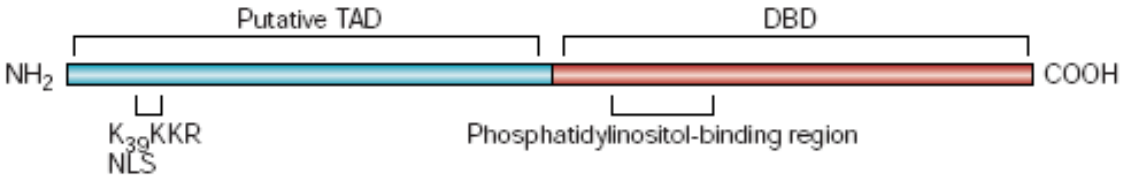

Figure 8. A diagrammatic representation of the TUB protein.

The aminoterminal domain contains the nuclear localizing signal (NLS), and has the transcriptional-activating activity (TAD Transcriptional activation domain). The conserved carboxyterminal tubby-domain contains the DNA binding domain and the phosphatidylinositol-binding region, which anchors the TUB to the cell membrane before it is released by phospholipase Cβ (PLC β)-mediated cleavage of the phosphatidylinositol bisphosphate. All TULP-family members have similar features to those shown above-all have a carboxyterminal tubby-domain, but their aminoterminal regions are less conserved (Carroll *et al.,* 2004).

Recently, Boggon *et* al., 1999 reported the high resolution crystal structure of the tubby-domain. This sheds the light on structure based function of this conserved domain, where deviation from the native state as a result of mutation results in altered phenotype. The structure of tubby reveals a striking fold in which a central hydrophobic helix at the carboxyterminus wholly traverses the interior of a closed 12-stranded β barrel. The tubby β barrel adopts an alternating up-down nearest-neighbor topology, such that hydrogen bonding is in the antiparallel mode for all strands. The strands of the barrel are numbered from 1-12 in a sequence order. Several excursions in the loops between these strands are observed. A three stranded β sheet intervenes in the 9 and 10 connections and are designated as 9A, 9B, and 9C. Similarly, four helices, H4, H6A, H6B, and H8, are found in the corresponding loop regions between strands of the main barrel. The barrel is slightly oblong, with C_α to C_α widths across it varying between 18 and 22 Å. From top to bottom, the barrel measures ~ 18 Å. The whole domain has a maximum dimension of 40 Å in the direction parallel to the central helix H12, and 51 Å in the perpendicular plane. Helix H0 at the NH_2-terminus caps the top of the barrel, and the long hydrophobic helix H12 traverses the inside of the barrel from top to bottom. This helix forms an integral contact with every part of the hydrophobic core. Thus, in the tubby mice, the entire hydrophobic core of this domain will be disrupted, and it is therefore almost certain that no functional protein can be produced.

In tubby mice, retinal degeneration is characterized by a progressive loss of photoreceptor cells beginning ~ 3 weeks after birth. Interestingly, the causative mutations in TUB leading to mouse phenotype and TULP1 leading to the disease in the patients (Lewis *et al*., 1999; Noben-Trauth *et al*., 1996) are at the identical donor splice site (Banerjee *et al*., 1998). Both mutations would be expected to alter the evolutionarily conserved carboxyterminal end of these related molecules.

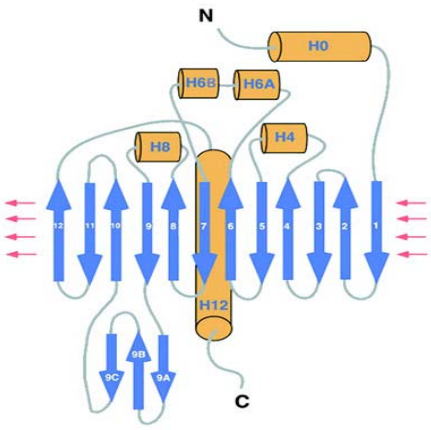

Figure 9. Topology diagram of the tubby COOH-terminal domains.

The small red arrows indicate the continuation of hydrogen bonding between β-strands 1 and 12 to form a closed barrel (Boggon *et al*., 1999).

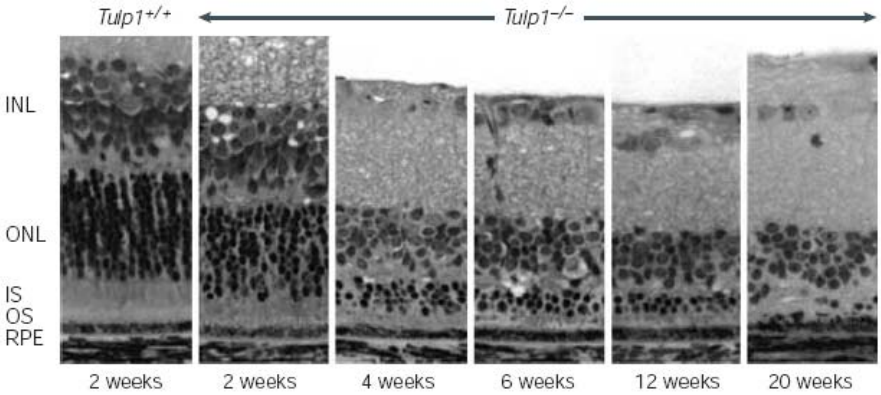

Figure 10. TULP 1 loss and retinal degeneration.

Light microscopy showing retinal degeneration in Tulp1 $^{-/-}$ mice. A2-week old Tulp1 $^{+/+}$ mice is shown on the left as a control. Shortening of the inner segment (IS) and outer segment (OS) of photoreceptor cells is apparent by 2 weeks of age. At 4 weeks, the outer nuclear layer (ONL) is greatly reduced. The degeneration is progressive over 20 weeks. INL, inner nuclear layer; RPE, retinal pigment layer. Scale bar, 20µm. (Carroll *et al*., 2004).

TULP 1 is implicated in the genetic origin of human Retinitis pigmentosa 14 (RP-14), a heterogeneous group of inherited retinal diseases in which the rod and cone photoreceptor cells degenerate, leading to blindness (Hagstrom *et al*., 1998). Mutations in the TULP1 gene are found in approximately 1% to 2% of patients with autosomal recessive RP (Gu *et al*., 1998). To date, 14 different mutations have been found in the TULP1 gene, including 4 splice-site mutations, 2 frame-shift mutations, 1 nonsense mutation, and 7 missense mutations (Banerjee *et al*., 1998; Gu *et al*., 1998). A genomic search for linkage led to the identification and refinement of a locus on chromosome 6p designated as RP-14 (Shugart *et al*., 1995). TULP1 mutations have a very severe visual impairment. The profound and early photoreceptor degeneration (both rod and cone) suggests a critical functional role for TULP 1. The disease can be inherited in an autosomal recessive, autosomal dominant or X-linked fashion. Nystagmus and reduced visual acuity is the prominent early feature of the disease expression. This early central visual loss is probably because of central retinal photoreceptor maldevelopment, dysfunction, or degeneration as a part of the generalized retinopathy.

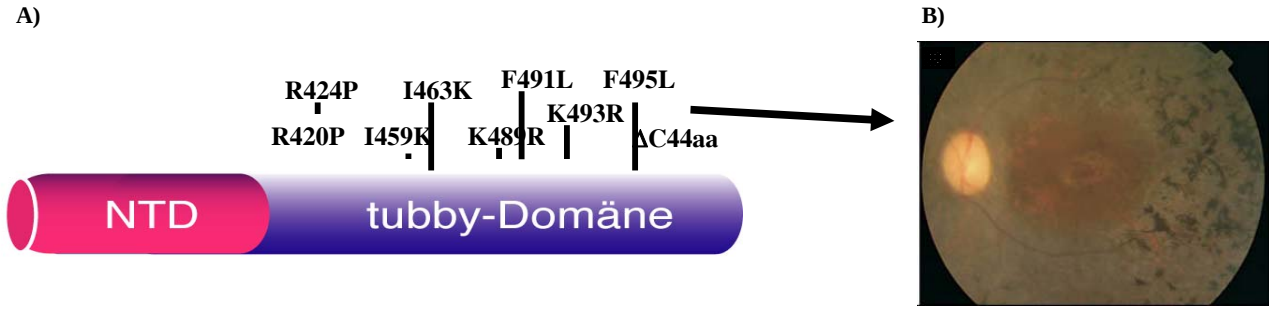

Figure 11. Mutations associated with RP and its phenotype.

A) Location of various hTULP 1 mutations on carboxyterminal tubby domain. NTD, aminoterminal transactivation domain. **B)** Fundus photograph of the left eye of RP patient showing diffuse bone spicule pigmentation extending to the macular region, narrowed arterioles, disc pallor, and atrophy of the pigment epithelium. (den Hollander *et al*., 2007).

This postnatal loss of vision suggests a fundamental role for TULP1 in retinal differentiation. Further, the observation that all retinal neuroblasts were TULP1-positive indicates that this protein may be involved in development of both photoreceptors and inner retinal neurons (Milam *et al*., 2000). Apoptosis is the common fate of photoreceptors in retinitis pigmentosa (Wenzel *et al*., 2005), which leads to the loss of the inner and outer segments of the photoreceptors. All of the studied TULP1 mutations affect a conserved amino acid residue in the carboxyterminal tubby-domain of TULP1.

Thus, on the basis of contiguous arrangement of these mutants, and its role in changes of surface charges it's postulated that this surface might form a protein or nucleic acid binding site.

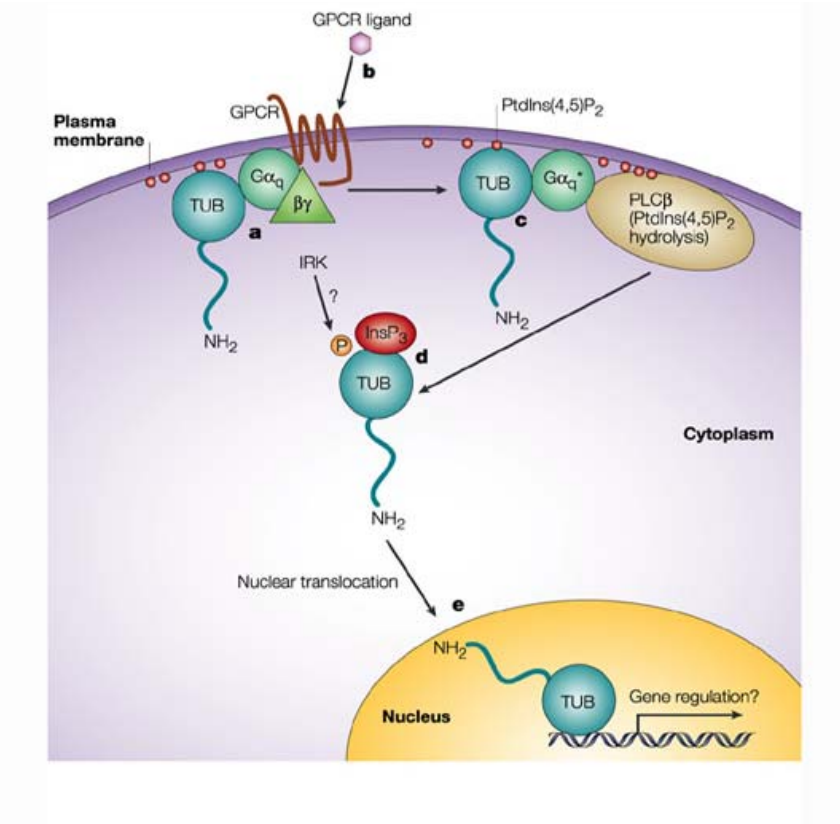

Figure 12. Schematic model of $G\alpha_q$ signaling through tubby proteins.

a) In the basal state, TUB resides on the membranes through phosphatidylinositol-4,5-bisphosphate (PtdIns(4,5) P_2) binding, presumably complexed to $G\alpha_q$. **b)** On G-protein-coupled receptor (GPCR) activation, $G\alpha_q$ is activated (as indicated by an asterisk) and released from the receptor. **c)** $G\alpha_q$ then activates phospholipase Cβ (PLCβ), which leads to cleavage of (PtdIns P_2) into inositol triphosphates ($InsP_3$). **d)** TUB is subsequently released from the cell membrane and then translocates into the nucleus. **e)** Once in the nucleus, TUB could be involved in the gene regulation. How TUB phosphorylation by the insulin receptor kinase (IRK) fits into this pathway remains unknown; this receptor tyrosine kinase might operate independently of this pathway. (Carroll *et al*., 2004).

1.8 Working hypothesis

RIBEYE is the major component of synaptic ribbons. Therefore, it probably has a major influence on the structure and function of synaptic ribbons. Deciphering the structural and functional aspects of RIBEYE was the goal of the present study.

2 Materials and Methods

2.1 Materials

2.1.1 Host Strains

2.1.1.1 Bacterial strains

Bacterial Strain	Genotype	Source and Reference
E.coli DH10B	F- *mcr*A Δ(*mrr-hsd*RMS-*mcr*BC) φ80*lac*ZΔM15 Δ*lac*X74 *rec*A1 *end*A1 *ara*D139 Δ(*ara, leu*)7697 *gal*U *gal*K λ- *rps*L *nup*G	Invitrogen, Grant *et al*., 1990.
E.coli BL21 (DE 3)	F^- *omp*T *hsd*S_B($r_B^-m_B^-$) *gal dcm* (DE3)	Invitrogen, Grodberg und Dunn, 1988.
E.coli JC 201	*PlsC* (derived from SM2-1 by P1 transduction using SO1023 as donor, selecting met^+, tet^s)	Gifted, Coleman, 1990.

2.1.1.2 *Saccharomyces cerevisiae* strains

Yeast strain	Genotype	Source and Reference
AH 109	*MATa , trp1-901, leu2-3, 112, ura3-52, his3-200, Gal4Δ, gal80Δ, LYS2::GAL1*$_{UAS}$*-GAL1*$_{TATA}$*-HIS3, GAL2*$_{UAS}$*-GAL2*$_{TATA}$*-ADE2, URA3::MEL1*$_{UAS}$*-MEL1*$_{TATA}$*-lacZ MEL1*	Clontech Laboratories Inc. James *et al*., 1996.
Y 187	*MATα , ura3-52, his3-200, ade2-101, trp1-901, leu2-3 ,112, gal4Δ, met-, gal80Δ, MEL 1 URA3::GAL1*$_{UAS}$*–GAL1*$_{TATA}$*-lacZ*	Clontech Laboratories Inc. Harper *et al*., 1993.

2.1.1.3 COS 7 cell line

Cell type	Features	Source and Reference
COS 7 cells	African green monkey kidney fibroblast-like cell line suitable for transfection by vectors requiring expression of SV40 T-antigen. The presence of T-antigen, retains complete permissiveness for lytic growth of SV40, supports the replication of ts A209 virus at 40°C, and supports the replication of pure population of SV40 mutants with deletions in the early region. The line was derived from the CV-1 cell line (ATCC CCL-70) by transformation with an origin defective mutant of SV40 which codes for wild type T antigen.	Gifted by T. C. Südhof Gluzman *et al*., 1981.

2.1.1.4 R28 cell line

Cell type	Features	Source and Reference
R28 cells	Retinal progenitor cells from rat retina. It retains neuronal properties and also expresses photoreceptor-specific proteins, e.g. recoverin, opsins and beta-arrestins.	Gifted by G.M Seigel Seigel *et al*., 2004.

2.1.1.5 *Pichia pastoris* strain

Yeast strain	Genotype	Features	Source and Reference
GS115	*his 4*	The Histidine auxotrophy is complemented by the expression vector carrying the *HIS 4* gene for the selection.	Invitrogen, Cregg *et al*., 1993.

2.1.2 Plasmid Vectors

2.1.2.1 *Escherichia coli* cloning vectors

Vectors	Features	Antibiotic resistance	Source and Reference
pGEX-KG	Genes cloned will be expressed as fusions to the C-terminus of GST, tac promotor, lac^q repressor	Ampicillin	Gifted by T. C. Südhof Schmitz *et al*., 2000.
pMAL c2	Genes cloned will be expressed as fusions to the C-terminus of MBP, tac promoter, lac^q repressor	Ampicillin	New England BioLabs Guan *et al*., 1988.

2.1.2.2 Yeast two-hybrid vectors

Vectors	Features	Antibiotic resistance	Source and Reference
pACT 2	Production of C- terminal GAL 4 (AD) fusion protein. Fusion protein targeted to yeast nucleus by SV40 NLS. P_{ADH1} constitutive promoter, T 7 promotor, HA epitope tag, leucine nutritional marker for selection in yeast. Replicates in *E.coli* (pUC) and *S. cerevisiae* (2µ)	Ampicillin	Clontech Laboratories Inc.
pGBKT 7	Production of C- terminal GAL 4 (BD) fusion protein. P_{ADH1} constitutive promoter, c-Myc tag, tryptophan nutritional marker for selection in yeast. Replicates in *E.coli* (pUC) and *S. cerevisiae* (2µ) plasmid.	Kanamycin	Clontech Laboratories Inc. Louret *et al.,* 1997.
pGADT 7	Production of C- terminal GAL 4 (AD) fusion protein. Fusion protein targeted to yeast nucleus by SV40 NLS that have been added to the activation domain sequence. P_{ADH1} constitutive promoter, T 7 promotor, HA epitope tag, Leucine nutritional marker for selection in yeast. Replicates in *E.coli* (pUC) and *S. cerevisae* (2µ).	Ampicillin	Clontech Laboratories Inc. Chien *et al.,* 1991.
pSE1111	Negative control vector (Bait) Gal4AD		Tai *et al*., 1999.
pSE1112	Negative control vector (Prey) Gal4BD		Tai *et al*., 1999.

2.1.2.3 Eukaryotic expression vectors

Vectors	Features	Antibiotic resistance	Source and Reference
pEGFP-N1	Genes cloned will be expressed as fusions to the N-terminus of EGFP (Excitation maximum 488nm; emission maximum 507 nm). Immediate early promoter of CMV. SV 40 polyadenylation signals downstream of the EGFP gene direct proper processing of the 3´end of the EGFP mRNA. pUC origin of replication and an f1 origin.	Neomycin/Kanamycin	Clontech Laboratories Inc. Chalfie *et al*., 1994.
pmRFP	Genes cloned will be expressed as fusions to the N-terminus of RFP (Excitation maximum nm 584; emission maximum 607 nm). Immediate early promoter of CMV. SV 40 polyadenylation signals downstream of the EGFP gene direct proper processing of the 3´end of the EGFP mRNA. pUC origin of replication and an f 1 origin.	Neomycin/Kanamycin	Clontech Laboratories Inc. Campbell *et al*., 2002.

2.1.2.4 *Pichia pastoris* vector

Vectors	Features	Antibiotic resistance	Source
pPIC 3.5 K	Plasmid allows *in vivo* multiple integration in *Pichia* genome. It contains five unique restriction sites in MCS. It's optimized for the intracellular expression of the gene of interest. Requires ATG codon for proper translational initiation. *HIS 4* selection in *Pichia.* For insertion at *HIS 4* linearized with *Sal 1*	Ampicillin / Kanamycin	Invitrogen

2.1.3 Antibodies

Primary antibody (for Immunohistochemistry and western blot)				
Antigen	**Monoclonal/Polyclonal**	**Raised source**	**Source and Reference**	**Working concentration**
Tulp1 (winden)	Polyclonal	Rabbit	Lab made (Unpublished)	1:100
RIBEYE U_{2656}	Polyclonal	Rabbit	Lab made Schmitz *et al*., 2000.	1:10,000
GST	Monoclonal	Mouse	NEB	1:10,000
MBP	Monoclonal	Mouse	NEB Narayanan *et.al*., 1994.	1:10,000
Tau RIBEYE	Polyclonal	Rabbit	Lab made Magupalli *et al*., 2008	1:10,000
EGFP T_{3743}	Polyclonal	Rabbit	Gifted by T.C. Südhof Texas, Dallas	1:10,000
GFP	Polyclonal	Rabbit	abcam Yamada *et al*., 2006.	1:1,000
Tulp1	Polyclonal	Rabbit	Chemicon North *et al*., 1997	1:100
β-tubulin	Monoclonal	Mouse	Sigma	1:500
Bassoon	Polyclonal	Rabbit	Synaptic Systems	1:500

Secondary antibody (for Immunohistochemistry and western blot)				
	Excitation wavelength (nm)	**Emission wavelength (nm)**	**Source and Reference**	**Working concentration**
Goat anti-Rabbit-Cy3	550	570	Sigma	1:1,000
Goat anti-Rabbit-Cy2	490	508	Sigma	1:1,000

Goat anti-Rabbit-POX	---	---	Sigma Wilson *et al.*, 1978.	1:10,000
Goat anti-Rabbit-Gold conjugate (10 nm)	---	---	Sigma Brada *et al.*, 1984.	1:10,000
Goat anti-Mouse-POX	---	---	Sigma Wilson *et al.*, 1978.	1:10,000

2.1.4 Plasmid clones

Clone number	Gene of interest	Cloned vector
845	RIBEYE(A) (Rat) Schmitz *et al.*, 2000	pEGFP N-1
864	RIBEYE(B) (Rat) Schmitz *et al.*, 2000	pGEX-KG
1672	TULP 1 full length(Bovine), Dr. Louise Köblitz, Unpublished	pCMV Tag 2B
3423	RIBEYE(B) (Rat) Schmitz *et al.*, 2000	pGEX-KG
467	RIBEYE(FL) (Rat) Schmitz *et al.*, 2000	pBluescript SK
310	RIBEYE(B) (Rat) Schmitz *et al.*, 2000	pEGFP N-1
311	RIBEYE(A/B) (Rat) Schmitz *et al.*, 2000	pEGFP N-1
1058	TULP 1 $_{1\text{-}546}$ (Bovine), Dr. Louise Köblitz, Unpublished	pACT2
904	TULP 1 (+PTNLS) (Bovine), Dr. Louise Köblitz, Unpublished	pACT2
906	TULP1 (-PTNLS) (Bovine), Dr. Louise Köblitz, Unpublished	pACT2
1029	TUBBY 1 $_{292\text{-}546}$(Bovine), Dr. Louise Köblitz, Unpublished	pACT2
1208	RIBEYE(A/B) (Rat) , Dr. Louise Köblitz, Unpublished	pGBKT7
2164	TULP1$_{353\text{-}546}$ (1051) (Bovine), Dr. Louise Köblitz, Unpublished	pACT2
1070	TUBBY 1 $_{292\text{-}546}$ (Bovine), Dr. Louise Köblitz, Unpublished	pGEX-KG
3008	RIBEYE(B) F904W (Rat), Dr. Karin Schwarz, Unpublished	pGBKT7

2.1.5 Oligonucleotides

Forward PCR primers

Underlined: restriction site, bold/underlined: first matching codon

Primer no:	Oligonucleotide sequence	Restriction site
REA 355 F	5´- TTTGGATCCTT**ATG**CCGGTTCCCAGCAG - 3´	BamH I
REA 388 F	5´- TTTGAATTCTT**ATG**CCGGTTCCCAGCAG - 3´	EcoR I
REA 389 F	5´- TTTGAATTCTT**AGT**AGCTTCAGCCACCG - 3´	EcoR I
REA 401 F	5´- TTTGAATTCTT**TCT**GGATATAGCTCTCCTA - 3´	EcoR I
REA 412 F	5´- TTTGGATCCTT**GAG**CTGGTAAACCACCGT - 3´	BamH I
REA 413 F	5´- TTTGGATCCTT**GTG**CCCAGCTACGGAGT - 3´	BamH I
REA 418 F	5´- TTTGGATCCTT**AGT**AGCTTCAGCCACCGA - 3´	BamH I
REB 406 F	5´- TTTTCCATGGTT**ATC**CGCCCCCAGATCATGA - 3´	Nco I
REA 384 F	5´- TTTGAATTC **TGC**AGGACAGAGATGCAGTT - 3´	EcoR I
REA 734 F	5´- TTTGAATTC **ATG**CCGGTTCCCAGCAG - 3´	EcoR I
REA 840 F	5´- TTTTGAATTC **ATG**CCGGTTCCCAGCAG- 3´	EcoR I
REB 353 F	5´- GTTCCATGGAG**ATC**CGCCCCCAGATCAT- 3´	Nco I
REB 508 F	5´- TTTTGAATTCTT**ATC**CCATCTGCTGCAGT - 3´	EcoR I
TULP1 595 F	5´-TTTTCCATGGTT**GTG**GACGAACCCCAGG - 3´	Nco I
TULP1 664 F	5´-TTTTAAGCTTCCACCATG**GTG**GACGAAC - 3´	Hind III
REB 837 F	5´-TTTTCTCGAGTGCCACCATG**ATC**CGCCCCCAGATCAT- 3´	Xho I
REB 839 F	5´-TTTTCTCGAGTGCCACC**ATG**CCGGTTCCCAGCAG - 3´	Xho I
REB 879 F	5´-TTTGAATTCTT**CCA**TCCAGGGGCACCA - 3´	EcoR I
REB 98 F	5´-TTAGAATTC **ATG**CCGGTTCCCAGCAGG - 3´	EcoR I
REB 96 F	5´-TTCACAATTG **ATC**CGCCCCCAGATCATG - 3´	Mun I
REA 415 F	5´-TTTGGATCCTT**CCA**ACATGCCTGGTTGTG - 3´	BamH I

Reverse PCR primers

Underlined: restriction site, bold/underlined: first matching codon

Primer no:	Oligonucleotide sequence	Restriction site
REA 356R	5´- TTTCTCGAG **ACT**TGGTTCTGGTGTTAGCA - 3´	Xho I
REA 390R	5´- TTTCTCGAG **ACT**TGGTTCTGGTGTTAGC - 3´	Xho I
REA 394R	5´- TTTCTCGAGG**TTC**CCTCTTAAGCAGTTC - 3´	Xho I
REA 395R	5´- TTTCTCGA**GGC**AGAGTAAGTAGCTGCT- 3´	Xho I
REA 396R	5´- TTTCTCGAGCT**CAG**CAGGGCCAAAAAC - 3´	Xho I
REA 397R	5´- TTTCTCGAGT**AGA**GTCAACGGGTCTTTC - 3´	Xho I
REA 398R	5´- TTTCTCGAG **ACT**CCCAGATTCCCGGTA - 3´	Xho I
REA 399R	5´- TTTCTCGAG **GTC**GCCATAGTAGTCTTGT - 3´	Xho I
REA 393R	5´- TTTCTCGAG **GCC**ATAAGTCAGAGAACTT - 3´	Xho I
REA 735R	5´- TTTTGCGGCCGCTTA**ACT**TGGTTCTGGTGTTAG - 3´	Not I
REA 841R	5´- TTTTTGTCGAC **ACT**TGGTTCTGGTGTTAGC - 3´	Sal I
REA 385R	5´- TTTTTCTAGA **TGT**GTGGAGACTTTGCCTG - 3´	Xba I
REB 405R	5´- TTTTCTCGAG **CTA**TTGCTCGTTGGGGTGCT - 3´	Xho I
REB 354R	5´-GTTCTCGAG **CTA**TTGCTCGTTGGGGT - 3´	Xho I
REA 391R	5´- TTTCTCGAG **GTG**GCTGAAGCTACT - 3´	Xho I
REB 509R	5´-TTTTCTCGAG **GCT**GTACCAGGCTGTGT - 3´	Xho I
REB 836R	5´-TTTTGGATCCCT**ACT**TGGTTCTGGTGTTAGC - 3´	Bam H I
REB 838R	5´-TTTTAGATCTCT**TTG**CTCGTTGGGGTGCT - 3´	Bgl II
REB 404R	5´-TTTTCTCGAG C**CAC**ACCTACAATGCCT - 3´	Xho I
TULP 1 596 R	5´-TTTTCTCGAGTT**TCA**CTCGCAGGCCAGC - 3´	Xho I
TULP 1 644 R	5´-TTTTCTCGAGT**GTC**ATCAGCGTGGACAAT - 3´	Xho I
TULP 1 647 R	5´-TTTTTGTCGACTT**CTC**GCAGGCCAGCTTC - 3´	Sal I
REA 881R	5´-TTTCTCGAGT**GGA**CCGATGGCGGGGT- 3´	Xho I
REA 119R	5´-TTCCTCGAG **ACT**TGGTTCTGGTGTTAGCAT- 3´	Xho I
REB 97 R	5´-TTCACTAGT **CTA**TTGCTCGTTGGGGTGC- 3´	Spe I

Mutant and COMBO Oligonucleotides

Forward mutated PCR primers

Underlined: mutated bases, bold/underlined: first matching codon

Primer no:	Oligonucleotide sequence
TULP 1 603 F $_{PTSNL}$	5´-CCCACCTCCAATCTG **CGA**GGAGGGGAGAATTT - 3´
TULP 1 637 F $_{R\ 424\ P}$	5´-**CCC**CGGCCCATGACGGTCATCATTCCTGG - 3´
TULP 1 639 F $_{I\ 463\ K}$	5´-**AGC**CTCAAGGAGCTGCACAACAAGCCCCCCAT - 3´
TULP 1 641 F $_{F\ 495\ L}$	5´-**AAT** TTACAGATTGTCCACGCTGATGACCCCG - 3´
TULP 1 646 F $_{K\ 493\ R}$	5´-**TCA**GTCAGAAATTTCCAGATTGTCCACGTCGATGAC - 3´
REB 505 F (COMBO)	5´-TGCCATATCCTCAATCTGGGAGGAGGAGCTGCTCGGATCC-3´
REB 523 F	5´-**AAC**ATCCCATCTGCTGCAGGAGGATCTTACAGCGAACAAGCATCA-3´
REB 866 F	5´-**TAC**TTACAGAACGGGATAGAGCGG - 3´
REB 868 F	5´-**CAT**GAGTCTCAGCCCTTCAGCTTT- 3´
REB 870 F	5´-**CCC**TTCAGCTGGGCTCAGGGCCCA- 3´
REB 872 F	5´-**GGC**CCATTGCAGGATGCTCCAAAT- 3´
REB 876 F	5´-**CAC**CACCTCGCCAATGACTTCACC - 3´

Reverse mutated PCR primers

Underlined: mutated bases, bold/underlined: first matching codon

Primer no:	Oligonucleotide sequence
TULP 1 604 R $_{PTSNL}$	5´-CAGATTGGAGGTGGG **ATC**GCTAGAGATGAGGTA - 3´
TULP 1 638 R $_{R\ 424\ P}$	5´-**CAT** GGGCCGGGGACCTCGGAAGCCCAGC- 3´
TULP 1 640 R $_{I\ 463\ K}$	5´-**CAG**CTCCTTGAGGCTCTCCAGTGTCTTGTTCTG - 3´
TULP 1 642 R $_{F\ 495\ L}$	5´-**GAC**AATCTGTAAATTCTTGACTGAGGCCTGG - 3´
TULP 1 643 R $_{K\ 493\ R}$	5´-**CTG**GAAATT TCTGACTGAGGCCTGGGTGACTCG - 3´
REB 504R (COMBO)	5´-GGATCCGAGCAGCTCCTCCTCCCAGATTGAGGATATGGCA- 3´
REB 522R	5´-**TGA**TGCTTGTTCGCTGTTAGATCCTCCTGCAGCAGATGGGATGTT -3´
REB 867R	5´-**CCG**CTCTATCCCGTTCTGTAAGTA - 3´
REB 869R	5´-**AAA**GCTGAAGGGCTGAGACTCATG- 3´
REB 871R	5´-**TGG**GCCCTGAGCCCAGCTGAAGGG- 3´
REB 873R	5´-**ATT**TGGAGCATCCTGCAATGGGCC- 3´
REB 877R	5´-**GGT**GAAGTCATTGGCGAGGTGGTG- 3´

2.1.6 PCR products

Amino acids	Forward primer	Reverse primer	Template clone	Vector
RE(A) $_{1-563}$	REA 355 F	REA 356 R	RIBEYE(A) (Rat) # 845	pACT 2
RE(A) $_{364-563(LONG, A2)}$	REA 389 F	REA 390 R	RIBEYE(A) (Rat) # 845	pACT 2
RE(A) $_{1-496}$	REA 388 F	REA 394 R	RIBEYE(A) (Rat) # 845	pACT 2
RE(A) $_{1-424}$	REA 388 F	REA 395 R	RIBEYE(A) (Rat) # 845	pACT 2
RE(A) $_{1-291}$	REA 388 F	REA 396 R	RIBEYE(A) (Rat) # 845	pACT 2
RE(A) $_{1-216}$	REA 388 F	REA 397 R	RIBEYE(A) (Rat) # 845	pACT 2
RE(A) $_{1-162}$	REA 388 F	REA 398 R	RIBEYE(A) (Rat) # 845	pACT 2
RE(A) $_{1-105(A1)}$	REA 388 F	REA 399 R	RIBEYE(A) (Rat) # 845	pACT 2
RE(A) $_{1-41}$	REA 388 F	REA 393 R	RIBEYE(A) (Rat) # 845	pACT 2
RE(A) $_{438-563(SHORT, A2)}$	REA 401 F	REA 390 R	RIBEYE(A) (Rat) # 845	pACT 2
RE(A) $_{1-563}$	REA 98 F	REA 119 R	RIBEYE(A) (Rat) # 845	pGBKT 7
RE(A) $_{364-563}$	REA 418 F	REA 390 R	RIBEYE(A) (Rat) # 845	pGBKT 7
RE(A) $_{1-563}$	REA 734 F	REA 735 R	RIBEYE(A) (Rat) # 845	pPIC 3.5 K
RE(A) $_{1-563}$	REA 840 F	REA 841 R	RIBEYE(A) (Rat) # 845	pMALc-2
RE(A) $_{343-536}$	REA 384 F	REA 385 R	RIBEYE(A) (Rat) # 845	pMALc-2
RE(B) $_{564-988}$	REB 406 F	REB 405 R	RIBEYE(B) (Rat) # 864	pACT 2
RE(A) $_{1-368}$	REA 388 F	REA 391 R	RIBEYE(A) (Rat) # 845	pACT 2
RE(B) $_{564-988 (C683S)}$	REB 353 F	REB 354 R	RE(B) $_{(C683S)}$ (Rat) # 3468	pGBKT 7
RE(B) $_{564-988}$	REB 96 F	REB 97 R	RIBEYE(B) (Rat) # 864	pMALc-2
RE(A) $_{1-563}$	REB 839 F	REB 836 R	RIBEYE(A) (Rat) # 845	mRFP
RE(B) $_{564-988}$	REB 837 F	REB 838 R	RIBEYE(B) (Rat) # 3423	mRFP
RE(B) $_{564-988}$	REB 406 F	REB 405 R	RIBEYE(B) (Rat) # 864	pGBKT 7
RE(A) $_{106-363(A3)}$	REA 879 F	REA 881 R	RIBEYE(A) (Rat) # 845	pACT 2
RE(B) $_{564-938}$	REB 406 F	REB 404 R	RIBEYE(B) (Rat) # 864	pGBKT 7
TULP 1$_{\Delta 503-546}$	TULP1 595 F	TULP1 644 R	TULP full length # 1672	pACT 2
TULP 1 $_{292-546}$	TULP1 664 F	TULP1 647 R	TULP full length # 1672	EGFP N-1
RE(A) $_{223-563}$	REA 415 F	REA 390 R	RIBEYE(A) (Rat) # 845	pGBKT 7
RE(A) $_{128-563}$	REA 413 F	REA 390 R	RIBEYE(A) (Rat) # 845	pGBKT 7
RE(A) $_{49-563}$	REA 412 F	REA 390 R	RIBEYE(A) (Rat) # 845	pGBKT 7
RE(B) $_{672-872}$	REB 508 F	REB 509 R	RIBEYE(B) (Rat) # 864	pACT 2

Mutants generated by COMBO PCR

Amino acids	Forward primer	Reverse primer	Outward For./ Rev. primer	Template clone	Vector
RE(B)$_{564-988\Delta DL}$	REB 505 F	REB 504 R	353 F/354 R	RIBEYE(B) (Rat) # 864	pGADT 7
RE(B)$_{SBD}$	REB 523 F	REB 522 F	353 F/354 R	RIBEYE(B) (Rat) # 864	pACT 2
RE(B)$_{SBD}$	REB 523 F	REB 522 F	353 F/354 R	RIBEYE(B) (Rat) # 864	pGBKT 7
RE(B)$_{D\ 758\ N}$	REB 866 F	REB 867 R	353 F/354 R	RIBEYE(FL) (Rat) # 467	pGBKT 7
RE(B)$_{E\ 854Q}$	REB 868 F	REB 869 R	353 F/354 R	RIBEYE(FL) (Rat) # 467	pGBKT 7
RE(B)$_{F\ 848W}$	REB 870 F	REB 871 R	353 F/354 R	RIBEYE(FL) (Rat) # 467	pGBKT 7
RE(B)$_{K\ 854\ Q}$	REB 872 F	REB 873 R	353 F/354 R	RIBEYE(FL) (Rat) # 467	pGBKT 7
RE(B)$_{I\ 796\ A}$	REB 876 F	REB 877 R	353 F/354 R	RIBEYE(FL) (Rat) # 467	pGBKT 7
TULP 1 $_{PTSNL}$	TULP1 603 F	TULP1 604 R	595 F/596 R	TULP full length # 1672	pACT 2
TULP 1$_{R\ 424\ P}$	TULP1 637 F	TULP1 638 R	595 F/596 R	TULP full length # 1672	pACT 2
TULP 1$_{I\ 463\ K}$	TULP1 639 F	TULP1 640 R	595 F/596 R	TULP full length # 1672	pACT 2
TULP 1$_{F\ 495\ L}$	TULP1 641 F	TULP1 642 R	595 F/596 R	TULP full length # 1672	pACT 2
TULP 1$_{K\ 493\ R}$	TULP1 646 F	TULP1 643 R	595 F/596 R	TULP full length # 1672	pACT 2

2.1.7 Subcloning products

Subcloned product	Vector	Restriction site	Parent vector	Restriction site (for cloning)	Excised by
RE(A) $_{1-105(A1)}$	pGBKT 7	5´-BamH I / Sal I -3´	RE(A) $_{1-105\ (A1)}$	pACT 2	5´-EcoR I / Xho I- 3´ , 5´-BamH1 / Xho1-3´
RE(A) $_{438-563}$	pGBKT 7	5´-BamH I / Sal I -3´	RE(A) $_{438-563}$	pACT 2	5´-EcoR I / Xho I- 3´ , 5´-BamH1 / Xho1-3´
RE(A) $_{1-563}$	pGEX-KG	5´-EcoR I / Xho I -3´	RE(A) $_{1-563}$	pACT 2	5´-EcoR I / Xho I- 3´ , 5´-EcoR1 / Xho1-3´
RE(A) $_{1-105(A1)}$	pMALc-2	5´-BamH I / Sal I -3´	RE(A) $_{1-105\ (A1)}$	pGEX-KG	5´-EcoR I / Xho I- 3´ , 5´-BamH1 / Xho1-3´
RE(A) $_{1-105(A1)}$	pGEX-KG	5´-EcoR I / Xho I -3´	RE(A) $_{1-105\ (A1)}$	pACT 2	5´-EcoR I / Xho I- 3´ , 5´-EcoR1 / Xho1-3´
RE(A) $_{438-563(SHORT,\ A2)}$	pGEX-KG	5´-EcoR I / Xho I -3´	RE(A) $_{438-563}$	pACT 2	5´-EcoR I / Xho I- 3´ , 5´-EcoR1 / Xho1-3´
RE(B) $_{669-869\ (NBD)}$	pACT 2	5´-EcoR I / Xho I -3´	RE(B) $_{669-869}$	pGEX-KG	5´-EcoR I / Xho I- 3´ , 5´-EcoR1 / Xho1-3´
RE(B) $_{669-869\ (NBD)}$	pGBKT 7	5´-Nco I / Sal I -3´	RE(B) $_{669-869}$	pACT 2	5´-EcoR I / Xho I- 3´ , 5´-Nco 1 / Xho1-3´
RE(A) $_{106-363(SHORT,\ A3)}$	pGBKT 7	5´-BamH I / Sal I -3´	RE(A) $_{106-363(A3)}$	pACT 2	5´-EcoR I / Xho I- 3´ , 5´-BamH1/ Xho1-3´
RE(B) $_{G\ 730\ A}$	pGBKT 7	5´-Nco I / Sal I -3´	RE(B) $_{G\ 730\ A}$	pGEX-KG	5´-Nco I / Xho I- 3´ , 5´-Nco 1 / Xho1-3´
RE(A) $_{106-363(A3)}$	pMALc-2	5´-BamH I / Sal I -3´	RE(A) $_{106-363(A3)}$	pGEX-KG	5´-EcoR I / Xho I- 3´ , 5´-BamH1/ Xho1-3´

2.1.8 Sequencing primers

Bold/underlined: first matching codon

Primer no:	Oligonucleotide sequence	Description
P 686 F	5´-GA**CTG**GTTCCAATTGACAAGC - 3´	5´ AOX 1
P 687 R	5´-**GCA**AATGGCATTCTGACATCC - 3´	3´ AOX 1
P 662 F	5´-**TCC**ACCTCCTACACGGTG- 3´	RIBEYE (A) Forward
P 688 F	5´-**GGA**TATAGCTCTCCTACCCCTTG- 3´	RIBEYE (A) Forward
P 722 R	5´-**TAA**TCTAGAATCAGGTTGTTC-3´	RIBEYE (A) Reverse

2.1.9 Enzyme, Proteins and molecular weight standards

Product	Company
Bovine serum albumin	Sigma
100 bp DNA-Leiter Roti® Mark	Roth
T4 DNA ligase	Roche Diagnostics
Low range protein standard Roti® Mark	Roth
Lysozyme	Roth
Restriction enzymes	New England Biolabs
Serum (for Cell Culture): FCS and NCS	PAA
Taq polymerase	peQLab

2.1.10 Reaction Kits

Kits	Company
Expand long template PCR system	Roche Diagnostics
Gel extraction kit	Qiagen
PCR kit	Sigma
PCR purification kit	Qiagen
Super Signal West Femto	PIERCE Biotechnology

2.1.11 Reagents and chemicals

Reagent/ Chemical	Company
Acetic acid	Roth
Agar-Agar	Roth
Agarose	peQLab
3-amino-1,2,4-trazole (ATZ)	Sigma
Ammonium peroxodisulfate	Roth
Ampicillin	Roth
Benzoyl peroxide	Sigma
Biotin	Calbiochem
Bovine Serum albumin (BSA)	Roth
Bradford protein assay reagent, 5X dye	Roth
Chloroquine	Sigma
Coomassie Brilliant Blue R 250	Roth
CSM-HIS	QBiogene
DEAE –Dextran hydrochloride	Fluka
Dimethylsulfoxide (DMSO)	Roth
Disodiumhydrogen phosphate	Roth
Dithiothreitol (DTT)	Sigma
dNTP´s PCR-grade	Roth
EDTA	Roth
Ethanol	Roth
Ethidiumbromide	Roth
Glucose	Roth
(Stable) Glutamine (200mM)	PAA
Glutathione-Sepharose beads	Fluka
Glutraldehyde (25%, EM grade)	Agar Scientific Ltd.
Glycerin	Roth
Glycid ether	Serva
Glycine	Roth
IPTG	MP Biomedicals
Isopropanol	Roth
Kanamycin	Roth
L-Glutathione reduced	Fluka
Lithium acetate	Sigma
LR-Gold resin (London resin)	London Resin Company Ltd.
Magnesium chloride	Roth
Magnesium chloride hexahydrate	Roth
Maltose	Sigma
MEM vitamins (100X)	PAA
β-Mercaptoethanol	Roth
Methanol	Roth
NAD^+ (Oxidised)	Sigma
NADH (Reduced)	Sigma
N,N-Dimethylformamide (DMF)	Roth
Non-essential amino acids (100X)	GIBCO
Non-fat dry milk powder	Supermarket
Nonidet P-40	Sigma
(n-Propyl gallate) NPG	Sigma
Osmium tetroxide	Serva
Paraformaldehyde	Roth
PCR buffer 10X	Sigma

Peptone	Roth
Phenylmethylsulfonylfluoride (PMSF)	Sigma
Ponceau-S	Roth
Potassium Chloride	Roth
Potassium Hydrogen phosphate	Roth
Potassium phosphate	Roth
Rotiphorese Gel 30 (29% acrylamide, 0.8% bisacrylamide)	Roth
Saccharose	MP Biomedicals
Sodium acetate	Roth
Sodium azide	Merck
Sodium bicarbonate (7.5% solution)	PAA
Sodium Carbonate	Merk
Sodium Chloride	VWR
Sodium dihydrogen phosphate	Fluka
Sodium Lauryl sulfate	Roth
Sorbitol	Roth
Streptomycin	Fluka
TEMED	Roth
TRIS	Roth
Triton X-100	Roth
Tryptone	Roth
Uranyl acetate	Merck
Whatmann filter paper	Roth
Yeast extract	MP Biomedicals
Yeast Nitrogen Base with ammonium sulfate without amino acids	FORMEDIUM
X-Gal (5-Bromo-4-Chloro-3-indoyl-β-galactoside)	MP Biomedicals

2.1.12 Buffer and media

Buffer	Media composition
Agarose gel electrophoresis buffer (TAE) 50X Stock	242.0 g Tris base 57.1 ml glacial acetic acid 100.0 ml of 0.5M EDTA pH 8.0 Made up to 1 liter with dd water
Acetate buffer (Plasmid preparation)	3M Potassium acetate, pH 5.5
Alkaline lysis solution 1 (Plasmid preparation)	50mM Tris-HCl pH8.0 10mM EDTA 100µg/ml RNase A
Alkaline lysis solution 2 (Plasmid preparation)	0.2N Sodium Hydroxide 1% (w/v) SDS
3-amino-1,2,4-trazole (ATZ)	10mM in double distilled water (filter sterilized)

Ampicillin	100mg/ml in dd water, filter sterilized
BEDS solution	10mM bicine-NaOH, pH 8.3 3% (v/v) ethylene glycol 5% (v/v) dimethyl sulfoxide (DMSO) 1 M sorbitol
Binding buffer	100 mM Tris-HCl , pH8.0 150 mM NaCl 1 mM EDTA 1% Triton X-100
Blocking buffer 1	0.5% Triton X-100 in PBS
Blocking buffer 2	100mM Tris-HCl , pH8.0 150 mM NaCl 1% Triton X-100
Blocking buffer for Immunocytochemistry	0.5% Bovine serum albumin 0.25% Triton X-100
Bradford-reagent Roti®- Quant	1:5 dilution in dd water
Breaking buffer (*Saccharomyces cerevisiae*)	100mM Tris-HCl , pH8.0 1 mM β-Mercaptoethanol 20% glycerol
Breaking buffer (*Pichia pastoris*)	50mM sodium phosphate pH 7.4 1mM EDTA 5% glycerol 1mM PMSF 100mM NaCl
BSA restriction digestion 10mg/ml (100X)	1:10 dilution dd water
Chloroquinone	10mM stock in sterile dd water
Coomassie stain	600.0ml Isopropanol 1560.0ml dd water 240.0ml acetic acid 0.6 grams Coomassie Brilliant Blue R 250
COS cells lysis buffer	100mM Tris-HCl , pH 7.9 150mM NaCl 1mM EDTA 1% Triton X-100
Coomassie destaining solution (Polyacrylamide gel electrophoresis)	100.0ml Acetic acid 300.0ml Ethanol Made up to 1 liter with dd water

Dulbecco's modified Eagle's medium / 10% FCS (DMEM) (for COS cells)	900 ml DMEM 100.0 ml FCS (per liter)
Dulbecco's modified Eagle's medium / 10%NCS / R28 additions (DMEM) (for R28 cells)	1.25 ml Glutamine (200mM) 5.0 ml MEM vitamins (100X) 5.0 ml Non-essential amino acids (100X) 25.0 ml Sodium bicarbonate (7.5% solution) 50.0 ml NCS Made up to 500 ml with DMEM
ECL (Chemiluminescence detection system)	1:1 obtained with ECL 1 & ECL 2 (ECL1) 5.0ml 1M Tris-HCl , pH 8.5 500µl luminol 220µl PCA Made up to 50ml with dd water (ECL2) 5.0ml 1 M Tris-HCl , pH 8.5 32µl Hydrogen peroxide (30%) Made up to 50.0 ml with dd water
IPTG	0.1 M in PBS
LB (Lennox L Broth Base)	20 grams LB 1 liter dd water
LB Agar-Agar plates	20.0 g LB 15.0 g Agar-Agar 1 liter dd water Desired antibiotic (100mg/ml) was added, if necessary
Lithium acetate/ Tris-EDTA/ β-Mercaptoethanol (For making of electocompetent *Saccharomyces cerevisiae*)	100mM Lithium acetate 10mM β-Mercaptoethanol 1X Tris-EDTA Made up to 20.0 ml with dd water
o-Nitrophenyl-β-D-galactoside (ONPG)	4mg/ml in Z-buffer
PBS (for cell culture)	Commercial preparation (PAA)
PBS (for molecular biology) (5X stock)	40.0 g sodium chloride 1.0 g potassium chloride 7. 2 g disodium hydrogen phosphate 1.2 g potassium phosphate Made up to 1 liter with dd water and adjusted to pH 7.4
Phenylmethylsulfonylfluoride (PMSF) Stock solution	40mM in 100% Isopropanol or DMSO
Ponceau-S stain	30.0 g Trichloroaceticacid 5.0 g Ponceau S 1 liter dd water

Rotigel 30% (Roth, commercial preparation)	(SDS-PAGE 10%) 1.27 ml 1M Tris pH 8.8 1.67 ml 30% Acrylamide 50µl SDS 1ml 50% glycerol 3.3µl TEMED 25µl 10%APS 1 ml dd water
SDS- PAGE electrophoresis buffer	14.4 g glycine 3.03 g Tris 1.0 g SDS
SDS-PAGE loading buffer 4X Concentration	4.0 ml β-Mercaptoethanol 2.0 ml glycerol 2.0 ml 1M Tris HCl , pH 7.0 4.0 mg Bromophenol blue 2.0 ml dd water
Sodium acetate	3M sodium acetate in dd water, pH 5.2 adjusted with glacial acetic acid Sterilized by autoclaving
STES buffer	0.2 M Tris-HCl , pH 7.6 0.5 M NaCl 0.1% SDS (w/v) 0.01M EDTA , Autoclaved
Streptomycine	10mg/ml in dd water, filter sterilized
Sodium Carbonate	1M in dd water
2X TBS	28.0 ml 5M NaCl 3.0 ml 1M KCl 1.0 ml 1M $CaCl_2$ 0.5 ml 1M $MgCl_2$ 4.5 ml 200mM Na_2PO_4, pH 7.4 20.0 ml 1M Tris-HCl , pH 7.9 Made up to 500ml with dd water, sterile filtered and stored at +4°C.
Tris-EDTA (TE)	10 mM Tris-HCl , pH 7.4 1 mM EDTA , pH 8.0
Western transfer buffer (5X)	15.125 g Tris 72.05 g glycine 1 liter methanol Made upto 5 liter with dd water
X-Gal (stock solution)	20mg/ml in N,N-Dimethylformamide (DMF)
Yeast two-hybrid (Filter lift cocktail)	20.0 ml Z-buffer 340µl X-Gal (20mg/ml stock) 54.0µl β-Mercaptoethanol

YPD medium	50.0 g YPD in 1 liter dd water
Z-buffer	16.1g sodium phosphate dibasic heptahydrate 5.5 g sodium dihydrogenphosphate monohydrate 0.75 g potassium Chloride 0.246 g magnesium Sulphate heptahydrate 2.7 ml β-Mercaptoethanol , made up to 1 liter with dd water, pH 7.0 and stored at + 4° C

2.1.13 Miscellaneous consumables/materials

Product	Company
Blotting paper	GE healthcare
Electroporation cuvettes, 0.1, 0.2 &0.4 cm gapped	peQLab
Reaction tubes 0.2, 0.6ml, 1.5ml & 2 ml	Greiner bio-one
Glass beads (0.5mm)	Roth
Disposable petri dishes (85mm)	VWR
Polypropylene falcon tubes 15 ml and 50 ml	Greiner bio-one
PVDF membranes	GE healthcare
QIAprep spin colums	Qiagen
Culture flasks	SCHOTT & GEN, Mainz

2.1.14 Laboratory hardware equipments

Product	Company
Adjustable pipettes	Eppendorff
Agarose gel electrophoresis system	Peq-lab
Axiovert 200, AxioCam MRm (Camera)	Zeiss
Autoclave	Tuttnauer Systec 5050ELCV
Biofuge fresco	Heraeus
Biofuge primo R	Heraeus
Biofuge stratos	Heraeus
Chemidoc XRS system	Bio-Rad
Electroporator ECM399	BTX
Fluorescence microscope Axiovert 200 M	Zeiss
Freezer -80°C	Heraeus
100-mesh gold grid	Plano, Wetzlar, Germany

Hot air oven	Heraeus
Incubator for Bacteria /Yeast	Memmert
Incubator for cell culture	Thermo
Laminar Flow Model 1,2	Holten
Magnetic strirrer (Complete Set)	Neolab
Multifuge S-R	Heraeus
Orbital Shaker	Edmund Bühler Labortechnik
PCR master cycler gradient	Eppendorff
pH meter	Inolab
Polyacrylamide Gel system	GE healthcare
Power pack for Gel system	GE healthcare
Rotary wheel	Neolab
Refrigerated Incubator Shaker Innova 4320	New Brunswick Scientific
Steri cycle CO_2 incubator	Thermo ELECTRON CORPORATION
Sterile filtration device	Millipore
Thermomixer compact	Eppendorff
Transmission Electron Microscope	FEI, Tecnai G ^{2}
Ultracut Microtome (UltraCut S)	Leica
Ultrasound bandelin sonoplus	Bandelin Electronic, Berlin
Vortex	VWR International
Western blot transfer apparatus	HOEFER SCIENTIFIC INSTRUMENTS
Weighing balance CP64	Sartorius

2.2 Methods

2.2.1 DNA related techniques and cloning

2.2.1.1 PCR amplification of DNA fragments

The Polymerase Chain Reaction (PCR) is a technique to specifically amplify a segment of DNA using two sequence-specific, complimentary primers to the sequence of target DNA. PCR process comprises of three steps: 1) denaturation of the double-stranded DNA template to separate strands by heating, 2) cooled to a temperature that allows the oligonucleotide primers to anneal to their target DNA sequence and 3) extension of the DNA strand with thermostable DNA polymerase (Chein *et. al*., 1976). The cycle of denaturation, annealing, and DNA synthesis were repeated (usually for 40 cycles). Because the products of one round of amplification serve as templates for the next, each successive cycle essentially doubles the amount of the desired DNA product. A 50µl final reaction mixture consisted of:

Tube 1	Tube 2
2µl (sterile double distilled H_20)	38 µl (sterile double distilled H_20)
1µl (Forward Primer OD 5 or 10 pmoles/µl)	5µl (10X PCR buffer containing 25mM $MgCl_2$)
1µl (Reverse Primer OD 5 or 10 pmoles/µl))	1µl (10mM dNTPs)
1µl (template DNA, 1-10ng)	1µl (Taq DNA polymerase 1U/µl)

The PCR reaction mixture was incubated in a thermocycler at the following cycle conditions: 95°C(2-5 min) - {[95 °C (30 sec) - 55 °C (30 sec) - 72 °C (1 min)] 8 cycles} - {[94 °C (30 sec) - 65 °C (30 sec) - 72 °C (1 min)] 40 cycles} - 72 °C (7 min) - 4°C (∞). The preferred annealing temperatures for oligonucleotides were between 54°C-56°C and extension time of ~1min/1kb fragment was used. The PCR was routinely performed with a ´hot start´ (Erlich *et al*., 1991) to minimize unspecific priming. Hot start was achieved by mixing the contents of tube1 to tube2 after heating to 95°C. Correct amplification and the purity of PCR products were analyzed by agarose gel electrophoresis and sequencing.

2.2.1.2 Genomic DNA isolation

Linear DNA can generate stable transformants of *Pichia pastoris* via homologous recombination between the transforming DNA and regions of homology within the genome (Cregg *et al*., 1985; Cregg *et al*., 1989). In order to find positive clones, yeast cell colonies (*Pichia pastoris)* were grown to isolate genomic DNA. The turbid yeast cultures were sedimented at 13,000 rpm at RT for 5 minutes and the pellet was resuspended in 100µl of STES buffer. Additionally, 0.5mm glass beads (Roth) were added till it reaches the lower meniscus. 100µl of equilibrated phenol: chloroform: isoamyl alcohol mixture was added and the contents were vortexed at maximum speed for 1 minute at RT. The upper aqueous layer was carefully collected in a fresh reaction tube after centrifugation at 13,000 rpm, RT for 5 minutes. Aqueous layer was precipitated using 3M sodium acetate (pH 5.2) and isopropanol for 1 hour at -20°C. The genomic DNA was sedimented at 13,000rpm, +4°C for 30 minutes, washed once with 1 ml of 70% ethanol and sedimented again. The pellet was air dried completely and resuspended in 20µl of sterile double-distilled water. The quality and quantity of isolated genomic DNA was checked on agarose gel electrophoresis and absorbance ratio at $A_{260\ nm}$: $A_{280\ nm}$. Genomic DNA was stored at -20°C till used.

2.2.1.3 Genomic PCR

Genomic PCR was performed to determine if the gene of interest has integrated into the *Pichia* genome. The isolated genomic DNA (see section 2.2.1.2) was used as a template. Amplification of the gene of interest was carried out either with 5´ *AOX 1* primer paired with the 3´ *AOX 1* primer or gene specific primers to affirm the integration of gene of interest in the *Pichia* genome (see material section). However, it will not provide information on the site of integration. Appropriate positive (plasmid) and negative (genomic DNA from empty GS115 cells) controls were employed in the same reaction. A 50µl final reaction mixture consisted of:

10X	5µl	Reaction buffer	(Sigma)
25mM	5µl	Magnesium Chloride	(Peq Lab)
10pmoles/µl	1µl	For. Primer	(Invtirogen Illumina)
10pmoles/µl	1µl	Rev. Primer	(Invtirogen Illumina)
100mM (25mM each)	dNTPs		(Karl Roth)
Isolated genomic DNA	1µg template		(Quantified)
1U/µl Taq polymerase	1µl	Red Taq	(Sigma)

The reaction mixture was incubated on a thermocycler device and the hot start procedure was followed which consists of following cycles: 95°C (1-4 min) - {[95 °C (30 sec) - 55 °C (30 sec) - 72 °C (1 min)] 40 cycles} - 72 °C (10 min) - 4°C (∞). The preferred annealing temperatures for oligonucleotides were between 54°C-56°C and extension time of ~1min/1kb fragment was used. Correct amplification and the purity of PCR products were analyzed by agarose gel electrophoresis.

2.2.1.4 DNA Electrophoresis

Agarose gel electrophoresis was used for separation, identification and purification of DNA fragments. DNA samples were mixed with 4X DNA loading buffer. TAE buffer was used as an electrolyte and the separation was done at 5 volts/cm. Depending upon the size of DNA molecule to be resolved, the agarose concentration varied between 0.8%-2.5% (w/v). By virtue of negative charge, DNA moves towards anode. Under constant voltage the migration speed of linear, double-stranded DNA in agarose gel is proportional to the logarithm of its molecular weight. Fluorescent dye, ethidium bromide (Sharp *et al*., 1973) which intercalates into the resolved DNA fragments was visualized by UV light. DNA fragment size (5,000bp-100bp), quality and quantity of DNA were determined upon comparison with known molecular weight standards (100 bp DNA-Leiter Roti® Mark, Roth).

2.2.1.5 Purification of DNA

After gel electrophoresis and identification of the respective bands under UV light, the respective bands were excised with a sharp scalpel. DNA/PCR products were purified by using a QIA®quick Gel Extraction Kit (QIAGEN) in accordance with the manufacturer's instructions. Excised gel was solubilized in 1 ml of QX1 buffer containing 5µl of vortexed QIAX silica gel beads. Additionally, 10µl of 3M Sodium acetate (pH 5.2) was added. The solubilization process was carried out at 55°C for 15 minutes on 600 rpm thermoshaker. DNA bound to silica gel was sedimented at 13,000 rpm, RT for 1 minute. Pellet was resuspended completely in 1ml of QX1 buffer and pelleted down. The pellet was washed twice with 1 ml of PE wash buffer. The pellet was air dried completely to remove traces of ethanol. The DNA from dried pellet was eluted with 30µl of preheated double-distilled water (heated at 55°C). Elution was carried out at 55°C, 600 rpm for 15 minutes on a thermoshaker. The eluted DNA was collected as supernatant after sedimentation at 13,000 rpm, RT for 1 minute.

2.2.1.6 Restriction digestion of DNA

Restriction endonuclease catalyzes a sequence-specific cleavage of double-stranded DNA, resulting in cohesive ends or blunt ends. Restriction digests were performed according to the manufacturer's instruction concerning buffer selection, addition of BSA etc. The amount of restriction enzyme, DNA, buffer, ionic concentrations, temperature and the duration of incubation varies and depends upon the specific application. For a typical 30µl reaction, consisting of 1µg DNA, 3µl of 10X recommended buffer, 3µl of 10X BSA and 0.25 units of restriction enzyme were used. Digested fragments were separated on agarose gel electrophoresis followed by purification using QIA®quick Gel Extraction Kit (QIAGEN).

2.2.1.7 Ligation of DNA fragment

The T4 DNA ligase reaction catalyzes the repair of single-stranded nicks in duplex DNA restriction fragments having either blunt or cohesive ends. Ligations were carried out overnight at room temperature or 14°C (unless, otherwise mentioned) using a 1:4 molar ratio of vector to insert. The 20µl reaction mixture consisted of 10-200ng total DNA mass, proportionate quantity of digested vector, 1µl of T4 DNA ligase (1U/µl) and 2µl of T4 DNA ligase buffer(10X).

2.2.1.8 Precipitation of DNA

DNA was precipitated and desalted with ethanol as described in Molecular cloning 2nd edition. For this purpose, about 1/10 volume of 0.3M sodium acetate (pH 5.2) and two volumes of isopropanol were added to the DNA solution for precipitation. The DNA solution was incubated at -20°C for 1 hour and sedimented at 13,000 rpm, +4°C for 15 minutes. The DNA pellet was carefully washed once with 1 ml of 70% ethanol and sedimented at 13,000 rpm, +4°C for 15 minutes. Pellet was air dried and resuspended in 10µl of 1mM Tris HCl, pH (8.5).

2.1.1.9 Preparation of electocompetent cells

All procedures were carried out in sterile and aseptic environment to prepare electrocompetent *Escherichia coli* cells (DH10B, BL21 and JC201). The following paragraphs also cover the methodology used for the preparation of electocompetent *Saccharomyces cerevisiae* and *Pichia pastoris* cells.

Glycerol stock of bacteria (*E.coli*) cells were freshly streaked on LB plate and incubated overnight at 37°C. Temperature sensitive JC201 (Coleman, 1990) bacterial strain was grown at 30°C. Overnight 50 ml LB preculture was grown at 37°C/30°C, 160 rpm after single colony innoculation. 500 ml of main culture (in 2 liters flask) was prepared with inoculation of 20 ml overnight grown preculture. Cells were grown at 37°C/30°C, 160 rpm shaking till an optical density (OD) between 0.9-1.0 was achieved at 600nm (OD_{600}). Further steps were carried out at +4°C. The culture was transferred to a sterile falcon tubes and centrifuged at 3,500rpm, +4°C for 15 minutes. The cell pellet was washed thrice in the sterile, ice-cold, double-distilled water and centrifuged at 3,500rpm, +4°C for 15 minutes. The final washed pellet (~4ml) was resuspended in 5 ml sterile, ice-cold 10% glycerol (made in sterile water). Aliquot's of (50µl) cell suspension was made in prechilled 1.5 ml reaction tube, and frozen in liquid nitrogen. Electrocompetent cells were stored at -80°C for long term storage. Using this method, we achieved 6-8 $x10^8$ transformants/µg DNA.

Saccharomyces cerevisiae strains (AH109 and Y187) were streaked on YPD plates, and incubated at 30°C till the colonies appear. The electrocompetent yeasts were prepared as described by (Helmuth *et al*., 2001). As a laboratory practice, gene of interest cloned in pGBKT 7 and pACT 2 were electroporated in AH109 and Y187 respectively. Preculture was set up by inoculating a single yeast colony in 10 ml YPD broth and was incubated at 30°C overnight at 160 rpm in an orbital shaker. Around 100 ml main culture (in 200 ml baffled flask) was set up, using 0.5 ml of overnight preculture and was incubated at 30°C overnight at 160 rpm in an orbital shaker. Cells were harvested by centrifuging at 2,000 rpm, +4°C for 5 minutes in a sterile 50 ml falcon tube. Cell pellet was washed twice with 20 ml of sterile, cold, double-distilled water and concentrated every time by centrifugation at 2,000 rpm, +4°C for 5 minutes. Cell pellets were resuspended in 20 ml of 1M Sorbitol and collected by centrifugation. Afterwards, the pellet was resuspended in 20 ml volume of incubation mixture (100 mM LiAc, 10 mM β-mercaptoethanol and 1X TE buffer) and was incubated at 30°C for 30 minutes with 250 rpm shaking. Cells were again pelleted at 2,000 rpm, +4°C for 3 minutes and washed once with 20ml of 1M Sorbitol. Electrocompetent cells pellet were resuspended in a minimal volume (200µl) of 1M Sorbitol. They were used directly for the electroporation.

Pichia pastoris GS115 (*his* 4) strain was used for the electrocompetent cell preparation. Glycerol stock was streaked on YPD plate and incubated at 30°C for 48 hrs. The single colony from the grown plate was used to inoculate 10ml preculture in a 50 ml baffled flask. Cells were grown overnight at 30°C in a shaking incubator at 220 rpm to obtain preculture. The preculture was diluted to an OD between 0.1-0.15 at 600nm (OD_{600}), and was further incubated till the absorbance ranges between 0.8-1.0 at 600 nm (OD_{600}) was achieved. The yeast cells were sedimented at 2,000 rpm, +4°C for 3 minutes and washed twice in cold sterile double-distilled water. The sedimented cell pellet was resuspended in 9 ml of BEDS solution (see material section), containing 1ml of (0.1M) DTT. The cells were incubated for 5 minutes at 30°C with 100 rpm shaking. Afterwards, the cells were sedimented at 2,000 rpm, +4°C for 5 minutes and resuspended in a 1 ml of BEDS solution without DTT. Competent cells were used directly for the electroporation.

2.2.1.10 Transformation of electrocompetent cells

Electroporation is a very efficient method of *E.coli* transformation (Chassy and Flickinger, 1987). In presence of high electric field, the transient membrane opening leads to uptake of DNA by electrocompetent bacteria. For electroporation, 1µl of DNA solution containing (10-100ng) DNA was added to approximately 50µl thawed (on ice) electrocompetent bacteria (DH10B, BL21 and JC201). Resuspended contents were transferred to a prechilled, 1mm electroporation cuvette and subjected to a pulse of strong electric field in the electroporator at 1,200V. Immediately after electroporation, the entire contents of the cuvette was recovered by the addition of sterile LB medium and incubated at 37°C, 160 rpm for 1 hour. The recovered cells were sedimented at 3,500 rpm, RT for 1 minute. The cell pellet was resuspended in (50µl) of residual LB, and spreaded on a LB agar petri dishes containing appropriate antibiotics for selection of transformants. The petri dishes were sealed, incubated overnight at 37°C/30°C (JC201) and observed for growth.

Electrocompetent *Saccharomyces cerevisiae* were also electroporated with the recombinant DNA as described (Helmuth *et al*., 2001). For this purpose, electocompetent yeast (120µl) was mixed with 1 µl of DNA and transferred to 0.4mm electroporation cuvette. Cells were pulsed at 1,800V and collected immediately with 1 ml YPD medium. Cells were incubated at 30°C for 1 hour with 600 rpm shaking. Transformants were selected on selection plates. These were identified by plating bait and prey

plasmid constructs on –W (lacking amino acid tryptophan) and –L (lacking amino acid leucine) selective plates, respectively. Transformants with bait plasmids convert the AH109 yeasts to tryptophan protrophy and enables them to grow on –W plates. Similarly Y187 transformed with prey plasmids grow on –L plates. Water treated cells and competent cells alone served as controls. The Petri dishes were sealed, incubated at 30°C for 48 hrs and observed for growth.

Pichia pastoris were transformed by electroporation as described by Lin-Cereghino *et al*., 2005. Electrocompetent cells (40µl) were mixed with 10µg (~4µl) of linearized DNA. The contents were transferred to prechilled 2.0mm cuvette and incubated for 5 minutes on ice. The cells were pulsed at 1,500 V. Soon after electroporation, the cuvette was added with cold sterile 1M sorbitol and cells were drawn in to a sterile reaction tubes. The cells were centrifuged at 2,000 rpm, +4°C for 5 minutes and cell pellet was resuspended in residual 50µl supernatant. Cells were spreaded on plates containing YNB+dextrose+biotin+sorbitol+(CSM-HIS) or MD (minimal dextrose). Non-electroporated, electocompetent cells and the cells transfected with sterile water served as a control to rule any contamination incurred during the procedure. The plates were sealed, incubated at 30°C for 48 hrs and observed for growth.

2.2.1.11 Plasmid DNA preparation (mini preparation and maxi preparation method)

Plasmid DNA was prepared with alkaline lysis (Birnboim and Doly 1979). For plasmid mini-preparation, single bacteria colony was inoculated in 5ml LB medium (in 15ml falcon tubes) containing appropriate antibiotics and incubated overnight at 37°C with 160 rpm shaking. Turbid cultures were centrifuged at 3,500 rpm, +4°C for 15 minutes and the pellet was resuspended in 250µl of alkaline lysis solution 1 (see material section). The contents were transferred to a fresh reaction tube, 250µl of alkaline lysis solution 2 (see material section) was added and gently mixed by inverting the tube. The contents incubated at room temperature for 5 minutes. The lysed cells were neutralized with 350µl of acetate buffer (see material section), and the preparation was centrifuged at 13,000 rpm, +4°C for 30 minutes. Clear supernatant was added with 750 µl of isopropanol and centrifuged at 13,000 rpm (radius max./min. 10.7/5.6[cm]), +4°C for 45 minutes to precipitate the DNA. The pellet (containing plasmid DNA) was carefully washed with 1ml of 70% ethanol and centrifuged at 13,000 rpm, +4°C for 20 minutes. The washed pellet was air dried and resuspended in 50µl of 1mM Tris-HCl

(pH 8.5). DNA was digested with restriction enzymes to screen positive clones. Confirmed positive clones were inoculated for large scale plasmid DNA preparation (maxi preparation).

Positive clones were inoculated in 100ml LB medium (in 200 ml conical flask) containing appropriate antibiotics for plasmid DNA maxi-preparation. Overnight incubation was carried out at 37°C, 160 rpm. The cells were centrifuged at 3,500 rpm, +4°C for 20 minutes. The pellet was resuspended in 5ml of buffer1 (see material section). The contents were transferred to a fresh falcon tube, 5ml of lysis buffer 2 (see material section) was added and incubated at room temperature for 15 minutes after gently inverting the tubes. The lysed cells were neutralized with the addition of 8ml of buffer 3 (see material section). The resuspension was centrifuged at 8,500 rpm, +4°C for 30 minutes. Clear supernatant was collected, and added with 20 ml of isopropanol. DNA was precipitated by centrifugation at 13,000 rpm, +4°C for 1 hour. The pellet obtained was carefully washed with 20ml of 70% ethanol and centrifuged at 13,000 rpm, +4°C for 30 minutes. The washed pellet was air dried and resuspended in 1ml of 1mM Tris-HCl (pH 8.5). The DNA was digested with restriction enzymes to consolidate the proper identity of the large scale DNA preparation.

2.1.1.12 DNA Sequencing

DNA was sequenced with dideoxynucleotide method (Sanger *et al*., 1977a). DNA sequences were commercially obtained form MWG Biotech (Martinstried, Germany).

2.2.1.13 Glycerol stocks

For long term storage, 0.85ml of a logarithmic-phase *E. coli* culture was added to 0.15 ml of sterile glycerol (100%).The reaction tubes were vortexed to ensure even distribution of the bacterial cells and glycerol. Cells were frozen in liquid nitrogen and stored at -80°C. Duplicates were stored frozen at any time.

2.2.2 Protein related techniques

2.2.2.1 SDS-PAGE

Polyacrylamide gel electrophoresis under denaturing conditions in the presence of SDS (Sodium Dodecyl Sulfate) separates the proteins inversely proportional to the logarithm of their molecular mass (Laemmli, 1970). The presence of SDS molecules, mask the intrinsic charge of protein and create a relatively uniform negative charge distribution caused by the sulfate group on SDS. The reducing agent, β-Mercaptoethanol aids in reducing the existing disulphide bonds and hence, in denaturing of the proteins. Protein samples were solubilized by boiling at 97°C for 3 minutes in 4X SDS loading buffer and the protein components were resolved electrophoretically. Stacking gel was discarded after electrophoresis, and the resolving gel was stained in Coomassie for 10 minutes at room temperature on a shaker. Proteins bands were visualized by the Coomassie brilliant blue (R-250) staining. The excess stain was removed with destaining solution (see material section) to visualize the protein bands.

2.2.2.2 Western Blotting

"Blotting" refers to the transfer of biological samples from a gel to a membrane and their subsequent detection on the surface of the membrane. The first step in the western blotting procedure is to separate the macromolecules using gel electrophoresis. Following electrophoresis, the separated molecules were electrotransferred onto a nitrocellulose membrane. The proteins were electroblotted from Polyacrylamide gels onto nitrocellulose membrane. Electroblotting was carried out at 50V at +4°C and the duration was dependent on the size of protein to be transferred and the applied potential difference.The nitrocellulose membranes after blotting were stained with Ponceau-S and subsequently destained with PBS. The membrane was blocked for 1 hour at room temperature with 5% (w/v) non-fat dry milk (in PBS), on a shaker. For probing, the membrane was incubated overnight with primary antibody (depending upon antigen to be detected) at +4°C, on a shaker in appropriate dilutions (according to the manufacturer's instructions, see material section). The non-specifically membrane bound antibody was removed by washing thrice in PBS for 10 minutes each at room temperature. Secondary antibody incubation was carried out at room temperature for 1 hour on a shaker in appropriate dilutions (according to the manufacturer's instructions, see material section). Further, non-specifically membrane bound antibody was removed by washing thrice in PBS for 10 minutes. The

membrane was developed using ECL (see material section), the chemiluminiscence signals were acquired using Quantity One (BioRad) software.

2.2.2.3 Stripping of nitrocellulose membranes

Nitrocellulose membranes were reprobed with the different antibody for multiple purposes. The earlier signals were removed by stripping the blot with boiled 1% SDS (in PBS) in presence of 1ml of β-Mercaptoethanol. The incubation was carried out at room temperature on a shaker for 1 hour. The excess stripping solution was removed by washing with PBS at room temperature for 10 minutes. The membrane was blocked as stated earlier (see section 2.2.2.2) and reprobed with the desired antibodies and the signals were detected as mentioned earlier (see section 2.2.2.2).

2.2.2.4 Determination of protein concentrations

In the acidic environment of the reagent, protein binds to the Coomassie dye. This results in a spectral shift from the reddish/brown form of the dye (absorbance at 465nm) to the blue form of the dye (absorbance maximum at 595 nm). Therefore, the absorbance at 595 nm gives fairly linear concentration dependence for most soluble proteins. The standard calibration curve was routinely obtained by using duplicates of a known concentration of BSA, and the unknown concentration was determined (Bradford, 1976).

2.2.2.5 Recombinant Protein Expression

Recombinant proteins either GST or MBP tagged were routinely expressed in BL21 (DE3). On the other hand, RIBEYE (A)-domain as a full-length protein was difficult to express in BL21 (DE3) because of the presence of many proline, arginine and serine residues in amino acid composition. However, LPAAT-deficient JC201 bacteria (Coleman, 1990) was found as a useful strain to express RIBEYE(A)-construct. Bacterial fusion proteins were expressed in baffled shake flasks. For this purpose, isolated single colonies were inoculated, grown overnight in 50ml (in 200ml flask) LB medium containing 100µl ampicillin (100mg/ml) at 37°C, 220 rpm to obtain precultures. However, JC201 precultures were grown in 100µl ampicillin (100mg/ml) and 500µl streptomycin (10mg/ml)) at 30°C. Main cultures were prepared using 400 ml of LB containing 800µl of ampicillin with addition of 10ml overnight grown preculture. The cells were grown at 37°C/30°C (JC201), 220 rpm till the

starting absorbance of 0.1 reaches to 1.0 at 600 nm (OD_{600}). Cultures were induced with the addition of 400µl (100mM) IPTG for 4 hours at 30°C, 220 rpm. Cells were harvested by centrifugation at 3,500 rpm, +4°C for 30 minutes and washed thrice by resuspending in 50 ml cold PBS.

COS7 cells were used as second source for heterologous protein expression. On day 0, cells were splitted and plated at density of 3×10^5 on 60mm dishes, in 3 ml DMEM medium (containing 10% FCS). After 48 hours of growth, COS7 cells were transfected with the eukaryotic expression construct (either EGFP- or mRFP tagged) indicated in the experiments, using DEAE Dextran method (Ishtchenko *et al*., 1995). Cells were washed twice with 5 ml of PBS and incubated with 3.3ml transfection cocktail (1650µl of 2X TBS, 1257µl of sterile double distilled water, 330µl of DEAE Dextran and 10µl of DNA) for 30 minutes at 37°C, 5% CO_2. Transfection cocktail was aspirated and incubated with fresh 5 ml medium containing 5µl of chloroquine (10mM stock) for 3 hours at 37°C, 5% CO_2. Chloroquine containing medium was aspirated and cells were washed twice with 5 ml of PBS. Cells were shocked for 2 minutes at room temperature with 2ml of 20% glycerol (prepared in DMEM medium). Glycerol containing medium was aspirated and cells were washed twice gently with 5 ml of PBS. Fresh DMEM medium (5ml) was added and cells were incubated for 48-60 hours at 37°C with 5% CO_2.

Recombinant protein was also expressed in *Pichia pastoris*. Methylotrophic yeast, *Pichia pastoris* is an important source for the production of recombinant proteins, particularly for proteins which cannot be appropriately expressed in prokaryotic systems (Cregg *et* al., 2000; Barr *et al*., 1992; Brierley *et, al*., 1994; Clare *et al*., 1991b; Grinna *et al*., 1989). As a eukaryote, *Pichia pastoris* has many of the advantages of higher eukaryotic expression systems such as protein processing, protein folding and post-translational modification, while being as easy to manipulate as *E.coli* or *Saccharomyces cerevisiae* (Cregg *et al*., 2000; Tschopp *et al*., 1987b). It is faster, easier, and less expensive to use than other eukaryotic expression system such as baculovirus or mammalian tissue culture, and generally give higher expression levels. As yeast, it shares the advantages of molecular and genetic manipulations with *Saccharomyces*, and it has the added advantage of 10-to100-fold higher heterologous protein expression levels. These features make *Pichia* very useful as a protein expression system.

The majority of heterologous protein production in *Pichia pastoris* is based on the fact that enzymes required for the metabolism of methanol is only present when cells were grown on methanol (Egli *et al*., 1980). The enzyme alcohol oxidase (AOX) catalyzes the first step in the methanol utilization pathway, using molecular oxygen it oxidises methanol to formaldehyde and hydrogen peroxide. AOX is strategically sequestered within the peroxisome along with catalase, which degrades accumulated hydrogen peroxide (toxic by-product) to oxygen and water. Alcohol oxidase has a poor affinity for the oxygen, and *Pichia pastoris* compensates by generating large amounts of the enzyme (Cereghino *et al*., 2001a). The promotor regulating the production of alcohol oxidase is the one used to drive heterologous protein expression in *Pichia pastoris.* There are two genes that encode alcohol oxidase in *P. pastoris*: AOX1 and AOX2; AOX1 is responsible for a vast majority of alcohol oxidase activity in the cell and is transcriptionally regulated. Loss of *AOX1* gene, and thus a loss of most of the cell's alcohol oxidase activity, results in a strain that is phenotypically Mut^s (Methanol utilization slow). This results in a reduction in the cell's ability to metabolize methanol. These cells therefore, exhibit poor growth on methanol medium. On the other hand, Mut^+ (Methanol utilization plus) refers to the wild type ability of strains to metabolize methanol as the sole carbon source (Cregg *et. al*., 1993).

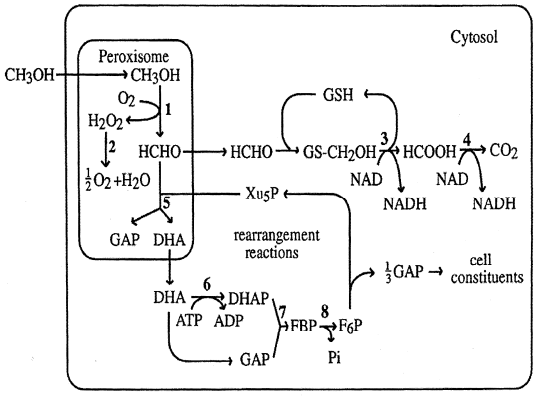

Figure 13. The methanol pathway in *Pichia pastoris*.

1) Alcohol oxidase; **2)** catalase; **3)** formaldehyde dehydrogenase; **4)** formate dehydrogenase; **5)** dihydroxyacetone synthase (DHAS); **6)** dihydroxyacetone kinase; **7)** fructose 1,6- bisphosphate aldolase; **8)** fructose 1,6-bisphospatase. The enzyme alcohol oxidase (AOX) catalyzes the first step generating formaldehyde and hydrogen peroxide. A portion of the formaldehyde generated by AOX leaves the peroxisomes and is further oxidized to formate and carbon dioxide by two cytoplasmic dehydrogenases, reactions that are a source of energy for cells growing on methanol. Two of the methanol pathway enzymes, AOX and DHAS, are present in high levels in cells grown on methanol but are not detectable in cells grown on most other carbon sources (e.g., glucose, glycerol, or ethanol) (Lin-Cereghino *et. al*., 2000).

P.pastoris exhibits a propensity for the homologous recombination between genomic and artificially introduced DNAs Fig.14-A,B&C. The strategy involves the cloning of gene of interest in the

expression vector, introduction of the expression vector into the *P.pastoris* genome, screening and expression of the recombinants.

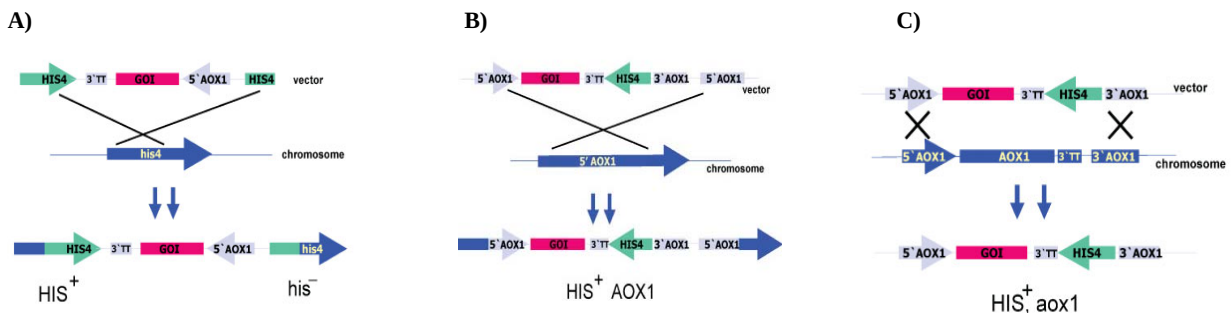

Figure 14. Recombination and integration in *Pichia pastoris* genome.

A) Integration into the *Pichia pastoris* genome, by gene insertion event at *his*4. In GS115, gene insertion events at the *his*4 locus arise from a single crossover event between the *his*4 locus in the chromosome and the *HIS* 4 gene on the vector. This results in the insertion of one or more copies of the vector at *his*4 locus. This is achieved by linearizing the recombinant vector at a restriction enzyme site located in *HIS*4 gene. **B)** Integration into the *Pichia pastoris* genome, by gene insertion event at *AOX* 1. This event arises from a single crossover event between the loci and any of the three *AOX* 1 regions on the vector: the *AOX* 1 promotor, the *AOX* 1 transcription termination region (TT), or sequences even further downstream of the *AOX* 1(3´ *AOX* 1). This is achieved by linearizing the recombinant vector at a restriction enzyme site located in the 5´ or 3´ *AOX* 1 regions. **C)** Integration into the *Pichia pastoris* genome, by gene replacement. These events arises as a result of double crossover between the *AOX* 1 promotor and 3´ *AOX* 1 regions of the vector and genome. This results is a complete removal of the *AOX* 1 coding region (i.e. gene replacement). However, these events are less likely to happen than single crossover events. (Daly *et. al*., 2005).

Optimal expression conditions are dependent on the characteristics of the protein being expressed. The conditions such as media, proteases, aeration, kinetics of growth temperature and shaking conditions determines the overall success rate. Growth kinetics of Mut^+ and Mut^s strains were similar on YPD or glycerol media. However, Mut^+ will grow faster than Mut^s when both were grown on methanol. The Mut^+ strains are less likely to become poisoned by methanol than Mut^s but are more likely to become oxygen limited (Romanos *et al*., 1995). Recombinant proteins can either be secreted or intracellularly expressed based on preferences (Barr *et al*., 1992; Scorer *et al*., 1993).

RIBEYE (A)-domain was intracellularly expressed in *Pichia pastoris*. In pilot experiment, with five positive clones the optimal conditions for the expression of protein was determined. The glycerol stocks of positive clones were streaked on the YNB+DEXTROSE+BIOTIN+SORBITOL+(CSM-HIS) containing plates and incubated at 30°C. All protein expression was carried out in baffled flask at 28°C - 30°C, in a shaking incubator at 220-250 rpm. BMGY/BMMY (Buffered Glycerol or Methanol) -complex medium were used for the expression and was about 10-30% of the total flask volume. A single colony was inoculated in 30 ml BMGY medium, in a 200ml baffled flask. The flasks were

covered with the loose fitting aluminum foil. Culture was incubated in a shaker at 30° C, 220 rpm, for 16-18 hrs till the OD range between 4-6 was achieved at 600nm (OD_{600}). The cells were centrifuged at 2,000 rpm, +4° C for 2 minutes, washed once with the cold PBS and sedimented as mentioned above. Washed cells were diluted in a BMMY medium, to a starting OD of 0.1 at 600nm (OD_{600}) for methanol induction. The culture was incubated further at 30° C, 220 rpm for 36 hours. Methanol was replaced after every 24 hours to a final volume of 1% (v/v). Further 1 ml aliquots of the induced culture were collected at time points such as 0hr, 6 hrs, 12hrs, 18hrs, 24hrs and 36hrs. The aliquots were centrifuged to separate the pellet and supernatant fractions. Both were separately stored at -86° C till they were analyzed. These conditions were applied on large scale culture to upscale the yield. The expression of protein was later deduced by western blot, using RIBEYE (A)-domain specific antibody.

2.2.2.6 Purification of Recombinant Protein

The expressed recombinant proteins were purified, before being used for experiments such as protein pull-downs and ribbon pull-down assays. *Escherichia coli* expressed GST and MBP-tagged fusion proteins were purified on the basis of their affinity towards glutathione-agarose beads and amylose resin respectively. The 15ml cell resuspension (in PBS) was incubated with 500µl of lysozyme (10mg/ml) for 1 hour at +4°C on a shaker and subsequently sonicated for 20 seconds, 4 rounds with in between 20 seconds interval. Cell free supernatant was obtained by 2 rounds of centrifugation at 13,000 rpm, +4°C for 1 hour. Glutathione-agarose beads (200µl) or amylose resin (200µl) was washed thrice in 50 ml of cold PBS solution and sedimented at 1,500 rpm, +4°C for 1 minute. The cell free supernatant from earlier step was incubated overnight with the beads/resin. Non-specific binding was reduced by washing bound protein (to beads/resin) six times with cold PBS. The washings were carried out for 30 minutes at +4°C on shaker and beads/resin were sedimented at 1,500 rpm for 1 minute at +4°C.

Recombinant protein expressed in COS 7 cells were visualized for expression patters, distribution of protein and transfection efficiency. The cells were afterwards processed for the extraction of recombinant protein. The petri dishes were placed on ice, and cells were scrapped down with policeman rubber scrapper. The cells were sedimented at 3,500 rpm (radius max./min. 12.4/6.0[cm]), +4° C for 20 minutes. Cells were washed once with cold PBS to remove serum proteins and were re-

sedimented. Recombinant protein was extracted by resuspending the cells in 300µl (for 3 petri dishes) of lysis buffer (100mM Tris-HCI (pH 8.0), 150 NaCl, 1mM EDTA, 1% Triton X-100). Additionally, 0.5mm glass beads were added, to the half of volume of the reaction tube. Cells were cracked with eight rounds of vigorous vortexing for 30 seconds, with an in between interval of 30 seconds. The supernatant was collected by centrifugation at 13,000 rpm, +4°C for 15 minutes and was used for assays.

Pichia pastoris transformed with RIBEYE(A)-pPIC3.5K was induced for 36 hours and processed for protein extraction. Cells were resuspended in 890µl of ice cold breaking buffer (50mM sodium phosphate (pH 7.4), 1mM EDTA, 5% glycerol, 1mM PMSF & 100mM NaCl). Proteins were released by mechanical cracking. The 0.5mm glass beads were filled to half of the reaction tube, and the cracking was performed at +4°C using high speed vortex. The cells were cracked 25 times for a period of 30 seconds, between vortexing the cells were chilled on ice for 30 seconds. The lysate was collected by blue pipette tip in a chilled reaction tube. The lysate was precleared from cell debris by centrifugation at 13,000 rpm, +4°C for 1 hour.

2.2.3 Protein - Protein Interaction

2.2.3.1 Yeast Two-Hybrid assay

Yeast two-hybrid is an important system to analyze and characterize protein-protein interactions (Fields *et al*., 1989). In a GAL4-based two-hybrid assay, a bait gene is expressed as a fusion to the GAL4 DNA-binding domain (DNA-BD), while another gene or cDNA is expressed as a fusion to the GAL4-activation domain (AD). Gal4 protein is a yeast transcription factor that normally controls genes responsible for galactose metabolism. Each Gal4- responsive gene contains a target site called an Upstream Activating Sequence, or UAS. When Gal4 binds the UAS, transcription is activated from a downstream promoter. By linking the GAL UAS with other metabolic genes (e.g., *ADE2, HIS3, MEL1* and *lacZ*) and by eliminating the wild-type GAL4 gene, yeast strains that change phenotype when Gal4 is activated are developed.

The following schematic drawing elucidates principle of the Gal4-based Yeast two-hybrid (YTH) system.

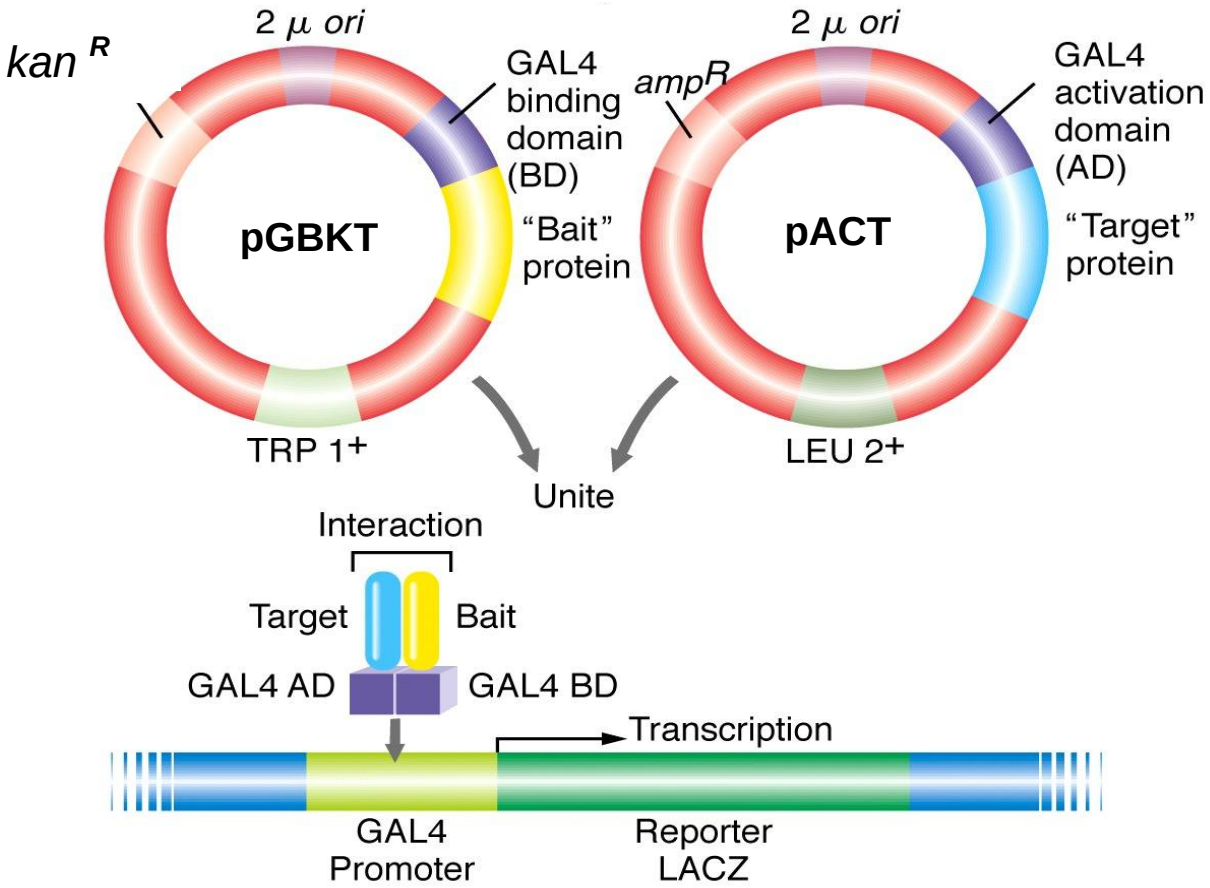

Figure 15. Principle of the Yeast two-hybrid system.

Two physically discrete modular domains of eukaryotic transcriptional activators were constituted by the (DNA-BD) (pGBKT7) and the (AD) activation domain (pACT2). The domains acts as independent modules: neither alone can activate transcription, but each domain continues to function when fused to other proteins. In the above case, protein of interest is expressed as a fusion to the DNA-BD. Another protein, or a cDNA library, is expressed as a fusion to the AD. If two proteins interact, the DNA-BD and AD are brought into close proximity and activate transcription of the reporter gene.

In a Yeast two-hybrid assay, the Gal4 DNA-binding (DNA-BD) and activation domains (AD)-expressed as fusions-are joined through a protein-protein interaction. Although the DNA- BD can bind UAS, it cannot activate the transcription by itself. Transcription is activated only when the other half of the protein, the Gal4 AD, joins the DNA-BD at the UAS. In the BD matchmaker systems, the AD consists of amino acids 768-881 of the Gal4 protein; the DNA-BD, amino acids 1-147. In addition, because two-hybrid is performed *in vivo*, the proteins are more likely to be in their native conformation, which may lead to increased sensitivity and accuracy of detection. When bait and library fusion proteins interact, the DNA-BD and AD are brought in proximity, thus activating transcription of four reporter genes. This will help yeast (*Saccharomyces cerevisiae)* to grow on

-ALWH plates (lacking Adenine, Leucine, Tryptophan and Histidine). The stringency was further increased by addition of 10 mM ATZ (3-amino-1, 2, 4-trazole). This system can be used to identify protein interactions, and to map interaction sites.

2.2.3.1.1 Yeast mating

A single yeast colony was picked from both –L and –W selective dropout plates. Colonies were resuspended in 1 ml YPD broth (in 2 ml reaction tubes). Selective dropout plates, –L and –W plates confers growth to the leucine synthesizing (pACT 2) and tryptophan synthesizing (pGBKT 7) colonies. The resuspended yeasts were incubated for 5 hours at 30°C on thermoshaker at 600 rpm. The mated yeasts were centrifuged at 3,000 rpm, +4°C for 5 minutes at the end of incubation. Yeast cell pellet was resuspended in 200 µl of residual YPD broth, after discarding most of the supernatant. 200µl of the above suspension was spreaded (100µl each) on –LW and –ALWH plates. Dropout –ALWH plates were spreaded with 100µl ATZ (10mM stock) prior to use. The plates are incubated at 30°C and observed for growth. Dropout –LW plate confers growth, when both plasmids are present in a same cell (diploid) and indicates mating efficiency. Growth on –ALWH plates indicates protein-protein interaction. For the matings pSE111 and pSE1112 (Bai and Elledge, 1996) as well as the empty bait and prey vectors were used as negative controls.

2.2.3.1.2 β-Galactosidase assays

In yeast two-hybrid system host strains, integrated nutritional reporter genes provide an elegant and sensitive growth selection. The *MATa* reporter strain AH109 contains three reporters - *HIS3, ADE2, and MEL1 (or lacZ)* under the control of upstream activating sequences (UASs) and TATA boxes. These promoters yield strong and specific responses to GAL 4 may be used as mating partner for the MATα Y187. When two transformants cultures are mated to each other, diploid cells are formed which contain four reporter genes: *HIS3, ADE2*, *MEL1,* and *lacZ*. The GAL 4DNA-BD binds to the GAL-UAS and, the AD is brought into proximity to the reporter genes promoter, there by activating transcription and permitting growth on selection medium and expression of α-galactosidase (*MEL1* product) and β-galactosidase (*lacZ* product) providing a qualitative assessment (filter lift) of protein-protein interaction. Quantitatively, the interaction is measured by β-galactosidase liquid assay as described (Wang *et al*., 1997; Stahl *et al*., 1999).

For qualitative β-galactosidase filter test, yeast cells were streaked on –LW/-ALWH plates and incubated for 48-60 hours at 30°C. Whatmann filter paper cut to proportionate size, placed onto the yeast colonies to make a replica of the yeast on the filter paper. The impressions of summary plate on whatman filter paper were probed in β-galactosidase filter test. The yeast cells were cracked by dipping filter paper bound to colonies, in liquid nitrogen for 30 sec. and thawed for 5 seconds. The liquid nitrogen cracked filter paper (containing the replica of cells) was placed gently on a layer of filters, earlier soaked in an incubation solution (10 ml ´Z´ buffer + 170 µl X-gal + 27µl β-Mercaptoethanol). Reaction was carried out at room temperature in a petridish with a covered lid. Filter lifts for the positive yeast clones were observed for the appearance of blue color in contrast to the corresponding controls. The time was recorded and the reaction was terminated by drying the filters at RT.

β-galactosidase liquid assay was performed as described by (Schneider *et al*., 1996). 5ml cell cultures were grown at 30°C, 600rpm in –LW / -ALWH medium to a density of 1×10^7 – 2×10^7 cells/ml. Cells were harvested by centrifugation at 2,000 rpm, +4°C for 5 minutes and all further steps were carried out at +4°C . Yeast cell pellet was resuspended in 250µl of breaking buffer (100mM Tris-HCl (pH 8.0), 1 mM β-Mercaptoethanol and 20% glycerol), and 0.5mm glass beads along with 12.5µl of PMSF (40mM) was added to the resuspension. Yeast cells were cracked by six rounds of vortex of 15 seconds duration, at top speed (10 seconds keeping cap of reaction tube on upside up position, 5 seconds in upside down position with 30 seconds in between interval). The cracked yeast cells were mixed with additional 250µl of breaking buffer and the whole liquid extract was aspirated using 1ml blue pipette tip. Extract was cleared by centrifugation at 13,000 rpm, +4°C for 20 minutes and used for assays. For assays, 100µl of precleared extract was mixed with 900µl of `Z buffer´ and incubated at 28°C for 5 minutes. Reaction was initiated with the addition of 200µl of ONPG (4mg/ml). Incubation was carried out at 28°C till the mixture acquires a pale yellow color. Reaction was terminated with addition of 0.5ml of Na_2CO_3 (1M). Reaction starting and termination times were recorded, and the optical density at 420 nm was measured. Protein concentration was estimated by Bradford method using BSA standards prepared in breaking buffer.

Specific activity was calculated according the formula:

$$(OD_{420} \times 1.7) / (0.0045 \times \text{protein concentration} \times \text{extract volume} \times \text{time})$$

OD_{420} is the optical density of the product, o-nitrophenol, at 420nm. The factor 1.7 corrects the reaction volume. The factor 0.0045 is the optical density of a 1nmole/ml solution of o-nitrophenol. Protein concentration is expressed in mg/ml. Extract volume is given in (ml), time is expressed in minutes. Specific activity is expressed as nmoles/minute/mg protein.

2.2.3.2 Protein pull-down assays

The Yeast two-hybrid findings were confirmed independently by protein pull-down assays. Recombinant proteins were expressed in bacteria, COS cells and *Pichia pastoris* host system as mentioned in the section (2.2.2.5). The purification steps were described in section (2.2.2.6).The protein pull-down procedure is described below.

2.2.3.2.1 Recombinant protein pull-downs (expressed in bacteria)

Following combination of bait and prey protein were studied in protein pull-down assays. (A1-GST; A1-MBP), (A1-GST; A2-MBP), (A2-GST; A2-MBP), (B-GST; A2-MBP), (full length A-GST; full length A-MBP) & (full length A-GST; full length B-MBP). GST fused proteins (bait) were immobilized on glutathione-sepharose beads, and was used to fish out eluted MBP fused prey protein if not denoted otherwise. Protein concentration was determined at 595 nm using the Bradford procedure (Bradford, 1951). Bait and prey proteins for experimentation were used in equimolar ratio along with respective controls. Eluates were precleared with 10µl of glutathione-agarose beads (per 1ml eluate) for 1 hour at +4°C on a rotary wheel. The bait proteins were either blocked in blocking buffer 1 (0.5% Triton X-100 in PBS or blocking buffer 2 (150mM NaCl, 100mM Tris-HCl (pH 8.0) & 1% Triton X-100) for 1 hour at +4°C on a rotary wheel. All of the studied bait and prey proteins, except (full length A-GST; full length A-MBP) were incubated in blocking buffer 1 (0.5% Triton X-100 in PBS), at +4°C for 12 hours by rotation in a 500µl reaction volume and washed subsequently in excess of corresponding blocking buffer.

In case of, (full length A-GST; full length B-MBP) pull-down, the blocking was performed in blocking buffer 2 containing (150mM NaCl, 100mM Tris-HCl (pH 8.0) & 1% Triton X-100). Eluates were precleared with 10µl of amylose resin (per 1ml eluate) for 1 hour at +4°C on a rotary wheel.

After blocking, bait (MBP-fused protein) and prey proteins (GST-fused protein) were further incubated in blocking buffer 2, for 3 hours at +4°C by rotation in a 500µl reaction volume. Later, the beads were washed with the corresponding blocking buffer. The washed beads were boiled in 20 µl of 4X SDS sample buffer. Proteins were resolved on SDS-PAGE and processed for western blotting as described in section 2.2.2.2.

2.2.3.2.2 Recombinant protein pull-downs (expressed in COS cells)

The tubby-domain of TULP1 was heterologously expressed in COS 7 cells as described in section (2.2.2.5). After 48 hours of transfection, the efficiency was confirmed by microscopic inspection of EGFP-tagged recombinant protein. The cells were afterwards processed for the extraction of recombinant protein as described in section (2.2.2.6). The precleared supernatant in equal volumes was incubated with an experimental and control immobilized bait RIBEYE(A)-GST and GST respectively, in an (3:1) equimolar ratio. The incubation was carried out for 12 hours on a rotary wheel at +4°C. The pellet was sedimented at 13,000 rpm, +4°C for 1 minute and washed with excess of corresponding lysis buffer. The beads were boiled in 20 µl of 4X sample buffer. Proteins were resolved on SDS-PAGE and processed for western blotting as described in section (2.2.2.2).

2.2.3.2.3 Recombinant protein pull-downs (expressed in Pichia pastoris)

Untagged RIBEYE (A)-domain was expressed intracellularly in *Pichia pastoris* and the protein was extracted as described in section 2.2.2.5 and 2.2.2.6 respectively. The precleared cell lysate was divided in two aliquots of 300µl volume. It was incubated for 5 hours in cold room on a rotary wheel, with the immobilized RIBEYE(A)FL as GST and GST alone (in equimolar ratio of 3:1 respectively). After incubation, samples were centrifuged and the pellets were washed and resolved using SDS-PAGE as described in section 2.2.2.1. The western blotting was performed as described in section 2.2.2.2. The membrane was probed with antibody against RIBEYE (A)-domain. Afterwards, the membrane was stripped as described in section 2.2.2.3., and incubated with antibody against GST to check equal loading of bait proteins.

2.2.3.3 Synaptic ribbons based pull-downs

Synaptic ribbons were isolated as described earlier (Schmitz *et. al*., 1996). Synaptic ribbons were used as bait in the pull-down experiments. These heavy organelles can be sedimented by low centrifugation such as 5,000 rpm at +4° C for 3 minutes. Eluted proteins (prey) were used in an equimolar ratio and incubated with the equal amount of the synaptic ribbons (180µg). The eluted fusion protein (prey) stays in supernatant, if not bound to the synaptic ribbons. A 500µl of reaction volume was constituted in blocking buffer 1 comprises of 0.5% Triton X-100 (in PBS) for 4 hours in a cold room on a rotary wheel. Thereafter, reaction tubes were centrifuged at 13,000 rpm, +4°C for 1minute and the ribbon pellet was washed with excess of corresponding blocking buffer. The samples were boiled at 97°C for 3 minutes. Proteins were resolved on 10% SDS-PAGE, and processed for western blotting as described in section 2.2.2.2. The membrane was probed with Anti-GST Antibody. Afterwards, the membrane was stripped as described in section 2.2.2.3, and incubated with Anti-RIBEYE (U_{2656}) antibody to check the equal ribbon fraction loading.

2.2.3.4 Morphological analysis of protein-protein interactions

2.2.3.4.1 Light microscopic analyses

Transfection of COS 7 cells was done with the DEAE-dextran method, as described by Ishtchenko *et al*., 1995 in section 2.2.2.5. After transfection, the cells were briefly washed with PBS to remove serum proteins. Cells were fixed with 1% paraformaldehyde (PFA) for 30 minutes at RT. Analysis of transfected cells was done by direct fluorescence if EGFP- or mRFP-tagged proteins were used. If not visible by EGFP or mRFP expression and localization of heterologously expressed protein was determined by indirect immunofluorescence microscopy.

Transfection of R28 cells were done with perfectin, according to the manufacturer's instructions (peQLab, Germany). R28 cells were grown in medium containing DMEM (10%NCS, see material section). 48 hours after transfection the cells were serum starved for 30 minutes. The cells were transfected with 2µg DNA (Perfectin kit). The transfection mixture (1ml for 3 cm diameter dishes) was retained in the petri dishes for 4 hours. Afterwards, the cells were washed with PBS and were grown in R28 medium and incubated at 37°C, 5% CO_2. The cells were fixed and visualized by indirect

immunofluorescence microscopy. Indirect immunofluorescence microscopy on cells was performed largely as previously described (Schmitz *et al*., 1996; von Kriegstein *et al*., 1999). Cells were fixed (1% PFA for 30 minutes) afterwards incubated with blocking buffer (0.5% bovine serum albumin, 0.25 % Triton X-100) for 1 hour at room temperature. The primary antibodies diluted in blocking buffer (see material sections) were added, and incubated overnight at +4°C. Thereafter, cells were washed multiple times with blocking buffer, secondary antibody (see material sections) was added (Cy2/Cy3-conjugated goat-anti-rabbit antibodies for polyclonal rabbit primary antibodies, or Cy2/Cy3 conjugated goat-anti-mouse antibodies for monoclonal mouse primary antibodies prepared in blocking buffer) and incubated for 1hour at RT. After subsequent washes with blocking buffer, cells were mounted in 60% glycerol in PBS that contained 1.5% n-propyl gallate in order to retard photobleaching. Controls were only incubated with secondary antibody. Samples were analysed and documented with an Axiovert 200M microscope equipped with respective filter blocks. The fluorescence images were documented with an AxioCam MRm camera (Zeiss).

2.2.3.4.2 Conventional transmission electron microscopy

Conventional transmission electron microscopy was performed largely as previously described (Schmitz and Drenckhahn, 1993). Transfected cells were fixed with (2.5% glutraldehyde+1%PFA) for overnight after brief washings with PBS. The fixed samples after several washes with PBS were post-fixed with 1% OsO_4 in H_20 (w/v) for 1 hour at RT. The samples were block-contrasted with 2% uranyl acetate in H_20 (w/v) for 3 hours at $+4^{O}C$, dehydrated with an ascending ethanol concentration series, and embedded in a resin mixture containing 49.6% glycid ether (1,2,3-propanetriol glycidyl ether, epoxy equivalent of 150) (w/v), 21% 2-dodecenylsuccinic acid anhydride(w/v), 29% methylnadic anhydride(w/v), and 4%2,4,6-tris(dimethylaminomethyl)phenol(w/v) (Serva, Heidelberg, Germany). The resin was polymerized at 60 ^{O}C for 12 hours. Sections were obtained with Ultracut Microtome (UltraCut S, Leica). Sections were analyzed with a digital transmission electron microscope (FEI, Tecnai G ^{2}) and digitally documented with AnalySIS software.

2.2.3.4.3 Postembedding immunogold electron microscopy

Immunogold electron microscopy was performed largely as previously described (Schmitz *et al*., 2000). Transfected cells were fixed using (0.1% glutraldehyde+2%PFA) as a pellet for 3 hours after

brief washings with PBS. Thereafter, cells were washed with PBS (six times, each for 10 minutes), dehydrated with ascending concentrations of ethanol, and embedded in LR-Gold resin (London resin) using benzoyl peroxide (0.5%) as a catalyst. Ultrathin sections (70nm) were cut and collected on uncoated 100-mesh gold grids. Sections were preincubated with 0.5% BSA in PBS, grids were transferred to primary antibody dilutions (Anti-RIBEYE at a 1:1000 dilution in 0.5% BSA in PBS), and primary antibody was detected by goat anti-rabbit secondary antibody conjugated to 10nm gold particles (Sigma; 1:100 dilution in blocking buffer). After extensive washes with PBS, immunogold complexes were fixed with 2.5% glutaraldehyde in PBS, and sections were contrasted with 2% uranyl acetate for 20 minutes at RT and analyzed with a digital TEM microscope (FEI, Tecnai G ^{2}). Controls were performed by either omitting the primary antibody of using irrelevant mono-and polyclonal antibodies, e.g., monoclonal and polyclonal antibodies against tubulin and the respective secondary antibodies.

2.2.3.5 NAD(H)-dependence of RIBEYE(A)-RIBEYE(B) interaction

Effect of NADH / NAD^+ on RIBEYE(A) with RIBEYE(B) interaction was studied using bacterial fusion protein. Full-length RIBEYE(A)-GST was used as a bait to fish out eluted prey RIBEYE(B)-MBP fusion protein. This setup was studied in the absence and presence of various concentration of NADH/NAD^+ . In a reaction volume of 500µl, 0.3 µM of bait- and prey- proteins were used. Beads with immobilized bait protein was earlier blocked in binding buffer (100mM Tris-HCl (pH 8.0), 150mM NaCl, 1mM EDTA & 1% Triton X-100) for 1 hour in a cold room on a rotary wheel and subsequently prey protein was added. The effect of NADH/NAD^+ on interaction was studied, by adding NADH / NAD^+ concentration ranging from 25nM-1.5µM in a binding buffer. The incubation was carried out for 3 hours at +4°C on a rotary wheel. The reaction tubes were centrifuged and the beads are washed in excess of corresponding binding buffer. The beads were boiled in 20µl of 4X sample buffer at 97°C for 3 minutes and the proteins were resolved on 10% SDS-PAGE, and processed for western blotting as described in section 2.2.2.2. The membrane was probed with Anti-MBP. Afterwards, the membrane was stripped (see section 2.2.2.3) and incubated with Anti-GST or Anti-RIBEYE (U_{2656}) antibody to check the equal bait protein loading.

3 Results

3.1 ANALYSIS OF RIBEYE-RIBEYE INTERACTIONS

3.1.1 Homo-dimerization of RIBEYE(A)-domain

In the Yeast two-hybrid (YTH) analyses, I found a strong self-interaction between the A-domain's of RIBEYE. RIBEYE(A)-domain interacts both with RIBEYE(A)-domain (Fig.16) as well as full length RIBEYE (consisting of A- and B- domains) (Fig.16-1; Magupalli *et al*., 2008) as judged by the growth of the respective mated yeasts on -ALWH selective plates (Fig.16-1:b) and expression of β-galactosidase marker gene activity as compared to the respective control matings. The control matings did not grow on –ALWH plates nor did they express β-galactosidase marker gene (Fig.16-1). The presence of both plasmids was shown by the growth on –LW plates. This was the case with all the studied mated partner combinations (Fig.16-1:a). Qualitatively the interaction was assessed by β-galactosidase filter test (Fig.16-1:c). Quantitatively, the strength of interaction was measured by β-galactosidase liquid assays (Fig.16-2). These findings from YTH i.e., homo-dimerization of RIBEYE (A)-domain was also confirmed at the protein level using two different protein pull-down assays (Fig.16-3&4). Immobilized RIBEYE(A)-MBP fusion protein (but not immobilized MBP alone) brings down soluble RIBEYE(A)-GST fusion protein (but not GST alone) in the protein pull-down assay (Fig.16-3). Similarly, immobilized RIBEYE(A)-GST specifically binds RIBEYE(A) from crude protein extracts of RIBEYE(A)-transgenic *P. pastoris* (Fig.16-4). GST control protein alone did not bind expressed RIBEYE(A) from *Pichia* extract. Thus, both YTH and protein pull-down data independently demonstrated that RIBEYE(A) interacts with RIBEYE(A). These initial findings suggested the presence of interacting site(s) on RIBEYE(A)-domain which aids in homo-dimerization of RIBEYE(A)-domains. In the next step, the interaction site(s) involved in intradomain RIBEYE(A)-RIBEYE(A) interaction were mapped using YTH assay.

1)

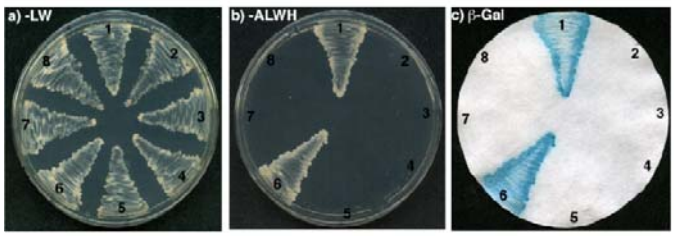

mating	bait	prey	-ALWH	βGal
1	RE(A)	RE(A)	+	+
2	pGBKT7	RE(A)	–	–
3	pSE1112	RE(A)	–	–
4	RE(A)	pACT2	–	–
5	RE(A)	pSE1111	–	–
6	RE(AB)	RE(A)	+	+
7	RE(AB)	pACT2	–	–
8	RE(AB)	pSE1111	–	–

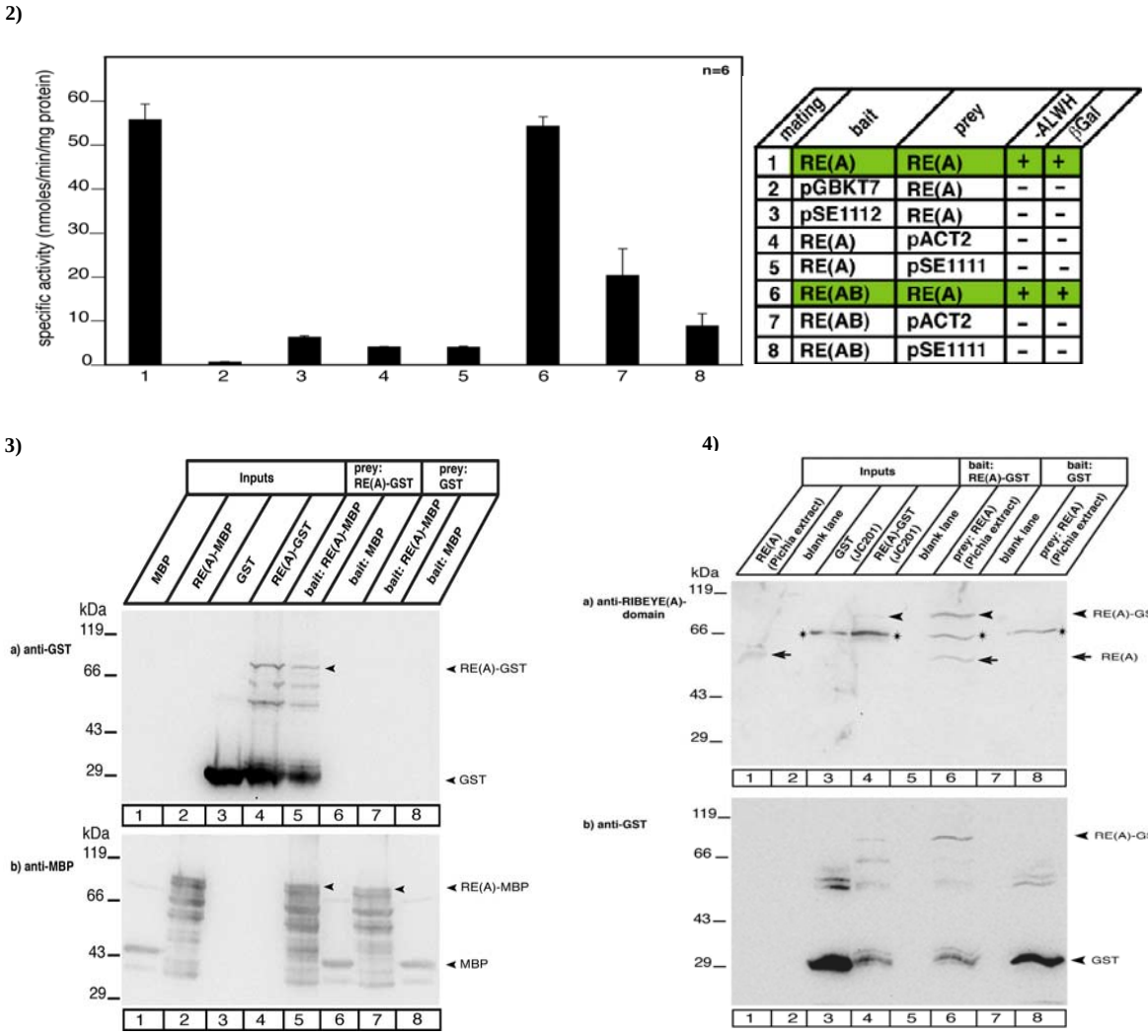

Figure 16. RIBEYE(A) interacts with RIBEYE(A) in YTH and pull-down assays.

1) Summary plates of YTH analyses obtained with the indicated bait and prey plasmids. a) Growth on –LW plates demonstrates the presence of the bait and prey plasmids in the mated yeasts. b) Growth on –ALWH selective medium demonstrates interaction between bait and prey proteins. For convenience, experimental bait-prey pairs were underlayered in color (green in case of interacting bait-prey pairs); control matings are non-colored. RIBEYE(A) interacts with RIBEYE(A) and full-length RIBEYE (RIBEYE(AB)) as judged by growth on selective plates (-ALWH) and expression of β-galactosidase expression (Fig. 16-1: b1,6 and c1,6 respectively). The respective control matings (autoactivation controls; yeast matings Fig. 16-1: b & c 2-5, 7-8) did not show growth on -ALWH plate and expression of β-galactosidase activity. Scoring (+) indicates the growth on –ALWH plate and β-galactosidase activity. **2)** Quantification of the β-galactosidase activities (liquid assays). Error bars represent s.e.m. **3)** RIBEYE(A) interacts with RIBEYE(A) in protein pull-down experiments (western blot analyses). RIBEYE(A)-MBP and MBP alone (control) were used as immobilized bait proteins and RIBEYE(A)-GST and GST alone (control) as soluble prey proteins. RIBEYE(A)-GST specifically binds to RIBEYE(A)-MBP (arrowhead in Fig. 16-3: a , lane 5). RIBEYE(A)-GST does not bind to MBP alone (Fig. 16-3: a, lane 6). GST alone also does not bind to RIBEYE(A)-MBP (Fig. 16-3: a, lane 7). Fig. 16-3: b shows the same blot as in (Fig. 16-3: a) but after stripping and reprobing of the nitrocellulose membrane with anti-MBP antibodies to show equal loading of bait proteins. Arrowheads shows RIBEYE(A)-MBP. **4)** RIBEYE(A)-GST also specifically binds intracellularly expressed RIBEYE(A) from a crude extract of RIBEYE(A)-transgenic *Pichia pastoris*. RIBEYE(A)-GST (lane 6) but not GST alone (lane 8) pulls-down untagged RIBEYE(A). The western blot was developed with an antibody against RIBEYE(A)-domain that simultaneously detects both untagged RIBEYE(A) which was used as prey protein as well as GST-tagged RIBEYE(A) which served as a bait protein. GST served as the control bait protein and did not pull-down RIBEYE(A) from the respective *Pichia pastoris* extract (Fig. 16-4: a). The pull-downed untagged RIBEYE(A) is labelled with an arrow in lane 6, the GST-tagged RIBEYE(A) is labelled with an arrowhead. The asterisk denotes an unspecific band detected by the antiserum against RIBEYE(A). The blot in Figure 16-4: b is same as in (Fig. 16-4: a) but after stripping and reprobing the membrane with anti-GST antibodies to show equal loading of bait proteins.

3.1.2 Mapping of RIBEYE(A)-RIBEYE(A) interaction(s)

Using YTH assay, I mapped the interaction sites involved in intradomain interactions (i.e., RIBEYE(A)-RIBEYE(A) interaction). For this purpose, amino- and carboxyterminal deletion constructs of RIBEYE(A) were generated, and tested for their ability to interact with full-length RIBEYE(A) in YTH assay. The outline of the complete RIBEYE molecule and the deletion constructs of the RIBEYE(A)-domain studied in the experiment are shown in Fig.17-1&2 respectively. The A-domain of RIBEYE consists of the aminoterminal 563 aa. Most of the carboxyterminal region of the RIBEYE(A)-domain could be omitted without abolishing the intradomain RIBEYE(A)-RIBEYE(A) interaction. RIBEYE(A) 1-105 was the shortest aminoterminal construct that still showed interaction with RIBEYE(A) full-length protein (Fig.17-2: prey7). Therefore, the aminoterminal portion of RIBEYE(A)-domain comprising the first 105 amino acids contains a binding site for another RIBEYE(A)-domain. This interaction site is denoted as “A1” in the following text. I also studied the aminoterminal deletion constructs of RIBEYE(A)-domain for their interaction with RIBEYE(A)-domain. Interesting, also aminoterminal deletion construct that lacks the previously identified RIBEYE(A1) binding site contained in the first 105 amino acids interacted with RIBEYE(A)-domain pointing to a second homo-dimerization site in the carboxyterminal region of the A-domain of RIBEYE. The minimal carboxyterminal region of the A-domain of RIBEYE that we found interacting with RIBEYE(A) was contained in a sequence stretch containing aa 438-563 (Fig.17-2: prey10) and was denoted as “A2” in the following text. I further tested whether the mid-region of RIBEYE which neither contain the aminoterminal A1 interaction site nor the carboxyterminal A2 interaction site for its capability to interact with RIBEYE(A). This region in the mid-portion of RIBEYE, denoted as “A3”, also interacts with RIBEYE(A) full length (Fig.17-2: prey 11). Thus, the A-domain of RIBEYE has three independent sites which were able to interact with full-length RIBEYE(A). The intermediate constructs, that contained either „A1“, „A2“, „A3“ interacted with full length RIBEYE(A) (Fig.17-2: prey 2-6&9). On this basis we concluded that three minimal interacting modules on RIBEYE(A)-domain can mediate RIBEYE(A)-RIBEYE(A) homo-dimerization. The interaction was judged by growth on –ALWH selective plates, and expression of β-galactosidase marker gene activity. All the tested RIBEYE constructs were not autoactivating as absence of growth on –ALWH and lack of expression of β-galactosidase activity. The summarized results as follows:

1)

2)

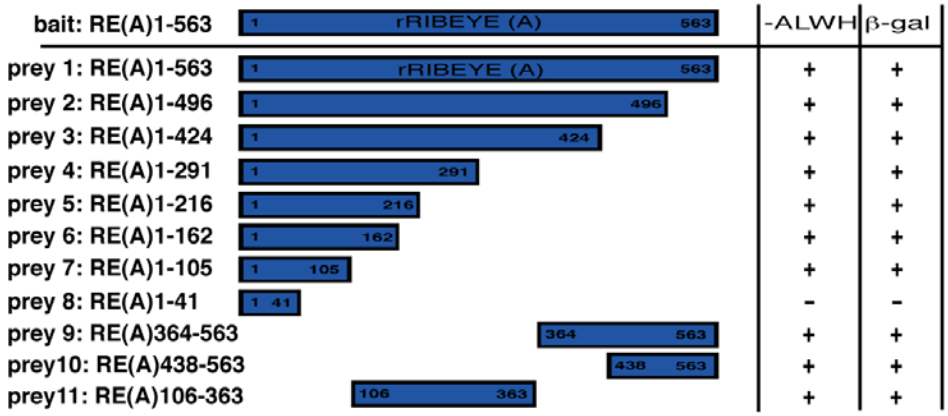

3)

a) b) c)

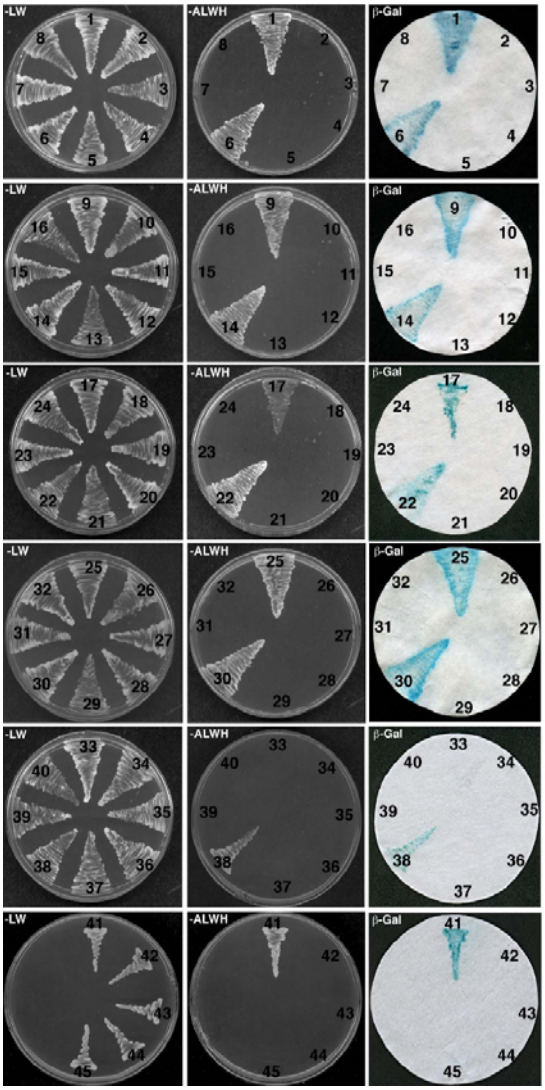

mating	bait	prey	-ALWH	β-Gal
1	RE(A)1-563	RE(A)1-563	+	+
2	pGBKT7	RE(A)1-563	-	-
3	pSE1112	RE(A)1-563	-	-
4	RE(A)1-563	pACT2	-	-
5	RE(A)1-563	pSE1111	-	-
6	RE(A)1-563	RE(A)1-291	+	+
7	pGBKT7	RE(A)1-291	-	-
8	pSE1112	RE(A)1-291	-	-
9	RE(A)1-563	RE(A)364-563	+	+
10	pGBKT7	RE(A)364-563	-	-
11	pSE1112	RE(A)364-563	-	-
12	RE(A)1-563	pACT2	-	-
13	RE(A)1-563	pSE1111	-	-
14	RE(A)1-563	RE(A)1-216	+	+
15	pGBKT7	RE(A)1-216	-	-
16	pSE1112	RE(A)1-216	-	-
17	RE(A)1-563	RE(A)438-563	+	+
18	pGBKT7	RE(A)438-563	-	-
19	pSE1112	RE(A)438-563	-	-
20	RE(A)1-563	pACT2	-	-
21	RE(A)1-563	pSE1111	-	-
22	RE(A)1-563	RE(A)1-424	+	+
23	pGBKT7	RE(A)1-424	-	-
24	pSE1112	RE(A)1-424	-	-
25	RE(A)1-563	RE(A)1-496	+	+
26	pGBKT7	RE(A)1-496	-	-
27	pSE1112	RE(A)1-496	-	-
28	RE(A)1-563	pACT2	-	-
29	RE(A)1-563	pSE1111	-	-
30	RE(A)1-563	RE(A)1-162	+	+
31	pGBKT7	RE(A)1-162	-	-
32	pSE1112	RE(A)1-162	-	-
33	RE(A)1-563	RE(A)1-41	-	-
34	pGBKT7	RE(A)1-41	-	-
35	pSE1112	RE(A)1-41	-	-
36	RE(A)1-563	pACT2	-	-
37	RE(A)1-563	pSE1111	-	-
38	RE(A)1-563	RE(A)1-105	+	+
39	pGBKT7	RE(A)1-105	-	-
40	pSE1112	RE(A)1-105	-	-
41	RE(A)1-563	RE(A)106-363	+	+
42	pGBKT7	RE(A)106-363	-	-
43	pSE1112	RE(A)106-363	-	-
44	RE(A)1-563	pACT2	-	-
45	RE(A)1-563	pSE1111	-	-

4)

Figure 17. Mapping of RIBEYE(A) -RIBEYE(A) interactions.

1) Schematic domain structure of RIBEYE showing the aminoterminal A-domain and the carboxyterminal B-domain. **2)** Stretch of amino acids covered in individual deletion construct. The indicated bait and prey plasmids were used to test for the interaction of the respective proteins in the YTH assay. YTH analyses revealed a N-terminal site (within the first 105 amino acids) that interacts with RIBEYE(A). This interaction site is denoted as "A1" (Fig. 17-2: prey 7). Similarly, YTH analyses of aminoterminal deletion constructs of RIBEYE(A) reveal a second interaction site in the carboxyterminal region of RIBEYE(A) that interacts with RIBEYE(A). This carboxyterminal interaction site is denoted as "A2" (Fig. 17-2: prey 9&10) and covers aa 438-563 (Fig. 17-2: prey 10). The "A3" region in the middle of RIBEYE(A) (aa 106-363) that does not contain "A1" and "A2" is also able to interact with full-length RIBEYE(A) (Fig. 17-2: prey 11). **3)** Summary of mapping analysis using qualitative YTH assay. For convenience, experimental bait-prey pairs were underlayered in color (green in case of interacting bait-prey pairs; yellow in case of non-interacting bait-prey pairs); control matings were non-colored. In (Fig. 17-3: a) growth on –LW plates demonstrates the presence of the bait and prey plasmids in the mated yeasts. Growth on –ALWH selective plates demonstrate the interaction between bait and prey proteins (Fig. 17-3: b). In the right panels, β-galactosidase activities were monitored by filter lift assay. Blue color indicates β-galactosidase activity. Positive control RIBEYE(A)-RIBEYE(A) interaction is shown in (mating #1), RIBEYE (A2) interacts with full length RIBEYE(A) (mating # 17), RIBEYE(A1) interacts with full length RIBEYE(A) (mating # 38) and RIBEYE (A3) interacts with full length RIBEYE(A) (mating # 41). All the tested RIBEYE constructs did not show auto-activation (mating # 2-5,7,8,10-13,15,16,18-21,23,24,26-29,31,32,34-37,39,40,42-45). Scoring (+) indicates the growth on –ALWH plate and β-galactosidase activity. **4)** Schematic representation of the identified RIBEYE-RIBEYE-interaction modules ("A1", "A2", "A3") in the A-domain of RIBEYE. RE(A), RIBEYE(A); RE(B), RIBEYE(B); rRIBEYE(A), rat RIBEYE(A); rRIBEYE(B), rat RIBEYE(B).

Next, I tested the number of possibilities by which the identified RIBEYE(A1), RIBEYE(A2) and RIBEYE(A3) interaction modules can interact among themselves.

3.1.3 Multiple interactions among RIBEYE(A)-domain interacting modules

In Yeast two-hybrid assays, I tested interactions between the identified minimal interaction modules (A1, A2 and A3) of the RIBEYE(A)-domain. I tested all possible interaction combinations between RIBEYE(A1), RIBEYE(A2) and RIBEYE(A3) using the YTH assay and found that multiple interactions exists between them. RIBEYE(A1) interacts with RIBEYE(A1), RIBEYE(A2) and RIBEYE(A3) (Fig.18-1,3&4). Similarly, RIBEYE(A2) interacts with RIBEYE(A2) in addition to RIBEYE(A1) (Fig.18-2&3). RIBEYE(A3) interacted with RIBEYE(A1) and RIBEYE(A3) (Fig.18-4). Qualitatively these interactions was assessed by β-galactosidase filter test. The individual modules were expressed as fusion proteins to validate the YTH findings. All these interactions could be confirmed biochemically by protein pull-down assays. RIBEYE(A1) interacts with RIBEYE (A1)(Fig.19-1), RIBEYE(A1) interacts with RIBEYE (A2)(Fig.19-4), RIBEYE(A1) interacts with RIBEYE (A3)(Fig.19-5), RIBEYE(A2) interacts with RIBEYE (A2)(Fig.19-2) and RIBEYE(A3)

interacts with RIBEYE (A3)(Fig.19-3). Thus, the “A1”, “A2” and “A3” interaction modules in the RIBEYE(A)-domain of RIBEYE allows multiple RIBEYE-RIBEYE interactions.

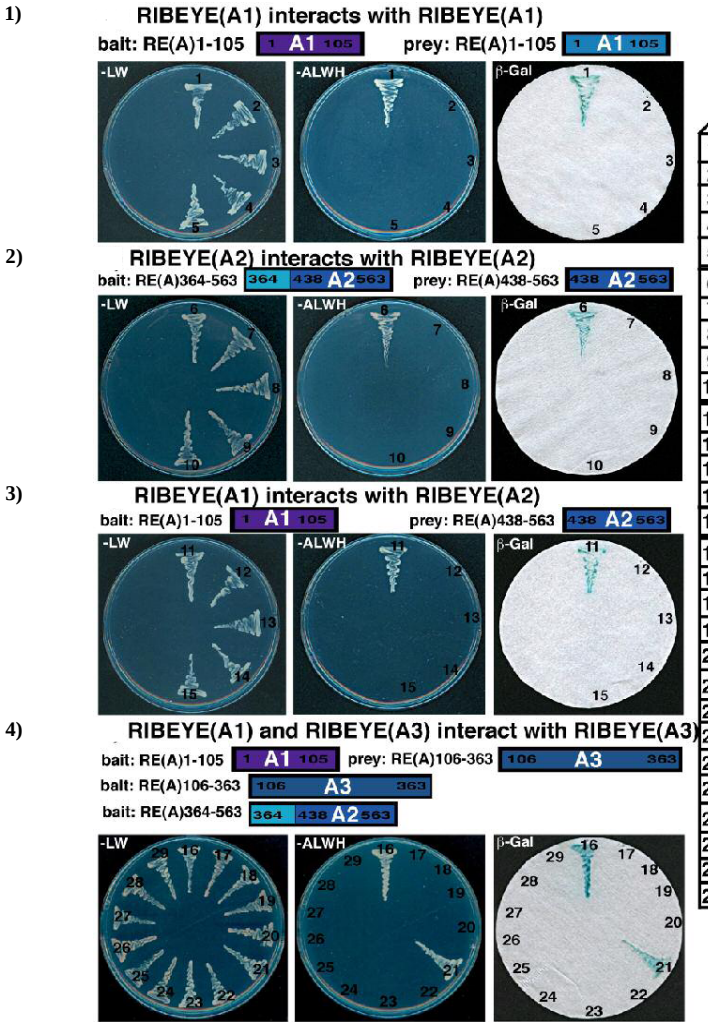

mating	bait	prey	-ALWH	βGal
1	RE(A)1-105	RE(A)1-105	+	+
2	pGBKT7	RE(A)1-105	–	–
3	pSE1112	RE(A)1-105	–	–
4	RE(A)1-105	pACT2	–	–
5	RE(A)1-105	pSE1111	–	–
6	RE(A)364-563	RE(A)438-563	+	+
7	pGBKT7	RE(A)438-563	–	–
8	pSE1112	RE(A)438-563	–	–
9	RE(A)364-563	pACT2	–	–
10	RE(A)364-563	pSE1111	–	–
11	RE(A)1-105	RE(A)438-563	+	+
12	pGBKT7	RE(A)438-563	–	–
13	pSE1112	RE(A)438-563	–	–
14	RE(A)1-105	pACT2	–	–
15	RE(A)1-105	pSE1111	–	–
16	RE(A)106-363	RE(A)106-363	+	+
17	pGBKT7	RE(A)106-363	–	–
18	pSE1112	RE(A)106-363	–	–
19	RE(A)106-363	pACT2	–	–
20	RE(A)106-363	pSE1111	–	–
21	RE(A)1-105	RE(A)106-363	+	+
22	RE(A)1-105	pACT2	–	–
23	RE(A)1-105	pSE1111	–	–
24	RE(A)364-563	RE(A)106-363	–	–
25	RE(A)364-563	pACT2	–	–
26	RE(A)364-563	pSE1111	–	–
27	RE(B)564-988	RE(A)106-363	–	–
28	RE(B)564-988	pACT2	–	–
29	RE(B)564-988	pSE1111	–	–

Figure 18. Multiple interactions among RIBEYE(A) -domain interaction modules in YTH assay.

The indicated, identified minimal interaction modules (“A1”, “A2” and “A3”) were tested in the YTH assay for their interaction with each other, in multiple combinations. For convenience, experimental bait-prey pairs were underlayered in color (green in case of interacting bait-prey pairs; yellow in case of non-interacting bait-prey pairs); control matings were non-colored. **1)** RIBEYE(A1) interacts with RIBEYE(A1) (mating #1). Matings #2-#5 show the respective indicated control matings. **2)** RIBEYE(A2) interacts with RIBEYE(A2) (mating #6). Matings #7-10 show the respective indicated control matings. **3)** RIBEYE(A1) interacts with RIBEYE(A2) (mating #11). Matings #12-15 show the respective indicated control matings. **4)** RIBEYE(A3) interact with RIBEYE(A3) and RIBEYE(A1) (matings #16&21 respectively). RIBEYE(A3) does not interact with RIBEYE(A2) & RIBEYE(B) (matings # 24 & 27 respectively). Matings #17-20, 22, 23, 25, 26, 28 and 29 shows the indicated control mating. All used RIBEYE constructs were not auto-activating. Scoring (+) indicates the growth on –ALWH plate and β-galactosidase activity.

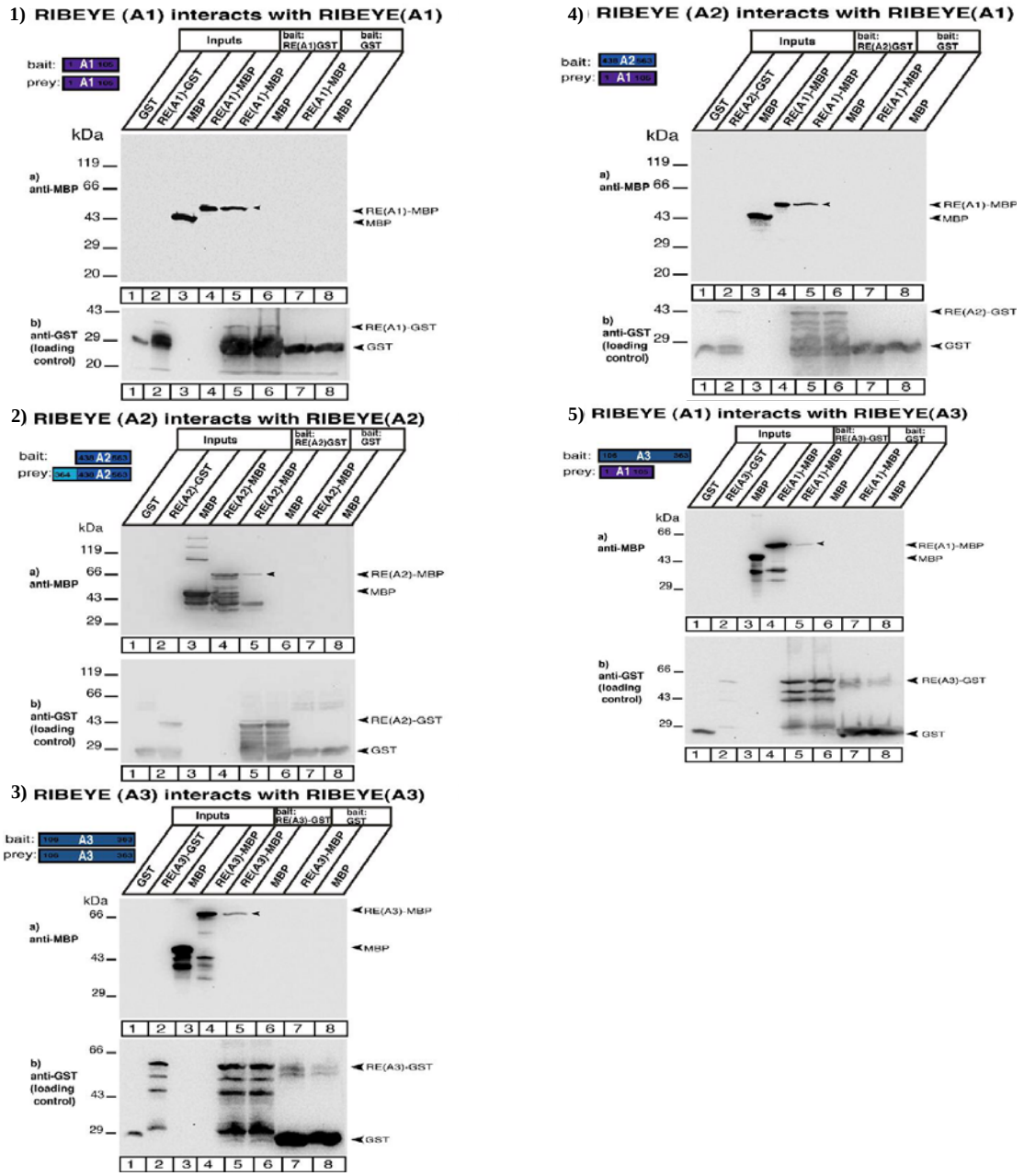

Figure 19. Multiple RIBEYE-RIBEYE interactions identified by YTH were confirmed by fusion protein pull-down assays.

The indicated, identified minimal interaction modules ("A1", "A2" and "A3") were tested in the protein pull-down assays for their interaction with each other, in multiple combinations. The membrane was first probed with anti-MBP (to detect pull-down product), stripped and re-probed with anti-GST to show equal bait protein loadings. **1)** RIBEYE(A1) interacts with RIBEYE(A1) (arrowhead, lane #5, anti- MBP). Anti-GST indicates equal bait loading. **2)** RIBEYE(A2) interacts with RIBEYE(A2) (arrowhead, lane #5, anti-MBP). Anti-GST indicates equal bait loading. **3)** RIBEYE(A3) interacts with RIBEYE(A3) (arrowhead, lane #5, anti-MBP). Anti-GST indicates equal bait loading. **4)** RIBEYE(A2) interacts with RIBEYE(A1) (arrowhead, lane #5, anti-MBP). Anti-GST indicates equal bait loading. **5)** RIBEYE(A1) interacts with RIBEYE(A3) (arrowhead, lane #5, anti-MBP). Anti-GST indicates equal bait loading.

3.1.4 Homo-dimerization of RIBEYE(B)-domain

Using YTH assay, I also showed homo-dimerization of the RIBEYE(B)-domain (Fig.20-1: b6&c6). Moreover, RIBEYE(B)-domain interacts with full length RIBEYE (consisting of A- and B-domains) (Fig.20-1: b1&c1). The homo-dimerization of RIBEYE(B)-domain is not very surprising: CtBP2 which is identical to RIBEYE(B)-domain (except for the first 20 amino acids) has been previously shown to homo-dimerize (Thio *et al*., 2004). CtBP1 also homo-dimerizes (Sewalt *et al*., 1999; Balasubramanian *et al*., 2003) and the structure of the CtBP1 dimer (tCtBP1) has been resolved (Kumar *et al*., 2002; Nardini *et al*., 2003). NAD(H) was found to stimulate the homo-dimerization of both CtBP1 and CtBP2 (Balasubramanian *et al*., 2003; Thio *et al*., 2004). Further, RIBEYE(B)-domains interaction with RIBEYE full length protein indicates that the A-domain of RIBEYE does not prevent homo-dimerization of RIBEYE(B)-domains (Fig.20-1; Magupalli *et al*., 2008). The homo-dimerization of RIBEYE(B)-domain is dependent on amino acids 689-716 which form the αB-loop-βC motif (homo-dimerization loop, HDL) of RIBEYE(B)-domain as judged by homology modelling (Fig.20-3:a). The αB-loop-βC motif in CtBP1 is important for homo-dimerization of CtBP1 (Nardini *et al*., 2003). In agreement with this prediction, homo-dimerization of RIBEYE(B)-domain is completely abolished if the homo-dimerization loop (HDL) is deleted (Fig.20-3:b). RIBEYE(B)ΔHDL no longer interact with RIBEYE(B)-domain (Fig.20-4). The RIBEYE (B) homo-dimerization interface is denoted as "B1" in the following text. The presence both plasmids (bait and prey) in the yeast were shown by growth on –LW plates, and were the case with all studied mated yeast combinations. The interaction was shown by the growth on –ALWH selective plates. Qualitatively, the interaction was assayed by β-galactosidase filter test (Fig.20-1&4). Quantitatively, the strength of interaction was shown by β-galactosidase liquid assays (Fig.20-2). Based on these findings, that RIBEYE (B) interacts with RIBEYE full length (consisting of A and B domains) I asked whether RIBEYE(B) also interacts with RIBEYE(A).

1)

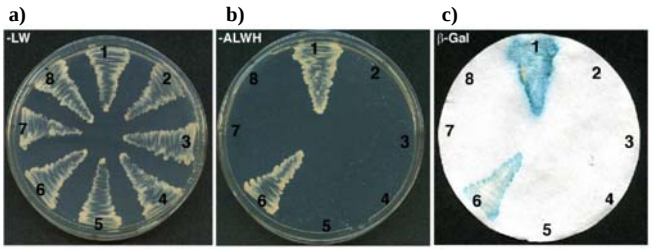

mating	bait	prey	-ALWH	β-Gal
1	RE(AB)	RE(B)	+	+
2	pGBKT7	RE(B)	-	-
3	pSE1112	RE(B)	-	-
4	RE(AB)	pACT2	-	-
5	RE(AB)	pSE1111	-	-
6	RE(B)	RE(B)	+	+
7	RE(B)	pACT2	-	-
8	RE(B)	pSE1111	-	-

2)

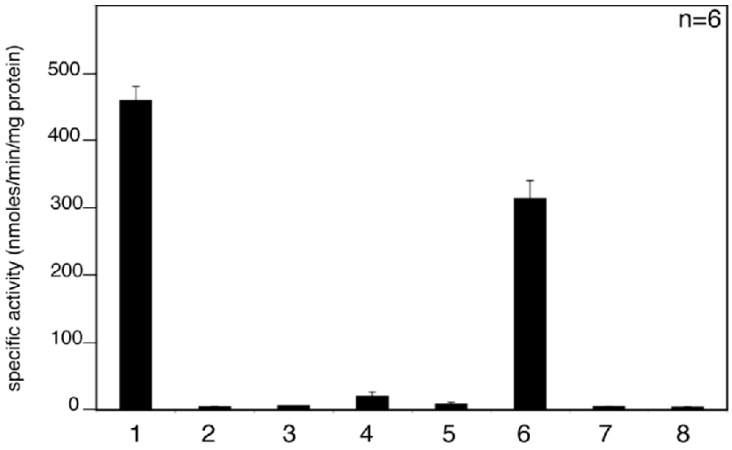

mating	bait	prey	-ALWH	βGal
1	RE(AB)	RE(B)	+	+
2	pGBKT7	RE(B)	-	-
3	pSE1112	RE(B)	-	-
4	RE(AB)	pACT2	-	-
5	RE(AB)	pSE1111	-	-
6	RE(B)	RE(B)	+	+
7	RE(B)	pACT2	-	-
8	RE(B)	pSE1111	-	-

3)

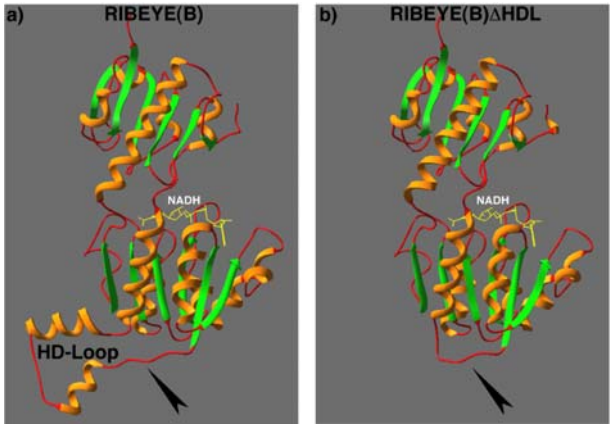

4)

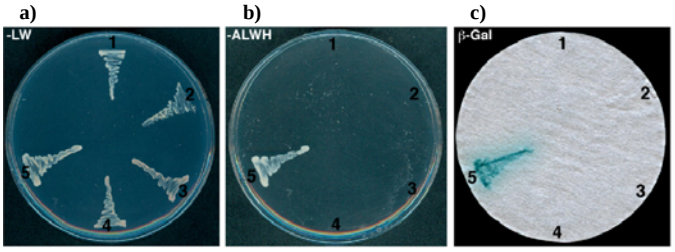

mating	bait	prey	-ALWH	βGal
1	RE(B)	RE(B)ΔHDL	-	-
2	RE(B)	RE(B)ΔHDL	-	-
3	pGBKT7	RE(B)	-	-
4	pSE1112	pACT2	-	-
5	RE(B)	RE(B)	+	+

Figure 20. Homo-dimerization of RIBEYE(B)-domain in YTH assay.

RIBEYE(B) interacts with RIBEYE(B) in YTH assay. For convenience, experimental bait-prey pairs were underlayered in color (green in case of interacting bait-prey pairs; yellow in case of non-interacting bait-prey pairs); control matings were non-colored. **1)** RIBEYE(B) interacts with full length RIBEYE and RIBEYE(B)in YTH (matings # 1&6 respectively). Control matings #2-5&7-8 indicates that the respective bait and prey constructs were not auto-activating. **2)** RIBEYE(B) homo-dimerizes with RIBEYE(B) in the YTH assay as demonstrated by quantitative analysis of β-galactosidase activity of the indicated yeasts. Error bars represent s.e.m. **3)** Structural model of RIBEYE(B)-domain. (a) wild type protein (b) and RIBEYE(B)ΔHDL with a deleted homo-dimerization loop. The NADH bound to RIBEYE is depicted in yellow. Arrowhead indicate the homo-dimerization loop (HD-loop). **4)** RIBEYE(B) homo-dimerization is dependent on HDL-loop as shown in the YTH assay. The interaction between RIBEYE(B) and RIBEYE(B) abolishes, when the HDL loop is deleted (matings # 1,2). Mating # 5 shows the positive control (RIBEYE(B)-RIBEYE(B)interaction). The other matings # 3 & 4 represent the indicated controls. Scoring (+) indicates the growth on –ALWH plate and β-galactosidase activity.

3.1.5 Hetero-dimerization of RIBEYE(A)- and RIBEYE(B)-domains

From the above findings, it's evident that RIBEYE(B) interacts with RIBEYE full length (consisting of A- and B-domains). Next, I tested the hypothesis, whether RIBEYE(B)-domain interacts with RIBEYE(A)-domain. In YTH, full length RIBEYE(B)-domain interacted with RIBEYE(A)-domain as judged by the growth on –ALWH selective plates. (Fig.21-1) and expression of the β-galactosidase marker gene activity (Fig.21-1: c1; Magupalli *et al.*, 2008). The β-galactosidase activity was quantitatively measured (Fig.21-2) and also confirmed by qualitative filter tests. The finding of YTH was further verified in protein pull-down assay (Fig.22). RIBEYE(A)-GST and GST alone (control protein) were used as immobilized bait proteins and RIBEYE(B)-MBP and MBP alone (control protein) as soluble prey proteins. After incubation, binding of the soluble prey proteins to the immobilized bait proteins was tested by probing with the indicated antibodies. RIBEYE(B)-MBP binds to RIBEYE(A)-GST (Fig.22a: arrowhead, lane 5) but not to GST alone (Fig.22a: lane 6). Fig.22b shows the same blot as in (Fig.22a) but after stripping and reprobing the membrane with anti-GST antibodies to confirm equal loading of bait proteins.

1)

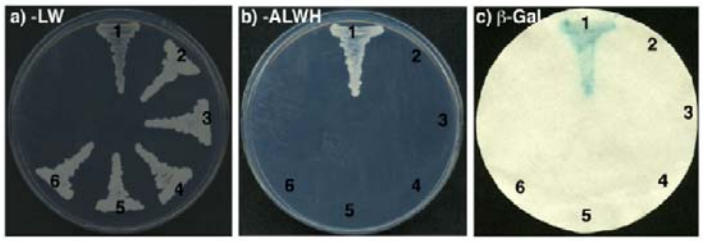

mating	bait	prey	-ALWH	β-Gal
1	RE(B)	RE(A)	+	+
2	RE(B)	pACT2	–	–
3	RE(B)	pSE1111	–	–
4	pGBKT7	RE(A)	–	–
5	pSE1112	RE(A)	–	–
6	pGBKT7	pACT2	–	–

2)

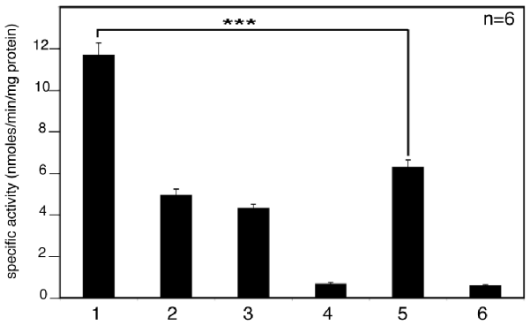

mating	bait	prey	-ALWH	β-Gal
1	RE(B)	RE(A)	+	+
2	RE(B)	pACT2	–	–
3	RE(B)	pSE1111	–	–
4	pGBKT7	RE(A)	–	–
5	pSE1112	RE(A)	–	–
6	pGBKT7	pACT2	–	–

Figure 21. Hetero-dimerization of RIBEYE(A) -RIBEYE(B) domains in YTH assay.

For convenience, experimental bait-prey pairs were underlayered in color (green in case of interacting bait-prey pairs); control matings are non-colored. **1)** Summary plates of YTH analyses obtained with the indicated bait and prey plasmids. Presence of bait and prey plasmids were indicated by growth on –LW plate (a). RIBEYE(A) interacts with RIBEYE(B) as judged by growth on –ALWH plates and β-galactosidase filter test (b1&c1) respectively. Matings # 2-6 are indicated controls. **2)** RIBEYE(A) interacts with RIBEYE(B) in the YTH assay as demonstrated by quantitative analysis of β-galactosidase activity of the indicated yeasts. Symbol (***) represents high significance, α=0.001. Error bars represent s.e.m. Scoring (+) indicates the growth on –ALWH plate and β-galactosidase activity.

Here, I demonstrated with further independent method that RIBEYE(A) specifically interacts with RIBEYE(B) and confirmed the YTH assay result. These findings suggests a presence of interaction site for interdomain RIBEYE(A)-RIBEYE(B) interaction.

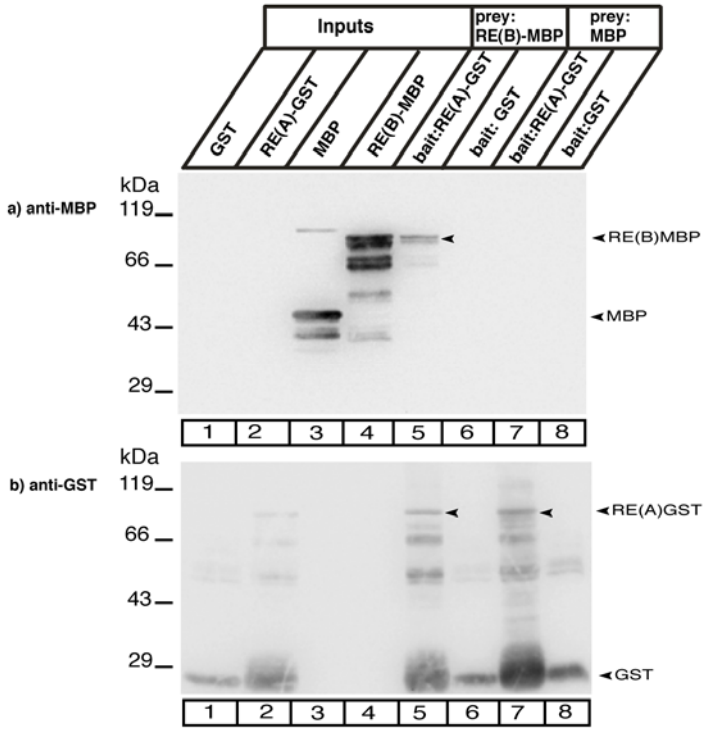

Figure 22. Hetero-dimerization of RIBEYE(A) -RIBEYE(B) domains in protein pull-down assay.

RIBEYE(A) interacts with RIBEYE(B) in protein pull-down assay. RIBEYE(A)-GST and GST alone (control protein) were used as immobilized bait proteins and RIBEYE(B)-MBP and MBP alone (control protein) as soluble prey proteins. After incubation, binding of the soluble prey proteins to the immobilized prey proteins was tested by western blotting with the indicated antibodies. RIBEYE(B)-MBP binds to RIBEYE(A)-GST (arrowhead , lane 5) but not to GST alone (lane 6). The blot in **(b)** is same as in **(a)** but after stripping and reprobing of the membrane with anti-GST antibodies to show equal loading of bait proteins.

3.1.6 Mapping of RIBEYE(A)-RIBEYE(B) interaction

In YTH assay, I mapped the interaction site involved in RIBEYE(A)-RIBEYE(B) interaction. Mapping analyses revealed that the "A2" interaction site in the carboxyterminal portion of the RIBEYE(A)-domain is the binding site for RIBEYE(B)-domain (Fig.23-2 and Fig.24-1). On RIBEYE(B), the NADH-binding sub-domain (NBD) is responsible for the interaction with RIBEYE(A)-domain (Fig.23-3 and Fig.24-2). The RIBEYE(B)ΔHDL is not responsible for the interactions between RIBEYE(A)-RIBEYE(B)-domains (Fig.23-3 and Fig.24-2:mating #1) and even with full length RIBEYE (AB) (Fig.24-3:mating #1). RIBEYE(B)ΔHDL which no longer homo-

dimerized with RIBEYE(B) (Fig.20-4), still interacted with RIBEYE(A) (Fig.24-2) and full length RIBEYE (Fig.24-3). The interaction is evident from the growth of the respective mated yeast on –ALWH selective plate and expression of β-galactosidase marker gene activity. Qualitatively the interaction was assessed by β-galactosidase filter test. These mapping data obtained by YTH analyses were confirmed by protein pull-down assay, where RIBEYE (A2) binds to full length RIBEYE(B), showing interaction between RIBEYE(A2) and RIBEYE(B)-domains (Fig.25).

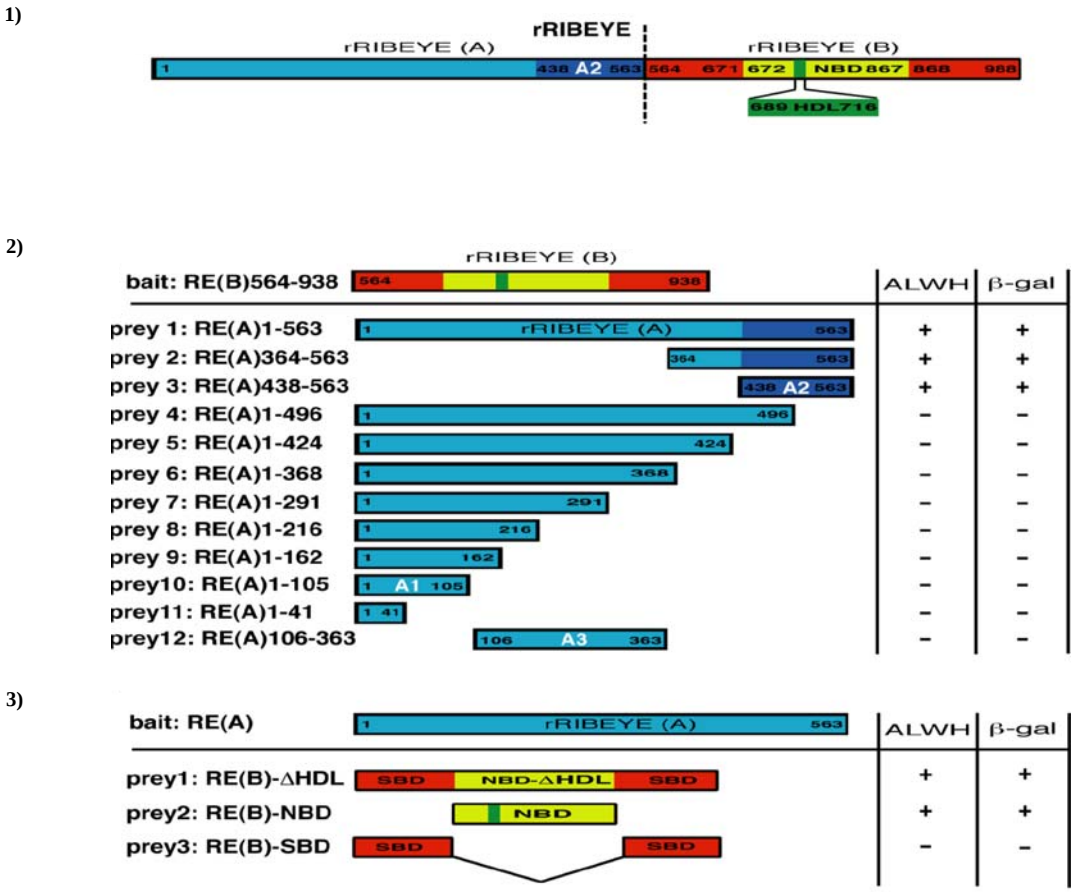

Figure 23. Mapping constructs used in RIBEYE(A) – RIBEYE(B) interaction in YTH assay.

1) Schematic domain structure of RIBEYE labelled either with known domain or mapped in these studies. The A-domain of RIBEYE is depicted in blue color. The substrate-binding sub-domain (SBD) of RIBEYE(B)-domain which consists of the amino- and carboxyterminal portions is depicted in red. The RIBEYE(B) homo-dimerization loop (HDL) is depicted in green within the yellow labelled NAD(H)-binding sub-domain. **2)** The indicated RIBEYE(A)-domain deletion construct (prey) were used in YTH assay along with bait RIBEYE(B). The RIBEYE(B) construct was the identified minimal stretch required for RIBEYE(A)-domain interaction. The minimal interaction modules were depicted as ("A1", "A2" and "A3"). **3)** The indicated RIBEYE(B)-domain deletion construct (prey) were used in YTH assay along with bait RIBEYE(A). Scoring (+) indicates the growth on –ALWH plate and β-galactosidase activity.

1)

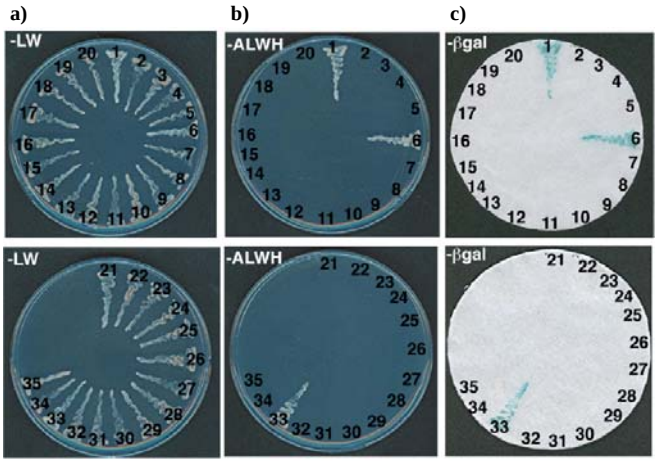

mating	bait	prey	-ALWH	βGal
1	RE(B)564-938	RE(A)1-563	+	+
2	RE(B)564-938	pACT2	–	–
3	RE(B)564-938	pSE1111	–	–
4	pGBKT7	RE(A)1-563	–	–
5	pSE1112	RE(A)1-563	–	–
6	RE(B)564-938	RE(A)364-563	+	+
7	pGBKT7	RE(A)364-563	–	–
8	pSE1112	RE(A)364-563	–	–
9	RE(B)564-938	RE(A)1-496	–	–
10	pGBKT7	RE(A)1-496	–	–
11	pSE1112	RE(A)1-496	–	–
12	RE(B)564-938	RE(A)1-424	–	–
13	pGBKT7	RE(A)1-424	–	–
14	pSE1112	RE(A)1-424	–	–
15	RE(B)564-938	RE(A)1-368	–	–
16	pGBKT7	RE(A)1-368	–	–
17	pSE1112	RE(A)1-368	–	–
18	RE(B)564-938	RE(A)1-291	–	–
19	pGBKT7	RE(A)1-291	–	–
20	pSE1112	RE(A)1-291	–	–
21	RE(B)564-938	RE(A)1-216	–	–
22	pGBKT7	RE(A)1-216	–	–
23	pSE1112	RE(A)1-216	–	–
24	RE(B)564-938	RE(A)1-162	–	–
25	pGBKT7	RE(A)1-162	–	–
26	pSE1112	RE(A)1-162	–	–
27	RE(B)564-938	RE(A)1-105	–	–
28	pGBKT7	RE(A)1-105	–	–
29	pSE1112	RE(A)1-105	–	–
30	RE(B)564-938	RE(A)1-41	–	–
31	pGBKT7	RE(A)1-41	–	–
32	pSE1112	RE(A)1-41	–	–
33	RE(B)564-938	RE(A)438-563	+	+
34	pGBKT7	RE(A)438-563	–	–
35	pSE1112	RE(A)438-563	–	–

2)

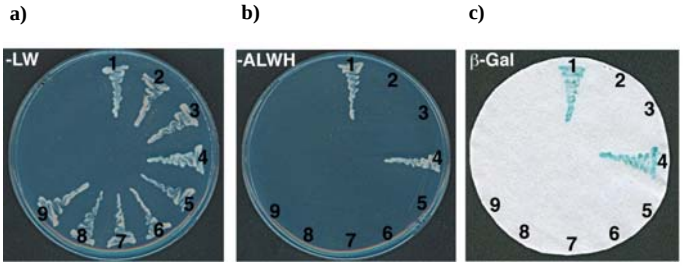

mating	bait	prey	-ALWH	βGal
1	RE(A)	RE(B)ΔHDL	+	+
2	pGBKT7	RE(B)ΔHDL	–	–
3	pSE1112	RE(B)ΔHDL	–	–
4	RE(A)	RE(B)NBD	+	+
5	pGBKT7	RE(B)NBD	–	–
6	pSE1112	RE(B)NBD	–	–
7	RE(A)	RE(B)SBD	–	–
8	pGBKT7	RE(B)SBD	–	–
9	pSE1112	RE(B)SBD	–	–

3)

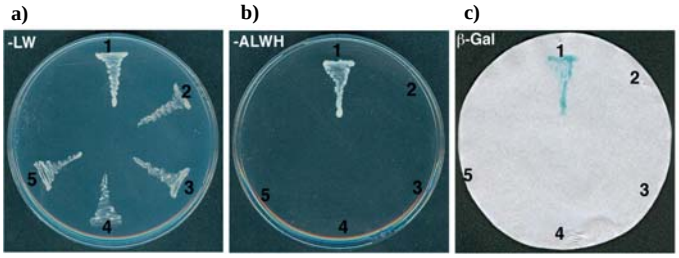

mating	bait	prey	-ALWH	βGal
1	RE(AB)	RE(B)ΔHDL	+	+
2	RE(AB)	pGADT7	–	–
3	RE(AB)	pSE1111	–	–
4	pGBKT7	RE(B)ΔHDL	–	–
5	pSE1112	RE(B)ΔHDL	–	–

Figure 24. Mapping of RIBEYE(A) -RIBEYE(B) interactions in YTH assay.

Analyses of RIBEYE(A)-RIBEYE(B) interaction mapping on A-domain, using the YTH assay. For convenience, experimental bait-prey pairs were underlayered in color (green in case of interacting bait-prey pairs; yellow in case of non-interacting bait-prey pairs); control matings were non-colored. **1)** Matings # 6 and 33 depicts that RIBEYE(B) interacts with carboxyterminal region of RIBEYE(A). Mating # 1 is a positive control indicating full length RIBEYE(A) interacts with RIBEYE(B). The other matings (# 2-5, 7-32, 34 and 35) are the respective indicated auto-activation controls and other mated RIBEYE constructs, which were comprehensively tested and found not to be interacting. **2)** Analyses of RIBEYE(A)-RIBEYE(B) interaction mapping on B-domain, using the YTH assay. The RIBEYE(B) homo-dimerization loop (HDL) is not essential for the interaction between RIBEYE(A) and RIBEYE(B) (mating #1). RIBEYE(B)ΔHDL (prey 1) still interacts with RIBEYE(A). The NAD(H) binding sub-domain (NBD) interacts with RIBEYE(A)-domain (mating # 4) but not the substrate-binding sub-domain (SBD) is responsible for interaction with RIBEYE(A) (mating # 7). **3)** Similarly, RIBEYE(B)ΔHDL is also shown to be not interfering with full length RIBEYE interaction (mating # 1). Scoring (+) indicates the growth on –ALWH plate and β-galactosidase activity.

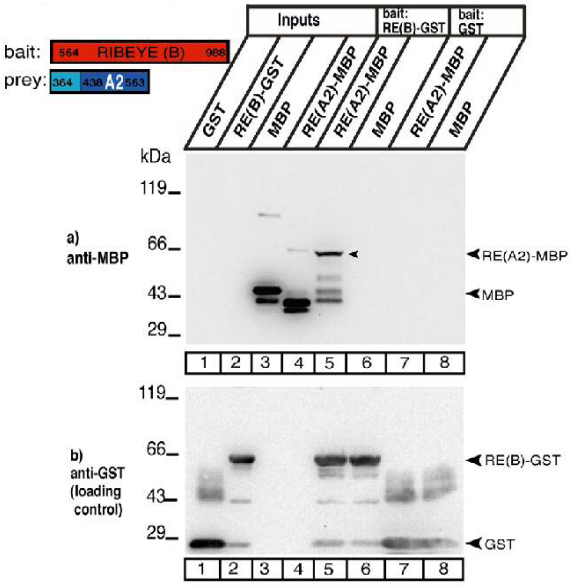

Figure 25. Mapping of RIBEYE(A)-RIBEYE(B) interactions in protein pull-down assay.

Carboxyterminal region of RIBEYE(A)-domain (i.e., A2) interacts with full-length RIBEYE(B) in pull-down assay. GST- tagged RIBEYE proteins were used as immobilized bait partners and MBP-tagged RIBEYE proteins were used as soluble prey partners. **a)** Binding of the prey proteins was analyzed by probing with antibodies against MBP. Only RIBEYE(B)-GST pulled down RIBEYE(A2)-MBP (arrowhead, lane 5) but not the control GST (lane 7). RIBEYE(B)-GST does not pull-down MBP (lane 6). **b)** Equal loading of bait partners was verified by stripping the same blot and reprobing with anti-GST to show equal loading of bait proteins.

3.1.7 RIBEYE(A)-RIBEYE(B) interaction mapping using NBD point mutants

In the above experiments, I had shown that the NBD sub-domain in RIBEYE(B) is the docking site for RIBEYE(A)-domain. Next, I mapped the interaction by mutating distinct amino acids in the NBD sub-domain of RIBEYE(B). These point mutants were tested for their ability to interact with RIBEYE(A)-domain. The mutation covered a broad region of NBD, and was tested for their role using YTH assay. I analyzed RIBEYE(B) point mutants RIBEYE(B)G730A, D758N, I796A, E844Q, F848W and K854Q which were located at the outer face of the NBD (Fig.26-1). All of these point mutations did not prevent homo-dimerization with RIBEYE(B) (Fig.26-2) and bound NADH (all except G730A) as judged by NADH-dependent energy transfer from tryptophan W867 to bound NADH (Alpadi *et al*., 2008) demonstrating the proper folding of these point mutants. Although these point mutants did not prevent homo-dimerization of RIBEYE(B), all of these point mutations (except for RIBEYE(B)K854Q) completely abolished interaction with RIBEYE(A) (Fig.27). This shows that

the two binding interfaces on RIBEYE(B) available for interaction with RIBEYE(A) and RIBEYE(B) and are distinct from each other although the interaction sites are spatially closely related. The binding site for RIBEYE(A) covers a large portion of the NBD (Fig.26-1). Interestingly, RIBEYE(B)G730, which is an essential component of the conserved NAD(H)-binding motif of RIBEYE (Schmitz *et al*., 2000), appears to be part of the interaction interface for RIBEYE(A): The point mutant RIBEYE(B)G730A that does not bind NAD(H) (Magupalli *et al*., 2008) can no longer interact with RIBEYE(A)(Fig.27C). We interpret the latter result that the binding sites for NAD(H) and for RIBEYE(A) are overlapping to a certain extent (see below and discussion). The docking site on RIBEYE(B) for RIBEYE(A) is denoted as "B2" in the following text.

1)

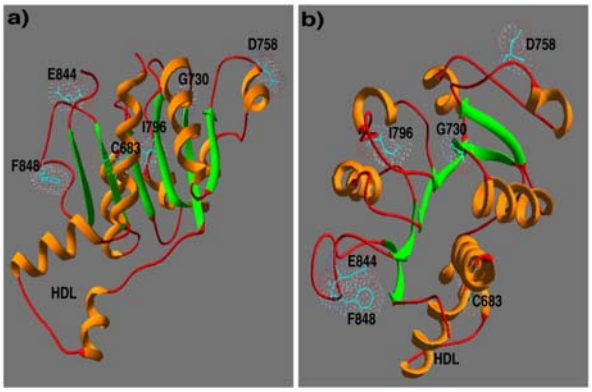

2)

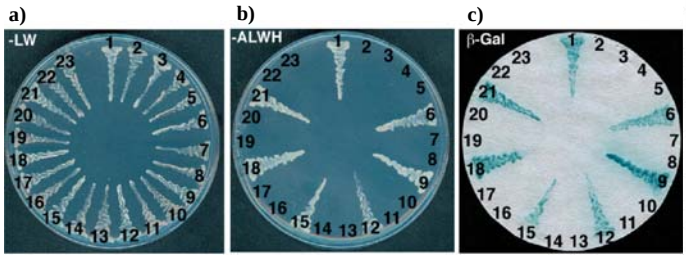

mating	bait	prey	-ALWH	βGal
1	RE(B)	RE(B)	+	+
2	pGBKT7	RE(B)	-	-
3	pSE1112	RE(B)	-	-
4	RE(B)	pACT2	-	-
5	RE(B)	pSE1111	-	-
6	RE(B)D758N	RE(B)	+	+
7	RE(B)D758N	pACT2	-	-
8	RE(B)D758N	pSE1111	-	-
9	RE(B)E844Q	RE(B)	+	+
10	RE(B)E844Q	pACT2	-	-
11	RE(B)E844Q	pSE1111	-	-
12	RE(B)F848W	RE(B)	+	+
13	RE(B)F848W	pACT2	-	-
14	RE(B)F848W	pSE1111	-	-
15	RE(B)K854Q	RE(B)	+	+
16	RE(B)K854Q	pACT2	-	-
17	RE(B)K854Q	pSE1111	-	-
18	RE(B)I796A	RE(B)	+	+
19	RE(B)I796A	pACT2	-	-
20	RE(B)I796A	pSE1111	-	-
21	RE(B)F904W	RE(B)	+	+
22	RE(B)F904W	pACT2	-	-
23	RE(B)F904W	pSE1111	-	-

Figure 26. Location of various NBD point mutants and its homo-dimerization with wildtype.

1) Model shows the location of various NBD point mutants on NAD(H) binding sub-domain. **a)** Lateral view of the NAD(H) binding sub-domain along with indicated point mutants. **b)** Top view of the NAD(H) binding sub-domain along with point mutants from the position of the bound NADH to the bottom of the molecule as seen in (a). **2)** The homo-dimerization was studied in YTH assay. For convenience, experimental bait-prey pairs were underlayered in color (green in case of interacting bait-prey pairs), control matings were non-colored. The studied point mutants RIBEYE(B)D758N, RIBEYE(B)E844Q, RIBEYE(B)F848W, RIBEYE(B)K854Q, RIBEYE (B) I796A and RIBEYE(B)F904W are all able to homo-dimerize (i.e., they interacts with wild type RIBEYE(B)). This is shown in (matings # 6, 9, 12, 15, 18, 21). Mating # 1 is a positive control (RIBEYE(B)-RIBEYE(B) interaction); the other (matings # 2-5, 7, 8, 10, 11, 13, 14, 16, 17, 19, 20, 22, 23) are the respective indicated controls. This study indicates that all the point mutated proteins were properly folded and were functional. None of the controls were auto-activating. Scoring (+) indicates the growth on –ALWH plate and β-galactosidase activity.

A)

mating	bait	prey	-ALWH	βGal
1	RE(B)	RE(A)	+	+
2	RE(B)	pACT2	-	-
3	RE(B)	pSE1111	-	-
4	pGBKT7	RE(A)	-	-
5	pSE1112	RE(A)	-	-
6	RE(B)C683S	RE(A)	-	-
7	RE(B)C683S	pACT2	-	-
8	RE(B)C683S	pSE1111	-	-
9	RE(B)C683S	RE(B)	+	+
10	pGBKT7	RE(B)	-	-
11	pSE1112	RE(B)	-	-

B)

mating	bait	prey	-ALWH	βGal
1	RE(B)	RE(A)	+	+
2	pGBKT7	RE(A)	-	-
3	pSE1112	RE(A)	-	-
4	RE(B)	pACT2	-	-
5	RE(B)	pSE1111	-	-
6	RE(B)F904W	RE(A)	+	+
7	RE(B)F904W	pACT2	-	-
8	RE(B)F904W	pSE1111	-	-
9	RE(B)K854Q	RE(A)	+	+
10	RE(B)K854Q	pACT2	-	-
11	RE(B)K854Q	pSE1111	-	-
12	RE(B)D758N	RE(A)	-	-
13	RE(B)D758N	pACT2	-	-
14	RE(B)D758N	pSE1111	-	-
15	RE(B)E844Q	RE(A)	-	-
16	RE(B)E844Q	pACT2	-	-
17	RE(B)E844Q	pSE1111	-	-
18	RE(B)F848W	RE(A)	-	-
19	RE(B)F848W	pACT2	-	-
20	RE(B)F848W	pSE1111	-	-
21	RE(B)I796A	RE(A)	-	-
22	RE(B)I796A	pACT2	-	-
23	RE(B)I796A	pSE1111	-	-

C)

mating	bait	prey	-ALWH	βGal
1	RE(B)	RE(A)	+	+
2	RE(B)	pACT2	-	-
3	RE(B)	pSE1111	-	-
4	pGBKT7	RE(A)	-	-
5	pSE1112	RE(A)	-	-
6	RE(B)G730A	RE(A)	-	-
7	RE(B)G730A	pACT2	-	-
8	RE(B)G730A	pSE1111	-	-
9	RE(B)G730A	RE(B)	+	+
10	pGBKT7	RE(B)	-	-
11	pSE1112	RE(B)	-	-
12	RE(B)	RE(B)	+	+

Figure 27. Mapping of RIBEYE(A) -RIBEYE(B) interaction using NBD point mutants in YTH assay.

For convenience, experimental bait-prey pairs were underlayered in color (green in case of interacting bait-prey pairs; yellow in case of non-interacting bait-prey pairs); control matings were non-colored. **A)** The RIBEYE (B) point mutant RIBEYE(B)C683S can no longer interact with RIBEYE (A) (mating # 6) but can still interact with RIBEYE (B) (mating # 9). Mating # 1 shows the positive control (RIBEYE (A) - RIBEYE (B) interaction. Matings (# 2-5, 7-8, 10-11) are controls. **B)** The RIBEYE point mutant RIBEYE (B) K854Q interacts both with RIBEYE (A) (mating # 9) as well as with RIBEYE (B) (Fig. 26). RIBEYE (B) F904W also interacts both with RIBEYE (A) (mating # 6) as well as with RIBEYE (B) (Fig. 26). In contrast, RIBEYE (B) D758N, RIBEYE (B) E844Q, RIBEYE (B) F848W and RIBEYE (B) I796A did no longer interact with RIBEYE (A) (matings # 12, 15, 18, 21) although all of these point mutants still interacted with RIBEYE (B) (Fig. 26). Mating # 1 represents the positive control (RIBEYE (A)-RIBEYE (B) interaction). Matings # 2-5, 7, 8, 10, 11, 13, 14, 16, 17, 19, 20, 22 and 23) represents the respective controls. **C)** The NADH binding-deficient RIBEYE(B)G730A can no longer interact with RIBEYE(A) (mating # 6) although it still interacts with RIBEYE(B) wild type protein (mating # 9). Mating # 12 is a positive control suggesting the RIBEYE(B) homo-dimerizes i.e., RIBEYE(B) interacts with RIBEYE(B) . None of the constructs were auto-activating. Scoring (+) indicates the growth on –ALWH plate and β-galactosidase activity.

3.1.8 NAD$^+$ and NAD(H) inhibit RIBEYE(A)-RIBEYE(B) interaction

In the previous experiment, I found that RIBEYE(A) binds to the NAD(H)-binding sub-domain of RIBEYE(B). It is known that RIBEYE (B) binds to NAD(H) with high affinity and shares a high sequence homology with D-isomer-specific 2- hydroxyl acid dehydrogenases (Schmitz *et al*., 2000). Since RIBEYE(A) docks to a broad interface of the NAD(H)-binding sub-domain of RIBEYE(B), I analyzed whether this interaction is dependent on NAD(H). This question I analyzed with protein pull-down assay. I used RIBEYE(A)-GST as immobilized bait and eluted RIBEYE(B)-MBP as soluble prey protein and checked for interaction of these proteins in the presence of increasing concentrations of NAD$^+$/NADH (Fig.28A&B). Increasing concentrations of NAD$^+$/NADH strongly inhibited RIBEYE(A)-RIBEYE(B) interaction. Both NAD$^+$ as well as NADH strongly inhibited RIBEYE(A)-RIBEYE(B) interaction at physiologically relevant low concentrations (Zhang *et al*., 2002 and Fjeld *et al*., 2003). The difference in binding of prey, RIBEYE(B) by bait RIBEYE(A) is quite evident in the conditions such as the presence and absence of NAD(H).

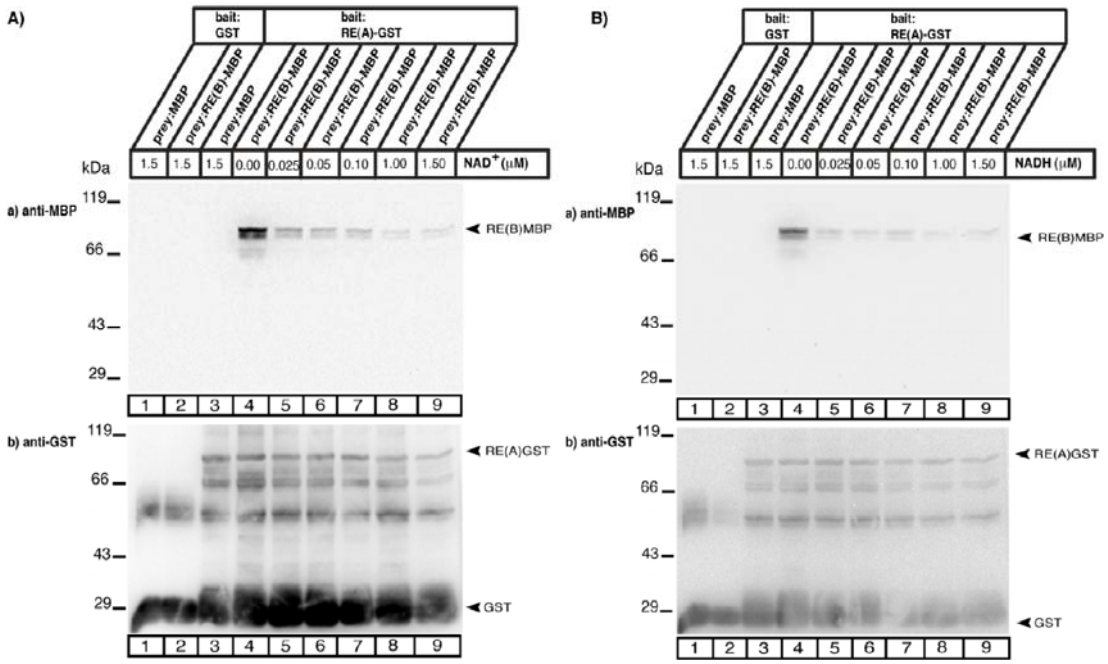

Figure 28. NAD$^+$ and NAD(H) inhibits RIBEYE(A) and RIBEYE(B) interaction.

0.3µM of immobilized RIBEYE(A)-GST fusion protein were incubated with 0.3µM of RE(B)-MBP in the presence of the indicated concentrations of NAD$^+$ (Fig. 28 **A**) or NADH (Fig. 28 **B**) for 3hrs at 4°C in binding buffer. a) Binding of the prey proteins was analyzed by probing with antibodies against MBP. b) Equal loading of bait partners was verified by stripping the same blot and reprobing with anti-GST to show equal loading of bait proteins.

3.1.9 RIBEYE co-aggregates in transfected cells

In order to determine whether the identified RIBEYE-RIBEYE-interactions can also occur *in vivo* within a cellular context, I transfected the indicated RIBEYE expression constructs that were differentially tagged either with EGFP or with mRFP in COS7 and the R28 retinal progenitor cell line (Seigel, 1996; Seigel *et al*., 2004). R28 cells express retinal and neuronal marker proteins (e.g. opsins, beta-2 arrestin, recoverin, neurotransmitter receptors, various pre- and postsynaptic proteins) in addition to stem cell/precursor cell markers (e.g. nestin) (Seigel *et al*., 2004). If transfected alone, both RIBEYE(A) as well as RIBEYE(AB) displayed a discrete, spot-like distribution whereas RIBEYE(B)-domain is diffusely distributed (Figs.29,30&31) as also previously described (Schmitz *et al*., 2000). If RIBEYE(A)-EGFP was cotransfected with RIBEYE(A)-mRFP both co-aggregated to the same protein clusters as judged by the large extend of colocalization of the EGFP and mRFP signals. Identical results were obtained if full-length RIBEYE(AB)-EGFP was cotransfected with RIBEYE(A)-mRFP (Fig.29:C&A) respectively. If RIBEYE(B)-EGFP was cotransfected with RIBEYE(B)-mRFP both signals remained diffusely distributed (Fig.30C and Fig.31E). Interestingly, if RIBEYE(B)-mRFP was cotransfected with RIBEYE(A)-EGFP, RIBEYE(B)-mRFP redistributed from a diffuse distribution (as typical for single transfected RIBEYE(B)), to a patchy, spot-like distribution that is typical for RIBEYE(A). Part of RIBEYE(B) remained diffusely distributed (Fig.29D,E and Fig.31D) probably due to the NAD(H) sensitivity of RIBEYE(B)-RIBEYE(A) interaction (see above). NAD(H) is ubiquitously present in the cytoplasm and expected to partly dissociate RIBEYE(A)-RIBEYE(B). Interestingly, in cells double-transfected with full-length RIBEYE(AB) and RIBEYE(B), RIBEYE(B) virtually completely redistributed from the diffuse distribution to the spot-like distribution typical for RIBEYE(AB) and perfectly colocalized with RIBEYE(AB) (Fig. 29B; Fig. 30B; and Fig. 31A). From these latter experiments we conclude, that both homotypic domain interactions (RIBEYE(B) - RIBEYE(B) interactions) as well as heterotypic domain interactions (RIBEYE(A)-RIBEYE(B) interactions) support the interaction between RIBEYE(AB) and RIBEYE(B). As judged by the nearly complete colocalization of RIBEYE(AB) and RIBEYE(B) compared with cells double-transfected with RIBEYE(A) and RIBEYE(B), we assume that a combination of homotypic and heterotypic domain interactions is probably stronger than a single type of homotypic interactions. Qualitatively identical results as described above for COS7 cells were also obtained with R28 cells (Fig.31). Together, the coaggregation and colocalization data in the transfected COS 7 and R28 cells indicate that the interaction sites between RIBEYE(A)-domain and RIBEYE(B)-domain, either between the

same type of domains (A-A, B-B) or between different domains (A-B), are also available within a cellular context.

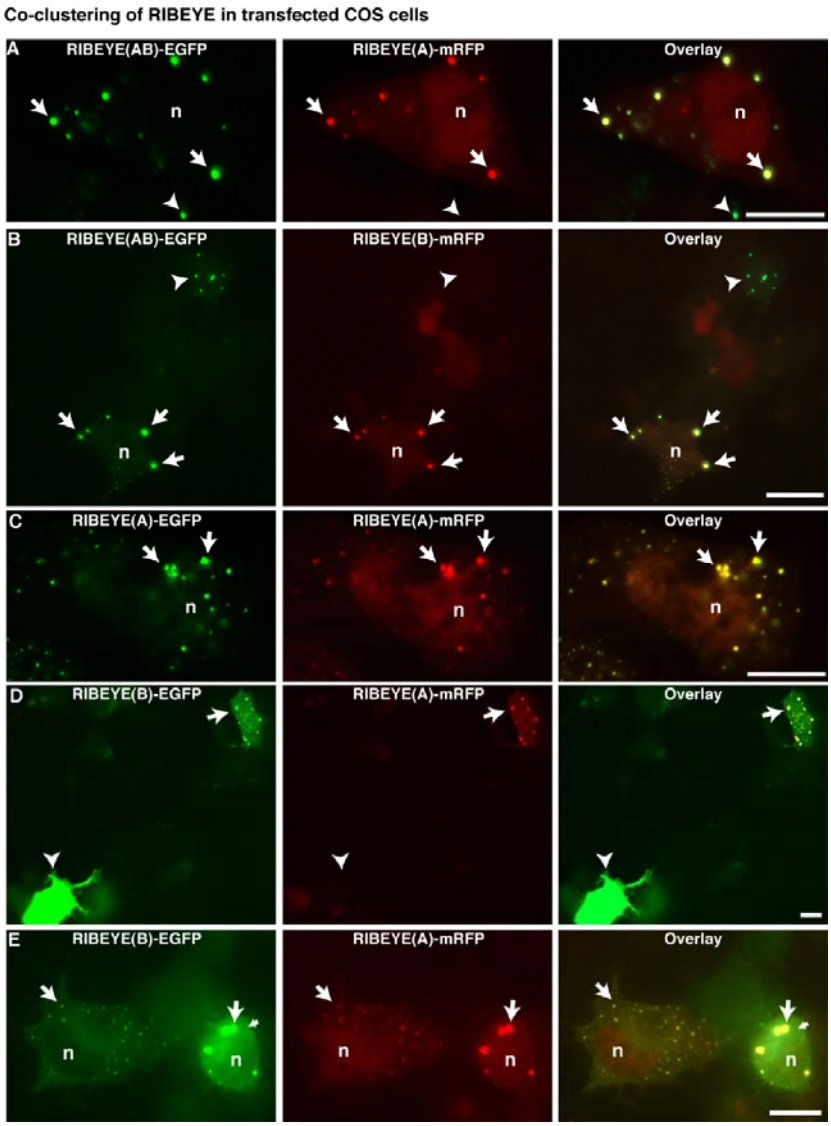

Figure 29. Co-clustering of different RIBEYE-proteins in cotransfected COS cells.

COS cells were transfected with the indicated mRFP- or EGFP-tagged RIBEYE constructs. Transfected cells were analyzed for the intracellular distribution of the respective proteins via direct epifluorescence microscopy. **A-B)** RIBEYE(AB)-EGFP co-aggregated and co-localized with RIBEYE(A)-mRFP (Fig. 29**A)** and RIBEYE(B)-mRFP (Fig. 29**B)** ; RIBEYE(B) is diffusely expressed in single-transfected cells (Schmitz *et al*., 2000; arrowhead in Fig. 29D, see also Figs. 30&31). The arrowhead in (Fig. 29**B)** shows a single transfected cell that is transfected only with RIBEYE(AB)-EGFP but not with RIBEYE(B)-mRFP. If RIBEYE(B) is cotransfected with RIBEYE(AB) (Fig. 29B), RIBEYE(B) virtually completely redistributed from a diffuse distribution into a spot-like, RIBEYE(AB)-typical distribution and co-localized with RIBEYE(AB), respectively (arrows in Fig. 29**B)**. RIBEYE(B) also redistributed from a diffuse to spot-like distribution if cotransfected with RIBEYE(A) (Fig. 29 **D, E**); part of RIBEYE(B) remained diffusely distributed (small arrow in E). The higher degree of co-distribution of RIBEYE(B) with RIBEYE(AB) in comparison to RIBEYE(A) probably represents the fact that more type of interactions can be formed between RIBEYE(B) and RIBEYE(AB) than between RIBEYE(B) and RIBEYE(A) alone (for summary, see Fig. 36). RIBEYE(A) also co-aggregated and co-localized with RIBEYE(A) (Fig. 29**C)**. For further examples of transfected COS cells, see also Fig. 30. R28 cells transfected with the respective plasmids produced qualitatively identical results (Fig. 31). Abbreviations. n, nucleus. Scale bars: 10µm.

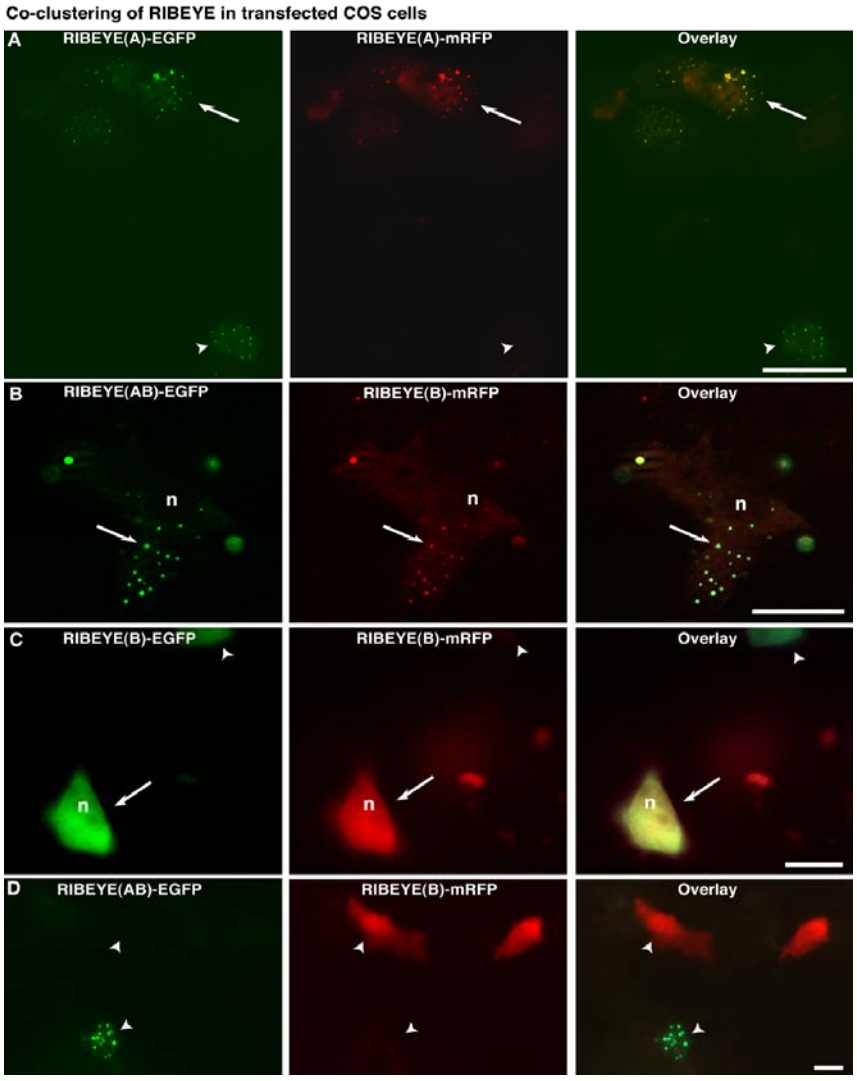

Figure 30. Co-clustering of different RIBEYE-proteins in cotransfected COS cells (continued).

Further examples of COS cells transfected with the indicated EGFP- or mRFP-tagged RIBEYE constructs. If single transfected RIBEYE (B) diffusely distributed **(**arrowhead in **D)** as previously described (Schmitz *et al*., 2000). The distribution is independent of the used fluorescent tag. In contrast, RIBEYE(A) and RIBEYE(AB) shows a discrete, punctuate distribution **(A&B)** as previously described (Schmitz *et al*., 2000). **A)** If RIBEYE(A) EGFP cotransfected with RIBEYE(A)mRFP both proteins co-aggregate into the same protein clusters (arrows). **B)** If RIBEYE(B) was cotransfected with RIBEYE(AB), RIBEYE(B) nearly completely redistributed to a spot-like distribution typical for RIBEYE(AB) (arrows) and only a small portion of RIBEYE(B) remained diffusely distributed. **D)** Cells are shown that are transfected either only with RIBEYE(AB) EGFP or only with RIBEYE(AB) mRFP to demonstrate the distribution of the respective proteins in single transfected cells. Arrowheads indicate single transfected cells. Abbreviations: n, nucleus. Scale bars: 10µm.

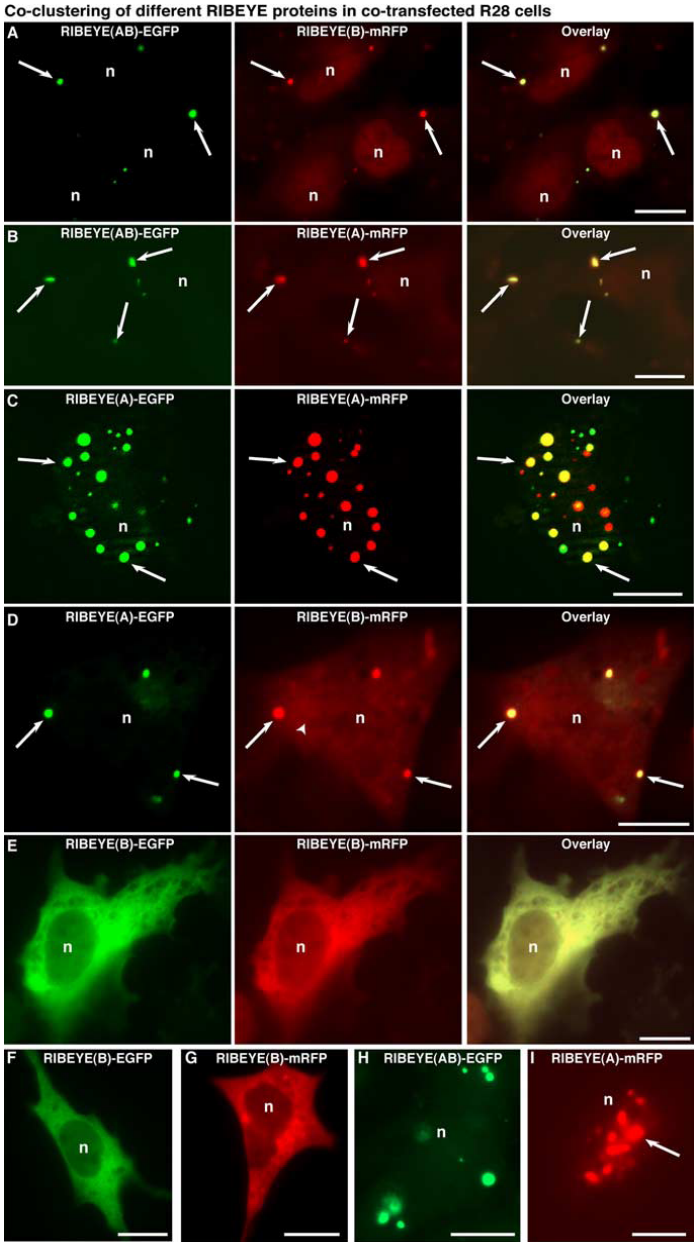

Figure 31. Co-clustering of different RIBEYE-proteins in cotransfected R28 cells.

A-H) R28 cells were transfected with the indicated EGFP- or mRFP-tagged RIBEYE constructs. Transfected cells were analyzed for the intracellular distribution of the respective fusion protein via direct epifluorescence microscopy. RIBEYE(AB) **(H)** and RIBEYE(A) (**I)** shows a discrete spot-like distribution, as already shown previously (Schmitz *et al*., 2000). In contrast, RIBEYE(B) is diffusely distributed in single-transfected cells (Schmitz *et al*., 2000) **(F**,**G)**. **A)** If, RIBEYE(B) is cotransfected with RIBEYE(AB), RIBEYE(B) virtually completely redistributed from a diffuse distribution into a spot-like, RIBEYE(AB)-typical distribution and colocalize with RIBEYE(AB) (arrows) (see also Fig. 29 & 30). **D)** RIBEYE(B) also redistributed from a diffuse to spot-like distribution if cotransfected with RIBEYE(A), part of RIBEYE(B) remained diffusely distributed (arrowhead) (see also Fig. 29). The higher degree of codistribution of RIBEYE(B) with RIBEYE(AB) compared with RIBEYE(A) probably represents the fact that more type of interactions can be formed between RIBEYE(B) and RIBEYE(AB) than between RIBEYE(B) and RIBEYE(A) (for a summary, see Fig. 36). RIBEYE(A) also coaggregates and colocalize with RIBEYE(A) **(C**, arrows**)**. If RIBEYE(B)-EFGP was cotransfected with RIBEYE(B)-mRFP both proteins remained diffusely distributed and did not generate a spot-like distribution **(E)**. The arrows in **(A-D)** point to intracellular RIBEYE aggregates that contain both type of the indicated differentially tagged RIBEYE proteins. The arrow in **(I)** points to an intracellular RIBEYE(A)-containing aggregate. COS cells transfected with the respective plasmids produced qualitatively identical results (Fig. 29&30). Abbreviations: n, Nucleus. Scale bars: 10µm.

3.1.10 Synaptic ribbons recruit externally added RIBEYE subunits(s)

In order to further characterize RIBEYE-RIBEYE interactions, I employed ribbon recruitments assays. In this experiment, purified RIBEYE domains as fusion protein were used as prey against synaptic ribbon fraction. It's known and evident that RIBEYE is the major components of the synaptic ribbons (Schmitz *et. al*., 2000) and amounts to 67% of total ribbon volume (Zenisek *et. al*., 2004). Yeast two-hybrid and the protein pull-downs were suggestive of RIBEYE (A) interacts RIBEYE (A) as well as RIBEYE (B). Based on this background information, I hypothesize that an isolated synaptic ribbon fraction should recruit RIBEYE(A)- and RIBEYE(B)-domains. Synaptic ribbons were purified as previously described (Schmitz *et al*., 1996; 2000). I tested whether isolated, RIBEYE-containing synaptic ribbons can recruit externally added RIBEYE(A)-GST and RIBEYE(B)-GST fusion proteins. GST alone was used as control protein. Purified synaptic ribbons binds soluble RIBEYE(B)-GST (lane 8) and RIBEYE(A)-GST(lane 9) fusion proteins (Fig.32). GST control protein did not bind to synaptic ribbons demonstrating the specificity of binding (lane 7).

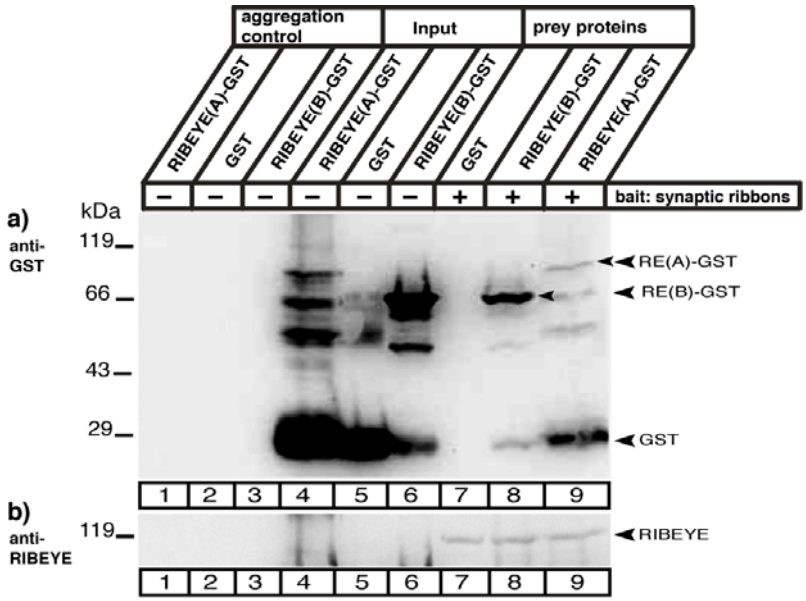

Figure 32. Synaptic ribbons recruit additionally added RIBEYE subunits.

Purified synaptic ribbons (180µg) were incubated with the indicated RIBEYE fusion proteins (approx. 3.5µM) and then sedimented by a 1min spin at 3,500 rpm. Fusion proteins that cosedimented with synaptic ribbons were detected by western blotting with the respective indicated antibodies. Lanes 4-6 show the respective input fractions, lane 1-3 the respective auto-aggregation controls of the soluble fusion proteins to test whether ribbon-independent sedimentation of fusion proteins occurs. The auto-aggregation controls show that in the absence of synaptic ribbons no fusion proteins are found in the pellet. In contrast, if synaptic ribbons were incubated with the fusion proteins the RIBEYE(A)-GST as well as RIBEYE(B)-GST could be sedimented by purified synaptic ribbons but not GST alone demonstrating the specificity of the binding of RIBEYE-fusion proteins to synaptic ribbons. The blot in (b) is same as in (a) but was stripped and reprobed with antibodies against RIBEYE (U2656) to show that equal amounts of purified synaptic ribbons were used as bait for the ribbon pull-downs. RIBEYE signals from isolated synaptic ribbons (bait) were denoted by an arrowhead in lanes 7-9.

Besides the full length RIBEYE(A)-domain the A1-MBP, A2-MBP and A3-MBP were tested for their ability to interact with the isolated synaptic ribbons (Fig.33). The A1 and A3 were found to be binding to the synaptic ribbons (lane7&8) respectively. The A2 was not interacting with the isolated synaptic ribbons (lane 9). This finding strengthens my earlier finding i.e., that full length RIBEYE(A) binds to the synaptic ribbon. Also, the binding of A1 and A3 to the synaptic ribbon as compared to A2 suggests that A3 binding site is exposed which then available for interaction. Most of the RIBEYE (A)-domain is buried inside the synaptic ribbons and part of it is exposed. Thus, the RIBEYE-RIBEYE interaction sites were accessible on synaptic ribbons. These were available to recruit externally added, additional RIBEYE proteins. This recruitment of additional RIBEYE subunits to pre-existing ribbons could explain the known dynamic growth and ultrastructural plasticity of synaptic ribbons (see discussion).

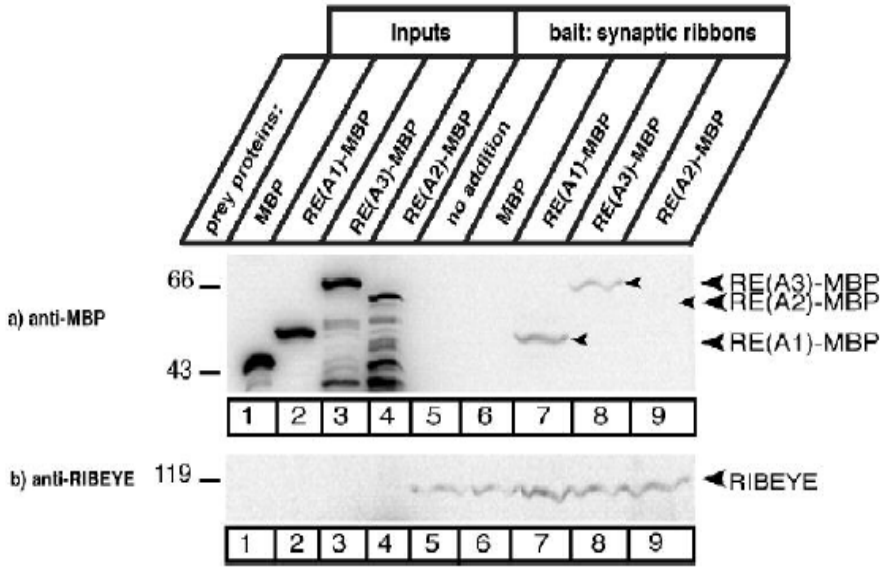

Figure 33. Synaptic ribbons recruits externally added RIBEYE(A) –sub-domains.

RIBEYE(A) sub-domains expressed as MBP-fusion proteins are recruited to synaptic ribbons in the same manner as GST-fusion proteins (Fig.32). RIBEYE(A1)-MBP and RIBEYE(A3)-MBP bound to synaptic ribbons (lanes7,8) whereas MBP alone did not (lane6) demonstrating the specificity of the interaction. Interestingly, RIBEYE(A2)-MBP did not bind to purified synaptic ribbons (lane9) although it efficiently interacted with RIBEYE(A) subunits (RIBEYE(A1), RIBEYE(A2)) in protein pull-down assays (Fig. 19). In Fig.33b, the same blot as in Fig.33a was stripped and reprobed with antibodies against RIBEYE (U2656) to show that equal amounts of purified synaptic ribbons were used as bait for the ribbon pull-downs. RIBEYE signal from isolated synaptic ribbons (bait) were denoted by an arrowhead in lanes 5-9. Lane 1-4 shows the input proteins.

3.1.11 RIBEYE-induced protein aggregates recruits endogenous bassoon

In order to further address the physiological relevance of the RIBEYE aggregates we tested whether these structures were related to bassoon, a physiological interaction partner of RIBEYE at the active zone of ribbon synapses (tom Dieck *et al*., 2005). Bassoon is endogenously expressed in R28 retinal precursor cells as judged by immunocytochemistry, western blotting, and RT-PCR (data not shown). Bassoon is distributed in R28 in a spot-like manner (Fig. 34D, arrowheads, in middle panel). The RIBEYE clusters in RIBEYE(AB-)EGFP transfected R28 cells largely formed around this bassoon-containing clusters and colocalized with bassoon (Fig.34A-C, arrows). The preferential colocalization between RIBEYE and its physiological interaction partner bassoon emphasizes the physiological relevance and ribbon-like partial function of the RIBEYE-containing protein aggregates.

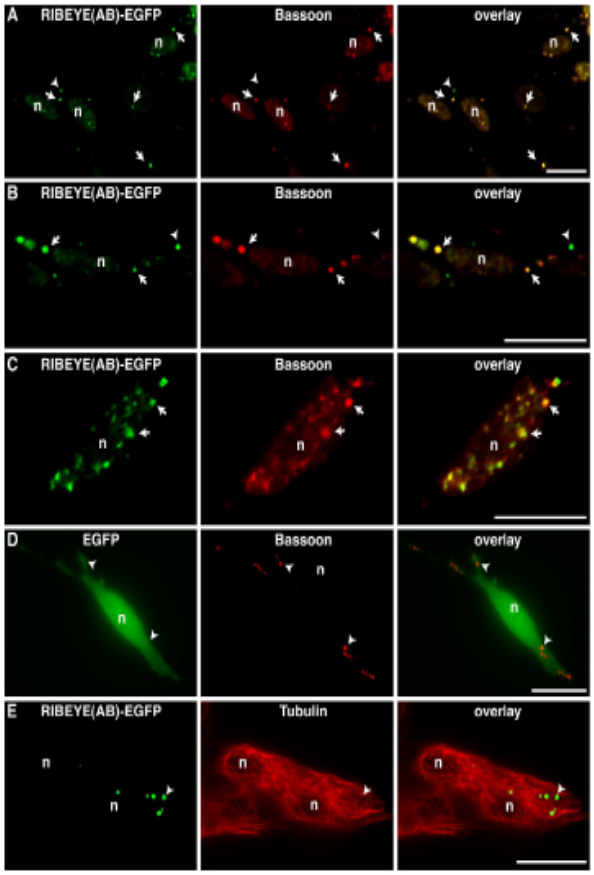

Figure 34. **RIBEYE co-assembles with the active zone protein bassoon in R28 cells.**

R28 retinal precursor cells were transfected with plasmids encoding for the indicated EGFP-tagged proteins. **A-E)** The distribution of the endogenously present active zone protein bassoon **(A-D)** or tubulin **(E)** was visualized by indirect immunofluorescence microscopy. In R28 cells, bassoon is endogenously present as discrete protein clusters **(A-C**, middle, arrows**)**. Heterologously expressed RIBEYE-EGFP co-aggregates with these pre-existing bassoon clusters **(A-C**, arrows**)** but not EGFP alone **(D)**. **D)** Endogenous bassoon (arrowheads) did not recruit EGFP alone. The arrowheads in **(A&B)** show RIBEYE clusters that aggregated independent of the endogenous bassoon. **E)** The RIBEYE(AB)-EGFP clusters (arrowhead) do not co-localize with microtubules, which were visualized by immunostaining with antibodies against tubulin. Abbreviations: n, Nucleus. Scale bars: 10µm.

3.1.12 Physiological role of RIBEYE induced protein aggregates

RIBEYE is the major component of synaptic ribbons and RIBEYE forms large protein clusters in transfected cells (Figs.29,30,31&34). Above we showed that, the RIBEYE co-aggregates at bassoon containing sites (see section 3.1.11). The *in vivo* recruitment of active zone protein bassoon by RIBEYE, mimics scenario similar to a synapse. Next, we were interested to analyze the ultrastructural appearance of the RIBEYE-containing aggregates by electron microscopy to find out whether these structures in transfected R28 cells have similarities with synaptic ribbons (Fig.35). Using conventional transmission electron microscopy, we observed large electron-dense aggregates in RIBEYE-EGFP transfected R28 cells (A-J) which were absent in control cells (K). Similar, large electron-dense protein aggregates were also present in RIBEYE(AB)-EGFP transfected COS cells but not in EGFP-transfected COS cells (data not shown). The large aggregates typically displayed a spherical shape with a diameter between of 200-500nm. These electron-dense structures were often surrounded by vesicles which in part were physically attached to the electron-dense aggregates via thin electron-dense stalks (arrowheads in Fig.35 A-J). These large spherical structures were strongly positive for RIBEYE by immunogold labelling with antibodies against RIBEYE (Fig.35 L-N) but not reactive with antibodies against tubulin (O) or RIBEYE pre-immune serum (P) (control incubations). These spherical structures have similarities to spherical synaptic ribbons of inner hair cells (for review, see Nouvian *at al*., 2006). Beside the large electron-dense particles we also found smaller aggregates which showed physical contacts between each other and which sometimes appeared to coalesce into larger, electron-dense structures (Fig.35 E, F). This could be explained as a result of direct RIBEYE-RIBEYE interaction, generating bigger structures. These structures were also partly physically linked to surrounding vesicles and show some resemblance to synaptic spheres, intermediate structures in the assembly and disassembly of synaptic ribbons (for review, see Vollrath and Spiwoks-Becker, 1996; see also discussion).

Our EM findings show the ribbon like-structures are generated as a result of multiple RIBEYE-RIBEYE interaction. Further, the proximity of these structures to the surrounding vesicles and membranes emphasizes the physiological relevance of these RIBEYE-containing structures.

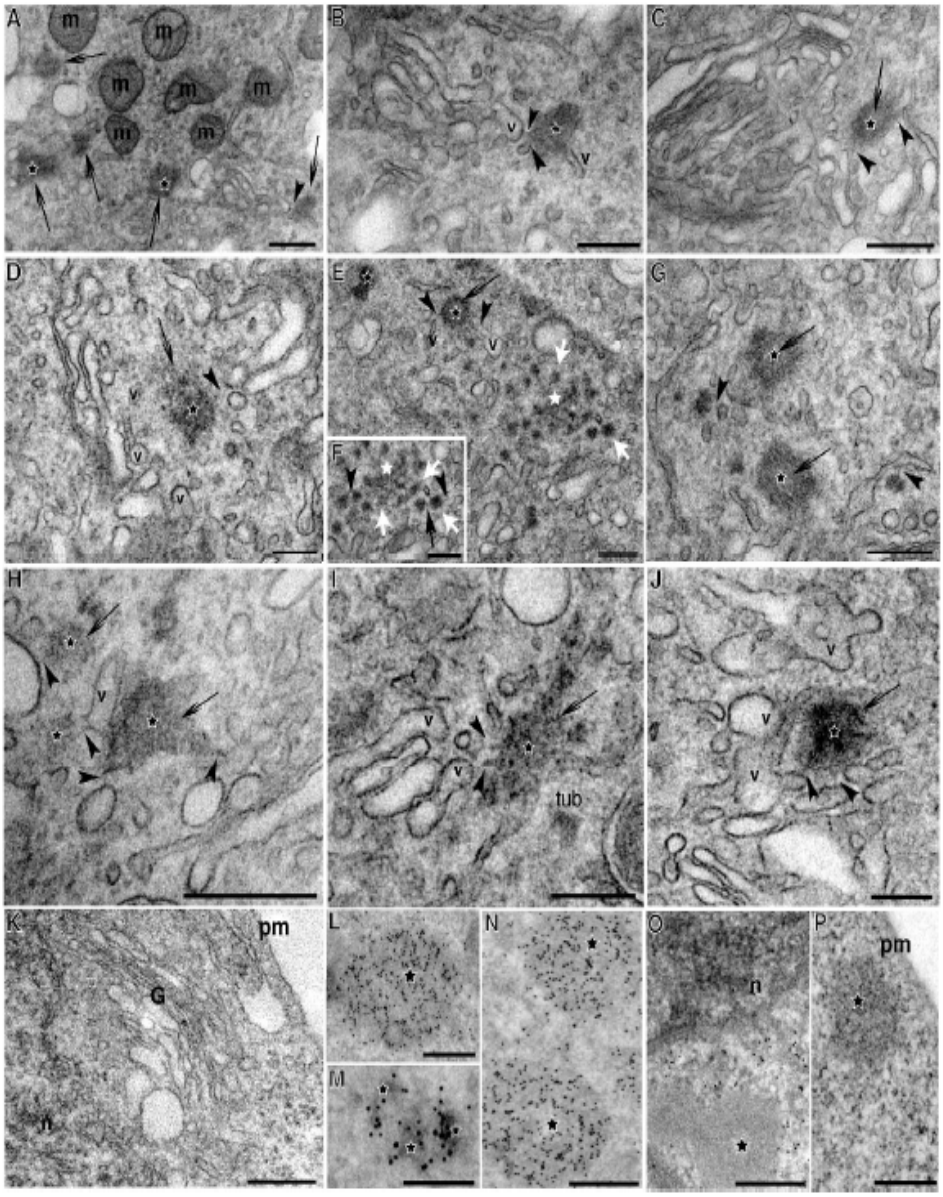

Figure 35. **Electron microscopy of RIBEYE -containing aggregates in transfected R28 cells**.

RIBEYE forms synaptic sphere-like structure in R28 cells. **A-K)** Conventional transmission microscopy of RE(AB)-EGFP- **(A-J)** and EGFP-transfected cells **(K)**. **L-P)** Immunogold electron microscopy of RE(AB)-EGFP-transfected cells immunolabeled with antibodies against RIBEYE **(L-N)**, tubulin **(O)** and control immunoglobulins **(**RIBEYE pre-immune; **P)**. **A)** Low magnification of RE(AB)-EGFP-transfected cells. Note the presence of large electron-dense material (200-500nm in diameter) in RIBEYE-transfected cells **(A-J**, asterisks and large black arrows**)**. These electron-dense structures are mostly spherical in shape **(A-G**, **J** asterisks**)**, although more irregular profiles are also present **(H**, **I** asterisks**)**. These electron-dense structures **(A-J)** were often surrounded by vesicles, which in part were physically attached to the electron-dense aggregates via thin electron-dense stalks **(A-J**, arrowheads**)**. In addition to the large electron-dense spheres, smaller electron-dense structures could be observed **(E**, **F**, white arrows**)**. Neighboring small electron-dense aggregates **(E**, **F**, white arrows**)** appear at least partly physically connected to each other **(F**, black arrow**)** and sometimes appeared to coalesce into larger, electron-dense structures **(E**, **F**, white asterisk**)**. **K)** Ultrastructure of a control-transfected cell. Both the large **(L**, **N)** as well as the small electron-dense aggregates **(M)** were strongly immunolabeled by RIBEYE antibodies. The aggregates were densely decorated by immunogold particles. **(O**, **P)** RE(AB)-EGFP transfected cell immunolabeled with antibodies against tubulin **(O)** and RIBEYE-pre-immune serum **(P)**. In no case a specific labelling of the electron-dense aggregates (asterisks) was observed. Abbreviations: n, Nucleus; m, mitochondria; G, Golgi apparatus; v, vesicles; tub, membrane tubule; pm, plasma membrane. Scale bars: 500nm **(A)**; 250nm **(B)**; 400nm **(C)**; 250nm **(D-F)** 300nm **(G-I)**; 250nm **(J)**; 400nm **(K)**; 200nm **(L-P)**.

3.1.13 Schematic RIBEYE-RIBEYE interaction model

On the basis of the genetic, biochemical and morphological findings we present here a summary of identified interaction. In the A-domain of RIBEYE three interaction modules are present which are denoted as A1, A2 and A3. In the B-domain of RIBEYE two interaction modules, denoted as B1 and B2, are present. Further, the intradomain RIBEYE(A2)- RIBEYE(B) interaction is inhibited by NAD(H). This could explain the dynamic nature of synaptic ribbons. All mapped interaction are summarized as shown in figure 36.

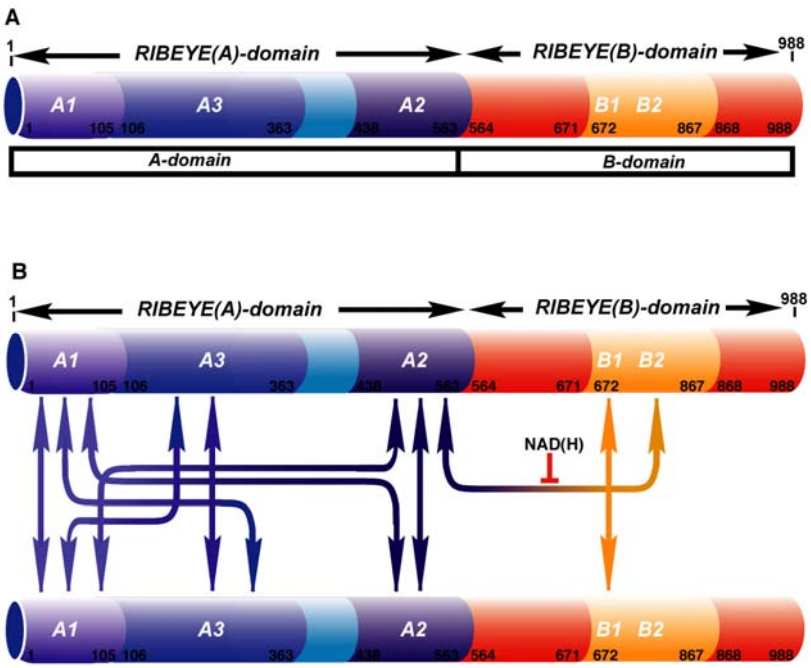

Figure 36. Schematic RIBEYE-RIBEYE interaction model.

A) Summarizes the identified RIBEYE-RIBEYE-interaction modules. In the A-domain of RIBEYE three interaction modules are present which are denoted as A1, A2 and A3. In the B-domain of RIBEYE two interaction modules, denoted as B1 and B2, were present. **B**) The interaction combinations between the identified interaction modules were summarized. Only for the upper RIBEYE molecule all possible intermolecular homotypic domain interactions were shown. Homotypic domain interactions, e.g. RIBEYE(A)-RIBEYE(A) interaction can be mediated by homotypic sub-domain interactions, e.g. RIBEYE(A1)-RIBEYE(A1), or by heterotypic sub-domain interaction, e.g. RIBEYE(A1)-RIBEYE(A2).

3.2 IDENTIFICATION AND FURTHER ANALYSIS OF RIBEYE -TULP 1 INTERACTIONS

3.2.1 RIBEYE interacts with the photoreceptor specific TULP1 in YTH assay

In the YTH screening, using RIBEYE(B)-domain as bait and a retinal cDNA library as prey we obtained a Tulp1 clone that encoded for large part of the tubby-domain of Tulp1 (Fig.37). TULP 1 is a photoreceptor specific phospholipids binding protein. Its exclusive expression in photoreceptors, which also station synaptic ribbons in the presynaptic terminals, made it an interesting candidate. It was further analyzed in the present study.

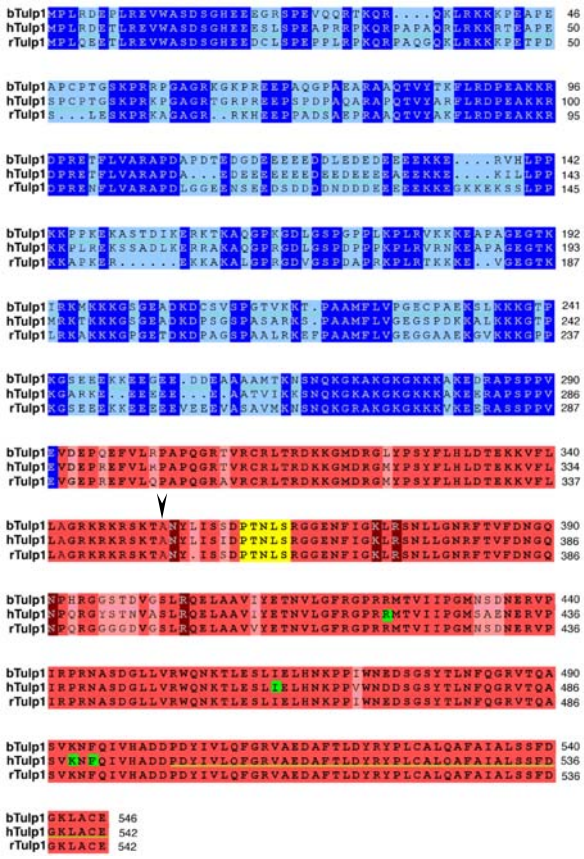

Figure 37. Amino acid sequence of bovine, human and rat TULP 1.

The sequences from bovine, human and rat are identified on the left as bTULP1, hTULP1, and rTULP1, respectively. Blue color indicates the Trans-activation domain (TAD) of TULP1. Residues in the TULP1 sequence that are shared among three species are highlighted in dark-blue color. Red color indicates the conserved tubby-domain. Yellow color indicates the PTNLS motif. Brown color indicates the amino acids implicated in phosphatidylinositol binding. Arrowhead indicates beginning of the coding region of the fished Tulp 1 prey clone. Amino acids marked in green are human TULP1 mutations. Underline with green color represents 44 amino acid exon deletion from tubby mouse. Accession number NCBI date bank: NP 067453 (mTulp1), CAI20251 (hTulp1).

The interaction between RIBEYE(B) and Tulp1 was further confirmed, by using RIBEYE(B) as bait and the entire tubby-domain of Tulp1 as prey in YTH assay. We found that RIBEYE(B) interacts with the tubby-domain of Tulp1 as judged by the growth on –ALWH selective plate and the β-galactosidase marker gene expression (Fig.38:Ba and C). All the studied constructs were not auto-activating in the YTH assay as shown by the corresponding control matings. I also tested whether full-length RIBEYE (RIBEYE(AB)) interacts with the tubby-domain of Tulp1 in the YTH assay. Indeed, also full length RIBEYE(AB) interacts with the tubby-domain of Tulp1 (Fig.38:Bb). These findings indicate that the A-domain RIBEYE did not prevent interaction of RIBEYE(B) with Tulp1. On the contrary, full length RIBEYE(AB) appeared to interact much stronger with the tubby-domain of Tulp1 then RIBEYE(B) alone (Fig.38:Bd and Ba). Therefore, I tested whether also the A-domain of RIBEYE could interact with the tubby-domain of Tulp1. YTH mating analysis indeed showed that RIBEYE(A) also interacts with tubby-domain of Tulp1(Fig.38:Bc). All the studied yeast constructs were not auto-activating demonstrating the specificity of interaction. Full-length RIBEYE not only interacted with the tubby-domain of Tulp1 but also with full-length Tulp1 (Fig.38:Bd)

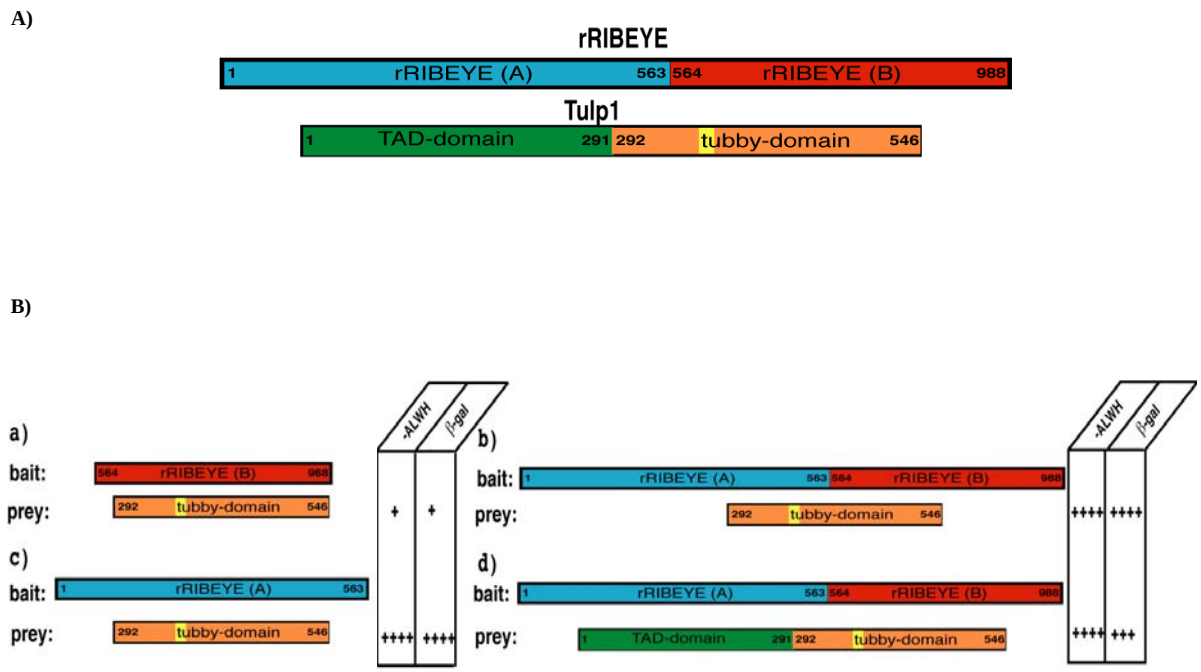

C)

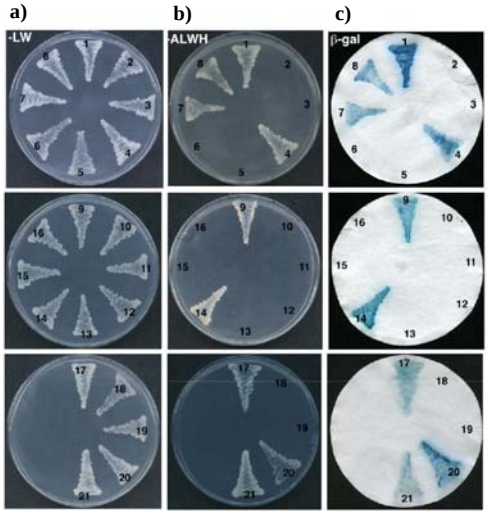

mating	bait	prey	-ALWH	β-Gal
1	RE(B)	Tulp1(353-546)	+	+
2	RE(B)	pACT2	–	–
3	RE(B)	pSE1111	–	–
4	RE(AB)	Tulp1(292-546)	+	+
5	pGBKT7	Tulp1(292-546)	–	–
6	pSE1112	Tulp1(292-546)	–	–
7	RE(A)	Tulp1(292-546)	+	+
8	RE(B)	Tulp1(292-546)	+	+
9	RE(AB)	Tulp1(353-546)	+	+
10	RE(AB)	pACT2	–	–
11	RE(AB)	pSE1111	–	–
12	pGBKT7	Tulp1(353-546)	–	–
13	pSE1112	Tulp1(353-546)	–	–
14	RE(A)	Tulp1(353-546)	+	+
15	RE(A)	pACT2	+	+
16	RE(A)	pSE1111	–	–
17	RE(AB)	Tulp1(1-546)	+	+
18	pGBKT7	Tulp1(1-546)	–	–
19	pSE1112	Tulp1(1-546)	–	–
20	RE(A)	Tulp1(1-546)	+	+
21	RE(B)	Tulp1(1-546)	+	+

Figure 38. RIBEYE interacts with TULP 1 in YTH assay.

A) Detailed outline of RIBEYE and TULP 1 constructs used in YTH assay. Two distinct domains of RIBEYE molecule were shown as A- and B- domains. These were represented by blue and red color respectively. Transactivation domain (TAD) and conserved tubby-domain of TULP1 were depicted in green and orange color respectively. Yellow color in tubby-domain represents the pentapeptide PTNLS motif. **B**) Interacting domains found in YTH assay. Tubby-domain interacts with **Ba)** RIBEYE(B) **Bb)** full length RIBEYE molecule. **Bc)** RIBEYE(A)-domain interacts with tubby-domain. **Bd)** and full-length TULP1 interacts with full-length RIBEYE. Scoring (+) indicates the number of colonies and the intensity of β-galactosidase activity on selective plates and filters, respectively. This was higher in case of full length RIBEYE as compared to RIBEYE(B)-domain alone. **C)** Summary of YTH matings. For convenience, experimental bait-prey pairs were underlayered in color (green in case of interacting bait-prey pairs); control matings are non-colored. **Ca)** Indicates the growth on -LW plates. **Cb)** Indicates the growth on selective –ALWH plates suggestive of interaction. **Cc)** Qualitatively the interaction is shown by β-galactosidase filter test. Scoring (+) indicated the growth on –ALWH plate and β-galactosidase activity.

3.2.2 RIBEYE interacts with photoreceptor specific TULP1 in pull-down assay

The YTH findings, was also confirmed at the protein level using GST pull-down assays (Fig.39). Immobilized RIBEYE(A)-GST fusion protein (but not immobilized GST alone) brings down TULP1-EGFP (but not EGFP alone) from COS7 cell lysate expressing respective recombinant protein (Fig.39a). Thus, two different approaches such as YTH and protein pull-down data independently demonstrated that RIBEYE(A) interacts with TULP1. These interaction suggested the presence of interacting site(s) on RIBEYE(A) and RIBEYE(B) domains. In the next step, the interaction site(s) involved in RIBEYE(A)-TULP1 interaction were mapped using YTH assay.

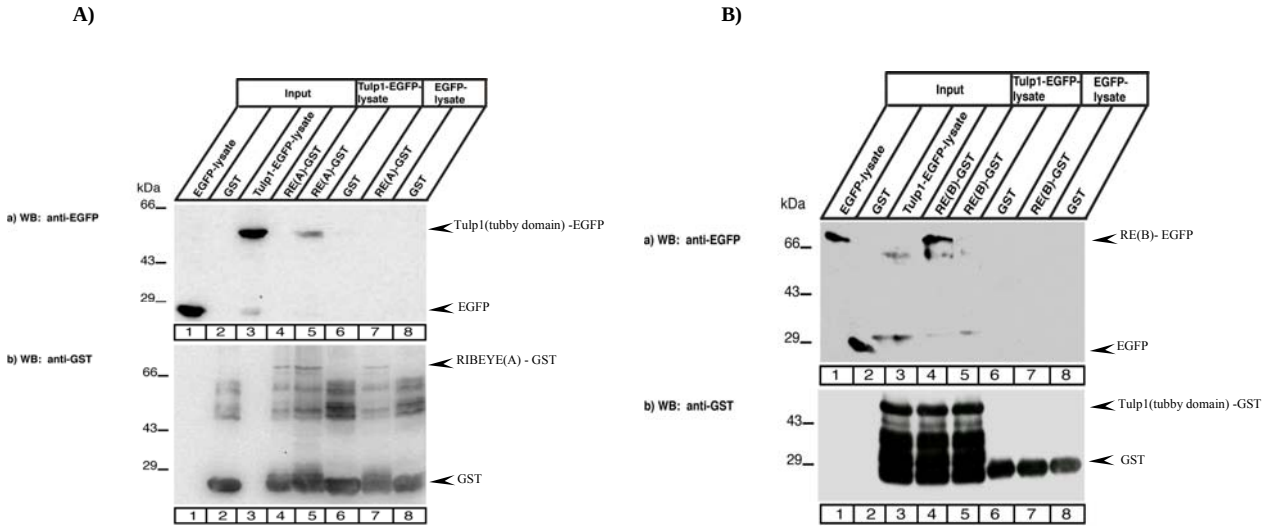

Figure 39. RIBEYE interacts with TULP 1 in GST pull-down assays.

GST pull-down assay was performed using different RIBEYE domains. **A)** RIBEYE(A) interacts with tubby-domain of TULP1. Immobilized RIBEYE(A)-GST (but not immobilized GST alone) binds TULP1-EGFP (not EGFP alone) from COS7 cell lysate. a) Pulled-down product in lane 5, shows bound TULP1 to RIBEYE(A). b) Shows the same blot as in a) but after stripping and reprobing with anti-GST antibodies to show equal loading of bait proteins. **B)** RIBEYE(B) interacts with the tubby-domain of TULP1. Blot was kindly provided by Dr. Louise Köblitz, who worked on RIBEYE(B) and Tulp1 interaction and is further continued in the present thesis work. Immobilized tubby-domain GST of TULP1 (but not immobilized GST alone) binds RIBEYE(B)-EGFP (not EGFP alone) from COS 7 cell lysate. a) Pulled-down product in lane 4, shows bound RIBEYE(B) to tubby-domain of Tulp1. b) Shows the same blot as in a) but after stripping and reprobing with anti-GST antibodies to show equal loading of bait proteins.

3.2.3 TULP1 is a dissociable peripheral component of synaptic ribbons

Tulp1 has been previously shown to be enriched in photoreceptor (Hagstrom *et al*., 2001; Ikeda *et al*., 1999; Milam *et al*., 2000; own observation) which then would be available to bind to synaptic ribbons (present study). To test this hypothesis, the synaptic ribbons were purified and tested for the presence of Tulp1 by western blotting. Synaptic ribbons purified according to the Schmitz *et al*., (1996) indeed contained Tulp1 (Fig.40). These purified ribbons lost their Tulp1 protein component if the ribbons were treated with high salt (2M KCl) and alkaline pH (pH11) conditions, where peripheral proteins are stripped (Schmitz *et al*., 2000). First, these data show that Tulp1 is a component of synaptic ribbons *in-situ*. Second, the Tulp 1 component can be dissociated from the ribbons by high salt/ alkaline pH it is most likely localized on the surface of the synaptic ribbons where it could interact with phosphorylated inositolphospholipids (see discussion).

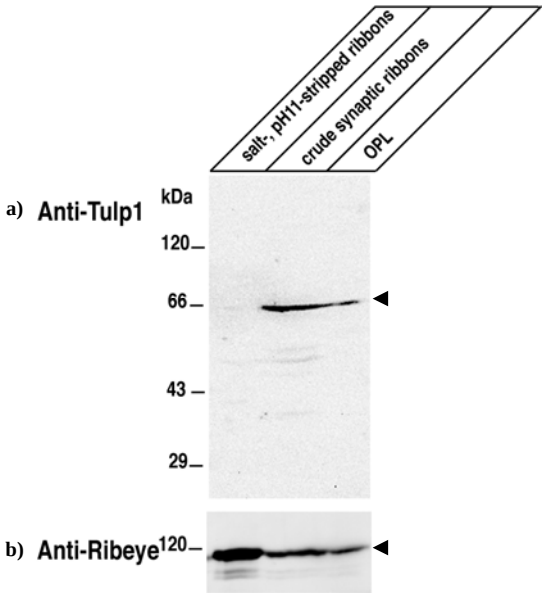

Figure 40. TULP 1 is a dissociable, peripheral component of synaptic ribbon.

Various synaptic fraction preparations from bovine retina were tested for the TULP1 immunoreactivity. The purified synapses of the outer plexiform layer (OPL) that contain photoreceptor ribbon synapses showed a TULP1 band. TULP1 immunoreactivity is enriched in crude synaptic ribbon preparation. Further, TULP 1 is dissociated from the synaptic ribbons, upon harsh treatment conditions such as high salt and high alkaline pH. **a)** The blot was probed with Anti-TULP1 (Chemicon) antibody. **b)** Shows the same blot as in a), but after stripping and reprobing with Anti-RIBEYE (U2656) antibody to show the equal loading of proteins.

3.2.4 Mapping of RIBEYE-TULP1 interactions

In the YTH assay, I mapped interaction sites for RIBEYE(A)-Tulp1 interaction by using various aminoterminal deletion construct of RIBEYE(A)-domain. As a positive control, full length RIBEYE(A)-domain interacts with tubby-domain. Much of the aminoterminal region (aa.1-363) of the RIBEYE(A)-domain can be deleted, without abrogating the interaction between RIBEYE(A) and Tulp1 (tubby-domain)(Fig.41B). The shortest deletion construct found to be interaction was between (364-563) amino acids (Fig.41C, mating #15). Further truncation of the aminoterminal, resulted in an abrogation of interaction. Therefore, amino acids 364-563 represent the binding site of Tulp1 on RIBEYE(A)-domain. This shows relatively a large part of RIBEYE(A)-domain is involved in interaction with TULP1. These interactions with TULP1 were judged by the ability of mated yeast to grow on –ALWH selective plate and expression of β-galactosidase marker gene activity. Qualitatively, the interaction was assessed by β-galactosidase filter tests (Fig.41:C).

A)

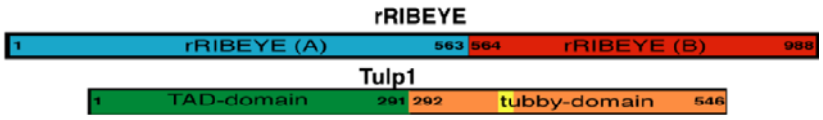

B)

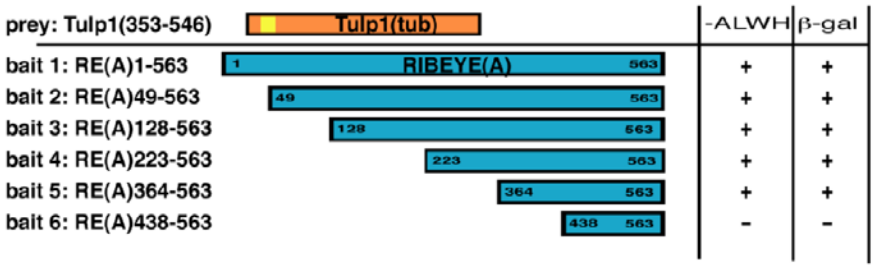

C)

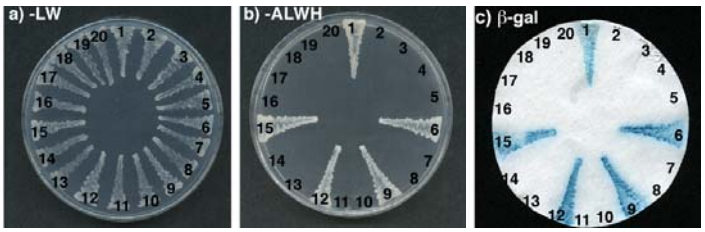

mating	bait	prey	-ALWH	β-Gal
1	RE(A)1-563	Tulp1(353-546)	+	+
2	RE(A)1-563	pACT2	–	–
3	RE(A)1-563	pSE1111	–	–
4	pGBKT7	Tulp1(353-546)	–	–
5	pSE1112	Tulp1(353-546)	–	–
6	RE(A)49-563	Tulp1(353-546)	+	+
7	RE(A)49-563	pACT2	–	–
8	RE(A)49-563	pSE1111	–	–
9	RE(A)128-563	Tulp1(353-546)	–	–
10	RE(A)128-563	pACT2	–	–
11	RE(A)128-563	pSE1111	–	–
12	RE(A)223-563	Tulp1(353-546)	+	+
13	RE(A)223-563	pACT2	+	+
14	RE(A)223-563	pSE1111	–	–
15	RE(A)364-563	Tulp1(353-546)	+	+
16	RE(A)364-563	pACT2	–	–
17	RE(A)364-563	pSE1111	–	–
18	RE(A)438-563	Tulp1(353-546)	–	–
19	RE(A)438-563	pACT2	–	–
20	RE(A)438-563	pSE1111	–	–

Figure 41. Mapping of RIBEYE(A) – TULP 1 interaction in YTH assays.

A) Detailed outline of RIBEYE and TULP 1 constructs used in YTH assay. RIBEYE A- and B-domains are represented in blue and red color respectively. Transactivation domain (TAD) and conserved tubby-domain of TULP1 were depicted in green and orange color respectively. Yellow color in tubby-domain represents the pentapeptide PTNLS motif. **B**) Overview of the aminoterminus deletion constructs of the RIBEYE(A)-domain studied in YTH assay. **3)** Summary of deletion mapping studied in YTH assay. For convenience, experimental bait-prey pairs were underlayered in color (green in case of interacting bait-prey pairs; yellow in case of non-interacting bait-prey pairs); control matings are non-colored. **Ca)** Indicates the growth on -LW plates. **Cb)** Indicates the growth on selective –ALWH plates suggestive of interaction. **Cc)** Qualitatively the interaction is shown by β-galactosidase filter test to qualitatively analyse the marker gene expression. Mating # 15 was the minimal mapped RIBEYE(A)-domain found to be interacting with RIBEYE(B)-domain. Scoring (+) indicates the growth on –ALWH plate and β-galactosidase activity.

Next, I mapped the interaction site(s) between RIBEYE(B) and TULP1. RIBEYE(B) consists of two globular sub-domain's, the NADH-binding domain (NBD) and the substrate binding domain (SBD).

The NBD also contains the dimerisation interface involved in RIBEYE(B) homo-dimerisation. By using YTH assay, I determined that the NBD sub-domain of RIBEYE(B) interacted with tubby-domain of Tulp1 (Fig.42:Cb, matings 1and 2). This interaction was evident from the growth on –ALWH selective plates and the expression of β-galactosidase marker gene (Fig.42:Cc). All the constructs were not auto-activating as concluded by the corresponding control matings. TULP1 contains a pentapeptide PTNLS motif (Fig.37) which has been shown as a potential interacting site for CtBP-binding proteins (Schaeper *et al*., 1995).

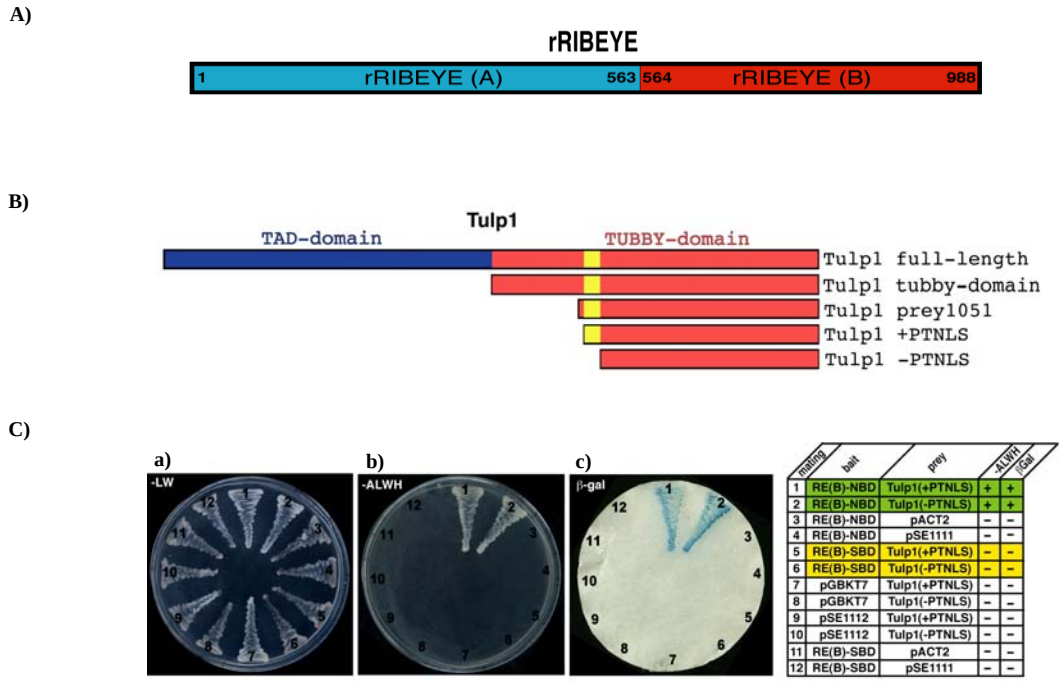

mating	bait	prey	-ALWH	β-Gal
1	RE(B)-NBD	Tulp1(+PTNLS)	+	+
2	RE(B)-NBD	Tulp1(-PTNLS)	+	+
3	RE(B)-NBD	pACT2	–	–
4	RE(B)-NBD	pSE1111	–	–
5	RE(B)-SBD	Tulp1(+PTNLS)	–	–
6	RE(B)-SBD	Tulp1(-PTNLS)	–	–
7	pGBKT7	Tulp1(+PTNLS)	–	–
8	pGBKT7	Tulp1(-PTNLS)	–	–
9	pSE1112	Tulp1(+PTNLS)	–	–
10	pSE1112	Tulp1(-PTNLS)	–	–
11	RE(B)-SBD	pACT2	–	–
12	RE(B)-SBD	pSE1111	–	–

Figure 42. Mapping of RIBEYE (B) – TULP 1 interaction in the presence/absence of PTNLS motif.

A) Schematic representation of RIBEYE molecule. RIBEYE(A)-domain is shown in blue color. Red color represent RIBEYE(B)-domain. **B)** Schematic representation of TULP1 domains and the deletion constructs used in YTH assay. Blue color indicates TAD domain. Red color indicates conserved tubby-domain. Yellow color indicates PTNLS motif. **C)** Summary of YTH interaction. For convenience, experimental bait-prey pairs were underlayered in color (green in case of interacting bait-prey pairs; yellow in case of non-interacting bait-prey pairs); control matings are non-colored. **Ca)** Indicates the growth on -LW plates. **Cb)** Indicates the growth on selective –ALWH plates, suggestive of interaction. **Cc)** Qualitatively the interaction is shown by β-galactosidase filter test. Matings # 1 and 2 indicate RIBEYE(B) interacts with TULP1, independent of PTNLS motif and on RIBEYE(B) it maps to NBD sub-domain. Scoring (+) indicates the growth on –ALWH plate and β-galactosidase activity.

Therefore, I tested the importance of PTNLS motif in RIBEYE(B) and Tulp1 interaction. For this purpose, I tested the deletion constructs that did/did not contains the PTNLS motif (Fig.42B). Furthermore, I generated a full-length tubby-domain construct containing a scrambled PTNLS motif

(PTSNL instead of PTNLS). All the constructs, which includes deletion construct with/without PTNLS motif, and the tubby-domain construct containing scrambled PTSNL motif interacted with Tulp1 (Fig.43c, mating # 2,3&4). These findings demonstrate that PTNLS motif is not decisive for interaction with RIBEYE(B).The interactions were assessed by the growth on –ALWH selective plates and the expression of β-galactosidase marker gene activity (Fig.43:b&c) respectively.

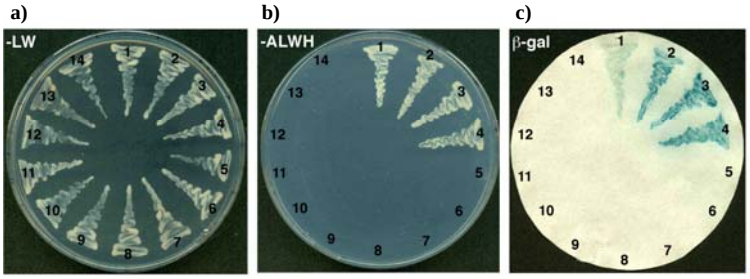

mating	bait	prey	-ALWH	β-Gal
1	RE(B)	Tulp1(tub,PTNLS)	+	+
2	RE(B)	Tulp1(+PTNLS)	+	+
3	RE(B)	Tulp1(-PTNLS)	+	+
4	RE(B)	Tulp1(tub,PTSNL)	+	+
5	RE(B)	pACT2	–	–
6	RE(B)	pSE1111	–	–
7	pGBKT7	Tulp1(tub,PTNLS)	–	–
8	pSE1112	Tulp1(tub,PTNLS)	–	–
9	pGBKT7	Tulp1(+PTNLS)	–	–
10	pSE1112	Tulp1(+PTNLS)	–	–
11	pGBKT7	Tulp1(-PTNLS)	–	–
12	pSE1112	Tulp1(-PTNLS)	–	–
13	pGBKT7	Tulp1(tub,PTSNL)	–	–
14	pSE1112	Tulp1(tub,PTSNL)	–	–

Figure 43. Mapping of RIBEYE (B) – TULP 1 interaction in the presence of scrambled PTNLS motif (to PTSNL).

Summary of YTH interaction. For convenience, experimental bait-prey pairs were underlayered in color (green in case of interacting bait-prey pairs); control matings are non-colored. **a)** Indicates the growth on -LW plates. **b)** Indicates the growth on selective –ALWH plates suggestive of interaction. **c)** Qualitatively the interaction is shown by β-galactosidase filter test. Scoring (+) indicates the growth on –ALWH plate and β-galactosidase activity.

3.2.5 Implication of human TULP1 mutants on RIBEYE-TULP1 interactions

TULP1 is a disease gene for severe, early onset form of Retinitis pigmentosa (RP-14) in humans. Distinct amino acids of Tulp1, when mutated are known to cause the disease phenotype (den-Hollander *et al*., 2007). I cloned the corresponding Tulp 1 mutants that causes RP in humans, and tested these diverse mutants for their capability to interact with RIBEYE(A) and RIBEYE(B) . These TULP1 mutations, identified from RP-14 patients, reveal a striking distribution pattern in the tubby structure. All these surface mutants (except K493R), cluster within a relatively small region of the large positively charged groove that wraps the tubby barrel. Some of these disease causing mutants, including (R424P) converts positive charged side chains to neutral ones, suggesting an important biological function dependent on the maintenance of a positive surface.

All of the tested RP disease mutants, except for (I463K) abrogated interaction of Tulp1 with RIBEYE(B) (Fig.44c, mating # 29).However, RIBEYE(A) and TULP1 interaction persists even after mutating the corresponding amino acids (Fig.44c, matings # 6,9,12,15 and 18), shown to be mutated in RP-14 patients. The interaction was judged by the growth of mated yeast on -ALWH selective

plates and the expression of β-galactosidase marker gene. These findings emphasizes the clinical importance of RIBEYE(B) and TULP1 interactions, which are selectively lost as compared to RIBEYE(A) in disease phenotype.

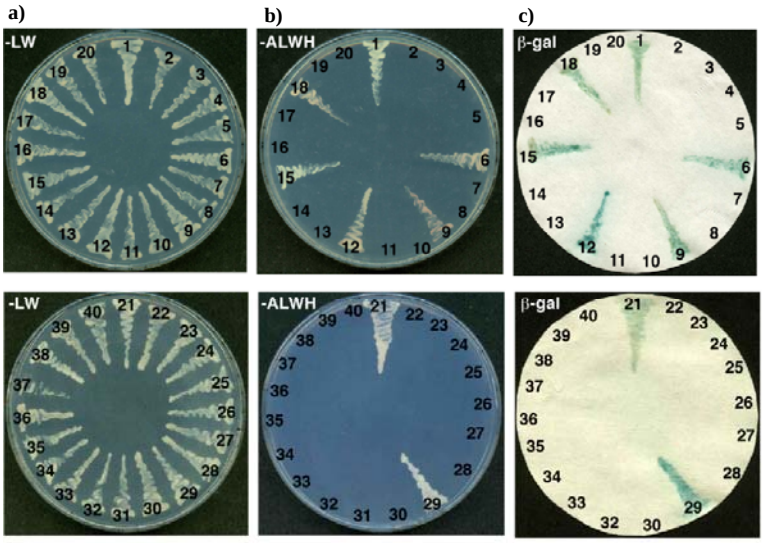

mating	bait	prey	-ALWH	βGal
1	RE(A)	Tulp1(292-546)	+	+
2	pGBKT7	Tulp1(292-546)	–	–
3	pSE1112	Tulp1(292-546)	–	–
4	RE(A)	pACT2	–	–
5	RE(A)	pSE1111	–	–
6	RE(A)	Tulp1(R424P)	+	+
7	pGBKT7	Tulp1(R424P)	–	–
8	pSE1112	Tulp1(R424P)	–	–
9	RE(A)	Tulp1(I463K)	+	+
10	pGBKT7	Tulp1(I463K)	–	–
11	pSE1112	Tulp1(I463K)	–	–
12	RE(A)	Tulp1(F495L)	+	+
13	pGBKT7	Tulp1(F495L)	–	–
14	pSE1112	Tulp1(F495L)	+	+
15	RE(A)	Tulp1(K493R)	+	+
16	pGBKT7	Tulp1(K493R)	–	–
17	pSE1112	Tulp1(K493R)	+	+
18	RE(A)	Tulp1(Δ503-546)	+	+
19	pGBKT7	Tulp1(Δ503-546)	–	–
20	pSE1112	Tulp1(Δ503-546)	–	–
21	RE(B)	Tulp1(292-546)	+	+
22	pGBKT7	Tulp1(292-546)	–	–
23	pSE1112	Tulp1(292-546)	–	–
24	RE(B)	pACT2	–	–
25	RE(B)	pSE1111	–	–
26	RE(B)	Tulp1(R424P)	–	–
27	pGBKT7	Tulp1(R424P)	–	–
28	pSE1112	Tulp1(R424P)	–	–
29	RE(B)	Tulp1(I463K)	+	+
30	pGBKT7	Tulp1(I463K)	–	–
31	pSE1112	Tulp1(I463K)	–	–
32	RE(B)	Tulp1(F495L)	–	–
33	pGBKT7	Tulp1(F495L)	–	–
34	pSE1112	Tulp1(F495L)	–	–
35	RE(B)	Tulp1(K493R)	–	–
36	pGBKT7	Tulp1(K493R)	–	–
37	pSE1112	Tulp1(K493R)	–	–
38	RE(B)	Tulp1(Δ503-546)	–	–
39	pGBKT7	Tulp1(Δ503-546)	–	–
40	pSE1112	Tulp1(Δ503-546)	–	–

Figure 44. Human TULP 1 mutations and its implication in interactions.

Summary of YTH interaction. For convenience, experimental bait-prey pairs were underlayered in color (green in case of interacting bait-prey pairs; yellow in case of non-interacting bait-prey pairs); control matings are non-colored. **a)** Indicates the growth on -LW plates. **b)** Indicates the growth on selective –ALWH plates suggestive of interaction. **c)** Qualitatively the interaction is shown by β-galactosidase filter test. Scoring (+) indicates the growth on –ALWH plate and β-galactosidase activity.

4 Discussion

Ribbon synapses rely heavily on extremely fast, tightly regulated, dynamically adjustable, and efficient neurotransmission. This demand is met by the presence of synaptic ribbons, the insignia of the high output ribbon synapses. Synaptic ribbons are large and dynamic macromolecular assemblies in the active zone of ribbon synapses. Their strategically location supports the tonic transmitter release in response to the incoming graded signals. The dimensions of synaptic ribbons can vary and are subject to changes e.g. in response to different lighting conditions/circadian rhythm probably reflecting structural adaptations to different degrees of synaptic activity (for review, see Vollrath and Spiwoks-Becker, 1996; Wagner, 1997). This is of paramount significance, as a sizable ribbon surface allows priming of large number of vesicles that are then immediately available for exocytosis (Schmitz *et al*., 2000). The conspicuous morphological changes in the ribbon structure will in turn result in a change in exocytotic efficiency. The governing molecular mechanism behind the changes such as differences in size, shape, appearance and disappearance has been so far unknown. At present, it is not clearly understood how the synaptic ribbon is assembled and how it functions in the synapse. Given the lead, the synaptic ribbons takes in ribbon synapse, its important to address the building blocks makes the ribbon(s) and its precise role in ribbon synapse.

In the present work, I attributed the changes in synaptic ribbon to its major component the RIBEYE. It's known that RIBEYE is the major component of synaptic ribbons and is present throughout the entire synaptic ribbon (Schmitz *et al*., 2000; Zenisek *et al*., 2004; Wan *et al*., 2005). RIBEYE has shown to be forming aggregates. Here, these aggregates are correlated as outcome of the physical RIBEYE-RIBEYE interactions. My findings demonstrate, RIBEYE as a scaffold protein that contains multiple interaction sites for other RIBEYE molecules. As a prototype for the entire synaptic ribbon, the multiple protein interactions of RIBEYE provide a molecular mechanism how the scaffold of the synaptic ribbon can be created from a single protein (RIBEYE). RIBEYE-RIBEYE interactions could link the individual RIBEYE units to together, generating and stabilizing the macromolecular structure of the synaptic ribbon. On the basis of genetic, biochemical and morphological data, I favour a structural role of RIBEYE in the synaptic ribbon architecture. In the second part of thesis, I showed that the synaptic ribbon contains TULP 1 and which interacts with RIBEYE scaffold. These

interactions were further characterized by independent assays. All together, these findings show how a synaptic ribbon is made and how it could function in synapse.

4.1 RIBEYE-RIBEYE interactions and the making of synaptic ribbons

Synaptic ribbons are large and dynamic macromolecular structures made up of limited subset of protein component. At present, it is not clearly understood how the synaptic ribbon is made and how it functions in the synapse. RIBEYE is the major and the unique protein component. Its presence makes a difference as compared to conventional synapse (Schmitz *et al*., 2000). In line with these findings, it's interesting to ask how a RIBEYE can form dynamic structure similar to that of synaptic ribbon. I tested the hypothesis in independent protein-protein interaction assays and found that RIBEYE has a tendency to self associate. In the present study, I demonstrated that RIBEYE is a scaffold protein that contains multiple interaction sites for the other RIBEYE molecules. The RIBEYE-RIBEYE interaction involves sites in the A-domain as well as B-domain of RIBEYE. The interactions among A-domains (homo-dimerization), B-domains (homo-dimerization) as well as hetero-dimerization of RIBEYE were confirmed by multiple independent approaches and the functional relevance of these interactions was studied.

I mapped the RIBEYE(A)-RIBEYE(A) homo-dimerization interaction using deletion constructs, and showed the presence of three interaction sites ("A1", "A2", "A3") on A-domain (Fig.17). Similarly, RIBEYE(B)-RIBEYE(B) homo-dimerization interaction is mediated by (B1) interaction site (Fig.20). Besides the homo-dimerizations, I showed RIBEYE(A)-domain interacts with RIBEYE(B)-domain (hetero-dimerization). The hetero-dimerization was facilitated by (A2) site of RIBEYE(A)-domain and, on RIBEYE(B)-domain it was mapped to (B2) site. Noteworthy, the RIBEYE-RIBEYE interactions involve sites in the A-domain as well as in the B-domain of RIBEYE, i.e. three distinct interaction sites("A1", "A2", "A3") on A-domain and two in the B-domain ("B1", "B2") (Fig.36).
These five interaction sites allow either homotypic domain interaction (interaction between the same type of domains; RIBEYE(A)-RIBEYE(A), RIBEYE(B)-RIBEYE(B)) or heterotypic domain interactions (RIBEYE(A)-RIBEYE(B)). Homotypic domain interactions can be either homotypic or heterotypic concerning the sub-domain involved. A homotypic domain interaction, e.g. RIBEYE(A)-

RIBEYE(A), can be mediated either by homotypic sub-domain interactions, e.g. RIBEYE (A1)-RIBEYE(A1), or by heterotypic sub-domain interactions, e.g. RIBEYE(A1)-RIBEYE(A2). This was confirmed by YTH and the protein pull-down assays. These experiments showed that RIBEYE(A)-domain can associate in multiple ways, besides interacting with B-domain via its A2 site (Figs.24&25). These experiments suggest that the ribbon is a product of multiple RIBEYE-RIBEYE interactions. In principle, the multiple interaction sites present on RIBEYE can be important for both intramolecular and intermolecular RIBEYE-RIBEYE interactions. Intermolecular RIBEYE-RIBEYE interactions could provide the three-dimensional scaffold of the synaptic ribbon as discussed above. Intramolecular RIBEYE-RIBEYE interactions could shield the interaction sites from unwanted intermolecular interactions to keep the protein soluble. Such a shielding of binding sites could be particularly important during development and to prevent the assembly of synaptic ribbons at unwanted, unphysiological subcellular sites (e.g. outside of the presynaptic terminal). Likely, the interaction between different RIBEYE domains and RIBEYE molecules is regulated. In the present study, we found that NAD(H) is an important regulator of RIBEYE interactions. RIBEYE(A)-RIBEYE(B) interactions are efficiently inhibited by low, physiological concentrations of NAD(H) (Zhang *et al*., 2002; Fjeld *et al*., 2003). Both NADH and NAD^+ are very efficient in disrupting RIBEYE(A)-RIBEYE(B) complexes. Thus, NAD(H) appears to act as a molecular switch that distinguishes between two different types of RIBEYE-RIBEYE interactions: in the presence of NAD(H), RIBEYE(A)-RIBEYE(B) are disassembled (this study) whereas RIBEYE(B)-RIBEYE(B) interactions are favored as judged by the NAD(H)-induced dimerization of CtBP2 (Thio *et al*., 2004). The binding interface on RIBEYE(B) for RIBEYE(B) interaction is spatially closely related but distinct from the binding interface of RIBEYE(B) for RIBEYE(A). This was shown by the analyses of point and deletion mutants of RIBEYE(B) that affect one type of interaction (RIBEYE(A)-RIBEYE(B) interaction) but not the other (RIBEYE(B)-RIBEYE(B) interaction) (Figs.24,26 and 27). The binding of NAD(H) could induce a conformation of RIBEYE(B) that favors homo-dimerization of RIBEYE(B) and that is incompatible with the formation of RIBEYE(B)-RIBEYE(A) hetero-dimers. RIBEYE(B)G730 is an essential part of the NADH binding motif and the RIBEYE(B)G730A point mutant does no longer interacts with RIBEYE(A). Therefore, one possible mechanism for the NADH-induced dissociation of the RIBEYE(A2)-RIBEYE(B) interaction could be that the NAD(H)-binding region of RIBEYE(B) is also part of the binding interface with RIBEYE(A). If NADH binds to RIBEYE it could displace RIBEYE(A) from RIBEYE(B) and stimulate homo-dimerization of

RIBEYE(B). By this way of thinking, NAD(H) would favor RIBEYE complexes that contain a homo-dimerized B-domain which is likely important for RIBEYE function. Additionally, RIBEYE(B) displaced from RIBEYE(A2) would make the A2-binding module available for RIBEYE(A)-RIBEYE(A)-interactions. By this mechanism, binding of NAD(H) could potentially initiate the assembly of synaptic ribbons. The NADH concentrations used in the present study are well in the range of the known cellular concentrations of NADH (Zhang *et al*., 2002; Fjeld *et al*., 2003) and thus very likely capable in regulating RIBEYE-RIBEYE interactions *in-situ*. The suggested modular assembly of the synaptic ribbon from individual RIBEYE units also provides a molecular explanation for the ultrastructural dynamics of synaptic ribbons by the addition or removal of RIBEYE subunits or rearrangements of RIBEYE-RIBEYE complexes.

The co-transfection experiments demonstrated that RIBEYE proteins interact with each other and co-aggregate into the same protein clusters. Given the fact that RIBEYE is the major component of synaptic ribbons (Schmitz *et al*., 2000; Zenisek *et al*., 2004; Wan *et al*., 2005) the multiple protein interactions of RIBEYE provide a molecular mechanism how the scaffold of the synaptic ribbon can be created. In agreement with this hypothesis, the RIBEYE aggregates in transfected R28 cells possess structural and functional similarities with synaptic ribbons. RIBEYE(AB)-transfected R28 cells formed electron-dense large protein-aggregates that were partly associated with surrounding vesicles and membrane compartments. The electron-dense aggregates were usually round in shape and resembled spherical synaptic ribbons of inner hair cells (Nouvian *et al*., 2006). Bar-shaped/plate shaped ribbons were not observed in the RIBEYE-transfected cells. Thus, the spherical synaptic ribbon is the “basal” type of synaptic ribbon structure that is built from RIBEYE and most likely additional factors are needed to build plate-shaped ribbons from spherical ribbons.

The plausible role of basal structures formed by RIBEYE, came from the colocalization studies with bassoon. The colocalization of RIBEYE with its physiological interaction partner bassoon in R28 cells emphasizes the physiological relevance of the RIBEYE-containing protein aggregates. Once the prototype of ribbon structures (RIBEYE structures) is formed they have tendency to co-localize with bassoon, suggesting that the RIBEYE-containing aggregates fulfill partial ribbon-like functions. Since RIBEYE is not the only component of synaptic ribbons (Schmitz *et al*., 2000; Wan *et al*., 2005) it

cannot be expected that RIBEYE alone makes fully mature ribbons, e.g. with a dense and regular association of synaptic vesicles. Very likely, other ribbon components are necessary to provide full-ribbon function and structure. Nevertheless, RIBEYE alone forms minimal ribbon structure which later on expected to be ornamented with other ribbon components. This is shown in the next part of discussion.

The ribbon recruitment experiments showed that binding sites for additional RIBEYE subunits are accessible and available on synaptic ribbons at a molecular level. Isolated synaptic ribbons (Schmitz *et al*., 1996, 2000) are able to bind externally added RIBEYE(B)- and also RIBEYE(A)-domains. The multiple RIBEYE-RIBEYE interaction sites in the A-domain suggest a predominantly structural role of the A-domain as previously suggested (Schmitz *et al*., 2000). Probably large portions of RIBEYE(A) are likely "buried" in the core of the synaptic ribbons. Still, part of the A-domain is accessible in isolated synaptic ribbons and therefore partly exposed. In ribbon pull-down experiments, both RIBEYE(A)- and RIBEYE(B)-domains were found to be binding synaptic ribbons (Fig.32). Further investigation with A-domain interacting modules suggests that, RIBEYE(A1) and RIBEYE(A3) but not RIBEYE(A2) did bind to purified synaptic ribbons. Since, RIBEYE(A2) can bind to both A1- and A2- interaction sites but not to the A3-interaction site, we suggest that A1 and A2 are located in the core of the ribbon where these sites are not available for interaction with RIBEYE(A2). In contrast, the A3 region is at least partly exposed on purified synaptic ribbons where it is free to interact with other protein, i.e. externally added RIBEYE(A1) and RIBEYE(A3) (Fig.33). Binding of RIBEYE(B) probably occurs via homo-dimerization of RIBEYE(B)-domains based on homologous findings with CtBP2 (Balasubramanian *et al*., 2003; Thio *et al*., 2004). This homo-dimerization is favored by the presence of NADH. Interestingly, RIBEYE(B) of synaptic ribbons does not bind RIBEYE(A2) although the respective fusion proteins can interact in a NAD(H)-dependent manner. Therefore, the RIBEYE(B) binding site for RIBEYE(A2) might be blocked or the binding is dis-favoured, e.g. by RIBEYE(B) homo-dimerization, or inhibited by NAD(H) bound at synaptic ribbons via the NBD of RIBEYE. Clearly these working hypotheses have to be analyzed by future investigations. Testing these assumptions will shed further light on the understanding of the construction and assembly of synaptic ribbons and how they work in the synapse.

In conclusion, the data show that RIBEYE is a scaffold protein with ideal properties to explain the assembly of synaptic ribbons as well as its ultrastructural dynamics via the modular assembly model. The capability to interact with other RIBEYE proteins in multiple ways could explain how a single protein, RIBEYE, builds the scaffold for the entire ribbon (Fig.36). Our transfection experiments actually show that RIBEYE can form aggregates that resemble spherical synaptic ribbons. The proposed modular assembly of the synaptic ribbon from individual RIBEYE subunits provides a molecular basis for the ultrastructural plasticity of synaptic ribbons (e.g. changes in size and shape of the ribbon). The binding of externally added RIBEYE to purified synaptic ribbons mimics the growth of synaptic ribbons that occurs *in-situ* e.g. under darkness in the mouse retina (Balkema *et al*., 2001; Spiwoks-Becker *et al*., 2004; Hull *et al*., 2006). Similarly, RIBEYE- aggregates appeared to be able to coalesce into larger structures at the ultrastructural level. The regulation of RIBEYE-RIBEYE interactions, e.g. by NAD(H), could contribute to the regulation of structural plasticity of synaptic ribbons.

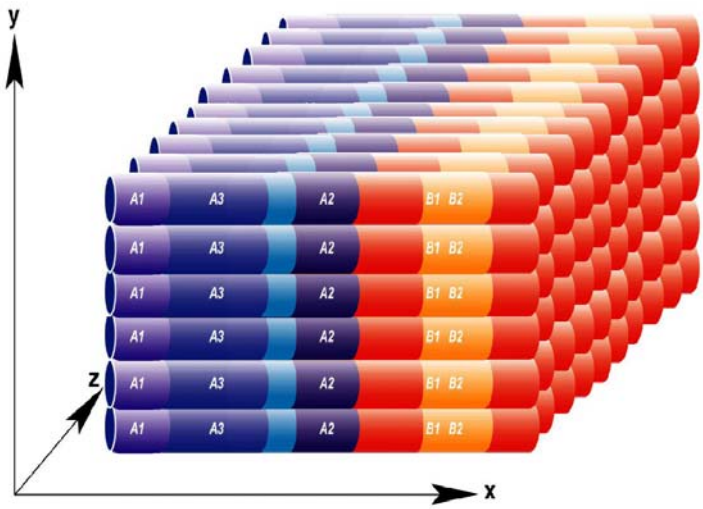

Figure 45. Working hypothesis on the assembly of ribbons from RIBEYE units.

A simplified, schematic working model is presented how RIBEYE-RIBEYE interactions could build the scaffold of the synaptic ribbon from individual RIBEYE subunits. In this model RIBEYE is depicted as a "linear" protein. For simplicity, a non-staggered association of RIBEYE units is depicted based on homotypic RIBEYE-RIBEYE interactions. A possible, staggered interaction based on heterotypic RIBEYE-RIBEYE interactions is not included. x,y,and z represent the three-dimensional axis.

4.2 RIBEYE-TULP1 interaction

Association of synaptic ribbons with large number of vesicles is prerequisite for faster release. RIBEYE being the major component of synaptic ribbons (Schmitz *et al*, 2000), and forms ribbon like structures. Understanding the ribbon formation and its function in the synapse is also necessary to decipher genetic diseases which affects vision and hearing. It's expected that other proteins interact with the RIBEYE scaffold, to provide a certain physiological function at the ribbon scaffold or to stabilize the ribbon. This was shown by the second part of thesis work in which I characterized the interaction of RIBEYE with TULP1. TULP1 is a ~70 KDa protein whose diseases phenotypes are well established. It's mutation, selectively affects the vision in humans. Heckenlively *et al*., 1995 and Ohlemiller *et al*., 1995 have reported that the histopathological changes in the eyes and the ears of tubby mice are similar to those seen in individuals with Ushers syndrome. It's intriguing to ascertain the role of these two proteins. The interaction of these proteins will likely be important for a better understanding on the disease phenotype. TULP1 was isolated as an interacting partner of RIBEYE using a retinal cDNA library.

Photoreceptor specific TULP1, is one among the isoforms of TULP gene family members. TULP1 binds to phospholipids via its tubby-domain. The exclusive expression of RIBEYE and TULP1 in retina, and the role of TULP1 in disease phenotype further make it an interesting candidate, playing a pivotal role in maintaining normal physiology of the retina. In the second part of study, I elucidated the role of entire RIBEYE in interaction with TULP1 and supported the findings with independent approaches. In this part of my thesis, I further continued Dr. Louise Köblitz findings who earlier showed that RIBEYE(B) interacts with TULP1.

I showed that, RIBEYE(A) as well as full length RIBEYE interacts with photoreceptor specific TULP1. The presence of RIBEYE(A)-domain does not hinder the interaction. The presence of RIBEYE(A)-domain in addition to earlier reported RIBEYE(B)-domain, their joint role as a complete RIBEYE molecule in interaction is a new finding. RIBEYE(A) as well as RIBEYE(B) interacts with the tubby-domain of TULP1. These findings were independently corroborated by protein pull-down assay, where RIBEYE(A)-domain binds to the tubby-domain of TULP1. These data show, the involvement of complete RIBEYE molecule, as the two independent domains of RIBEYE molecule

are engaged in the interaction. Further, these interactions operate over entire length of ribbon, indicative of important function associated with these interactions.

Further strengthening evidences came from the *in-situ* ribbon fraction analysis. The entire length of synaptic ribbon is decorated with RIBEYE molecule (Schmitz *et al*., 2000). It is known that, TULP1 is enriched in the photoreceptors (Hagstrom *et al*., 2001; Ikeda *et al*., 1999; Milam *et al*., 2000; own observation), including the presynaptic terminals which contains synaptic ribbons. We shown that, purified synaptic ribbons are immunoreactive to TULP1 indicating its association with the synaptic ribbons. Further, this association is reduced when the ribbons are treated harshly with 2M KCl and alkaline conditions (pH 11). These similar treatments also results in stripping of peripheral membrane proteins (Schmitz *et al*., 2000). These data supports TULP1 as a peripheral component of synaptic ribbons. It's based on the fact, that TULP1 at the surface of synaptic ribbons it could be able to interact with phosphorylated inositolphospholipids of ribbon associated vesicles.

Using YTH assay, I mapped the regions involved in interaction. Mapping of the RIBEYE domains, revealed that a carboxyterminal (364-563 amino acids) of RIBEYE(A)-domain binds with the tubby-domain of TULP1. On the other hand, the similar tubby-domain binds to the NAD(H) binding region of the RIBEYE(B)-domain. Amino acid alignment showed a presence of classical penta-peptide PTNLS motif in tubby-domain. These (PXDLS) penta-peptide motifs had earlier shown as interacting site for CtBP binding proteins (Schaeper *et al*., 1995). The importance of this motif was tested using YTH assay, where I found that the penta-peptide motif is not important for interaction with RIBEYE(B)-domain. This hypothesis was tested in alternative way by scrambling the PTNLS motif to PTSNL which shown the similar results. These findings suggests that RIBEYE(B)-domain interacts with tubby-domain of TULP1 in the absence/presence of classical penta-peptide motif.

In next step, I ascertained the physiological role of these interactions in maintaining the healthy status of retina. It's known that, TULP1 is a disease gene for Retinitis pigmentosa (RP-14) that causes early onset severe retinitis pigmentosa in patients and photoreceptor degeneration in mice. It affects both rods and cones which harbors synaptic ribbons. It starts with progressive degeneration of retinal photoreceptors cells and leads to blindness. One would expect to know the outcome of this altered

scenario in ribbon synapse. Especially with the above finding, that TULP1 binds entire RIBEYE in which two domains of RIBEYE were found to be interacting. It would be intriguing to test these interactions in disease state and comparing them to that of wild type. In YTH assay, I tested the TULP1 mutated amino acids known to cause Retinitis pigmentosa in human for their ability to interact with RIBEYE domain. All of the studied mutations (R424P, I463K, F495L, K493R & Δ503-546) does not influence the interaction with RIBEYE(A)-domain. These interactions even persist in the mutated state. However, in case of RIBEYE(B)-TULP1 interactions all the mutants (except for the I463K) abrogates Tulp1-RIBEYE interactions. These findings implicates that the scaffold of ribbon is also affected in the disease phenotype further suggesting the clinical importance of these interactions.

This study also indicates a possible impact of phosphoinositides on synaptic ribbons via its binding partner TULP1. Phosphoinositides are known regulatory molecules in the synapse (De Camilli *et al*., 1996; Martin, 1998; Odorizzi *et al*., 2000). The reversible phosphorylation of their inositol ring generates a series of stereoisomers that can bind to cytosolic and membrane proteins with variable affinities and specificities. This could of enormous interest in ribbon synapse which has very fast recycling of vesicles. The generation of specific phosphoinositide species can be used as a mechanism to temporarily and spatially regulate the recruitment of cytosolic proteins. Because of these properties, phosphoinositides can ascribe an identity to a membrane for a defined role.

Recruitment of the phospholipid binding protein (TULP1) is certainly very important for an organelle that intimately associated with vesicles and membranes. This feature is of prime importance in ribbon synapses which rely on high traffic of the synaptic vesicles. TULP1 interaction with RIBEYE is of paramount significance in meeting the demands of ongoing trafficking and may serve multiple purposes. Phosphoinositides has potential to bind cytosolic proteins to the bilayer. In the same line, the presence of $PI(4,5)P_2$ which is highly concentrated at plasma membrane may serve as an anchor to position ribbon to the plasma membrane. Since, the phosphorylation state and hydrolysis of PIP_2 in the membranes could be changed very rapidly, which could be switch for membrane association and dissociation. This mechanism could possibly explain the observed attachment and detachment of ribbons from the active zones. Thus, membrane phosphoinositides can participate in attachment of ribbon to the active synapse. Phosphoinositides could be involved in recruiting of the synaptic vesicles

to a ribbon surface in a stimulus dependent manner. During exocytosis $PI(4,5)P_2$, which is concentrated in the plasma membrane, makes the membrane as the appropriate target for vesicle fusion, and regulates the membrane component of the exocytotic machinery. PIP_2 is known to be important for vesicle priming (Grishenin *et al*., 2004). The rapid excess-membrane retrieval that is produced by strong synapse stimulation may be regulated by $PI(4,5)P_2$-triggered actin polymerization. This scenario is similar to the exocytosis in ribbon synapse where a strong stimulus leads to the attachment of vesicles to the ribbon surface (Zenisek *et al*., 2008). This could be supported by the local changes in the phosphoinositides upon stimulation. Likely the two phases are working in concert in ribbon synapse.

Spatially segregated membrane domain enriched for phosphoinositides would exhibit a positive membrane curvature (Chernomordik *et al*., 1996) that could contribute to the remodeling of the bilayer for even such as membrane budding and fusion. The recruitment of the phosphoinositide binding protein (TULP1) to ribbon, could allow the assembly of signal transduction complexes, cytoskeletal membrane attachments, coated membrane domain for bud formation, and scaffold for membrane fusion reactions.

Our results provide evidence for a critical role of phosphoinositide binding protein TULP 1 at the ribbon synapse. Interaction between RIBEYE and TULP1 have broad implication and suits to the rapid events in trafficking specific to photoreceptor cells.

5 References

Alpadi, K., Magupalli, V.G., Käppel, S., Köblitz, L., Schwarz, K., Seigel, G.M., Sung, C.H and Schmitz, F. (2008). RIBEYE recruits Munc119, a mammalian ortholog of the *C. elegans* protein unc119, to synaptic ribbons of photoreceptor ribbon synapses. J. Biol. Chem. 283, 26461-26467.

Bai, C., and Elledge, S.J. (1996). Gene identification using the yeast two-hybrid system. Methods Enzymol. 273, 331-347.

Balasubramanian, P., Zhao, L.J., and Chinnadurai, G. (2003). Nicotinamide adenine dinucleotide stimulates oligomerization, interaction with adenovirus E1A and an intrinsic dehydrogenase activity of CtBP. FEBS Lett. 537, 157-160.

Balkema, G.W., Cusick, K., and Nguyen, T.H. (2001). Diurnal variation in synaptic ribbon length and visual threshold. Vis. Neurosci.18, 789-797.

Banerjee, P., Kleyn, P.W., Knowles, J.A., Lewis, C.A., Ross, B.M., Parano, E., Kovats, S.G., Lee, J.J., Penchaszadeh G.K., Ott, J., Jacobson, S.G., and Gillam, T.C. (1998). TULP1 mutations in two extended Dominican kindreds with autosomal recessive Retinitis pigmentosa. Nature Genetics.18, 177-179.

Barr, K.A., Hopkins, S.A., and Sreekrishna, K. (1992). Protocol for Efficient Secretion of HAS Developed from *Pichia pastoris.* Pharm. Eng.12, 48-51.

Birnboim, H.C., and Doly, J. (1979). A rapid alkaline procedure for screening recombinant plasmid DNA. Nucleic Acids Res. 7, 1513-1523.

Boggon, T.J., Shan, W.S., Santagata, S., Myers, S.C., and Shapiro, L. (1999). Implication of Tubby proteins as Transcription factors by Structure-Based Functional Analysis. Science. 286, 2119-2125.

Brada, D., and Roth, J. (1984).‘‘Golden blot”–Detection of polyclonal and monoclonal antibodies bound to antigens on nitrocellulose by protein A-gold complexes. Anal. Biochem. 142, 79-83.

Bradford, M. (1976). A rapid and sensitive method for the quantitation of microgram quantities of protein utilizing the principle of protein-dye binding. Anal. Biochem. 72, 248-254.

Brandstätter, J., Wässle, H., Betz, H., and Morgans, C.W. (1996a). The plasma membrane protein SNAP-25, but not syntaxin, is present at photoreceptor and bipolar cell synapses in the rat retina. Eur. J. Neurosci. 8, 823-828.

Brandstätter, J.H., Löhrke, S., Morgans, C.W., and Wässle, H.(1996b). Distributions of two homologous synaptic vesicle proteins, synaptophorin and synaptophysin, in the mammalian retina. J. Comp. Neurol. 370, 1-10.

Brandstätter, J.H., Fletcher, E.L., Garner, C.C., Gundelfinger, E.D., and Wassle, H. (1999). Differential expression of the presynaptic cytomatrix protein bassoon among ribbon synapses in the mammalian retina. Eur. J. Neurosci. 11, 3683-3693.

Brierley, R. A., Davis, G.R., and Holtz, G.C. (1994). Production of Insulin-Like Growth Factor-1 in Methylotrophic Yeast. United States Patent. 5, 324, 639.

Campbell, R.E., Tour, O., Palmer, A.E., Steinbach, P.A., Baird, G.S., Zacharias, D.A., and Tsien, R.Y. (2002). A monomeric red fluorescent protein. Proc. Natl. Acad. Sci. USA. 99, 7877-7782.

Carroll, K., Gomez, C., and Shapiro, L. (2004). Tubby proteins: The plot thickens. Nature Reviews Mol. Cell Biol. 5, 55-64.

Cereghino, G.P.L., Cereghino, J.L., and Sunga, A.J. (2001a). New selectable marker/auxotrophic host strain combinations for molecular genetic manipulation of *Pichia pastoris*. Gene. 263, 159-169.

Chalfie, Y., Tu, G., Ward, E.W., and Prasher, D. (1994). Green fluorescent protein as a marker for gene expression. Science. 263, 802-805.

Chassy B.M., and Flickinger, J.L. (1987). Transformation of *Loctobacillius casei* by electroporation. FEMS Microbiol. Letters. 44, 173-177.

Chein, A., Edgar, D.B., and Trela J.M. (1976). Deoxyribonucleic acid polymerase from the extreme thermophile *Thermus aquaticus.* J. Bacteriol. 127, 1550-1557.

Chernomordik, L. (1996). Non-bilayer lipids and biological fusion intermediates. Chem. Phy. Lipids. 81, 203-213.

Chien, C.T., Bartel, P.L., Sternglanz, R., and Fields, S. (1991). The two-hybrid system: a method to identify and clone genes for proteins that interact with a protein of interest. Proc. Natl. Acad. Sci. 88, 9578-9582.

Chinnadurai, G. (2002). CtBP, an unconventional transcriptional corepressor in development and oncogenesis. Mol. Cell. 9, 213-224.

Chinnadurai, G. (2003). CtBP family proteins: more than transcriptional corepressors. Bioessays. 25, 9-12.

Clare, J.J., Romanos, M.A., Rayment, F.B., Rowedder, J.E., Smith, M.A., Payne, M.M., Sreekrishna, K., and Henwood, C.A. (1991b). Production of epidermal growth factor in yeast: high-level secretion using *Pichia pastoris* strains containing multiple gene copies. Gene.105, 205-212.

Coleman, J. (1990). Characterization of *Escherichia Coli* cells deficient in 1-acyl-sn-glycerol-3-phosphate acyltransferase activity. J.Biol.Chem. 265, 17215-17221.

Cregg J.M., Barringer, K.J., and Hessler, A.Y. (1985). *Pichia pastoris* as a host system for transformations. Mol. Cell Biol. 5, 3376-3385.

Cregg J.M., Madden, K.R., Barringer, K.J., Thill, G., and Stillman, C.A. (1989). Functional characterization of two alcohol oxidase genes from the yeast, *Pichia pastoris* as a host system for transformations. Mol. Cell Biol. 9, 1316-1323.

Cregg J.M., Vedvick, T.S., and Raschke, W. (1993). Recent advances in the expression of foreign genes in *Pichia pastoris.* Bio/Technology.11, 905-910.

Cregg, J.M., Cereghino, L., Shi, J., and Higgins, D.R. (2000). Recombinant protein expression in *Pichia pastoris.* Mol. Biotech. 16, 23-52.

Daily, R., and Hearn T.W.M. (2005). Expression of heterologous proteins in *Pichia pastoris*: a useful experimental tool in protein engineering and production. Journal of Molecular Recognition.18, 119-138.

De Camilli, P., Emr, S.D., McPherson, P.S., and Novick, P. (1996). Phosphoinositides as regulators in membrane traffic. Science. 271, 1533-1539.

den Hollander, A.I., van Lith-Verhoeven, J.J., Arends, M.L., Storm, T.M., Cremers, F.P., and Hoyng, C.B. (2007). Novel Compound Heterozygous TULP1 Mutations in a Family with severe Early-Onset Retinitis Pigmentosa. Arch. Ophthalmol. 125, 932-935.

Dowling, J.E. (1987).The retina: An Approachable Part of the Brain. Cambridge, MA. Harvard University Press.

Egli, T., van Dijjen, J.P., Veenuis, M., Harder, W., and Fiechter, A. (1980). Methanol metabolism in yeasts: regulation of the synthesis of catabolic enzymes. Arch. Microbiol. 124, 115-121.

Erlich, H.A., Gelfand, D., and Sninsky J.J. (1991). Recent advances in the polymerase chain reaction. Science. 252, 1643-1651.

Fields, S., and Song, O. (1989). A novel genetic system to detect protein-protein interactions. Nature. 340, 245-246.

Fjeld, C.C., Birdsong, W.T., and Goodman, R.H. (2003). Differential binding of NAD^+ and NADH allows the transcriptional corepressor carboxyl-terminal binding protein to serve as a metabolic sensor. Proc. Natl. Acad. Sci. U S A. 100, 9202-9207.

Fuchs, P.A. (2005). Time and intensity coding at the hair cell's ribbon synapse. J. Physiol. 566, 7-12.

Geppert, M., Ulrich, B., Green, D.G., Takei, K., Daniels, L., De Camilli, P., Südhof, T.C., and Hammer, R.E. (1994). Synaptic targeting domains of synapsins 1 revealed by transgenic expression in photoreceptor cells. EMBO J. 13, 3720-3727.

Gluzman, Y. (1981). SV40-transformed simian cells support the replication of early SV40 mutants. Cell. 23, 175-182.

Grant, S.G., Jessee, J., Bloom, F.R., and Hanahan, D. (1990). Differential plasmid rescue from transgenic mouse DNAs into *Escherichia coli* methylation-restriction mutants. Proc. Natl. Acad. Sci. USA. 87, 4645-4649.

Grinna, L.S., and Tschopp, J.F. (1989). Size Distribution and General Structural Features of N-Linked Oligosaccharides from Methylotrophic Yeast *Pichia pastoris.* Yeast. 5, 107-115.

Grishanin, R.N., Kowalchyk, J.A., Ann, K., Earles, C.A., Chapman, E.R., Gerona, R.R., and Martin, T.F. (2004). CAPS acts at a perfusion step in dense-core vesicle exocytosis as a PIP2 binding protein. Neuron. 43, 551-562.

Grodberg, J., and Dunn, J.J. (1988). ompT encodes the *Escherichia coli* outer membrane protease that cleaves T7 RNA polymerase during purification. J. Bacteriol. 170, 1245-1253.

Gu, S.M., Lennon, A., and Li, Y. (1998).Tubby-like protein-1 mutations in autosomal recessive retinitis pigmentosa. Lancet. 351, 1103-1104.

Guan C.D., Lib.P., Riggsa. P.D., and Inouyeb, H. (1988). Vectors that facilitate the expression and purification of foreign peptides in *Escherichia coli* by fusion to maltose-binding protein. Gene. 67, 21-30.

Hagstrom, S.A., North, M.A., Nishina, P.M., Berson, E.L., and Dryja, T.P. (1998). Recessive mutations in the gene encoding tubby-like protein TULP1 in patients with retinitis pigmentosa. Nature Genetics. 18, 174-176.

Hagstrom, S.A., Adamian, M., Scimeca, M., Pawlyk, B.S., Yue, G., and Li, T. (2001). A role for the Tubby-like protein 1 in rhodopsin transport. Invest. Ophthalmo. Vis. Sci. 42, 1955-1962.

Harper, J.W., Adami, G.R., Wie, N., Keyomarski, K., and Elledge, S.J.(1993). The p21 Cdk-interacting protein Cip1 is a potent inhibitor of G1 cyclin-dependent kinases. Cell. 75, 805-816.

Heckenlively, J.R., Chang, B., Erway, L.C., Peng, C., Hawes, N.L., Hageman, G.S., and Roderick, T.H. (1995). Mouse model for Usher syndrome: linkage mapping suggests homology to Usher type 1 reported at human chromosome 11p15. Proc. Natl. Acad. Sci. USA. 92, 11100-11104.

Heidelberger, R., and Matthews, G. (1992). Calcium influx and calcium current in single synaptic terminals of goldfish retinal bipolar neurons. J. Physiol. 447, 235-256.

Heidelberger, R., Thoreson, W.B., and Witkovsky, P. (2005). Synaptic transmission at retinal ribbon synapses. Prog. Retin. Eye Res. 24, 682-720.

Helmuth, M., Altrock, W., Bockers, T.M., Gundelfinger, E.D., and Kreutz, M.R. (2001).An electrotransfection protocol for yeast two-hybrid library screening. Anal. Biochem. 293, 149-152.

Hopsu, V.K., and Arstila, A.U. (1964). An appearent somato-somatic synaptic structure in the pineal gland of the rat. Exp. Cell Res. 37, 484-487.

Hull, C., Studholme, K., Yazulla, S., and von Gresdorff, H. (2006). Diurnal changes in exocytosis and the number of synaptic ribbons at active zones of an ON-type bipolar cell terminal. J. Neurophysiol. 96, 2025-2033.

Ichtchenko, K., Hata, Y., Nguyen, T., Ullrich, B., Missler, M., Moomaw, C., and Südhof, T.C. (1995). Neuroligin 1: A splice-site specific ligand for α-neurexins. Cell. 81, 435–443.

Ikeda, S., He, W., Ikeda, A., Naggert, J.K., North, M.A., and Nishina, P.M. (1999). Cell-specific expression of Tubby gene family members (*tub, Tulp1, 2 and 3*) in the retina. Invest. Ophthalmo. Vis. Sci. 40, 2706-2712.

James, P., Haliaday, J., and Craig, E.A. (1996).Genomic libraries and host strain designed for highly efficient two hybrid selection in yeast. Genetics. 144, 1425-1436.

Jastrow, H., von Mach, M.A., and Vollrath, L. (1997). The shape of synaptic ribbons in the rat pineal gland. Cell Tissue Res. 287, 255-261.

Kapeller, R., Moriarty, A., Strauss, A., Stubdal, H., Theriault, K., Siebert, E., Chickering, T., Morgenstern, J.P., Tartaglia, L.A., and Lillie, J. (1999). Tyrosine phosphorylation of tub and its association with Src homology 2 domain containing proteins implicate tub in intracellular signalling by insulin. J. Biol. Chem. 274, 24980-24986.

Khimich, D., Nouvian, R., Pujol, R., Tom Dieck, S., Egner, A., Gundelfinger, E.D., and Moser, T. (2005). Hair cell synaptic ribbons are essential for synchronous auditory signalling. Nature. 434, 889-894.

Kumar, V., Carlson, J.E., Ohgi, K.A., Edwards, T.A., Rose, D.W., Escalante, C.R., Rosenfeld, M.G., Aggarwal, A.K. (2002). Transcription corepressor CtBP is an NAD(+)-regulated dehydrogenase. Mol. Cell.10, 857-869.

Laemmli, U.K. (1970). Cleavage of structural proteins during the assembly of the head of bacteriophage T4. Nature. 227, 680-685.

Lenzi, D., Runyeon, J.W., Crum, J., Ellisman, M.H., and Roberts, W.M. (1999). Synaptic vesicle populations in saccular hair cells reconstructed by electron tomography. J. Neurosci.19, 119-132.

Lewis, C.A., Batlle, I.R., Batlle, K.G.R., Banerjee, P., Cideciyan, A.V., Huang, J., Aleman, T.S., Huang, Y., Ott, J., Gilliam, T.C., Knowles, J.A., and Jacobson, S.G. (1999). Invest. Ophthalmo. Vis. Sci. 40, 2106-2114.

Lin-Cereghino, J., and Cregg, J.M. (2000). Heterologous protein expression in the methylotrophic yeast *Pichia pastoris*. FEMS Microbiol. Reviews. 24, 45-66.

Lin-Cereghino, J., Wong, W.W., Xiong, S., Giang, W., Luong, L.T., Vu, J., Johnson, S.D., and Lin-Cereghino, G.P. (2005). Condensed protocol for competent cell preparation and transformation of the methylotrophic yeast Pichia pastoris. Biotechniques. 38, 44-48.

Louret, O., Doignon, F., and Crouzet, M. (1997). Stable DNA-Binding Yeast vector allowing high bait expression for use in the Two-Hybrid system. Bio Techniques. 23, 816-820.

Magupalli, V.G., Schwarz, K., Alpadi, K., Natarajan, S., Seigel, G.M., and Schmitz, F. (2008). Multiple Ribeye-Ribeye interactions create a dynamic scaffold for the formation of synaptic ribbon. J. Neurosci. 28, 7954-7967.

Mandell, J.W., Townes-Anderson, E., Czemik, A.J., Cameron, R., Greengard, P., and De Camilli, P. (1990). Synapsins in the vertebrate retina: absence from ribbon synapses and heterogeneous distribution among conventional synapses. Neuron. 5, 19-33.

Martin, T.F. (1998). Phosphoinositide lipids as signaling molecules: common themes for signal transduction, cytoskeletal regulation, and membrane trafficking. Annu. Rev. Cell. Dev. Biol.14, 231-264.

Milam, A.H., Hendrickson, A.E., Xiao, M., Smith, J.E., Possin, D.E., John, S.K., and Nishina, P.M. (2000). Localization of Tubby-like Protein 1 in developing and adult human retinas. Invest. Ophthalmol. & Vis. Sci. 41, 2352-2356.

Morgans, C.W., Brandstätter, J.H., Kellerman, J., Betz, H., and Wässle, H. (1996). A SNARE complex containing syntaxin 3 is present in ribbon synapses of the retina. J. Neurosci. 19, 1027-1037.

Muresan, V., Lyass, A., and Schnapp, B.J. (1999).The kinesin motor KIF3A is a component of the presynaptic ribbon in vertebrate photoreceptors. J. Neurosci.19, 1027-1037.

Narayanan, S.R. (1994). Preparative affinity chromatography of proteins. J. Chromato. A. 658, 237-258.

Nardini, M., Spano, S., Cericola, C., Pesce, A., Massaro, A., Millo, E., Luini, A., Corda, D., and Bolognesi, M. (2003). CtBP/BARS: a dual-function protein involved in transcription co-repression and Golgi membrane fission. EMBO J. 22, 3122-3130.

Nishina. P., North, M., and Ikeda, A. (1998). Molecular characterization of a novel *tubby* gene family member, *TULP 3,* in mouse and humans. Genomics. 54, 215-220.

Noben-Trauth, K., Naggert, J.K., North, M.A., and Nishina, P.M. (1996). A candidate gene for the mouse mutation tubby. Nature. 380, 534-538.

North, M.A., Naggert, J.K., Yan, Y., Noben-Trauth, K., and Nishina, P.M. (1997). Molecular characterization of TUB, TULP1, and TULP2, members of the novel tubby gene family and their possible relation to ocular diseases. Proc. Natl. Acad. Sci. USA. 94, 3128-3133.

Nouvian, R., Beutner, D., Parsons, T.D., and Moser, T. (2006). Structure and function of the hair cell ribbon synapse. J. Membr. Biol. 209, 153-165.

Odorizzi, G., Babst, M., and Emr, S.D. (2000). Phosphoinositide signalling and the regulation of membrane trafficking in yeast. Trends Biochem. Sci. 25, 229-235.

Ohlemiller, K.K., Hughes, R.M., Mosinger-Ogilvie, J., Speck, J.D., Grosof, D.H., and Silverman, M.S. (1995). Cochlear and retinal degeneration in the tubby mouse. Neuroreport. 6, 845-849.

Pappas, G.D., and Waxman, S.G. (1972). Synaptic fine structure-morphological correlates of chemical and electrotonic transmission. In Structure and Function of synapse, ed. G. D Pappas and D. P. Purpura. New York: Raven Press, pp. 1-43.

Parsons, T.D., Lenzi, D., Almers, W., and Roberts, W.M. (1994). Calcium-triggered exocytosis and endocytosis in an isolated presynaptic cell: capacitance measurements in saccular hair cells. Neuron. 13, 875-883.

Parsons, T.D., and Sterling, P. (2003). Synaptic Ribbon: conveyor belt or safety belt? Neuron. 37, 379-382.

Poortinga, G., Watanbe, M., and Parkhurst, S.M. (1998). *Drosophila* CtBP: a hairy-interacting protein required for embryonic segmentation and hairy-mediated transcriptional repression. EMBO J. 17, 2067-2078.

Prescott, ED., and Zenisek, D. (2005). Recent progress towards understanding the synaptic ribbon. Curr. Opin. Neurobiol.15, 431-436.

Romanos, M.A. (1995). Advances in the use of *Pichia pastoris* for high level gene expression. Current Opinion Biotechnology. 6, 527-533.

Sambrook, J., Fritsch, E.F., and Maniatis, T. (1989). Molecular cloning: A Laboratory manual. (Cold Spring Harbor Laboratory, Cold Spring Harbor NY). Press. 2nd edition.

Sanger, F., Nicklen S., and Coulson A.R. (1977a). DNA sequencing with chain-terminating inhibitors. Proc. Natl. Acad. Sci. 74, 5463-5467.

Santagata, S., Boggon, T.J., Baird, C.L., Gomez, C.A., Zhao, J., Shan, W.S., Myszka, D.G., and Shapiro, L. (2001). G-protein signalling through tubby proteins. Science. 292, 2041-2050.

Schaeper, U., Boyd, J.M., Verma, S., Uhlmann, E., Subramanian, T., and Chinnadurai, G. (1995). Molecular cloning and characterization of a cellular phosphoprotein that interacts with a conserved C-terminal domain of adenovirus E1A involved in negative modulation of oncogenic tarnsformation. Proc. Natl. Acad. Sci. USA. 92, 10467-10471.

Schlüter, O.M., Schnell, E., Verhage, M., Tzonopoulos, T., Nicholl, R.A., Janz, R., Malenka, R.C., Geppert, M., and Südhof, T.C. (1999). Rabphilin Knock-out mice reveal rat rabphilin is not required for rab3 function in neurotransmitter release. J. Neurosci. 19, 5834-5846.

Schmitz, F., and Drenckhahn, D. (1993). Distribution of actin in cone photoreceptor synapses. Histochemistry. 100, 35-40.

Schmitz, F., Bechmann, M., and Drenckhahn, D. (1996). Purification of synaptic ribbons, structural components of the photoreceptor active zone complex. J. Neurosci. 16, 7109-7116.

Schmitz, F., Königstorfer, A., and Südhof, T.C. (2000). RIBEYE, a component of synaptic ribbons: a protein's journey through evolution provides insight into synaptic ribbon function. Neuron. 28, 857-872.

Schmitz, F., Tabares, L., Khimich, D., Strenzke, N., de la Villa-Polo, P., Castellano-Munoz, M., Bulankina, A., Moser, T., Fernandez-Chacon, R., and Südhof, T.C. (2006). CSPalpha-deficiency causes massive and rapid photoreceptor degeneration. Proc. Natl. Acad. Sci. USA. 103, 2926-2931.

Schneider, S., Buchert, M., and Hovens, C.M. (1996). An *in vitro* assay of β-galactosidase from yeast. *Bio Techniques*. 20, 960-962.

Scorer, C.A., Buckholz, R.G., Clare, J.J., and Romanos, M.A. (1993). The intracellular production and Secretion of HIV-1 Envelope Protein in the Methylotrophic Yeast *Pichia pastoris.* Gene.136, 111-119.

Seigel, G.M. (1996). Establishment of an E1A-immortalized retinal cell culture. In Vitro Cell Dev. Biol. Anim. 32, 66-68.

Seigel, G.M., Sun, W., Wang, J., Hershberger, D.H., Campbell, L.M., and Salvi, R.J. (2004). Neuronal gene expression and function in the growth-stimulated R28 retinal precursor cell line. Curr. Eye Res. 28, 257-269.

Sewalt, R.G., Gunster, M.J., van der, V. J., Satijn, D.P., and Otte, A.P. (1999). C-Terminal binding protein is a transcriptional repressor that interacts with a specific class of vertebrate Polycomb proteins. Mol. Cell Biol. 19, 777-787.

Sharp, P.A., Sugden, B., and Sambrook, J. (1973). Detection of two restriction endonuclease activities in *Haemophilus parainfluenzae* using analytical agarose-ethidium bromide electrophoresis. Biochemistry. 12, 3055-3063.

Shugart, Y., Banerjee, P., Knowles, J.A., Lewis, C.A., Jacobson, S.G., Matise, T.C., Penchaszadeh, G., Gilliam, T.C., and Ott, J. (1995). Fine genetic mapping of a gene for autosomal recessive retinitis pigmentosa on chromosome 6p21. Am. J. Hum. Genet. 57, 499-502.

Singer, J.H. (2007). Multivesicular release and saturation of glutamatergic signalling at retinal ribbon synapses. J. Physiol. 580, 23-29.

Smith, C.A., and Sjöstrand, F.S. (1961). A synaptic structure in the hair cells of the guinea pig cochlea. J. Ultrastruct. Res. 5, 523-556.

Spiwoks-Becker, I., Glas, M., Lasarzik, I., and Vollrath, L. (2004). Mouse photoreceptor synaptic ribbons lose and regain material in response to illumination changes. Eur. J. Neurosci. 19, 1559-1571.

Stahl, B., Diehlmann. A., and Südhof, T.C. (1999). Direct interaction of Alzheimer's disease-related presenilin 1 with armadillo protein p0071. J. Biol. Chem. 274, 9141-9148.

Sterling, P. (1998). The retina. In The Synaptic Organization of the Brain, Fourth Edition, G.Shepherd, ed. (New York: Oxford University Press), pp. 205-253.

Sterling, P., and Matthews, G. (2005). Structure and function of ribbon synapses. Trends Neurosci. 28, 20-29.

Stevens, C.F., and Tsujimoto, T. (1995). Estimates for the pool size of releasable quanta at a single central synapse and for the time required to refill the pool. Proc. Nat. Acad. Sci. 92, 846-849.

Tachibana, M. (1999). Regulation of transmitter release from retinal bipolar cells. Prog. Biophys. Mol. Biol. 72, 109-133.

Tai, A.W., Chuang, J.Z., Bode, C., Wolfrum, U., and Sung, C.H. (1999). Rhodopsin´s carboxy-terminal cytoplasmic tail acts as a membrane receptor for cytoplasmic dynein by binding to the dynein light chain Tctex-1.Cell. 97, 877-887.

Thio, S.S., Bonventre, J.V., and Hsu, S.I. (2004). The CtBP2 co-repressor is regulated by NADH-dependent dimerization and possesses a novel N-terminal repression domain. Nucleic Acids Res. 32, 1836-1847.

tom Dieck, S., Altrock, W.D., Kessels, M.M., Qualmann, B., Regus, H., Brauner, D., Fejtov′a, A., Bracko, O., Grundelfinger, E.D., and Brandstätter, J.H. (2005). Molecular dissection of the photoreceptor ribbon synapse: physical interaction of Bassoon and RIBEYE is essential for the assembly of the ribbon complex. J. Cell Biol.168, 825-836.

tom Dieck, S., and Brandstätter, J.H. (2006). Ribbon synapses of the retina. Cell and Tissue Research 326, 339-346.

Trujillo-Cenoz, O. (1972). The structural organization of the compound eye in insects. In Handbook of Sensory Physiology, Volume VII/2, Physiology of Photoreceptor Organs, M.G.F. Fuortes, ed. (New York: Springer Verlag), 5-62.

Tschopp, J.F., Severlow, G., Kosson, R., Craig, W., and Grinna, L. (1987b). High Level Secretion of Glycosylated invertase in the Methylotrophic Yeast *Pichia pastoris.* Bio/Technology 5, 1305-1308.

Ullrich, B., and Südhof, T.C. (1994). Distribution of synaptic markers in the retina: implications for synaptic vesicle traffic in ribbon synapses. J. Physiol. 88, 249-257.

Vollrath, L., and Spiworks-Becker, I. (1996). Plasticity of retinal ribbon synapses. Microsc. Res. Tec. 35, 472-487.

Von Gresdorff, H., Vardi, E., Matthews, G., and Sterling, P. (1996). Evidence that vesicles on the synaptic ribbon of retinal bipolar neurons can be rapidly released. Neuron. 16, 1221-1227.

Von Gresdorff, H. (2001). Synaptic ribbons: versatile signal transducers. Neuron. 29, 7-10.

Von Kriegstein, K., Schmitz, F., Link, E., and Südhof, T.C. (1999). Distribution of synaptic vesicle proteins in the mammalian retina identifies obligatory and facultative components of ribbon synapses. Eur. J. Neurosci. 11, 1335-1348.

Wagner, H.J. (1997). Presynaptic bodies ("ribbons"): from ultrastructural observations to molecular perspectives. Cell Tissue Res. 287, 435-446.

Wan, L., Almers, W., and Chen, W. (2005). Two ribeye genes in teleosts: the role of ribeye in ribbon formation and bipolar cell development. J. Neurosci. 25, 941-949.

Wang, Y., Okamoto, M., Schmitz, F., Hofmann, K., and Südhof, T.C. (1997). Rim is a putative Rab3 effector in regulating synaptic-vesicle fusion. Nature. 388, 593-598.

Wenzel, A., Grimm, C., Samardzija, M., and Reme, C.E. (2005). Molecular mechanism of light-induced photoreceptor apoptosis and neuroprotection for retinal degeneration. Prog. Retin. Eye Res. 24, 275-306.

Wilson, M. and Nakane, P. (1978). Immunofluorescence and Related staining Technique. Elsevier/North Holland Biomedical Press, Amsterdam p 215.

Yamada, H.Y., and Gorbsky, G.J. (2006). Tumor suppressor candidate TSSC5 is regulated by UbcH6 and a novel ubiquitin ligase RING105. Oncogene. 25, 1330-1339.

Zenisek, D., Horst, N.K., Merrifield, C., Sterling, P., and Matthews, G. (2004). Visualizing synaptic ribbons in the living cell. J. Neurosci. 24, 9752-9759.

Zenisek, D. (2008). Vesicle association and exocytosis at ribbon and extraribbon sites in retinal bipolar cell presynaptic terminals. Proc. Natl. Acad. Sci. USA. 105, 4922-4927.

Zhang, Q., Piston, D.W., and Goodman, R.H. (2002). Regulation of Corepressor Function by Nuclear NADH. Science. 295, 1895-1897.

APPENDICES

List of figures

Figure 1. Schematic overview of the mammalian retina. 8
Figure 2. Detailed anatomy of the outer portion of mammalian retina. 9
Figure 3. Ultrastructural representation of a retinal ribbon synapse. 10
Figure 4. 3D representation of synaptic ribbons. 12
Figure 5. Domain structures of RIBEYE, CtBP2, CtBP1, and phosphoglycerate dehydrogenase. 14

Figure 6. Structure of the Human Gene Encoding RIBEYE and CtBP2. 14
Figure 7. Working Model for the role of RIBEYE in the function of synaptic ribbons. 15
Figure 8. A diagrammatic representation of the TUB protein. 17
Figure 9. Topology diagram of the tubby COOH-terminal domains. 18
Figure 10. Tulp1 loss and retinal degeneration. 18

Figure 11. Mutations associated with RP and its phenotype. 19
Figure 12. Schematic model of $G\alpha_q$ signaling through tubby proteins. 20
Figure 13. The methanol pathway in *Pichia pastoris*. 49
Figure 14. Recombination and integration in *Pichia pastoris* genome. 50
Figure 15. Principle of the Yeast two-hybrid system. 53

Figure 16. RIBEYE(A) interacts with RIBEYE(A) in YTH and pull-down assays . 62
Figure 17. Mapping of RIBEYE(A)-RIBEYE(A) interactions. 65
Figure 18. Multiple interaction among RIBEYE(A)-domain interaction modules in YTH assay. 66
Figure19. Multiple RIBEYE- RIBEYE interactions identified by YTH are confirmed by fusion protein pull-down assays. 67
Figure 20. Homo-dimerization of RIBEYE(B)-domain in YTH assay. 69

Figure 21. Hetero-dimerization of RIBEYE(A)-RIBEYE(B)domains in YTH assay. 70
Figure 22. Hetero-dimerization of RIBEYE(A)-RIBEYE(B)domains in protein pull-down assay. 71
Figure 23. Mapping construct used in RIBEYE(A)-RIBEYE(B) interaction in YTH assay. 72
Figure 24. Mapping of RIBEYE(A)-RIBEYE(B) interaction in YTH assay. 73
Figure 25. Mapping of RIBEYE(A)-RIBEYE(B) interaction in protein pull-down assay. 74

Figure 26. Location of various NBD point mutants and its homo-dimerization with wild type. 75
Figure 27. Mapping of RIBEYE(A)-RIBEYE(B) interaction using NBD point mutants in YTH assay. 76
Figure 28. NAD^+ and NAD(H) inhibits RIBEYE(A) and RIBEYE(B) interaction. 77
Figure 29. Co-clustering of different RIBEYE-proteins in cotransfected COS cells. 79
Figure 30. Co-clustering of different RIBEYE-proteins in cotransfected COS cells (continued). 80

Figure 31. Co-clustering of different RIBEYE-proteins in cotransfected R28 cells. 81
Figure 32. Synaptic ribbon recruits externally added RIBEYE subunits. 82
Figure 33. Synaptic ribbon recruits externally added RIBEYE(A) sub-domains. 83
Figure 34. RIBEYE co-assembles with the active zone protein bassoon in R28 cells. 84
Figure 35. Electron microscopy of RIBEYE-containing aggregates in transfected R28 cells. 86

Figure 36. Schematic RIBEYE-RIBEYE interaction model. 87
Figure 37. Amino acid sequence of bovine, human and rat TULP1. 88
Figure 38. RIBEYE interacts with TULP1 in YTH assays. 90
Figure 39. RIBEYE interacts with TULP1 in protein pull-down assays. 91
Figure 40. TULP1 is a dissociable, peripheral component of synaptic ribbon. 92

Figure 41. Mapping of RIBEYE(A)-TULP1 interaction in YTH assay. 93
Figure 42. Mapping of RIBEYE(B)-TULP1 interaction in the presence/absence of PTNLS motif. 94
Figure 43. Mapping of RIBEYE(B)-TULP1 interaction in the presence of scrambled PTNLS motif (to PTSNL). 95
Figure 44. Human TULP1 mutations and its implication in interactions. 96
Figure 45. Working hypothesis on the assembly of ribbons from RIBEYE units. 102

List of abbreviations

µg	microgram
µl	microlitre
ΔDL	Deletion of dimerisation loop
A	Adenine
$A_{260\ nm}$	Absorbance at 260 nm
$A_{280\ nm}$	Absorbance at 280 nm
aa	Amino acids
AD	Activation Domain
-ALWH	Drop out medium lacking Adenine, Leucine, Tryptophan and Histidine
Amp	Ampicillin
AOX1	Alcohol oxidase1
AOX2	Alcohol oxidase1
BARS	brefeldin A-ADP ribosylated substrate
bc	Bipolar cell
BD	Binding Domain
BMGY	Buffered glycerol complex medium
BMMY	Buffered methanol complex medium
bp	base pair
BSA	Bovine serum albumin
C	Celsius
cDNA	complementary DNA
CSM-HIS	Complete supplement mixture lacking histidine
CtBP1	C-terminal Binding Protein 1
CtBP2	C-terminal Binding Protein 2
Cy2	Carbocyanin
Cy3	Indocarbocyanin
ddH_2O	double distilled water
DEAE dextran	Diethylaminoethyldextran
DMEM	Dulbecco´s Modified Eagle's Medium
DNA	Deoxyribonucleicacid
dNTP	deoxyribonucleotides
DTT	Dithiothreitol
ECL	Enhanced chemiluminiscence
E. coli	*Escherichia coli*
EGFP	Enhanced Green Fluorescent Protein
EDTA	Ethylenediaminetetrachloroacteic acid
EM	Electron microscopy
F	Forward
For. Primer	Forward primer
Gal	Galactose
GCL	Ganglion cell layer
GFP	Green Fluorescent Protein

GST	Glutathione S-transferase
H	Histidine
Hc	Horizontal cell
INL	Inner nuclear layer
IPTG	Isopropyl-β-D-Thiogalactopyranoside
IPL	Inner plexiform layer
IS	Inner segments
Kb	Kilobases
kDa	kilo Dalton
-L	Yeast selection medium lacking Leucine
LB	Luria-Bertani medium
LPAAT	Lysophosphatidic acid acyltransferase
LR gold	LR-Gold resin (London resin)
-LW	Yeast selection medium lacking Leucine and Tryptophan
MBP	Maltose binding protein
MCS	Multiple cloning site
min(s)	minute(s)
ml	millilitre
mRFP	monomeric red fluorescent protein
Mut^s	Methanol utilization slow (slow growth in the presence methanol)
Mut^+	Methanol utilization plus (fast growth in presence of methanol)
MW	Molecular weight
NAD	oxidised Nicotinamide adenine dinucleotide
NADH	reduced Nicotinamide adenine dinucleotide
NBD	NADH binding sub-domain
ng	nanogram
nm	nanometer
NLS	Nuclear localization signal
OD	Optical density
OLM	Outer limiting membrane
ONL	Outer nuclear layer
ONPG	o-Nitrophenyl-β-D-galactoside
OPL	Outer plexiform layer
OS	Outer segments
P	Primer
PBS	Phosphate Buffered Saline
PCR	Polymerase Chain Reaction
PFA	Paraformaldehyde
PMSF	Phenylmethanesulphonylfluoride
PtdIns $(4,5)P_2$	Phosphatidylinositol 4,5-bisphosphate
PtdIns $(3,4)P_2$	Phosphatidylinositol 3,4-bisphosphate
PtdIns $(3,4,5)P_3$	Phosphatidylinositol 3,4,5-triphosphate
R	Reverse
RE(A)	RIBEYE(A)-Domain
RE(B)	RIBEYE(B)-Domain
Rev. primer	Reverse primer

RP-14	Retinitis pigmentosa -14
rpm	revolutions per minute
RT	room temperature
RT-PCR	Reverse transcription-PCR
SBD	Substrate binding sub-domain
SD	Synthetic Drop out medium
SDS	Sodiumdodecylsulfate
SDS-PAGE	SDS Polyacrylamide gel electrophoresis
s.e.m	Standard error of mean
TAD	Transcriptional activation domain
TAE	Tris Acetate EDTA
TE	Tris EDTA
Tris	Trishydroxymethylaminomethane
TULP1	Tubby-like protein1
U	Unit
V	Volts
V/V	volume/volume
-W	Yeast selection medium lacking Tryptophan
X-Gal	5-Bromo-4-chloro-3-indolyl-β-D-galactopyranoside
YPD	Yeast extract, peptone, and dextrose
YTH	Yeast two-hybrid

Curriculum Vitae

Venkat Giri Magupalli

Address for correspondence:

Anatomy and Cell Biology Department,
Medical faculty, Saarland University,
Building 61, Homburg/Saar, D-66421,
Germany

Tel: +49 6841-1626199
E-mail: venkatgirim@gmail.com

Residence address:

Apartment E-47,
Steinhübel-12,
Homburg/Saar, D-66421,
Germany

Personal data:

First name:	Venkat Giri
Family name:	Magupalli
Date of Birth:	28th March 1980
Sex:	Male
Place of Birth:	Orissa, India
Nationality:	Indian

Scientific publications:

Multiple Ribeye-Ribeye interactions create a dynamic scaffold for the formation of synaptic ribbon. Venkat Giri Magupalli, Karin Schwarz, Kannan Alpadi, Sivaraman Natarajan, Gail M. Seigel and Frank Schmitz. Journal of Neuroscience. 28, 7954-7967.

RIBEYE recruits Munc119, a mammalian ortholog of the *C. elegans* protein unc119, to synaptic ribbons of photoreceptor ribbon synapses. Kannan Alpadi, Venkat Giri Magupalli, Stefanie Käppel, Louise Köblitz, Karin Schwarz, Gail M. Seigel, Ching-Hwa Sung and Frank Schmitz. Journal of Biological Chemistry. 283, 26461-26467.

The Retinitis Pigmentosa disease protein TULP1 is a component of synaptic ribbons, and interacts with RIBEYE. Venkat Giri Magupalli, Louise Köblitz, Kannan Alpadi, C.H. Sung and Frank Schmitz. (Manuscript in preparation).

Academic Qualifications:

September 2008
Doctorate in Philosophy (Ph.D), University of Saarlandes, Germany. Thesis work was carried out under the supervision of Prof. Dr. med. Frank Schmitz (Chair of Neuroanatomy, Department of Anatomy and Cell Biology).

July 2003
Masters of Science (M.Sc), University of Hyderabad, Hyderabad, India.
First class with Distinction.

July 2001
Bachelors of Science (B.Sc) Honours, Utkal University, Bhubaneswar, Orissa.
First class with Distinction.

July 1997
Secondary School Leaving Certificate (S.S.L.C), Kendriya Vidyalaya No:1, Bhubaneswar, Orissa.
First class.

Research experience:

October 2004-June 2008
Molecular and Functional characterization of RIBEYE and interacting proteins. Institute for Anatomy and Cell Biology, Medical faculty, Saarland University, Homburg (Saar).

July 2002-July 2003
Serotonin circadian rhythms in Suprachiasmatic nucleus and Pineal gland of rat brain. University of Hyderabad, India.

Honours / distinctions:

IBRO (International Brain Research Organisation) fellowship for attending 3rd Asia-Pacific Associate School of Neuroscience (2004), India.

Gold medal in Masters Degree of Science (M.Sc), University of Hyderabad, India.

University Merit Scholarship in Masters Degree of Science. University of Hyderabad, India.

Fourth position in Bachelor (Honours) Degree; Utkal University, India.

National Merit Scholarship in Bachelor (Honours) Degree, Ministry of Human Resource Development (Government of India), New Delhi, India.

National player of Hockey, Sport Authority of India, Salt-lake City, India.

Abstract / Poster presentation:

Multiple Ribeye-Ribeye interactions create a dynamic scaffold for the formation of synaptic ribbon. Venkat Giri Magupalli, Karin Schwarz, Kannan Alpadi, Sivaraman Natarajan, Gail M. Seigel and Frank Schmitz.
Molecular pathways in health and disease of the nervous system. Annual Meeting, Homburg/Saar, Germany, 2008.

Scientific membership and Research grants awarded:

Member of Society for Neuroscience (SFN).

University of Saarlandes, Medicine faculty Homburger Forschungsförderungsprogramm HOMFOR 2006 and Zentrale Forschungskommission (ZFK) 2006.

Cellular/Molecular

Multiple RIBEYE–RIBEYE Interactions Create a Dynamic Scaffold for the Formation of Synaptic Ribbons

Venkat Giri Magupalli,[1] Karin Schwarz,[1] Kannan Alpadi,[1] Sivaraman Natarajan,[1] Gail M. Seigel,[2] and Frank Schmitz[1]

[1]Department of Neuroanatomy, Institute for Anatomy and Cell Biology, Saarland University, Medical School Homburg/Saar, 66421 Homburg/Saar, Germany, and [2]Department of Ophthalmology, Physiology and Biophysics, State University of New York at Buffalo, Buffalo, New York 14214

Synaptic ribbons are large, dynamic structures in the active zone complex of ribbon synapses and important for the physiological properties of these tonically active synapses. RIBEYE is a unique and major protein component of synaptic ribbons. The aim of the present study was to understand how the synaptic ribbon is built and how the construction of the ribbon could contribute to its ultrastructural plasticity. In the present study, we demonstrate that RIBEYE self-associates using different independent approaches (yeast two-hybrid analyses, protein pull downs, synaptic ribbon–RIBEYE interaction assays, coaggregation experiments, transmission electron microscopy and immunogold electron microscopy). The A-domain [RIBEYE(A)] and B-domain [RIBEYE(B)] of RIBEYE contain five distinct sites for RIBEYE–RIBEYE interactions. Three interaction sites are present in the A-domain of RIBEYE and mediate RIBEYE(A)–RIBEYE(A) homodimerization and heterodimerization with the B-domain. The docking site for RIBEYE(A) on RIBEYE(B) is topographically and functionally different from the RIBEYE(B) homodimerization interface and is negatively regulated by nicotinamide adenine dinucleotide. The identified multiple RIBEYE–RIBEYE interactions have the potential to build the synaptic ribbon: heterologously expressed RIBEYE forms large electron-dense aggregates that are in part physically associated with surrounding vesicles and membrane compartments. These structures resemble spherical synaptic ribbons. These ribbon-like structures coassemble with the active zone protein bassoon, an interaction partner of RIBEYE at the active zone of ribbon synapses, emphasizing the physiological relevance of these RIBEYE-containing aggregates. Based on the identified multiple RIBEYE–RIBEYE interactions, we provide a molecular mechanism for the dynamic assembly of synaptic ribbons from individual RIBEYE subunits.

Key words: **synaptic ribbon; ribbon synapse; RIBEYE; retina; active zones; exocytosis**

Introduction

Ribbon synapses are specialized chemical synapses, e.g., in the retina and inner ear, capable to maintain rapid exocytosis of synaptic vesicles for prolonged periods of time (for review, see Fuchs, 2005; Heidelberger et al., 2005; Prescott and Zenisek, 2005; Sterling and Matthews, 2005; Nouvian et al., 2006; Singer, 2007). For this purpose, ribbon synapses are equipped with presynaptic specializations, the synaptic ribbons, which are considered to speed vesicle trafficking (for review, see tom Dieck and Brandstätter, 2006; Nouvian et al., 2006; Sterling and Matthews, 2005). Synaptic ribbons are large presynaptic structures associated with the active zone complex of ribbon synapses (for review, see Wagner, 1997). Synaptic ribbons of photoreceptor synapses are plate-like structures in three-dimensional representations that can be >500 nm in length and depth. In EM sections, retinal synaptic ribbons usually appear bar-shaped, and inner ear synaptic ribbons are usually spherical structures (for review, see Nouvian et al., 2006). Also in the retina, the assembly of the bar-shaped ribbon is believed to go through spherical ribbon intermediates, the so called synaptic spheres (for review, see Vollrath and Spiwoks-Becker, 1996; Spiwoks-Becker et al., 2004). The dimensions of synaptic ribbons in the retina can vary and are subject to changes, e.g., in response to different stimuli (lighting conditions/circadian rhythm), probably reflecting structural adaptations to different degrees of synaptic activity (for review, see Vollrath and Spiwoks-Becker, 1996; Wagner, 1997). Regardless of their shape, synaptic ribbons are associated with large amounts of synaptic vesicles and other membrane compartments (for review, see Sterling and Matthews, 2005).

We have previously identified a novel protein, "RIBEYE," as a unique and specific component of synaptic ribbons (Schmitz et al., 2000). RIBEYE is present in synaptic ribbons of all vertebrate ribbon synapses (Schmitz et al., 2000, 2006; Zenisek et al., 2004; Khimich et al., 2005; tom Dieck et al., 2005; Wan et al., 2005) (for review, see tom Dieck and Brandstätter, 2006). RIBEYE consists of a unique A-domain [RIBEYE(A)] and B-domain [RIBEYE(B)] that is identical to CtBP2 except for the first 20 aa (Schmitz et al., 2000). The B-domain of RIBEYE binds nicotinamide adenine dinucleotide (NAD^+ or NADH [NAD(H)]) with high affinity

Received Jan. 29, 2008; revised June 21, 2008; accepted June 21, 2008.

This work was supported by Deutsche Forschungsgemeinschaft Grant SFB530 TP C11 and HOMFOR (F.S.), and by Research to Prevent Blindness and National Institutes of Health Infrastructure Grant R24EY016662 (G.M.S.). We thank Drs. M. J. Schmitt and L. Köblitz (Saarland University) for the donation of plasmids and yeast strains; Dr. Susanne tom Dieck (Max Planck Institute for Brain Research Frankfurt) for the gift of anti-rat RIBEYE(A) antibody; Dr. H. T. McMahon (Medical Research Council, Cambridge, UK) for the donation of JC201 bacteria; and Dr. Jutta Schmitz-Kraemer for critically reading this manuscript.

Correspondence should be addressed to Dr. Frank Schmitz, Department of Neuroanatomy, Institute for Anatomy and Cell Biology, Saarland University, Medical School Homburg/Saar, Kirrbergerstrasse, Building 61, 66421 Homburg/Saar, Germany. E-mail: frank.schmitz@uniklinik-saarland.de.

DOI:10.1523/JNEUROSCI.1964-08.2008

Copyright © 2008 Society for Neuroscience 0270-6474/08/287954-14$15.00/0

and belongs to a family of D-isomer-specific 2-hydroxy acid dehydrogenases (Schmitz et al., 2000). The structural analysis of these proteins, e.g., of CtBP1, revealed the presence of two globular subdomains, namely an NAD(H)-binding subdomain (NBD) and the substrate-binding subdomain (SBD) (for a review, see Chinnadurai, 2002; Kumar et al., 2002; Nardini et al., 2003).

Previous data indicated that RIBEYE is the major component of synaptic ribbons (Schmitz et al., 2000; Zenisek et al., 2004; Wan et al., 2005). In the present study, we analyzed functional properties of RIBEYE and demonstrate that RIBEYE is capable to interact with itself. RIBEYE–RIBEYE interactions are mediated through three binding sites in the A-domain and two binding sites in the B-domain enabling multiple RIBEYE–RIBEYE interactions. RIBEYE–RIBEYE interactions can generate the three-dimensional scaffold of the synaptic ribbon and provide a molecular mechanism for the ultrastructural plasticity of these presynaptic structures.

Materials and Methods

Plasmids. Details on all plasmids and antibodies used in this study are posted in the supplemental Methods (available at www.jneurosci.org as supplemental material).

Yeast two-hybrid methods. We used the galactosidase-4 (Gal4)-based Matchmaker Yeast Two-Hybrid System (Clontech) according to the manufacturer's instructions. The cDNA of the respective bait proteins were cloned in frame with the Gal4-DNA-binding domain of pGBKT7. The cDNA of the indicated prey proteins were cloned in frame with the Gal4-activation domain of pACT2 or pGADT7. The bait and prey plasmids confer tryptophan and leucine prototrophy to the respective auxotrophic yeast strains. Yeast strains Y187 and AH109 were used that contain distinct auxotrophic marker genes: AH109 contained *MATa*, *trp1–901*, *leu2-3,112*, *ura3-52*, *his3-200*, *gal4*Δ, *gal80*Δ, *LYS2::GAL1*$_{UAS}$-*GAL1*$_{TATA}$-*HIS3*, *GAL2*$_{UAS}$-*GAL2*$_{TATA}$-*ADE2*, and *URA3::MEL1*$_{UAS}$-*MEL1*$_{TATA}$-*lacZ* (James et al., 1996); Y187 contained *MAT*α, *ura3-52*, *his3-200*, *ade2-101*, *trp1-901,leu2-3,112*, *gal4*Δ, *met*, *gal80*Δ, and *URA3::GAL1*$_{UAS}$-*GAL1*$_{TATA}$-*lacZ* (Harper et al., 1993). Bait plasmids were always electroporated into AH109 yeast, whereas all prey plasmids were transformed into Y187. Preparation of electrocompetent yeasts and electroporation of yeasts were done as described previously (Helmuth et al., 2001). For identifying transformants, yeasts were plated on the respective selective plates to identify the resulting convertants to the respective prototrophy (drop out media Clontech/QBiogene). For interaction analyses, AH109 yeasts containing the respective bait plasmid were mated with Y187 yeasts containing the respective prey plasmid. Mating was performed for 5 h at 30°C in 1 ml of YPD medium (yeast extract, peptone, and dextrose) with heavy vortexing. For assessing mating efficiency, half of the mated sample was streaked on −LW plates [containing synthetic complete yeast medium without leucine (L) and without tryptophan (W)], and the other half was plated on −ALWH selective plate [containing synthetic complete yeast medium without adenine (A), L, W, and histidine (H)] with 10 mM 3-amino-1,2,4-triazole added. For the matings, pSE1111 and pSE1112 (Bai and Elledge, 1996) as well as the empty bait and prey vectors were used as negative controls. Expression of β-galactosidase (β-gal) marker gene expression were qualitatively analyzed by filter assays and quantitatively with liquid assays as described previously (Wang et al., 1997; Stahl et al., 1999).

Expression of RIBEYE(A)-domain. RIBEYE(A)-glutathione *S*-transferase (GST) is difficult to express in conventional prokaryotic expression systems because of its high contents of proline, serine, glycine, and arginine residues (Schmitz et al., 2000) (our unpublished observations). We identified two expression systems to express full-length RIBEYE(A)-GST fusion protein. One source were LPAAT (lysophosphatidic acid acyltransferase)-deficient JC201 bacteria (Coleman, 1990), which express full-length RIBEYE(A)-GST fusion protein although part of it is processed to smaller fragments (see Figs. 1 *B*, 4 *B*, 6 *A*, *B*, 10 *B*; supplemental Fig. 1 *B*, available at www.jneurosci.org as supplemental material). The second source were methylotropic yeast *Pichia pastoris* (Cereghino and Cregg, 2000). Electroporation of JC201 and expression and purification of RIBEYE(A)-GST fusion protein was performed according to standard procedures (Schmitz et al., 2000). A certain degree of proteolytic processing of RIBEYE(A) is present in both of these systems. The proteolytic processing cannot be prevented even under optimized fermenting conditions using the BioFlo 110 fermenter (New Brunswick Scientific) with constant oxygenation of the medium, pH control, different induction times, and different induction temperatures (data not shown).

Intracellular expression of untagged RIBEYE(A) in Pichia pastoris. *Pichia pastoris* yeast strain GS115 (*his4*) (Invitrogen) was used for heterologous protein expression (Lin-Cereghino et al., 2005). Yeast cultures were grown at 30°C on synthetic minimal medium containing 0.67% yeast nitrogen base (without amino acids supplemented with ammonium sulfate and appropriate amino acid-base; Formedium). RE(A)pPIC3.5K was electroporated into freshly made electrocompetent yeasts GS115 (*his4*) as described (Lin-Cereghino et al., 2005). For electroporation, 10 μg of purified and *Sal*I-linearized plasmid DNA was used. Electroporation was performed at 1500 V (BTX ECM 399 electroporator; Biogentronix) with 2 mm gapped prechilled cuvette (Peqlab). Recombinant His$^+$ clones were selected on MD (minimal dextrose) plates (0.67% yeast nitrogen base without amino acids, 0.077% CSM-His, 2% dextrose, 0.00004% biotin, 1 M sorbitol, 1.5% agar–agar). Genomic integration of the electroporated construct was confirmed through genomic PCR (5′-AOX1-primer: GACTGGTTCCAATTGACAAGC; 3′-AOX1-primer: GCAAATGGCATTCTGACATCC). For induction of fusion protein, yeasts were first cultured in BMGY medium (1% yeast extract, 2% peptone, 0.67% yeast nitrogen base without amino acids, 0.00004% biotin, 1% glycerol, 0.1 M potassium-phosphate buffer, pH 6) at 30°C to an optical density at 600 nm (OD_{600}) of 2–6. Induction was achieved in BMMY medium (same as BMGY with 0.5% methanol instead of glycerol) at 30°C, starting the culture at an OD_{600} of 1. After every 24 h, methanol was replenished to the final volume of 0.5%. After 36 h of induction, the cells were pelleted (1500 rpm, 5 min, 4°C) and processed for extraction of fusion protein. Induced *Pichia pastoris* yeasts were mechanically cracked with 0.5 mm glass beads (Biospec/Roth) in breaking buffer (50 mM sodium phosphate, pH 7.4, 100 mM NaCl, 1 mM EDTA, 5% glycerol, 1 mM PMSF). For this purpose, 100 μl cell pellet were resuspended in 890 μl of ice-cold breaking buffer. To this mixture, ~500 μl of glass beads were added. The cracking was performed at +4°C using high-speed vortex (25× vortexing for 30 s; between vortexing, samples were chilled 30 s on ice). The lysate was centrifuged twice (13,000 rpm, 1 h at 4°C). Subsequently, the supernatant was precleared with 20 μl empty glutathione-agarose beads (Fluka) for 1 h at 4°C on a rotary wheel.

Protein pull-down assays using bacterial fusion protein. For pull-down experiments using pairs of GST- and maltose-binding protein (MBP)-tagged fusion proteins, the GST-tagged fusion proteins were usually kept immobilized on glutathione beads whereas MBP fusion proteins were used as solublized prey proteins if not denoted otherwise. Bait and prey proteins were used in equimolar amounts along with the respective control proteins. Protein concentrations were determined using the Bradford method (Bradford, 1976). For pull-down experiments, fusion protein eluates were precleared with 10 μl of empty glutathione Sepharose beads (per 1 ml of eluate) for 1 h at 4°C. Binding was performed in PBS that contained 0.5% Triton X-100 at 4°C for 12 h on a rotary wheel (500 μl incubation volume) if not denoted otherwise. Pellets were washed five times by adding an excess of PBS/Triton X-100 and subsequent spinning (13,000 rpm, 1 min, 4°C). Pellets were boiled in SDS-sample buffer and subsequently subjected to Western blot analyses with the indicated antibodies.

Miscellaneous methods. For the preparation of synaptic ribbons, synaptic ribbons were purified as described previously (Schmitz et al., 1996, 2000). Standard protein techniques were performed as described previously (Schmitz et al., 2000). For reprobing of Western blots, nitrocellulose sheets were treated with prewarmed (90°C) stripping buffer (1% SDS, 10 mM β-mercaptoethanol in PBS) and incubated at room temperature for 1 h. Immunofluorescence microscopy was performed as described previously (Schmitz et al., 2000, 2006) using a Zeiss Axiovert 200M microscope (Carl Zeiss) equipped for conventional epifluorescence microscopy with the respective filter sets for enhanced green fluorescent protein (EGFP) and monomeric red fluorescent protein (mRFP)

and equipped with an Apotome (Zeiss) to make optical sections. Transfection of COS cells was done as described previously with the DEAE-dextran method (Schmitz et al., 2000). R28 cells were transfected by lipofection using perfectin (Peqlab) according to the manufacturer's instructions. Transfected cells were usually analyzed by fluorescence microscopy 48 h after transfection if not denoted otherwise. Conventional transmission, immunogold electron microscopy, and quantification of radioactive NAD^+-binding to RIBEYE fusion proteins were performed as described previously (Schmitz et al., 1996, 2000). Thrombin cleavage of GST-tagged fusion protein was performed mostly as described previously (Chadli et al., 2000).

Results

Homodimerization of RIBEYE(A)

We used the yeast two-hybrid (YTH) system to determine whether the A-domain of RIBEYE can homodimerize. In YTH, we observed a strong self-interaction between the A-domains of RIBEYE as judged by growth on −ALWH-selective plates and expression of the β-galactosidase marker gene activity compared with the respective control matings (Fig. 1*A*, mating 1; supplemental Fig. 1*A*, available at www.jneurosci.org as supplemental material). RIBEYE(A) also interacted with full-length RIBEYE [RIBEYE(AB)] (Fig. 1*A*, mating 6). The RIBEYE-expressing yeasts were not autoactivating in YTH, as demonstrated by the lack of growth on −ALWH plates and analysis of β-galactosidase expression of the respective control matings (Fig. 1*A*, matings 2–5, 7, 8). Quantitative β-galactosidase activities determined in liquid assays are shown in supplemental Figure 1*A* (available at www.jneurosci.org as supplemental material). The homodimerization of RIBEYE(A) observed in the YTH system was also confirmed at the protein level using two different pull-down assays (Fig. 1*B*; supplemental Fig. 1*B*, available at www.jneurosci.org as supplemental material). Immobilized RIBEYE(A)-MBP fusion protein (but not immobilized MBP alone) bound soluble RIBEYE(A)-GST fusion protein (but not GST alone) (Fig. 1*B*). Similarly, immobilized RIBEYE(A)-GST specifically bound RIBEYE(A) from crude protein extracts of RIBEYE(A)-transgenic *Pichia pastoris* (supplemental Fig. 1*B*, available at www.jneurosci.org as supplemental material). GST control protein alone did not bind RIBEYE(A) from the *Pichia pastoris* extract. Thus, both YTH and protein pull-down data independently demonstrated that RIBEYE(A) interacts with RIBEYE(A).

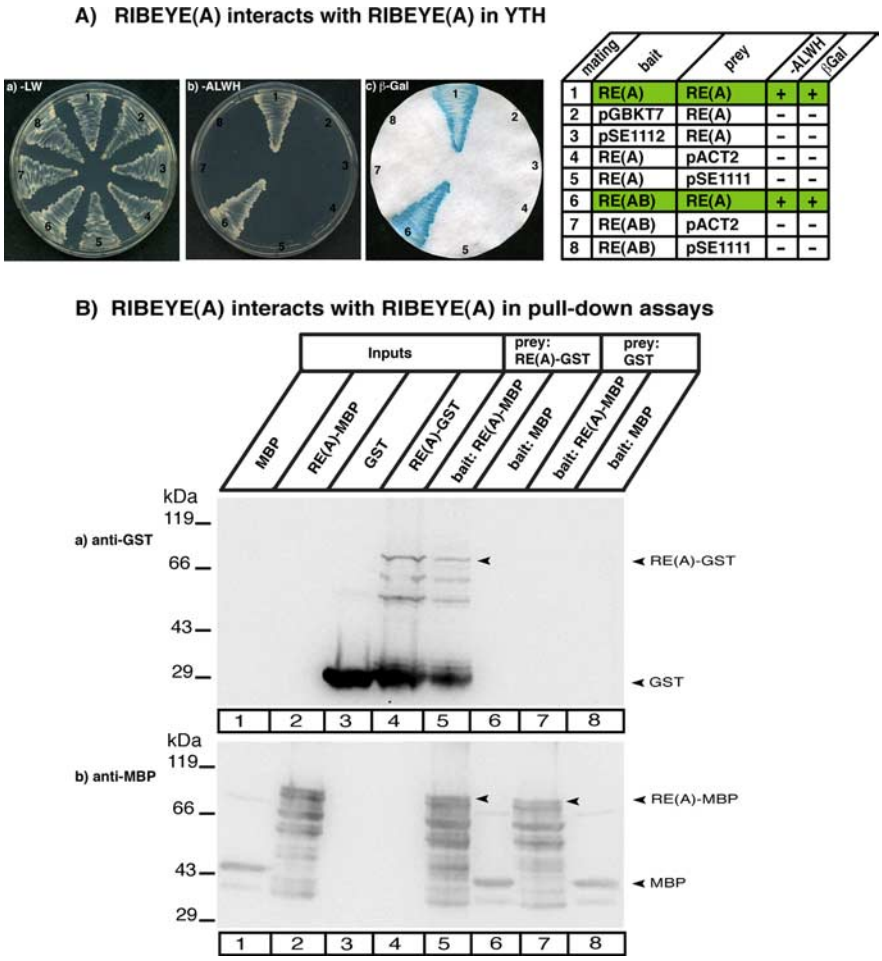

Figure 1. RIBEYE(A) interacts with RIBEYE(A). ***A***, RIBEYE(A) interacts with RIBEYE(A) in YTH. Summary plates of YTH analyses obtained with the indicated bait and prey plasmids. The indicated yeast clones growing on selective medium either for the presence of bait and prey plasmids (−LW dropout medium) or selective for protein–protein interaction (−ALWH dropout medium). For convenience, experimental bait–prey pairs are underlayered in color (green in case of interacting bait–prey pairs; control matings are not colored). RIBEYE(A) interacts with RIBEYE(A) and RIBEYE(AB) as judged by growth on selective plates (−ALWH) and expression of β-galactosidase expression (yeast matings 1, 6; ***Ab***, ***Ac***). The respective control matings (autoactivation controls; yeast matings 2–5, 7–8) did not show growth on −ALWH plates and expression of β-galactosidase activity. For quantification of the β-gal activities, see also supplemental Figure 1*A* (available at www.jneurosci.org as supplemental material). Growth on −LW plates (***Aa***) demonstrates the presence of the bait and prey plasmids in the mated yeasts. ***Ba***, ***Bb***, RIBEYE(A) interacts with RIBEYE(A) in protein pull-down experiments (Western blot analyses). RIBEYE(A)-MBP and MBP alone (control) were used as immobilized bait proteins and RIBEYE(A)-GST and GST alone (control) as soluble prey proteins. RIBEYE(A)-GST specifically binds to RIBEYE(A)-MBP (***Ba***, lane 5, arrowhead). RIBEYE(A)-GST does not bind to MBP alone (***Ba***, lane 6). GST alone also does not bind to RIBEYE(A)-MBP (***Ba***, lane 7). ***Bb*** shows the same blot as in ***Ba*** after stripping and reprobing of the nitrocellulose with anti-MBP antibodies to show equal loading of bait proteins. RIBEYE(A)-GST also specifically binds intracellularly expressed RIBEYE(A) from a crude extract of RIBEYE(A)-transgenic *Pichia pastoris* (supplemental Fig. 1*B*, available at www.jneurosci.org as supplemental material). RE(AB), full-length RIBEYE; RE(A), RIBEYE(A).

Mapping of RIBEYE(A)–RIBEYE(A) interaction

In the rat, RIBEYE(A) consists of the N-terminal 563 aa. To map the interaction sites important for RIBEYE(A)–RIBEYE(A)-interaction, we generated C- and N-terminal deletion constructs of RIBEYE(A) and tested them for their capability to interact with full-length RIBEYE(A) in YTH (Fig. 2*A*,*B*; supplemental Fig. 2, available at www.jneurosci.org as supplemental material). Most of the C-terminal region of the A-domain could be removed without abolishing the interaction with RIBEYE(A). RIBEYE(A)1–105 was the shortest N-terminal construct that could interact with full-length RIBEYE(A)-domain (Fig. 2*B*, prey 7). Therefore, the first 105 N-terminal amino acids contain a binding site for RIBEYE(A), which is subsequently denoted as the "A1" interaction site. We also analyzed N-terminal deletions of RIBEYE(A) for their interaction with full-length RIBEYE(A) (Fig. 2*B*; supplemental Fig. 2, available at www.jneurosci.org as supplemental material). Interestingly, N-terminal deletion constructs of RIBEYE that did not contain the previously identified RIBEYE(A1)-binding site also interacted with RIBEYE(A) (Fig.

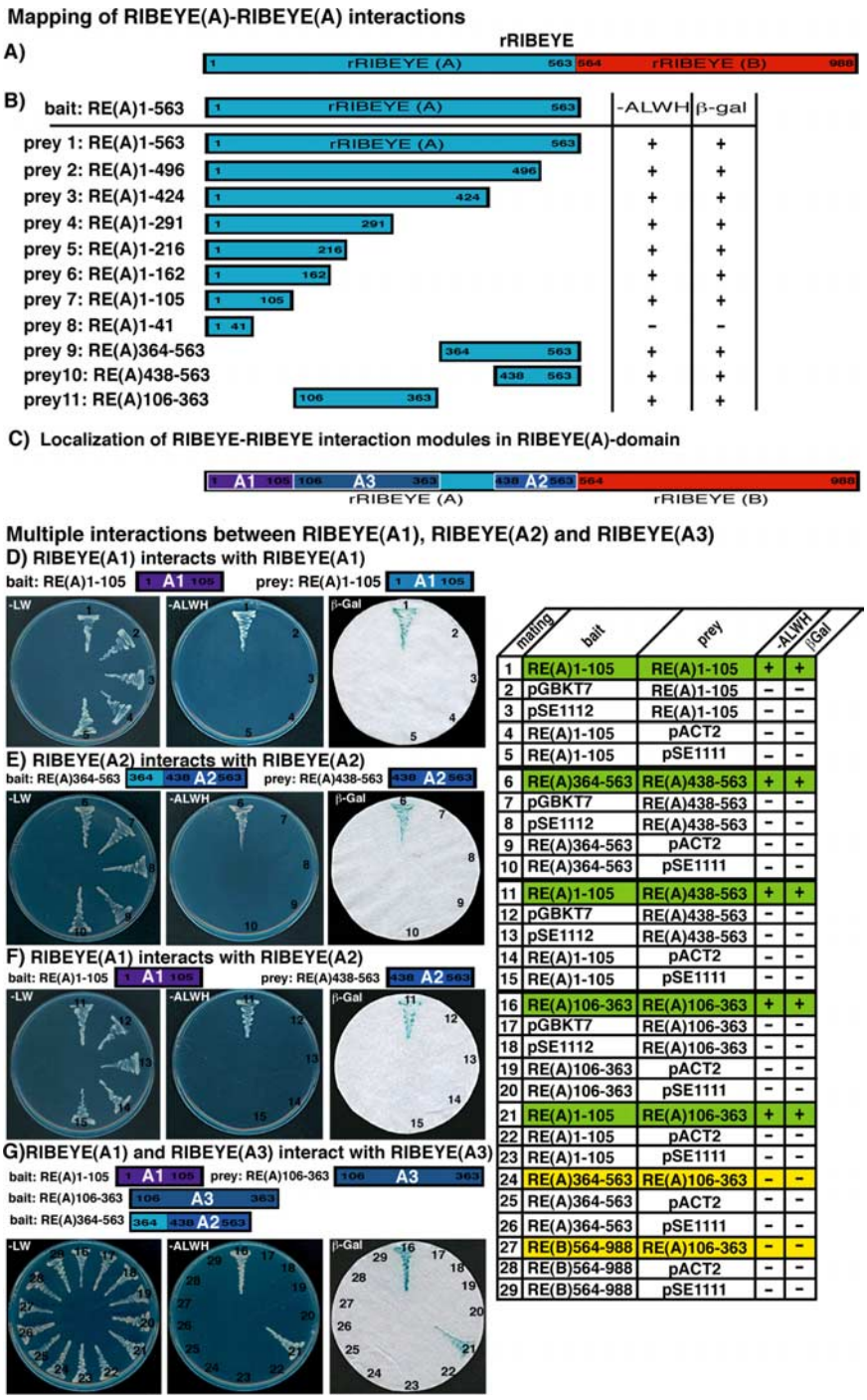

mating	bait	prey	-ALWH	β-Gal
1	RE(A)1-105	RE(A)1-105	+	+
2	pGBKT7	RE(A)1-105	–	–
3	pSE1112	RE(A)1-105	–	–
4	RE(A)1-105	pACT2	–	–
5	RE(A)1-105	pSE1111	–	–
6	RE(A)364-563	RE(A)438-563	+	+
7	pGBKT7	RE(A)438-563	–	–
8	pSE1112	RE(A)438-563	–	–
9	RE(A)364-563	pACT2	–	–
10	RE(A)364-563	pSE1111	–	–
11	RE(A)1-105	RE(A)438-563	+	+
12	pGBKT7	RE(A)438-563	–	–
13	pSE1112	RE(A)438-563	–	–
14	RE(A)1-105	pACT2	–	–
15	RE(A)1-105	pSE1111	–	–
16	RE(A)106-363	RE(A)106-363	+	+
17	pGBKT7	RE(A)106-363	–	–
18	pSE1112	RE(A)106-363	–	–
19	RE(A)106-363	pACT2	–	–
20	RE(A)106-363	pSE1111	–	–
21	RE(A)1-105	RE(A)106-363	+	+
22	RE(A)1-105	pACT2	–	–
23	RE(A)1-105	pSE1111	–	–
24	RE(A)364-563	RE(A)106-363	–	–
25	RE(A)364-563	pACT2	–	–
26	RE(A)364-563	pSE1111	–	–
27	RE(B)564-988	RE(A)106-363	–	–
28	RE(B)564-988	pACT2	–	–
29	RE(B)564-988	pSE1111	–	–

Figure 2. Mapping of RIBEYE(A)–RIBEYE(A) interactions. ***A***, Schematic domain structure of RIBEYE showing the N-terminal A-domain and the C-terminal B-domain. ***B***, ***C***, Summary of mapping analyses. The indicated bait and prey plasmids were used to test for the interaction of the respective proteins in the YTH system. YTH analyses of the C-terminal deletion constructs of RIBEYE(A) reveal an N-terminal site (within the first 105 aa) that interacts with RIBEYE(A). This interaction site is denoted as A1 (***C***). YTH analyses of N-terminal deletion constructs of RIBEYE(A) reveal a second interaction site in the C-terminal region of RIBEYE(A) that interacts with RIBEYE(A). This C-terminal interaction site is denoted as A2 (***C***) and covers amino acids 438–563. The A3 region (***C***) in the middle of RIBEYE(A) (amino acids 106–363) that does not contain A1 and A2 is also able to interact with full-length RIBEYE(A). ***C***, Schematic representation of the identified RIBEYE–RIBEYE interaction modules (A1, A2, A3) in the A-domain of RIBEYE. ***D–G***, The indicated minimal interaction modules (A1, A2, and A3) were tested in the YTH system for interaction with each other. For convenience, experimental bait–prey pairs are underlayered in color (green for interacting bait–prey pairs; yellow for noninteracting bait–prey pairs); control matings are not colored. ***D***, RIBEYE(A1) interacts with RIBEYE(A1) (mating 1). Matings 2–5 show the respective indicated control matings. ***E***, RIBEYE(A2) interacts with RIBEYE(A2) (mating 6). Matings 7–10 show the respective indicated control matings. ***F***, RIBEYE(A1) interacts with RIBEYE(A2) (mating 11). Matings 12–15 show the respective indicated control matings. ***G***, RIBEYE(A1) and RIBEYE(A3) interact with RIBEYE(A3) (matings 21, 16). RIBEYE(A3) does not interact with RIBEYE(B) (mating 27). Matings 22, 23, 17–20, 28, and 29 show the respective indicated control matings. No used RIBEYE constructs were autoactivating. RIBEYE(A2) does not interact with RIBEYE(A3) (mating 24). Matings 25 and 26 show the respective control matings. RE(A), RIBEYE(A); RE(B), RIBEYE(B).

2*B*, preys 9, 10; supplemental Fig. 2, available at www.jneurosci.org as supplemental material), pointing to a second homodimerization site in the C-terminal region of RIBEYE(A). We identified RIBEYE(A)438–563 as the smallest C-terminal portion of RIBEYE(A) that interacts with RIBEYE(A) (Fig. 2*B*; supplemental Fig. 2, available at www.jneurosci.org as supplemental material). This C-terminal RIBEYE(A) interaction site is denoted as "A2" in the following text. We further tested whether the midregion of RIBEYE(A), which does neither contain the N-terminal A1 interaction site nor the C-terminal A2 interaction site for its capability to interact with RIBEYE(A). This region in the midportion of RIBEYE(A), denoted as "A3," also interacted with RIBEYE(A) (Fig. 2*B*, prey 11). Thus, the A-domain of RIBEYE has three independent sites which are able to interact with full-length RIBEYE(A) (summarized in Fig. 2*C*). Supplemental Figure 2 (available at www.jneurosci.org as supplemental material) demonstrates that all of the tested RIBEYE constructs were not autoactivating as judged by the absence of growth on −ALWH and lack of expression of β-galactosidase activity.

The A1, A2, and A3 interaction modules in the A-domain of RIBEYE allow multiple RIBEYE–RIBEYE interactions

Next, we tested whether the identified RIBEYE(A1), RIBEYE(A2), and RIBEYE(A3) interaction modules in the A-domain of RIBEYE could interact with each other. We tested all possible interaction combinations between RIBEYE(A1), RIBEYE(A2) and RIBEYE(A3) in the YTH system and found that multiple interactions could take place between them. RIBEYE(A1) interacts with RIBEYE(A1), RIBEYE(A2), and RIBEYE(A3) (Fig. 2*D*,*F*,*G*). Similarly, RIBEYE(A2) interacted with RIBEYE(A2) and RIBEYE(A1) but not RIBEYE(A3) (Fig. 2*E*–*G*). RIBEYE(A3) interacted with RIBEYE(A1) and RIBEYE(A3) but not RIBEYE(A2) (Fig. 2*G*). All of these interactions between RIBEYE(A) subdomains characterized in the YTH system were confirmed by protein pull-down analyses using the respective fusion proteins (Fig. 3*A*–*D*,*F*).

Homodimerization of RIBEYE(B)

With the YTH system, we confirmed homodimerization of the B-domain of RIBEYE (supplemental Fig. 3*A*,*B*, available at www.jneurosci.org as supplemental material). The homodimerization of RIBEYE(B) is not very surprising: CtBP2,

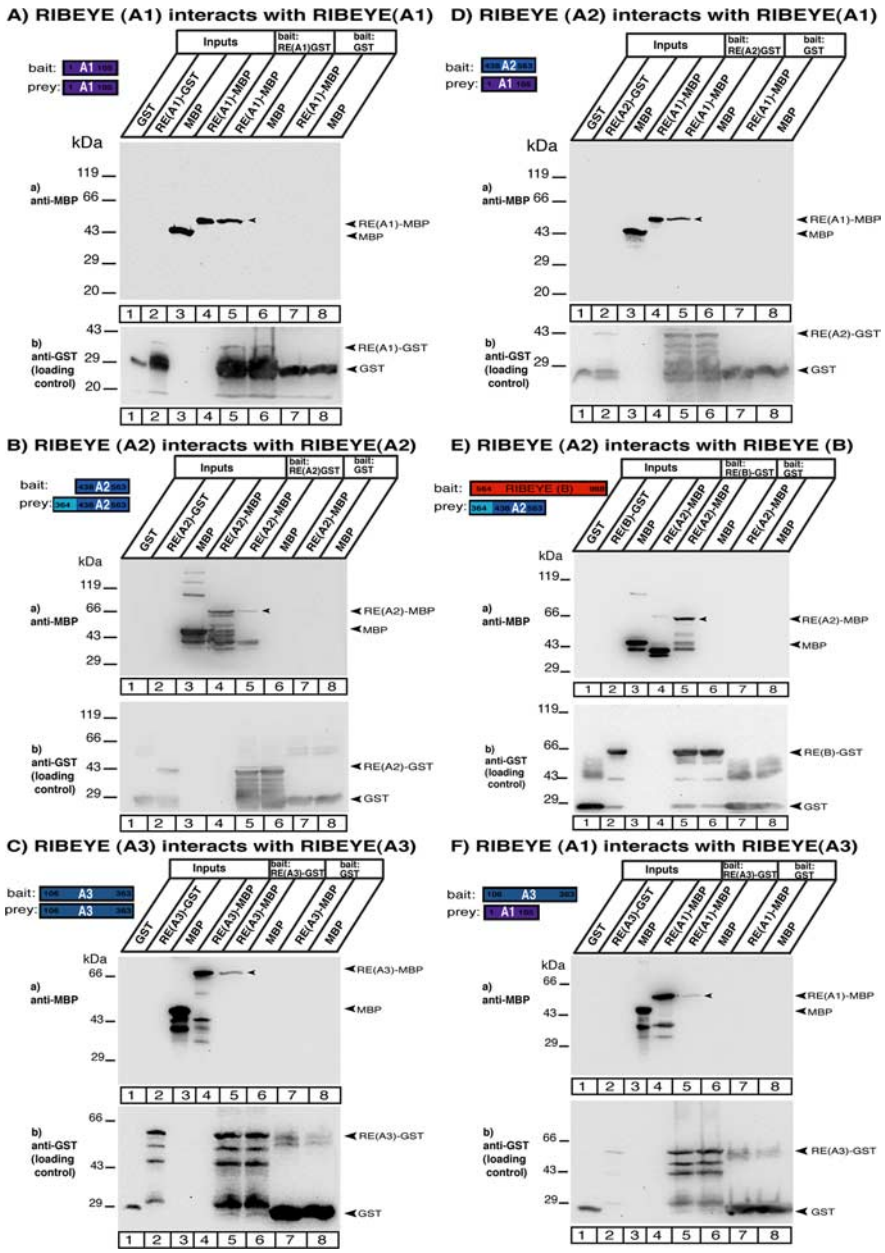

Figure 3. Multiple RIBEYE–RIBEYE interactions identified by YTH are confirmed by fusion protein pull-down experiments. Interaction analyses of the indicated RIBEYE subdomains in fusion protein pull-down analyses. GST-tagged RIBEYE proteins were used as immobilized bait proteins and eluted MBP-tagged RIBEYE proteins as soluble prey proteins. Binding of the prey proteins was analyzed by Western blotting with antibodies against MBP. Equal loading was verified by reprobing the respective blot (after stripping) with antibodies against GST. ***Aa***, ***Ab***, RIBEYE(A1) interacts with RIBEYE(A1). RIBEYE(A1)-GST (lanes 5, 6) and GST alone (lanes 7, 8; control protein) were tested for their ability to pull down RIBEYE(A1)-MBP. MBP alone served as control prey protein. Only RIBEYE(A1)-GST pulled down RIBEYE(A1)-MBP (lane 5) but not the control bait protein GST (lane 7). RIBEYE(A1)-GST does not pull down MBP alone (lane 6). ***Ab*** shows the same blot as in ***Aa*** after stripping and reprobing of the nitrocellulose with anti-GST antibodies to show equal loading of bait proteins. Lanes 1–4 show the indicated input proteins. ***Ba***, ***Bb***, RIBEYE(A2) interacts with RIBEYE(A2). RIBEYE(A2)-GST (lanes 5, 6) and GST alone (lanes 7, 8; control protein) were tested for their ability to pull down RIBEYE(A2)-MBP. MBP alone served as control prey protein. Only RIBEYE(A2)-GST pulled down RIBEYE(A2)-MBP (lane 5) but not the control bait protein GST (lane 7). RIBEYE(A2)-GST does not pull down MBP alone (lane 6). ***Bb*** shows the same blot as in ***Ba*** after stripping and reprobing of the nitrocellulose with anti-GST antibodies to show equal loading of bait proteins. Lanes 1–4 show the indicated input proteins. ***Ca***, ***Cb***, RIBEYE(A3) interacts with RIBEYE(A3). RIBEYE(A3)-GST (lanes 5, 6) and GST alone (lanes 7, 8; control protein) were tested for their ability to pull down RIBEYE(A3)-MBP. MBP alone served as control prey protein. Only RIBEYE(A3)-GST pulled down RIBEYE(A3)-MBP (lane 5) but not the control bait protein GST (lane 7). RIBEYE(A3)-GST does not pull down MBP alone (lane 6). ***Cb*** shows the same blot as in ***Ca*** after stripping and reprobing of the nitrocellulose with anti-GST antibodies to show equal loading of bait proteins. Lanes 1–4 show the indicated input proteins. ***Da***, ***Db***, RIBEYE(A2) interacts with RIBEYE(A1). RIBEYE(A2)-GST (lanes 5, 6) and GST alone (lanes 7, 8; control protein) were tested for their ability to pull down RIBEYE(A1)-MBP. MBP alone served as control prey protein. Only RIBEYE(A2)-GST pulled down RIBEYE(A1)-MBP (lane 5) but not the control bait protein GST (lane 7). RIBEYE(A2)-GST does not pull down MBP alone (lane 6). ***Db*** shows the same blot as in ***Da*** after stripping and reprobing of the nitrocellulose with anti-GST antibodies to show equal loading of bait proteins. Lanes 1–4 show the indicated input proteins. ***Ea***, ***Eb***, RIBEYE(B) interacts with RIBEYE(A2). RIBEYE(B)-GST (lanes 5, 6) and GST alone (lanes 7, 8; control protein) were tested for their ability to pull down RIBEYE(A2)-MBP. MBP alone served as control prey protein. Only RIBEYE(B)-GST pulled down RIBEYE(A2)-MBP (lane 5) but not the control bait protein GST (lane 7). RIBEYE(B)-GST does not pull down MBP alone (lane 6). ***Eb*** shows the same blot as in ***Ea*** after stripping and reprobing of the nitrocellulose with anti-GST antibodies to show equal loading of bait proteins. Lanes 1–4 show the indicated input proteins. ***Fa***, ***Fb***, RIBEYE(A3) interacts with RIBEYE(A1). RIBEYE(A3)-GST (lanes 5, 6) and GST alone (lanes 7, 8; control protein) were tested for their ability to pull down RIBEYE(A1)-MBP. MBP alone served as control prey protein. Only RIBEYE(A3)-GST pulled down RIBEYE(A1)-MBP (lane 5) but not the control bait protein GST (lane 7). RIBEYE(A3)-GST does not pull down MBP alone (lane 6). ***Fb*** shows the same blot as in ***Fa*** after stripping and reprobing of the nitrocellulose with anti-GST antibodies to show equal loading of bait proteins. Lanes 1–4 show the indicated input proteins. RE(A), RIBEYE(A); RE(B), RIBEYE(B).

which is identical to RIBEYE(B) (except for the first 20 aa) has been shown previously to homodimerize (Thio et al., 2004). CtBP1 also homodimerizes (Sewalt et al., 1999; Balasubramanian et al., 2003), and the structure of the CtBP1 dimer (tCtBP1) has been resolved (Kumar et al., 2002; Nardini et al., 2003). NAD(H) was found to stimulate the homodimerization of both CtBP1 and CtBP2 (Balasubramanian et al., 2003; Thio et al., 2004).

RIBEYE(B) also interacted with RIBEYE full-length protein indicating that the A-domain of RIBEYE does not prevent homodimerization of RIBEYE(B)-domains (supplemental Fig. 3*A*,*B*, available at www.jneurosci.org as supplemental material). The homodimerization of RIBEYE(B) is dependent on amino acids 689–716, which form the αB-loop-αC motif [homodimerization loop (HDL)] of RIBEYE(B) as judged by homology modeling (supplemental Fig. 3*D*, available at www.jneurosci.org as supplemental material). The αB-loop-αC motif in CtBP1 is important for homodimerization of CtBP1 (Nardini et al., 2003). In agreement with this prediction, homodimerization of RIBEYE(B) is completely abolished if the HDL is deleted (supplemental Fig. 3*C*, matings 1, 2, available at www.jneurosci.org as supplemental material). RIBEYE(B)ΔHDL no longer interacted with RIBEYE(B) (supplemental Fig. 3, available at www.jneurosci.org as supplemental material). The RIBEYE(B) homodimerization interface is denoted as "B1" in the following text.

Heterodimerization of RIBEYE(B) and RIBEYE(A)

We used the YTH system to test whether RIBEYE(B) can also interact with

←

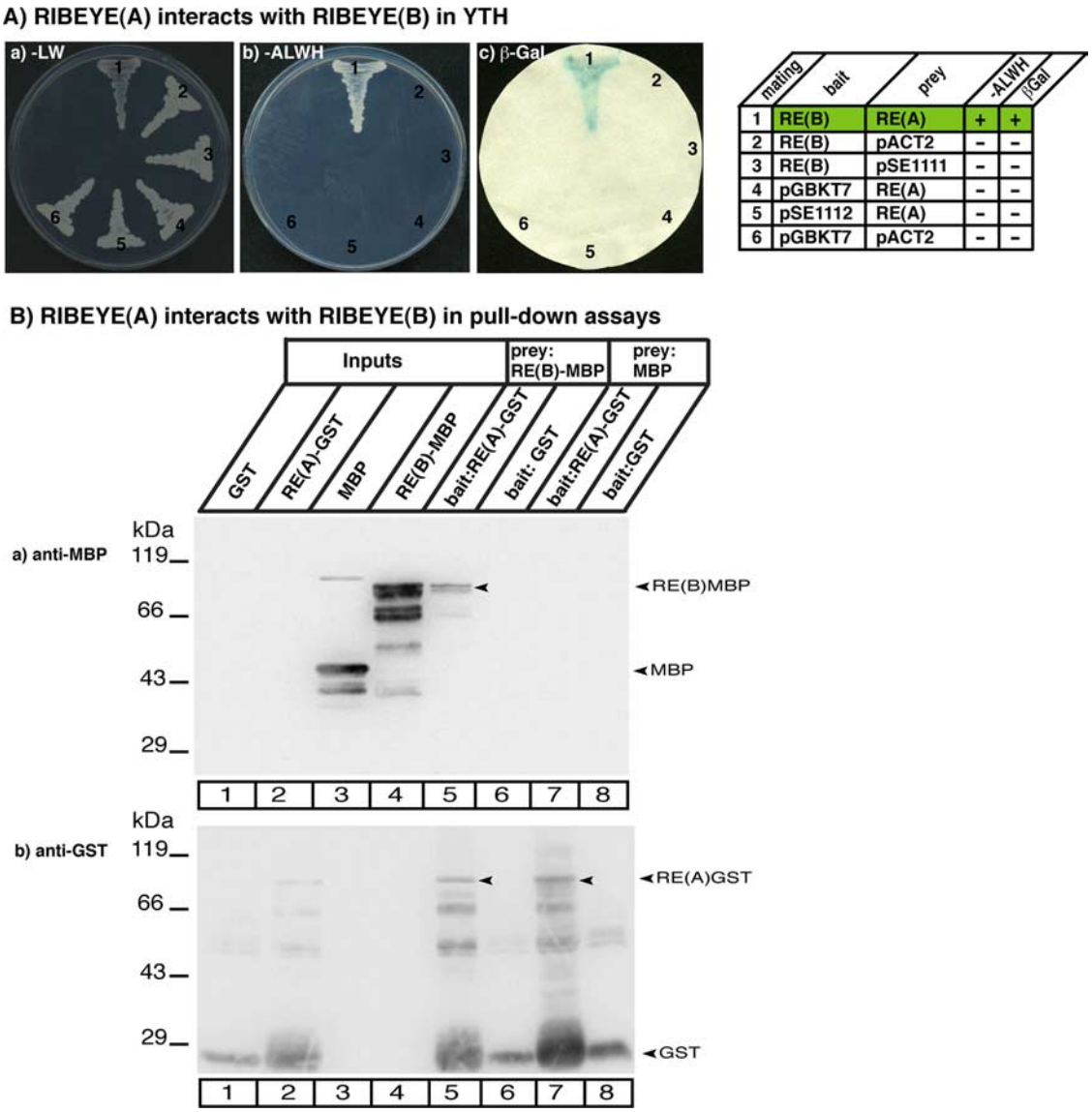

Figure 4. RIBEYE(A) interacts with RIBEYE(B). ***A***, Analyses of RIBEYE(A)–RIBEYE(B) interactions using the YTH system. Summary plates of YTH analyses obtained with the indicated bait and prey plasmids. For convenience, experimental bait–prey pairs are underlayered in color (green for interacting bait–prey pairs; control matings are not colored). RIBEYE(A) interacts with RIBEYE(B) as judged by growth on −ALWH plates and expression of β-galactosidase activity (***Ab***, ***Ac***, mating 1). ***Ba***, ***Bb***, RIBEYE(A) interacts with RIBEYE(B) in protein pull-down experiments. RIBEYE(A)-GST and GST alone (control protein) were used as immobilized bait proteins and RIBEYE(B)-MBP and MBP alone (control protein) as soluble prey proteins. After incubation, binding of the soluble prey proteins to the immobilized bait proteins was tested by Western blotting with the indicated antibodies. ***Ba***, RIBEYE(B)-MBP binds to RIBEYE(A)-GST (lane 5, arrowhead) but not to GST alone (lane 6). MBP alone binds neither to RIBEYE(A)-GST (lane 7) nor to GST alone (lane 8). ***Bb***, The same blot as in ***Ba*** after stripping and reprobing of the nitrocellulose with anti-GST antibodies to show equal loading of bait proteins. RE(A), RIBEYE(A); RE(B), RIBEYE(B).

RIBEYE(A). RIBEYE(B) showed a robust interaction with RIBEYE(A) in the YTH system as judged by growth on −ALWH selective plates and β-galactosidase marker gene expression (Fig. 4, mating 1; supplemental Figs. 4, 5, mating 1, available at www.jneurosci.org as supplemental material). This interaction between RIBEYE(A) and RIBEYE(B) was verified at the protein level using protein pull-down analyses (Fig. 4*B*). RIBEYE(A)-GST fusion protein, but not GST alone, specifically interacted with RIBEYE(B)-MBP fusion protein (but not with MBP alone) as judged by protein pull-down analyses (Fig. 4*B*). We used the YTH system to map the respective interaction sites for RIBEYE(B)–RIBEYE(A) interaction. Mapping analyses revealed that the A2 interaction site in the C-terminal portion of the RIBEYE(A) is the binding site for RIBEYE(B) (Fig. 5; supplemental Fig. 4*B*, available at www.jneurosci.org as supplemental material). On RIBEYE(B), the NBD is responsible for the interaction with RIBEYE(A) (Fig. 5*C*; supplemental Fig. 4*C*, available at www.jneurosci.org as supplemental material). These mapping data obtained by YTH analyses were confirmed by protein–protein pull-down analyses that showed interaction between RIBEYE(A2) and RIBEYE(B) (Fig. 3*E*). We used deletion and point mutants of RIBEYE(B) to further analyze the binding site of RIBEYE(A) on the NBD of RIBEYE(B) in detail. First, we tested whether the RIBEYE(B)ΔHDL deletion mutant that is no longer able to homodimerize with RIBEYE(B) (supplemental Fig. 3*C*,*D*, available at www.jneurosci.org as supplemental material) is still able to interact with RIBEYE(A). Indeed, RIBEYE(B)ΔHDL is able to interact with RIBEYE(A) as well as with full-length RIBEYE [RIBEYE(AB)] (Fig. 5*C*; supplemental Figs. 4*C*, 7, available at www.jneurosci.org as supplemental material). Next, we

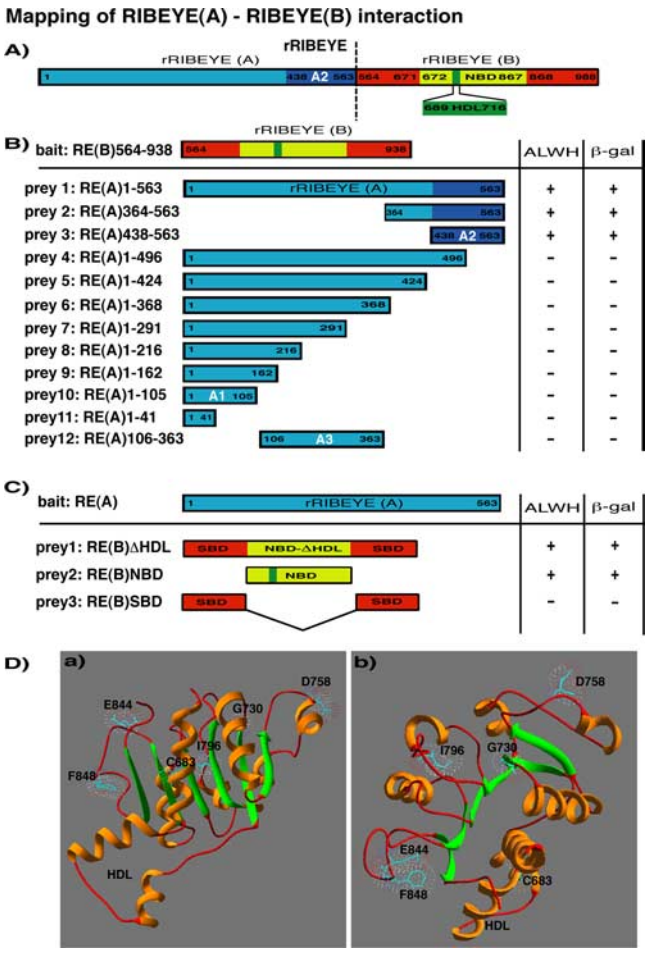

Figure 5. Mapping of RIBEYE(A)–RIBEYE(B) interaction in YTH. ***A***, Schematic domain structure of RIBEYE. The A-domain of RIBEYE is depicted in blue, the SBD of RIBEYE(B), which consists of the N- and C-terminal portions of the B-domain, is depicted in red. The HDL is depicted in green within the yellow-labeled NBD of RIBEYE(B). ***B***, ***C***, The indicated bait and prey plasmids were used to test for the interaction of the respective proteins in the YTH system. ***B***, YTH analyses of C- and N-terminal deletion constructs of RIBEYE(A) reveal that the RIBEYE(A2) site is responsible for interaction with RIBEYE(B). ***C***, YTH analyses of the indicated constructs of RIBEYE(B) reveal that the NBD (prey 2), but not the SBD (prey 3), is responsible for interaction with RIBEYE(A). The RIBEYE(B) HDL is not essential for the interaction between RIBEYE(A) and RIBEYE(B). RIBEYE(B)ΔHDL (prey 1) still interacts with RIBEYE(A). ***Da***, ***Db***, Summary of the location of distinct amino acids on the NBD that are essential for binding of RIBEYE(A). If these amino acids on the NBD of RIBEYE(B) are point mutated, RIBEYE(A) can no longer bind to RIBEYE(B) (supplemental Fig. 5, available at www.jneurosci.org as supplemental material). The lack of binding of the RIBEYE(B) point mutants to RIBEYE(A) is not caused by misfolding of the respective point mutants because all of these RIBEYE(B) point mutants homodimerized with RIBEYE(B) (supplemental Fig. 6, available at www.jneurosci.org as supplemental material). ***Da***, A lateral view of the NBD of RIBEYE(B). ***Db***, A top view on the NBD from the position of the bound NADH to the "bottom" of the molecule as seen in ***Da***. RE(A), RIBEYE(A); RE(B), RIBEYE(B).

tested different point mutants of the NBD of RIBEYE(B) for their interaction with RIBEYE(A) and RIBEYE(B). We analyzed RIBEYE(B) point mutants RIBEYE(B)G730A, D758N, I796A, E844Q, F848W, and K854Q, which are located at the outer face of the NBD (Fig. 5*D*). All of these point mutations did not prevent homodimerization with RIBEYE(B) (supplemental Figs. 5*C*, 6, available at www.jneurosci.org as supplemental material). Furthermore, RIBEYE(B)D758N, I796A, E844Q, F848W, and K854Q bound NADH as judged by NADH-dependent energy transfer from tryptophan W867 to bound NADH [performed as described by Fjeld et al. (2003)] (data not shown), demonstrating the proper folding of these point mutants. Although these point mutants did not prevent homodimerization of RIBEYE(B), all of these point mutations [except for RIBEYE(B)K854Q] completely abolished interaction with RIBEYE(A) (supplemental Fig. 5*A–C*, available at www.jneurosci.org as supplemental material). This shows that the two binding interfaces on RIBEYE(B) available for interaction with RIBEYE(A) and RIBEYE(B) are distinct from each other, albeit spatially closely related. The binding site for RIBEYE(A) covers a large portion of the NBD (Fig. 5*D*; supplemental Fig. 5, available at www.jneurosci.org as supplemental material). Interestingly, RIBEYE(B)G730, which is an essential component of the conserved NAD(H)-binding motif of RIBEYE (Schmitz et al., 2000), appears to be part of the interaction interface for RIBEYE(A): the point mutant RIBEYE(B)G730A (Fig. 5*D*) that does not bind NAD(H) (supplemental Fig. 5*D*, available at www.jneurosci.org as supplemental material) can no longer interact with RIBEYE(A) (supplemental Fig. 5*C*, available at www.jneurosci.org as supplemental material). We interpret the latter result to mean that the binding sites for NAD(H) and for RIBEYE(A) are overlapping to a certain extent (see below and Discussion). The docking site on RIBEYE(B) for RIBEYE(A) is denoted as "B2" in the following text.

NADH and NAD$^+$ inhibit RIBEYE(A)–RIBEYE(B) interaction

Because RIBEYE(A) docks to a broad interface of the NAD(H)-binding subdomain of RIBEYE(B), we analyzed whether this interaction is dependent on NAD(H). To analyze this question, we applied the pull-down assay described in Materials and Methods. We used RIBEYE(A)-GST as immobilized bait and eluted RIBEYE(B)-MBP as soluble prey protein and checked for interaction of these proteins in the presence of increasing concentrations of NADH/NAD$^+$ (Fig. 6). Increasing concentrations of NADH/NAD$^+$ strongly inhibited RIBEYE(A)–RIBEYE(B) interaction. Both NAD$^+$ as well as NADH strongly inhibited RIBEYE(A)–RIBEYE(B) interaction already at low physiological concentrations. The tested concentrations of NAD(H) are within the cellular concentration range of NAD(H) known from other studies (Zhang et al., 2002; Fjeld et al., 2003). The NAD(H) concentrations did not have any influence on the control pull downs. At all NADH/NAD$^+$ concentrations used, there was no unspecific binding of RIBEYE(B)-MBP to GST alone (supplemental Fig. 8, available at www.jneurosci.org as supplemental material). The identified interactions between the different subdomains of RIBEYE and their regulation via NAD(H) are summarized in Figure 11*B*.

RIBEYE coaggregates with other RIBEYE molecules in transfected R28 and COS cells

To determine whether the identified RIBEYE–RIBEYE interactions can also occur within the cellular context, we performed cell transfections with the indicated RIBEYE expression constructs that were differentially tagged either with EGFP or with mRFP. For transfection, we used COS7 cells and the R28 retinal progenitor cell line (Seigel, 1996; Seigel et al., 2004). R28 cells express retinal and neuronal marker proteins (e.g., opsins, β-2 arrestin, recoverin, neurotransmitter receptors, and various presynaptic and postsynaptic proteins) in addition to stem cell/precursor cell markers (e.g., nestin) (Seigel et al., 2004). If transfected alone, both RIBEYE(A) as well as RIBEYE(AB) displayed a discrete, spot-like distribution, whereas RIBEYE(B) is diffusely distributed (Fig. 7; supplemental Figs. 9–11, available at www.jneurosci.org as supplemental material), as also described previously (Schmitz et al., 2000). If RIBEYE(A)-EGFP was cotrans-

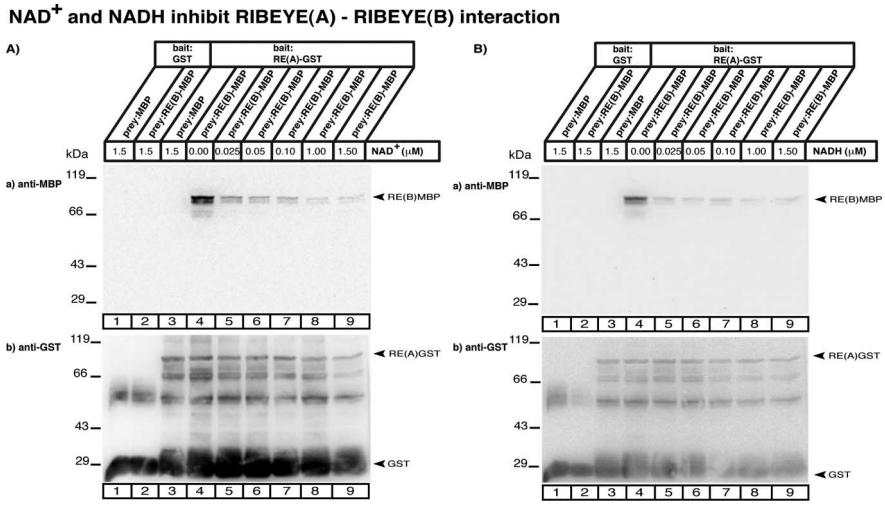

Figure 6. NADH and NAD$^+$ inhibit RIBEYE(A)–RIBEYE(B) interaction. ***Aa–Bb***, Immobilized RIBEYE(A)-GST fusion protein (0.3 μM) was incubated with 0.3 μM RIBEYE(B)-MBP in the presence of the indicated concentrations of NAD$^+$ (***Aa***, ***Ab***) or NADH (***Ba***, ***Bb***) for 3 h at 4°C in binding buffer (100 mM Tris-HCl, pH 8.0, 150 mM NaCl, 1 mM EDTA, 1% Triton X-100). After several washes with binding buffer, the pellets were boiled with SDS-sample buffer and analyzed for binding of RIBEYE(B)-MBP by Western blot analyses and probing of the Western blots with anti-MBP antibodies. Both NAD$^+$ and NADH strongly inhibited binding of RIBEYE(B) to RIBEYE(A). ***Ab***, ***Bb***, Respective loading controls in which the same blots as shown in ***Aa*** and ***Ba*** were incubated with GST antibodies after stripping of the respective blots. RE(A), RIBEYE(A); RE(B), RIBEYE(B).

fected with RIBEYE(A)-mRFP both coaggregated to the same protein clusters as judged by the large extend of colocalization of the EGFP and mRFP signals (Fig. 7*C*, arrows; supplemental Figs. 10*C*, 11*A*, available at www.jneurosci.org as supplemental material). Identical results were obtained when full-length RIBEYE(AB)-EGFP was cotransfected with RIBEYE(A)-mRFP (Fig. 7*B*, arrows). If RIBEYE(B)-EGFP was cotransfected with RIBEYE(B)-mRFP, both signals remained diffusely distributed (Fig. 7*E*). Interestingly, whenever RIBEYE(B)-mRFP was cotransfected with RIBEYE(A)-EGFP, RIBEYE(B)-mRFP redistributed from a diffuse distribution [as typical for single transfected RIBEYE(B)], to a patchy, spot-like distribution that is typical for RIBEYE(A) (Fig. 7*D*, arrow). Part of RIBEYE(B) remained diffusely distributed (Fig. 7*D*, arrowhead; supplemental Fig. 10*D*,*E*, available at www.jneurosci.org as supplemental material) probably because of the NAD(H) sensitivity of the RIBEYE(B)–RIBEYE(A) interaction (see above). NAD(H) is ubiquitously present in the cytoplasm and expected to partly dissociate RIBEYE(A)–RIBEYE(B) complexes. Interestingly, in cells double-transfected with full-length RIBEYE(AB) and RIBEYE(B), RIBEYE(B) virtually completely redistributed from the diffuse distribution to the spot-like distribution typical for RIBEYE(AB) and perfectly colocalized with RIBEYE(AB) (Fig. 7*A*, arrows; supplemental Figs. 9, 10*B*, 11*B*, available at www.jneurosci.org as supplemental material). From these latter experiments, we conclude that both homotypic domain interactions [RIBEYE(B)–RIBEYE(B) interactions] as well as heterotypic domain interactions [RIBEYE(A)–RIBEYE(B) interactions] support the interaction between RIBEYE(AB) and RIBEYE(B). As judged by the nearly complete colocalization of RIBEYE(AB) and RIBEYE(B) compared with cells double-transfected with RIBEYE(A) and RIBEYE(B), we assume that a combination of homotypic and heterotypic domain interactions is probably stronger than a single type of homotypic interactions. Qualitatively identical results were obtained for R28 cells (Fig. 7; supplemental Fig. 9, available at www.jneurosci.org as supplemental material) and COS cells (supplemental Figs. 10, 11, available at www.jneurosci.org as supplemental material). Also in COS cells, RIBEYE(A) coaggregated with RIBEYE(AB) (supplemental Fig. 10*A*, available at www.jneurosci.org as supplemental material) and RIBEYE(A) (supplemental Figs. 10*C*, 11*A*, available at www.jneurosci.org as supplemental material). Similarly, RIBEYE(B) translocated from a completely diffuse distribution to a spot-like distribution if cotransfected with RIBEYE(A) or RIBEYE(AB) [in 98 and 99%, respectively, of double-transfected cells in 100 randomly picked double-transfected cells vs 3% spot-like distribution in cells transfected with RIBEYE(B) only].

Interestingly, if RIBEYE(AB)-EGFP-transfected cells were analyzed already a few hours after transfection, the RIBEYE(AB)-containing aggregates appeared smaller and more numerous than at later time points suggesting that the smaller protein clusters could mature/coalesce to the bigger protein aggregates that are predominant at later time points (supplemental Fig. 9, available at www.jneurosci.org as supplemental material).

In conclusion, the coaggregation and colocalization data in the transfected COS and R28 cells indicate that the interaction sites between RIBEYE(A) and RIBEYE(B), either between the same type of domains (A–A, B–B) or between different domains (A–B), are also available within a cellular context.

Electron microscopy of RIBEYE-containing aggregates in transfected R28 cells

RIBEYE is the major component of synaptic ribbons and RIBEYE forms large protein aggregates in transfected cells (Fig. 7). We analyzed the ultrastructural appearance of the RIBEYE-containing aggregates by electron microscopy to find out whether these structures have similarities with synaptic ribbons (Fig. 8). Using conventional transmission electron microscopy, we observed large electron-dense aggregates in RIBEYE-EGFP-transfected R28 cells (Fig. 8*A–J*), which were absent in control cells (K). Similar, large electron-dense protein aggregates were also present in RIBEYE(AB)-EGFP-transfected COS cells but not in EGFP-transfected COS cells (data not shown). The large aggregates typically displayed a spherical shape with a diameter between of 200–500 nm. These electron-dense structures were often surrounded by vesicles which in part were physically attached to the electron-dense aggregates via thin electron-dense stalks (Fig. 8*A–J*, arrowheads). These large spherical structures were strongly positive for RIBEYE by immunogold labeling with antibodies against RIBEYE (Fig. 8*L–N*) but not reactive with antibodies against tubulin (*O*) or RIBEYE preimmune serum (*P*) (control incubations). These spherical structures have similarities to spherical synaptic ribbons of inner hair cells (for review, see Nouvian at al., 2006). Beside the large electron-dense particles we also found smaller aggregates which showed physical contacts between each other and which sometimes appeared to coalesce into larger, electron-dense structures (Fig. 8*E*,*F*). These structures were also partly physically linked to surrounding vesicles and show some resemblance to synaptic spheres, intermediate structures in the assembly and disassembly of synaptic ribbons

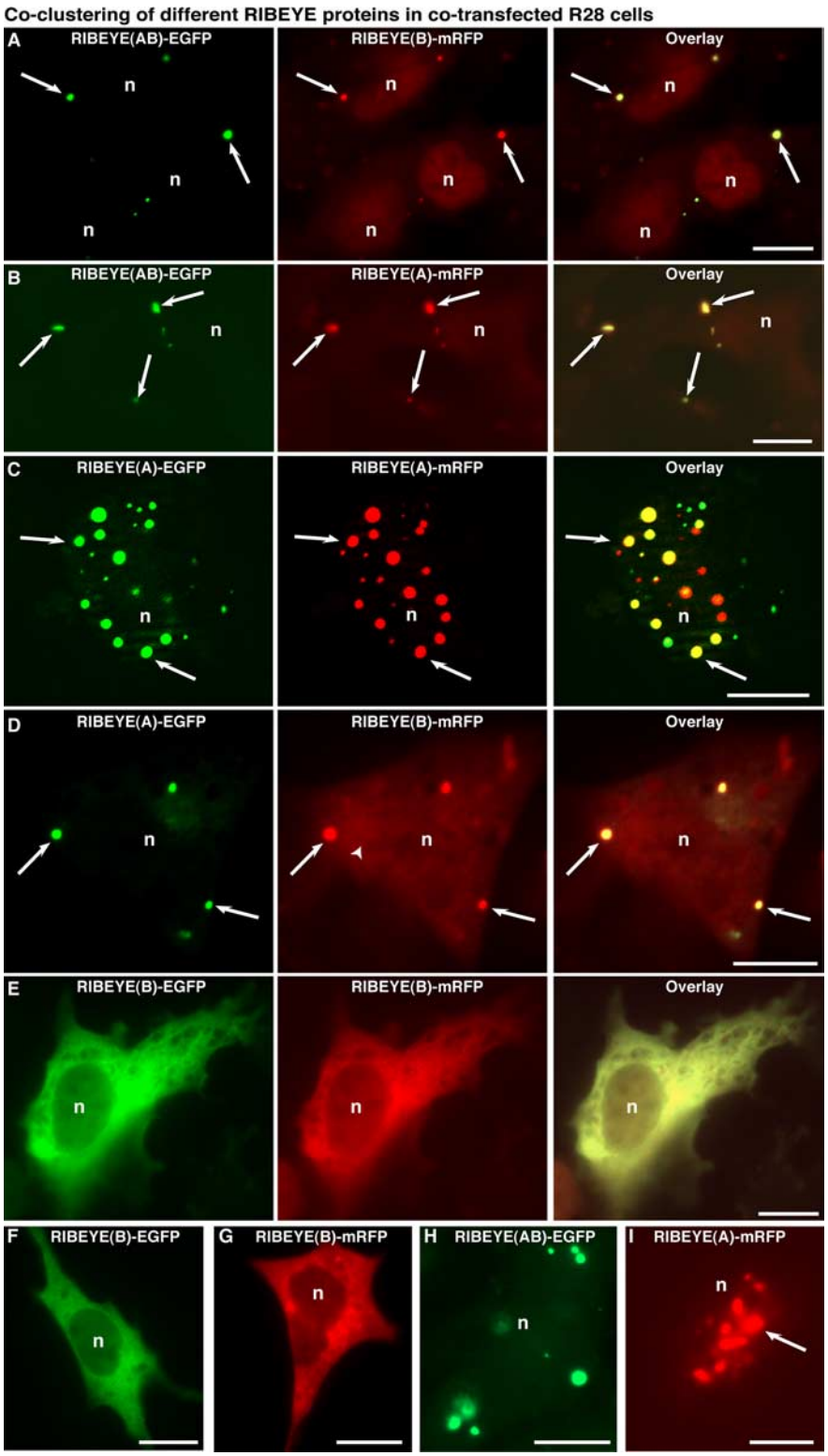

Figure 7. Coclustering of different RIBEYE-proteins in cotransfected R28 cells. ***A–H***, R28 cells were transfected with the indicated mRFP- or EGFP-tagged RIBEYE constructs. Transfected cells were analyzed for the intracellular distribution of the respective proteins via direct epifluorescence microscopy. RIBEYE(AB) (***H***) and RIBEYE(A) (***I***) show a discrete spot-like distribution, as already shown previously (Schmitz et al., 2000). In contrast, RIBEYE(B) is diffusely distributed in single-transfected cells (Schmitz et al., 2000) (***F***,***G***). ***A***, If RIBEYE(B) is cotransfected with RIBEYE(AB) (supplemental Fig. 9, available at www.jneurosci.org as supplemental material), RIBEYE(B) virtually completely redistributed from a diffuse distribution into a spot-like, RIBEYE(AB)-typical distribution and colocalized with RIBEYE(AB) (arrows) (supplemental Fig. 9 *A*, *B*, available at www.jneurosci.org as supplemental material). ***D***, RIBEYE(B) also redistributed from a diffuse to spot-like distribution if cotransfected with RIBEYE(A) (supplemental Fig. 9*C*, available at www.jneurosci.org as supplemental material); part of RIBEYE(B) remained diffusely distributed (arrowhead). The higher degree of codistribution of RIBEYE(B) with RIBEYE(AB) compared with RIBEYE(A) probably represents the fact that more types of interactions can be formed between RIBEYE(B) and RIBEYE(AB) than between RIBEYE(B) and RIBEYE(A) alone (for a summary, see Fig. 11). RIBEYE(A) also coaggregated and colocalized with RIBEYE(A) (***C***, arrows). ***E***, If RIBEYE(B)-EGFP was cotransfected with RIBEYE(B)-mRFP, both proteins remained diffusely distributed and did not generate a spot-like distribution. For additional examples of transfected R28 cells, see supplemental Figure 9 (available at www.jneurosci.org as supplemental material). The arrows in ***A–D*** point to intracellular RIBEYE aggregates that contain both types of the indicated differentially tagged RIBEYE proteins. The arrow in ***I*** points to an intracellular RIBEYE(A)-containing aggregate. COS cells transfected with the respective plasmids produced qualitatively identical results (supplemental Figs. 10, 11, available at www.jneurosci.org as supplemental material). n, Nucleus. Scale bars, 10 μm.

(for review, see Vollrath and Spiwoks-Becker, 1996) (see Discussion).

RIBEYE coaggregates at bassoon-containing sites in retinal R28 progenitor cells

To further address the physiological relevance of the RIBEYE aggregates, we tested whether these structures are related to bassoon, a physiological interaction partner of RIBEYE at the active zone of ribbon synapses (tom Dieck et al., 2005). Bassoon is endogenously expressed in R28 retinal precursor cells as judged by immunocytochemistry (Fig. 9), Western blotting (supplemental Fig. 9*D*, available at www.jneurosci.org as supplemental material) and reverse transcription-PCR (data not shown). Bassoon is distributed in R28 in a spot-like manner (Fig. 9*D*, arrowheads). The RIBEYE clusters in RIBEYE(AB)-EGFP-transfected R28 cells primarily formed around this bassoon-containing clusters and colocalized with bassoon (Fig. 9*A–C*, arrows). The preferential colocalization between RIBEYE and its physiological interaction partner bassoon emphasizes the physiological relevance and ribbon-like partial function of the RIBEYE-containing protein aggregates.

Purified synaptic ribbons recruit externally added RIBEYE(A) and RIBEYE(B)

Next, we tested whether isolated, purified synaptic ribbons can recruit externally added RIBEYE(B)-GST and RIBEYE(A)-GST fusion proteins (Fig. 10). GST alone was used as control protein. Purified synaptic ribbons bound soluble RIBEYE(A)-GST and RIBEYE(B)-GST fusion proteins (Fig. 10*A*,*B*). GST control protein did not bind to synaptic ribbons (Fig. 10*Aa*, lane 6, *Ba*, lane 6) demonstrating the specificity of binding. Thus, the RIBEYE–RIBEYE in-

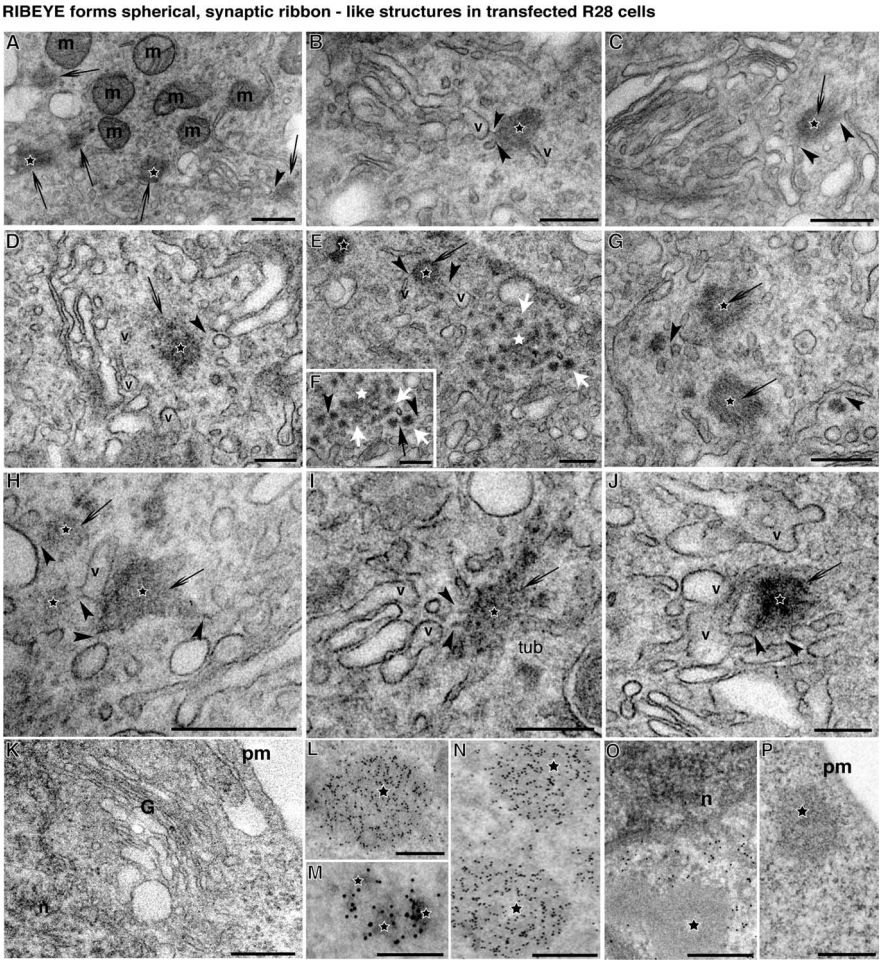

Figure 8. Electron microscopy of RIBEYE-containing aggregates in transfected R28 cells. ***A–K***, Conventional transmission microscopy of RE(AB)-EGFP- (***A–J***) and EGFP-transfected cells (***K***). ***L–P***, Immunogold electron microscopy of RE(AB)-EGFP-transfected cells immunolabeled with antibodies against RIBEYE (***L–N***), tubulin (***O***), and control immunoglobulins (RIBEYE preimmune; ***P***). ***A***, Low magnification of RE(AB)-EGFP-transfected cells. Note the presence of large electron-dense material (200–500 nm in diameter) in RIBEYE-transfected cells (***A–J***, asterisks and black arrows). These electron-dense structures are mostly spherical in shape (***A–G***, ***J***, asterisks), although more irregular profiles are also present (***H***, ***I***, asterisks). These electron-dense structures (***A–J***) were often surrounded by vesicles, which in part were physically attached to the electron-dense aggregates via thin electron-dense stalks (***A–J***, arrowheads). In addition to the large electron-dense spheres, smaller electron-dense structures could be observed (***E***, ***F***, white arrows). Neighboring small electron-dense aggregates (***E***, ***F***, white arrows) appear at least partly physically connected to each other (***F***, black arrow) and sometimes appeared to coalesce into larger, electron-dense structures (***E***, ***F***, white asterisk). ***K***, Ultrastructure of a control-transfected cell. ***L–N***, Both the large (***L***, ***N***) as well as the small (***M***) electron-dense aggregates were strongly immunolabeled by RIBEYE antibodies. The aggregates were densely decorated by immunogold particles. ***O***, ***P***, RE(AB)-EGFP-transfected cell immunolabeled with antibodies against tubulin (***O***) and RIBEYE-preimmune serum (***P***). In no case was a specific labeling of the electron-dense aggregates (asterisks) observed. n, Nucleus; m, mitochondria; G, Golgi apparatus; v, vesicles; tub, membrane tubule; pm, plasma membrane. Scale bars: ***A***, 500 nm; ***B***, 250 nm; ***C***, 400 nm; ***D–F***, 250 nm; ***G–I***, 300 nm; ***J***, 250 nm; ***K***, 400 nm; ***L–P***, 200 nm.

teraction sites are accessible on synaptic ribbons and available to recruit externally added, additional RIBEYE proteins. We verified that the binding of RIBEYE(A) to purified synaptic ribbons is independent of the attached GST tag by removing the GST tag by thrombin cleavage (Fig. 10*C*). Untagged RIBEYE(A) cosedimented with purified synaptic ribbons but not without synaptic ribbons, further confirming the specific binding of RIBEYE(A) to purified synaptic ribbons. To further evaluate the binding of RIBEYE(A) to synaptic ribbons, we also tested whether RIBEYE(A1), RIBEYE(A2), and RIBEYE(A3) (used as purified MBP-tagged fusion proteins) were able to bind to purified synaptic ribbons. RIBEYE(A1)-MBP and RIBEYE(A3)-MBP bound to synaptic ribbons whereas MBP alone did not demonstrating the specificity of the interaction. Interestingly, RIBEYE(A2)-MBP did not bind to purified synaptic ribbons although it efficiently interacted with RIBEYE(A) subunits [RIBEYE(A1), RIBEYE(A2)] in protein pull-down assays (Fig. 3). We interpret these findings that the RIBEYE(A2)-binding sites/options are probably unavailable or blocked by other proteins on purified synaptic ribbons (see Discussion). The recruitment of additional RIBEYE subunits to preexisting ribbons could explain the known dynamic growth and ultrastructural plasticity of synaptic ribbons (see Discussion). Figure 11 depicts a simplified model that schematically shows how synaptic ribbons could be built from individual RIBEYE subunits via the identified RIBEYE–RIBEYE interactions.

Discussion

Synaptic ribbons are large and dynamic macromolecular constructions in the active zone of ribbon synapses. At present, it is not clearly understood how the synaptic ribbon is made and how it functions in the synapse. In the present study, we demonstrated that RIBEYE is a scaffold protein that contains multiple interaction sites for other RIBEYE molecules. Noteworthy, the RIBEYE–RIBEYE interactions involve sites in the A-domain as well as in the B-domain of RIBEYE, i.e., three distinct interaction sites in the A-domain (A1, A2, A3) and two in the B-domain (B1, B2). We have shown that these five interaction sites allow either homotypic domain interactions [interactions between same type of domains: RIBEYE(A)–RIBEYE(A), RIBEYE(B)–RIBEYE(B)] or heterotypic domain interactions [RIBEYE(A)–RIBEYE(B)]. Homotypic domain interactions can be either homotypic or heterotypic concerning the subdomain involved. A homotypic domain interaction, e.g., RIBEYE(A)–RIBEYE(A), can be mediated either by homotypic subdomain interactions, e.g., RIBEYE(A1)–RIBEYE(A1), or by heterotypic subdomain interactions, e.g., RIBEYE(A1)–RIBEYE(A2). The cotransfection experiments demonstrated that RIBEYE proteins interact with each other and coaggregate into the same protein clusters. Given the fact that RIBEYE is the major component of synaptic ribbons (Schmitz et al., 2000; Zenisek et al., 2004; Wan et al., 2005), the multiple protein interactions of RIBEYE provide a molecular mechanism how the scaffold of the synaptic ribbon can be created. RIBEYE–RIBEYE interactions could directly link the individual RIBEYE units to each other. Because RIBEYE is present throughout the entire synaptic ribbon, RIBEYE–RIBEYE interactions could thus generate and stabilize the macromolecular structure of the synaptic ribbon. The proposed modular model of synaptic ribbons could explain how the scaffold of the

synaptic ribbon is formed mostly from a single protein component (RIBEYE). In agreement with this hypothesis, the RIBEYE aggregates in transfected R28 cells possess structural and functional similarities with synaptic ribbons. RIBEYE(AB)-transfected R28 cells formed electron-dense large protein aggregates that were partly associated with surrounding vesicles and membrane compartments. The electron-dense aggregates were usually round in shape and resembled spherical synaptic ribbons of inner hair cells (Nouvian et al., 2006). Bar-shaped/plate-shaped ribbons were not observed in the RIBEYE-transfected cells. Thus, the spherical synaptic ribbon appears to be the "basal" type of synaptic ribbon structure that is built from RIBEYE and most likely additional factors are needed to build plate-shaped ribbons from spherical ribbons. The colocalization of RIBEYE with its physiological interaction partner bassoon in R28 cells emphasizes the physiological relevance of the RIBEYE-containing protein aggregates and suggest that the RIBEYE-containing aggregates fulfill partial ribbon-like functions. Because RIBEYE is not the only component of synaptic ribbons (Schmitz et al., 2000; Wan et al., 2005), it cannot be expected that RIBEYE alone makes fully mature ribbons, e.g., with a dense and regular association of synaptic vesicles. Very likely, additional ribbon components are necessary to provide full-ribbon function and structure.

In principle, the multiple interaction sites present on RIBEYE can be important for both intramolecular and intermolecular RIBEYE–RIBEYE interactions. Intermolecular RIBEYE–RIBEYE interactions could provide the three-dimensional scaffold of the synaptic ribbon as discussed above. Intramolecular RIBEYE–RIBEYE interactions could shield the interaction sites from unwanted intermolecular interactions to keep the protein soluble. Such a shielding of binding sites could be particularly important during development and to prevent the assembly of synaptic ribbons at unwanted, unphysiological subcellular sites (e.g., outside of the presynaptic terminal).

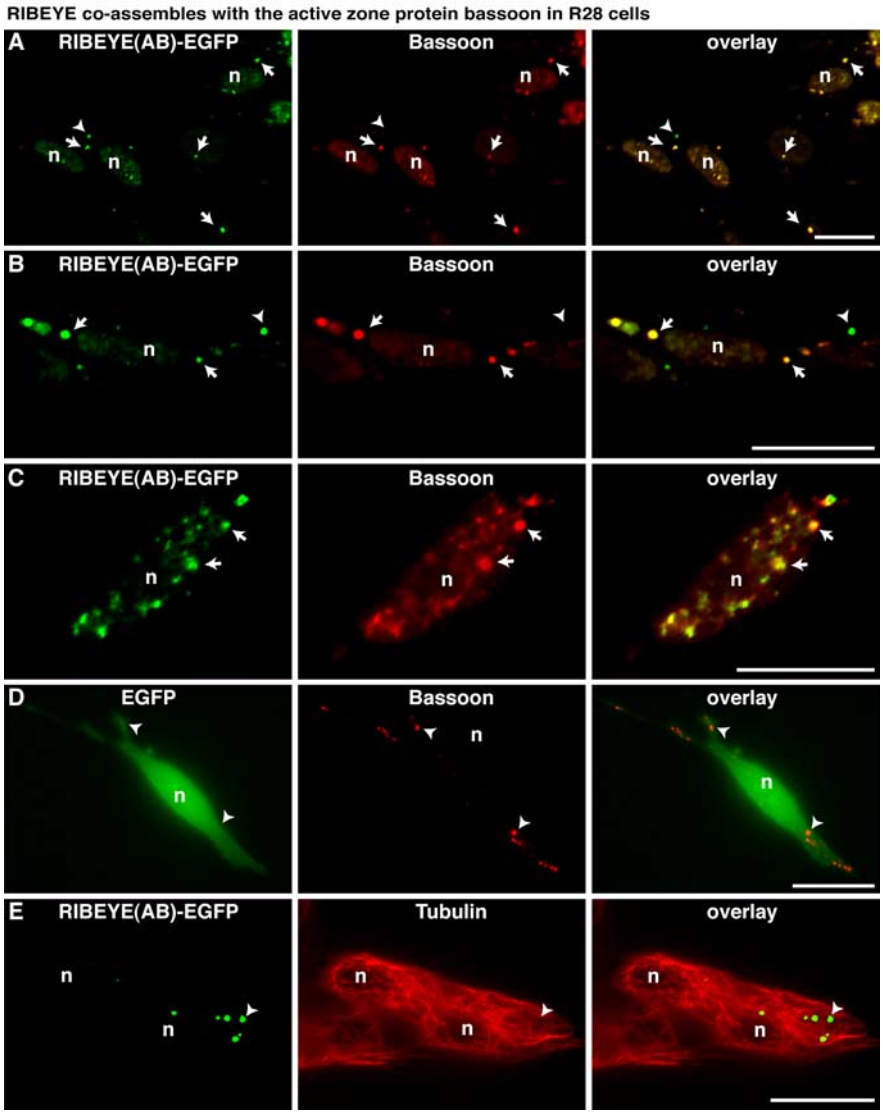

Figure 9. The RIBEYE-induced protein aggregates recruit endogenous bassoon. R28 retinal precursor cells were transfected with plasmids encoding for the indicated EGFP-tagged proteins. ***A–E***, The distribution of the endogenously present active-zone protein bassoon (***A–D***) or tubulin (***E***) was visualized by indirect immunofluorescence microscopy. In R28 cells, bassoon is endogenously present as discrete protein clusters (***A–C***, middle, arrows). Heterologously expressed RIBEYE-EGFP coaggregates with these preexisting bassoon clusters (***A–C***, arrows) but not EGFP alone (***D***). ***D***, Endogenous bassoon (arrowheads) did not recruit EGFP alone. The arrowheads in ***A*** and ***B*** show RIBEYE clusters that aggregated independent of the endogenous bassoon. ***E***, The RIBEYE(AB)-EGFP clusters (arrowhead) do not colocalize with microtubules, which were visualized by immunostaining with antibodies against tubulin. n, Nucleus. Scale bars, 10 μm.

It is likely that the interaction between different RIBEYE domains and RIBEYE molecules is regulated. In the present study, we found that NAD(H) is an important regulator of RIBEYE interactions. RIBEYE(A)–RIBEYE(B) interactions are efficiently inhibited by low, physiological concentrations of NAD(H). Both NADH and NAD^+ are very efficient in disrupting RIBEYE(A)–RIBEYE(B) complexes. Thus, NAD(H) appears to act as a molecular switch that distinguishes between two different types of RIBEYE–RIBEYE interactions: in the presence of NAD(H), RIBEYE(A)–RIBEYE(B) interactions are disassembled (this study), whereas RIBEYE(B)–RIBEYE(B) interactions are favored as judged by the NAD(H)-induced dimerization of CtBP2 (Thio et al., 2004). The binding interface on RIBEYE(B) for RIBEYE(B) interaction is spatially closely related but distinct from the binding interface on RIBEYE(B) for RIBEYE(A). This was shown by the analyses of point and deletion mutants of RIBEYE(B) that affect one type of interaction [RIBEYE(A)–RIBEYE(B) interaction] but not the other [RIBEYE(B)–RIBEYE(B) interaction] (Fig. 5*C*,*D*; supplemental Figs. 5, 6, available at www.jneurosci.org as supplemental material). The binding of NAD(H) could induce a conformation of RIBEYE(B) that favors homodimerization of RIBEYE(B) and that is incompatible with the formation of RIBEYE(B)–RIBEYE(A) heterodimers. RIBEYE(B)G730 is an essential part of the NADH-binding motif and the RIBEYE(B)G730A point mutant no longer interacts with RIBEYE(A). Therefore, one possible mechanism for the NADH-induced dissociation of the RIBEYE(A2)–RIBEYE(B) interaction

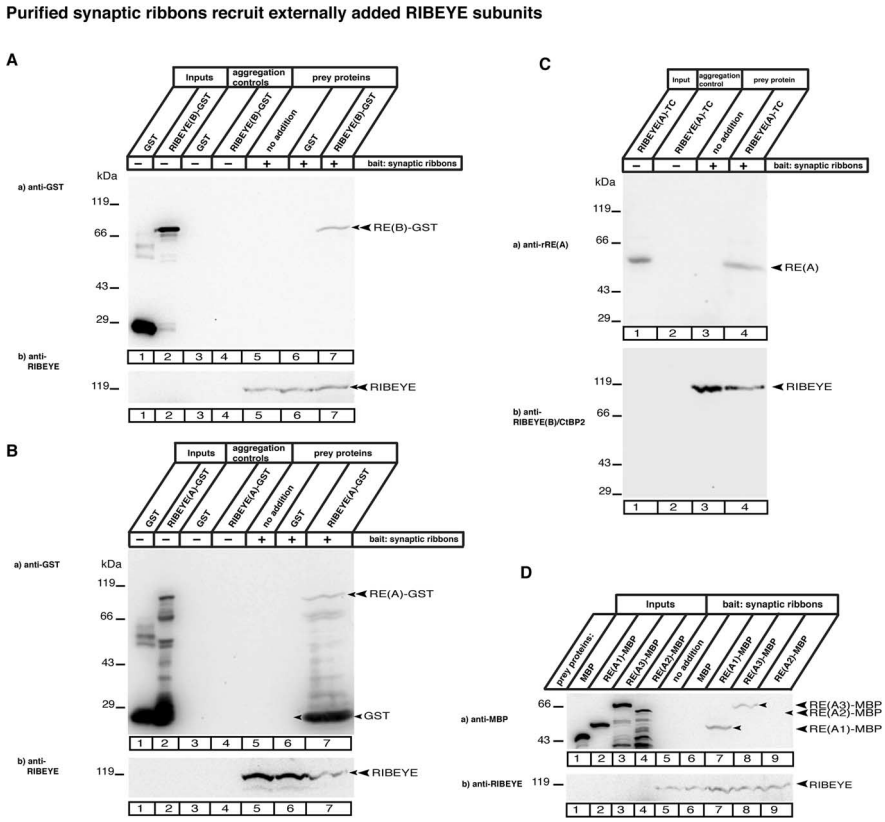

Figure 10. Synaptic ribbons recruit externally added RIBEYE subunits. Purified synaptic ribbons (180 μg) were incubated with the indicated RIBEYE fusion proteins (~3.5 μM) and then sedimented by a 1 min spin at 3.500 rpm. Fusion proteins that cosedimented with synaptic ribbons were detected by Western blotting with the indicated antibodies. ***Aa–Bb***, Lanes 1 and 2 show the respective input fractions, and lanes 3 and 4 the respective autoaggregation controls of the soluble fusion proteins to test whether ribbon-independent sedimentation of fusion proteins occurs. The autoaggregation controls show that in the absence of synaptic ribbons, no fusion proteins are found in the pellet. In contrast, if synaptic ribbons were incubated with the fusion proteins, both RIBEYE(A)-GST (***B***) as well as RIBEYE(B)-GST (***A***) sedimented with purified synaptic ribbons indicating binding to synaptic ribbons. In contrast, GST alone did not cosediment with synaptic ribbons (lane 6), demonstrating the specificity of the binding of RIBEYE fusion proteins to synaptic ribbons. As outlined in Materials and Methods, RIBEYE(A)-GST cannot be expressed exclusively as an unprocessed protein even under fermenter conditions, probably because of its high contents of proline residues and the extended shape of the molecule. In addition to full-length RIBEYE(A), degradation bands of RIBEYE(A)-GST are also visible. But full-length RIBEYE(A) is clearly expressed and binds to purified synaptic ribbons (***Ba***, lane 7), whereas GST alone does not (***Ba***, lane 6). The indicated lower band in lane 7 at ~25 kDa is probably GST split-off from RE(A)-GST that piggybacks on RE(A)-GST bound to synaptic ribbons because GST is known to dimerize (Connell et al., 2008). In ***Ab*** and ***Bb***, the same blot as in ***Aa*** and ***Ba*** was stripped and reprobed with antibodies against RIBEYE (U2656) to show that equal amounts of purified synaptic ribbons were used as bait for the protein pull downs. RIBEYE signals of isolated bait synaptic ribbons are denoted by arrowheads (***Aa–Bb***, lanes 5–7). Recruitment of RIBEYE fusion protein is independent of the tag. ***Ca***, A further control to show that the recruitment of RE(A) to purified ribbons is mediated by RIBEYE(A) and not the GST-tag. Purified synaptic ribbons recruited RIBEYE(A), from which the GST-tag was removed by thrombin cleavage [RIBEYE(A)-TC, lane 4]. The autoaggregation control (lane 2) demonstrates that the coaggregation is dependent on the presence of synaptic ribbons and does not occur without ribbons. Binding of thrombin-cleaved rat RE(A) was detected by an antibody against RIBEYE(A) from the rat [anti-RE(A)] (tom Dieck et al., 2005). ***Cb***, Equal loadings of purified ribbons in lanes 3 and 4 was verified by Western blotting with a monoclonal antibody against RIBEYE(B)/CtBP2 (BD Transduction Laboratories). Lane 1 shows the input protein, RIBEYE(A) without GST-tag. ***Da***, RIBEYE(A) subdomains expressed as MBP fusion proteins are recruited to synaptic ribbons in the same manner as GST fusion proteins. RIBEYE(A1)-MBP and RIBEYE(A3)-MBP bound to synaptic ribbons (lanes 7, 8), whereas MBP alone did not (lane 6), demonstrating the specificity of the interaction. Interestingly, RIBEYE(A2)-MBP did not bind to purified synaptic ribbons (lane 9) although it efficiently interacted with RIBEYE(A) subunits [i.e., RIBEYE(A1), RIBEYE(A2)] in protein pull-down assays (Fig. 3). ***Db***, The same blot as in ***Da*** was stripped and reprobed with antibodies against RIBEYE (U2656) to show that equal amounts of purified synaptic ribbons were used as bait for the protein pull downs. RIBEYE signals of isolated bait synaptic ribbons are denoted by arrowheads (lanes 3–4 in ***Ca***, ***Cb***; lanes 5–9 in ***Da***, ***Db***). Lane 1–4 shows the input proteins (***Da***, ***Db***). RE, RIBEYE; RIBEYE(A)-TC, RIBEYE(A) generated from RIBEYE(A)-GST by a thrombin-mediated cleavage of the GST tag.

could be that the NAD(H)-binding region of RIBEYE(B) is also part of the binding interface with RIBEYE(A). If NADH binds to RIBEYE it could displace RIBEYE(A) from RIBEYE(B) and stimulate homodimerization of RIBEYE(B). By this way of thinking, NAD(H) would favor RIBEYE complexes that contain a homodimerized B-domain, which is likely important for RIBEYE function. Additionally, RIBEYE(B) displaced from RIBEYE(A2) would make the A2-binding module available for RIBEYE(A)–RIBEYE(A) interactions. By this mechanism, binding of NAD(H) could potentially initiate the assembly of synaptic ribbons. The NADH concentrations used in the present study are well in the range of the known cellular concentrations of NADH (Zhang et al., 2002; Fjeld et al., 2003) and thus very likely capable in regulating RIBEYE–RIBEYE interactions *in situ*.

The suggested modular assembly of the synaptic ribbon from individual RIBEYE units also provides a molecular explanation for the ultrastructural dynamics of synaptic ribbons by the addition or removal of RIBEYE subunits or rearrangements of RIBEYE–RIBEYE complexes. The ribbon recruitment experiments showed that binding sites for additional RIBEYE subunits are accessible and available on synaptic ribbons at a molecular level. Isolated synaptic ribbons (Schmitz et al., 1996, 2000) are able to bind externally added RIBEYE(B) and also RIBEYE(A). The multiple RIBEYE–RIBEYE interaction sites in the A-domain suggest a predominantly structural role of the A-domain as previously suggested (Schmitz et al., 2000). Probably large portions of RIBEYE(A) are likely "buried" in the core of the synaptic ribbons. Still, part of the A-domain is accessible in isolated synaptic ribbons and therefore partly exposed. In ribbon pull-down experiments (Fig. 10), RIBEYE(A1) and RIBEYE(A3) but not RIBEYE(A2) did bind to purified synaptic ribbons. Because RIBEYE(A2) can bind to both A1 and A2 interaction sites but not to the A3 interaction site, we suggest that A1 and A2 are located in the core of the ribbon, where these sites are not available for interaction with RIBEYE(A2). In contrast, the A3 region appears at least partly exposed on purified synaptic ribbons where it is free to interact with other protein, i.e., externally added RIBEYE(A1) and RIBEYE(A3) (Fig. 10*D*). Binding of RIBEYE(B) probably occurs via homodimerization of RIBEYE(B)-domains based on homologous findings with CtBP2 (Balasubramanian et al., 2003; Thio et al., 2004). This homodimerization is favored by the presence of NADH. Interestingly, RIBEYE(B) of synaptic ribbons does not bind RIBEYE(A2), although the respective fusion proteins can interact in an NAD(H)-dependent manner. Therefore, the RIBEYE(B)-binding site for RIBEYE(A2) might be blocked or the binding disfavored, e.g., by

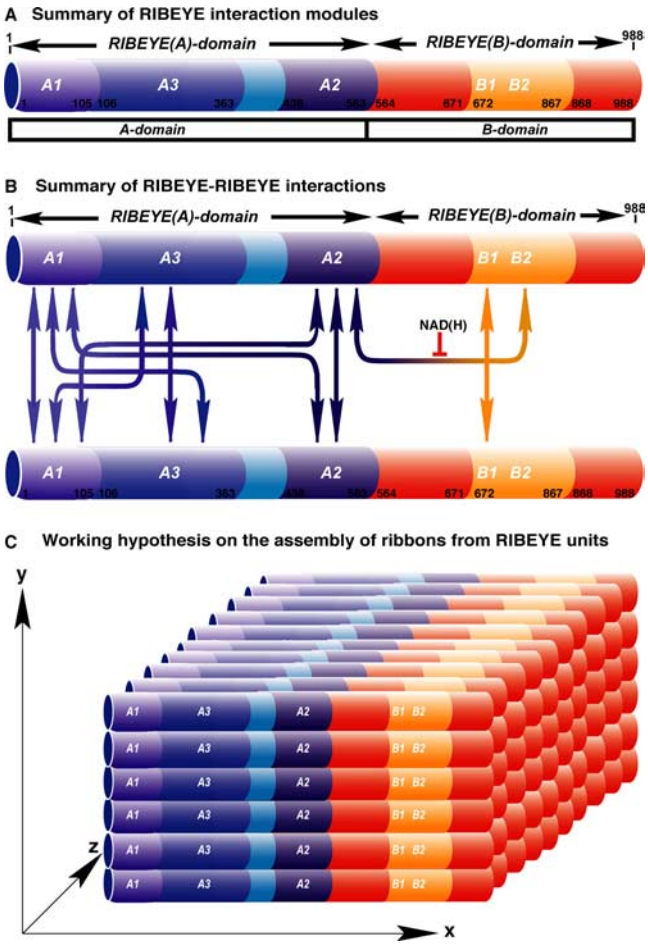

Figure 11. Schematic RIBEYE–RIBEYE interaction model. ***A***, Summary of the identified RIBEYE–RIBEYE interaction modules. In the A-domain of RIBEYE, three interaction modules are present, which are denoted as A1, A2, A3. In the B-domain of RIBEYE, two interaction modules, denoted as B1 and B2, are present. ***B***, Interaction combinations between the identified interaction modules are summarized. Only for the top RIBEYE molecule are all possible intermolecular homotypic domain interactions shown. Homotypic domain interactions, e.g., RIBEYE(A)–RIBEYE(A) interactions, can be mediated by homotypic subdomain interactions, e.g., RIBEYE(A1)–RIBEYE(A1), or by heterotypic subdomain interactions, e.g., RIBEYE(A1)–RIBEYE(A2). ***C***, A simplified, schematic working model shows how RIBEYE–RIBEYE interactions could build the scaffold of the synaptic ribbon from individual RIBEYE subunits. In this model, RIBEYE is depicted as a "linear" protein. For simplicity, a nonstaggered association of RIBEYE units is depicted based on homotypic RIBEYE–RIBEYE interactions. A possible, staggered interaction based on heterotypic RIBEYE–RIBEYE interactions is not included. *x*, *y*, and *z* represent the three-dimensional axis.

RIBEYE(B) homodimerization, or inhibited by NAD(H) bound at synaptic ribbons via the NBD of RIBEYE. Clearly, these working hypotheses have to be analyzed by future investigations and testing these assumptions will shed further light on the understanding of the construction and assembly of synaptic ribbons and how they work in the synapse.

In conclusion, our data show that RIBEYE is a scaffold protein with ideal properties to explain the assembly of synaptic ribbons as well as its ultrastructural dynamics via the modular assembly mechanism. The capability to interact with other RIBEYE proteins in multiple ways could explain how a single protein, RIBEYE, builds the scaffold for the entire ribbon (Fig. 11). Our transfection experiments actually show that RIBEYE can form aggregates that resemble spherical synaptic ribbons. The proposed modular assembly of the synaptic ribbon from individual RIBEYE subunits provides a molecular basis for the ultrastructural plasticity of synaptic ribbons (e.g., changes in size and shape of the ribbon). The binding of externally added RIBEYE to purified synaptic ribbons mimics the growth of synaptic ribbons that occurs *in situ*, e.g., under darkness in the mouse retina (Balkema et al., 2001; Spiwoks-Becker et al., 2004; Hull et al., 2006). Similarly, RIBEYE-aggregates increased in size over time in light microscopy (supplemental Fig. 9, available at www.jneurosci.org as supplemental material) and RIBEYE aggregates appeared to be able to coalesce into larger structures at the ultrastructural level. The regulation of RIBEYE–RIBEYE interactions, e.g., by NAD(H), could contribute to the regulation of structural plasticity of synaptic ribbons.

References

Bai C, Elledge SJ (1996) Gene identification using the yeast two-hybrid system. Methods Enzymol 273:331–347.

Balasubramanian P, Zhao LJ, Chinnadurai G (2003) Nicotinamide adenine dinucleotide stimulates oligomerization, interaction with adenovirus E1A and an intrinsic dehydrogenase activity of CtBP. FEBS Lett 537:157–160.

Balkema GW, Cusick K, Nguyen TH (2001) Diurnal variation in synaptic ribbon length and visual threshold. Vis Neurosci 18:789–797.

Bradford M (1976) A rapid and sensitive method for the quantitation of microgram quantities of protein utilizing the principle of protein-dye binding. Anal Biochem 72:248–254.

Cereghino JL, Cregg JM (2000) Heterologous protein expression in the methylotrophic yeast Pichia pastoris. FEMS Microbiol Rev 24:45–66.

Chadli A, Bouhouche I, Sullivan W, Stensgard B, McMahon N, Catelli MG, Toft DO (2000) Dimerization and N-terminal domain proximity underlie the function of the molecular chaperone heat shock protein 90. Proc Natl Acad Sci U S A 97:12524–12529.

Chinnadurai G (2002) CtBP, an unconventional transcriptional corepressor in development and oncogenesis. Mol Cell 9:213–224.

Coleman J (1990) Characterization of Escherichia coli cells deficient in 1-acyl-sn-glycerol-3- phosphate acyltransferase activity. J Biol Chem 265:17215–17221.

Connell E, Scott P, Davletov B (2008) Real time assay for monitoring membrane association of lipid-binding domains. Anal Biochem 377:83–88.

Fjeld CC, Birdsong WT, Goodman RH (2003) Differential binding of NAD^+ and NADH allows the transcriptional corepressor carboxyl-terminal binding protein to serve as a metabolic sensor. Proc Natl Acad Sci U S A 100:9202–9207.

Fuchs PA (2005) Time and intensity coding at the hair cell's ribbon synapse. J Physiol 566:7–12.

Harper JW, Adami GR, Wei N, Keyomarsi K, Elledge SJ (1993) The p21 Cdk-interacting protein Cip1 is a potent inhibitor of G1 cyclin-dependent kinases. Cell 75:805–816.

Heidelberger R, Thoreson WB, Witkovsky P (2005) Synaptic transmission at retinal ribbon synapses. Prog Retin Eye Res 24:682–720.

Helmuth M, Altrock W, Böckers TM, Gundelfinger ED, Kreutz MR (2001) An electrotransfection protocol for yeast two-hybrid library screening. Anal Biochem 293:149–152.

Hull C, Studholme K, Yazulla S, von Gersdorff H (2006) Diurnal changes in exocytosis and the number of synaptic ribbons at active zones of an ON-type bipolar cell terminal. J Neurophysiol 96:2025–2033.

James P, Halladay J, Craig EA (1996) Genomic libraries and a host strain designed for highly efficient two hybrid selection in yeast. Genetics 144:1425–1436.

Khimich D, Nouvian R, Pujol R, Tom Dieck S, Egner A, Gundelfinger ED, Moser T (2005) Hair cell synaptic ribbons are essential for synchronous auditory signalling. Nature 434:889–894.

Kumar V, Carlson JE, Ohgi KA, Edwards TA, Rose DW, Escalante CR, Rosenfeld MG, Aggarwal AK (2002) Transcription corepressor CtBP is an NAD(+)-regulated dehydrogenase. Mol Cell 10:857–869.

Lin-Cereghino J, Wong WW, Xiong S, Giang W, Luong LT, Vu J, Johnson SD, Lin-Cereghino GP (2005) Condensed protocol for competent cell preparation and transformation of the methylotrophic yeast Pichia pastoris. Biotechniques 38:44–48.

Nardini M, Spanò S, Cericola C, Pesce A, Massaro A, Millo E, Luini A, Corda D, Bolognesi M (2003) CtBP/BARS: a dual-function protein involved in

transcription co-repression and Golgi membrane fission. EMBO J 22:3122–3130.

Nouvian R, Beutner D, Parsons TD, Moser T (2006) Structure and function of the hair cell ribbon synapse. J Membr Biol 209:153–165.

Prescott ED, Zenisek D (2005) Recent progress towards understanding the synaptic ribbon. Curr Opin Neurobiol 15:431–436.

Schmitz F, Bechmann M, Drenckhahn D (1996) Purification of synaptic ribbons, structural components of the photoreceptor active zone complex. J Neurosci 16:7109–7116.

Schmitz F, Königstorfer A, Südhof TC (2000) RIBEYE, a component of synaptic ribbons: a protein's journey through evolution provides insight into synaptic ribbon function. Neuron 28:857–872.

Schmitz F, Tabares L, Khimich D, Strenzke N, de la Villa-Polo P, Castellano-Muñoz M, Bulankina A, Moser T, Fernández-Chacón R, Südhof TC (2006) CSPalpha-deficiency causes massive and rapid photoreceptor degeneration. Proc Natl Acad Sci U S A 103:2926–2931.

Seigel GM (1996) Establishment of an E1A-immortalized retinal cell culture. In Vitro Cell Dev Biol Anim 32:66–68.

Seigel GM, Sun W, Wang J, Hershberger DH, Campbell LM, Salvi RJ (2004) Neuronal gene expression and function in the growth-stimulated R28 retinal precursor cell line. Curr Eye Res 28:257–269.

Sewalt RG, Gunster MJ, van der Vlag J, Satijn DP, Otte AP (1999) C-Terminal binding protein is a transcriptional repressor that interacts with a specific class of vertebrate Polycomb proteins. Mol Cell Biol 19:777–787.

Singer JH (2007) Multivesicular release and saturation of glutamatergic signalling at retinal ribbon synapses. J Physiol 580:23–29.

Spiwoks-Becker I, Glas M, Lasarzik I, Vollrath L (2004) Mouse photoreceptor synaptic ribbons lose and regain material in response to illumination changes. Eur J Neurosci 19:1559–1571.

Stahl B, Diehlmann A, Südhof TC (1999) Direct interaction of Alzheimer's disease-related presenilin 1 with armadillo protein p0071. J Biol Chem 274:9141–9148.

Sterling P, Matthews G (2005) Structure and function of ribbon synapses. Trends Neurosci 28:20–29.

Thio SS, Bonventre JV, Hsu SI (2004) The CtBP2 co-repressor is regulated by NADH-dependent dimerization and possesses a novel N-terminal repression domain. Nucleic Acids Res 32:1836–1847.

tom Dieck S, Brandstätter JH (2006) Ribbon synapses of the retina. Cell Tissue Res 326:339–346.

tom Dieck S, Altrock WD, Kessels MM, Qualmann B, Regus H, Brauner D, Fejtová A, Bracko O, Gundelfinger ED, Brandstätter JH (2005) Molecular dissection of the photoreceptor ribbon synapse: physical interaction of Bassoon and RIBEYE is essential for the assembly of the ribbon complex. J Cell Biol 168:825–836.

Vollrath L, Spiwoks-Becker I (1996) Plasticity of retinal ribbon synapses. Microsc Res Tech 35:472–487.

Wagner HJ (1997) Presynaptic bodies ("ribbons"): from ultrastructural observations to molecular perspectives. Cell Tissue Res 287:435–446.

Wan L, Almers W, Chen W (2005) Two ribeye genes in teleosts: the role of Ribeye in ribbon formation and bipolar cell development. J Neurosci 25:941–949.

Wang Y, Okamoto M, Schmitz F, Hofmann K, Südhof TC (1997) Rim is a putative Rab3 effector in regulating synaptic-vesicle fusion. Nature 388:593–598.

Zenisek D, Horst NK, Merrifield C, Sterling P, Matthews G (2004) Visualizing synaptic ribbons in the living cell. J Neurosci 24:9752–9759.

Zhang Q, Piston DW, Goodman RH (2002) Regulation of corepressor function by nuclear NADH. Science 295:1895–1897.

Supplemental Material can be found at:
http://www.jbc.org/cgi/content/full/M801625200/DC1

THE JOURNAL OF BIOLOGICAL CHEMISTRY VOL. 283, NO. 39, pp. 26461–26467, September 26, 2008
© 2008 by The American Society for Biochemistry and Molecular Biology, Inc. Printed in the U.S.A.

RIBEYE Recruits Munc119, a Mammalian Ortholog of the *Caenorhabditis elegans* Protein unc119, to Synaptic Ribbons of Photoreceptor Synapses*[S]

Received for publication, February 28, 2008, and in revised form, July 7, 2008 Published, JBC Papers in Press, July 29, 2008, DOI 10.1074/jbc.M801625200

Kannan Alpadi[‡], Venkat Giri Magupalli[‡], Stefanie Käppel[‡], Louise Köblitz[‡], Karin Schwarz[‡], Gail M. Seigel[§1], Ching-Hwa Sung[¶], and Frank Schmitz[‡2]

From the [‡]Department of Neuroanatomy, Institute for Anatomy and Cell Biology, Saarland University, Medical School Homburg/Saar, 66421 Homburg/Saar, Germany, the [§]Department of Ophthalmology, Physiology, and Biophysics, SUNY University at Buffalo, Buffalo, New York 14214, and the [¶]Margaret M. Dyson Vision Research Institute, Department of Ophthalmology, Cell and Developmental Biology, Weill Medical College of Cornell University, New York, New York 10021

Munc119 (also denoted as RG4) is a mammalian ortholog of the *Caenorhabditis elegans* protein unc119 and is essential for vision and synaptic transmission at photoreceptor ribbon synapses by unknown molecular mechanisms. Munc119/RG4 is related to the prenyl-binding protein PrBP/δ and expressed at high levels in photoreceptor ribbon synapses. Synaptic ribbons are presynaptic specializations in the active zone of these tonically active synapses and contain RIBEYE as a unique and major component. In the present study, we identified Munc119 as a RIBEYE-interacting protein at photoreceptor ribbon synapses using five independent approaches. The PrBP/δ homology domain of Munc119 is essential for the interaction with the NADH binding region of RIBEYE(B) domain. But RIBEYE-Munc119 interaction does not depend on NADH binding. A RIBEYE point mutant (RE(B)E844Q) that no longer interacted with Munc119 still bound NADH, arguing that binding of Munc119 and NADH to RIBEYE are independent from each other. Our data indicate that Munc119 is a synaptic ribbon-associated component. We show that Munc119 can be recruited to synaptic ribbons via its interaction with RIBEYE. Our data suggest that the RIBEYE-Munc119 interaction is essential for synaptic transmission at the photoreceptor ribbon synapse.

Munc119 (also denoted as RG4, Ref. 1) is a mammalian ortholog of the *Caenorhabditis elegans* protein unc119 and essential for normal vision and synaptic transmission at photoreceptor synapses (1–3). Munc119/RG4 was initially identified by a differential display screen and shown to be expressed at high levels in photoreceptor synapses (1–3). Munc119 consists of an N-terminal, 77-amino acid long proline-rich region, and a 163-amino acid long C-terminal domain that shares significant sequence homology to the prenyl-binding protein PrBP/δ[3] (previously also denoted as the δ-subunit of photoreceptor cGMP-dependent phosphodiesterase (PDE6D) (4–6). The C-terminal PrBP/δ homology domain of Munc119 is highly conserved between species and is essential for Munc119 function (1–3). The essential function of Munc119 for synaptic transmission at photoreceptor synapses and for vision has been demonstrated in a cone rod dystrophy patient with a premature termination codon mutation (5). This termination codon mutation resulted in a Munc119 protein that lacked the PrBP/δ domain. Consistently, a transgenic mouse model that reproduced this premature termination codon mutation of Munc119 displayed similarly strong disturbances of synaptic transmission at photoreceptor synapses and defects in vision (5, 7, 8). The mechanism of how Munc119 works in photoreceptor synapses is not clear.

Photoreceptor synapses are mainly ribbon-type synapses (for review, see Refs. 9–11). Ribbon synapses are specialized, tonically active chemical synapses. To maintain tonic exocytosis, ribbon synapses are equipped with specialized presynaptic structures, the synaptic ribbons (for review, see Refs. 9–11). Synaptic ribbons are presynaptic structures in the active zone complex of these synapses and are associated with large amounts of synaptic vesicles (for review, see Refs. 9–11). The protein RIBEYE is a major component of synaptic ribbons and exclusively localized to these structures (12–14). RIBEYE consists of a unique A-domain and a B-domain, which is largely identical to CtBP2 (12). RIBEYE(B) domain belongs to a family of D-isomer-specific 2-hydroxy acid dehydrogenases and binds NAD(H) with high affinity (12). Structural analyses of the CtBP protein family that also includes RIBEYE (for review, see Ref. 15) revealed the presence of two distinct subdomains: a central NADH binding domain (NBD) and a substrate binding domain (SBD) (16, 17). The RIBEYE-specific substrate that binds to the

* This work was supported by the Sonderforschungsbereich 530 (SFB530) (TPC11) and by HOMFOR (to F. S.). The costs of publication of this article were defrayed in part by the payment of page charges. This article must therefore be hereby marked "*advertisement*" in accordance with 18 U.S.C. Section 1734 solely to indicate this fact.

The nucleotide sequence(s) reported in this paper has been submitted to the GenBank™/EBI Data Bank with accession number(s) BC103449.1.

[S] The on-line version of this article (available at http://www.jbc.org) contains supplemental materials and Figs. S1–S6.

[1] Supported by the Sybil Harrington Scholar Award from Research to Prevent Blindness and 5R24EY016662.

[2] To whom correspondence should be addressed: Dept. of Neuroanatomy, Institute for Anatomy and Cell Biology, Bldg. 61, Saarland University, Medical School Homburg/Saar, 66421 Homburg/Saar. Tel.: 49-6841-1626012; Fax: 49-6841-1626121; E-mail: frank.schmitz@uniklinikum-saarland.de.

[3] The abbreviations used are: PrBP/δ, prenyl-binding protein δ; RE, RIBEYE; RE(B), RIBEYE(B) domain; NBD, NAD(H) binding domain; SBD, substrate binding domain; RE(AB), full-length RIBEYE(AB); PRD, proline-rich domain of Munc119; YTH, yeast-two-hybrid; GST, glutathione *S*-transferase; MBP, maltose-binding protein.

Downloaded from www.jbc.org at Saarlaendische Univ. u. Landesbibl./Medizinische Abteilung Homburg/Saar on September 24, 2008

SBD is not yet known as well as the precise physiological function of RIBEYE in the synapse.

To better understand the physiological role and molecular composition of synaptic ribbons, we performed a YTH screen using the RIBEYE (B) domain as a bait. In this screen, we identified Munc119 as a potential RIBEYE-interacting protein.

EXPERIMENTAL PROCEDURES

Plasmids—Details on all plasmids are deposited as supplemental materials.

Yeast Two-hybrid Methods—For YTH analyses, the Gal4-based Matchmaker yeast two-hybrid system (Clontech) was used according to the manufacturer's instructions. For the YTH screening, we used a bovine retinal YTH cDNA library from the retina (18). The cDNA of the respective bait proteins were cloned in-frame with the Gal4-DNA binding domain of pGBKT7. The cDNA of the indicated prey proteins were cloned in-frame with the Gal4 activation domain of pACT2 or pGADT7. The bait and prey plasmids confer tryptophan and leucine prototrophy to the respective auxotrophic yeast strains. Yeast strains Y187 and AH109 were used that contain distinct auxotrophic marker genes: AH109 [MATa, trp1-901, leu2-3, 112, ura3-52, his3-200, Gal4Δ, gal80Δ, LYS2::$GAL1_{UAS}$-$GAL1_{TATA}$-HIS3, $GAL2_{UAS}$-$GAL2_{TATA}$-ADE2, URA3::$MEL1_{UAS}$-$MEL1_{TATA}$-lacZ] (19); Y187 [MATα, ura3-52, his3-200, ade2-101, trp1-901, leu2-3,112, gal4Δ,. met, gal80Δ, URA3::$GAL1_{UAS}$-$GAL1_{TATA}$-lacZ] (20). Bait plasmids were electroporated into AH109 yeast, prey plasmids into Y187 yeast. Preparation of electrocompetent yeasts and electroporation of yeasts were done as described (21). For identifying transformants, yeasts were plated on the respective selective plates to identify the resulting convertants to the respective prototrophy (drop out media Clontech/QBiogene). For interaction analyses, AH109 yeasts containing the respective bait plasmid were mated with Y187 yeasts containing the respective prey plasmid. Mating was performed for 5 h at 30 °C in 1 ml of YPD medium with heavy vortexing. For assessing mating efficiency, half of the mated sample was streaked on −LW plates, the other half was plated on −ALWH selective plate with 10 mM aminotriazole (3-amino 1,2,4-triazole, ATZ) added. For the matings, pSE1111 and pSE1112 that encode irrelevant proteins (22) as well as the empty bait and prey vectors were used as negative controls. Expression of β-galactosidase (β-gal) marker gene activity was qualitatively analyzed by filter assays and quantitatively with liquid assays as described (23, 24).

Cell Culture—COS- and R28 retinal progenitor cells were cultured as previously described (12, 25, 26). COS cells were transiently transfected with the DEAE-dextran method (12) or with lipofection using the perfectin reagent (PEQLAB) according to the manufacturer's instructions.

GST Pull-down Assays from Transfected COS Cells—COS cells were transfected with the indicated eukaryotic expression constructs (empty GSTpEBG, Munc119(1–240)-GSTpEBG and RE(B)-EGFP, see supplemental materials). For the experimental assays, Munc119(1–240)-GSTpEBG was co-transfected with RE(B)-EGFP. Empty GSTpEBG co-transfected with RE(B)-EGFP served as control assays. 48 h after transfection, the cells were collected from the plates and pelleted at 6,000 rpm for 5 min at 4 °C. All subsequent steps were performed at 4 °C if not denoted otherwise. The cell pellets were washed with ice-cold phosphate-buffered saline and lysed with 500 μl of ice-cold lysis buffer (100 mM Tris-HCl, pH 7.9, 150 mM NaCl, 1 mM EDTA containing 1% Triton X-100) for 30 min. Subsequently, the samples were centrifuged at 13,000 rpm for 15 min. The lysate from experiment and control assay were incubated overnight with 10 μl of washed glutathione-Sepharose beads each (Amersham Biosciences). After incubation, the samples were centrifuged at 13,000 rpm for 1 min, and the supernatants removed. The pellets were washed with ice-cold phosphate-buffered saline three times. The final pellets were boiled in 25 μl of SDS sample buffer and subjected to 10% SDS-PAGE followed by Western blot analyses with the indicated antibodies.

Immunoprecipitation from R28 Retinal Progenitor Cells—All steps were performed at 4 °C if not denoted otherwise. Washed R28 cell pellets were lysed with lysis buffer (100 mM Tris-HCl, pH 7.9, 150 mM NaCl, 1 mM EDTA, 1% Triton X-100) for 45 min on ice. The lysate was centrifuged twice at 13,000 rpm (15 min, Eppendorf centrifuge (Biofuge Fresco, rotor 3329), and supernatants were subsequently precleared by the addition of 20 μl of washed protein A-Sepharose beads (Sigma) and 10 μl of RIBEYE preimmune serum for 1 h. Following centrifugation (13,000 rpm, 1 min), the precleared lysate was divided into two equal aliquots and incubated either with 10 μl of control IgG (U2656 preimmune serum) or with 10 μl of anti-RIBEYE (U2656 immune serum) for overnight at 4 °C. After overnight incubation, 20 μl of washed protein A-Sepharose beads were added to the samples, and incubation was continued for another 1 h. Subsequently, samples were centrifuged and washed five times with incubation buffer. The washed protein A-Sepharose pellets were boiled in 30 μl of SDS sample buffer and analyzed by Western blot analyses as described below.

Immunoprecipitation from the Bovine Retina—All steps were performed at 4 °C if not denoted otherwise. For each immunoprecipitation, a freshly isolated bovine retina was incubated with 2 ml of lysis buffer (100 mM Tris-HCl, pH 7.9, 150 mM NaCl, 1 mM EDTA) containing 1% Triton X-100 for 30 min at 4 °C. Then the sample was centrifuged at 13,000 rpm for 15 min. Samples were transferred to 2-ml syringes and forcefully ejected through 23-gauge needles to mechanically disrupt the retinal tissue. Mechanical crushing through 23-gauge needles was repeated 40–50 times. The mechanical disruption is essential to fractionate synaptic ribbons and to make them accessible for immunoprecipitation. Without mechanical treatment, no RIBEYE was observed in the respective tissue lysate. After mechanical disruption, lysis was allowed to proceed for further 30 min on ice. Samples were centrifuged twice at 13,000 rpm for 30 min. The supernatant was incubated with 10 μl of Munc119 preimmune serum and 20 μl of washed protein A-Sepharose beads for 1 h at 4 °C. Afterward, the sample was centrifuged at 13,000 rpm for 15 min, and the precleared lysate was divided into two aliquots and incubated either with 10 μl of Munc119 immune serum (Munc119 V2T2.120) or with Munc119 preimmune serum (control IgG) together with 20 μl of washed protein A-Sepharose beads (overnight). After overnight incubation, samples were centrifuged at

Downloaded from www.jbc.org at Saarlaendische Univ. u. Landesbibl./Medizinische Abteilung Homburg/Saar on September 24, 2008

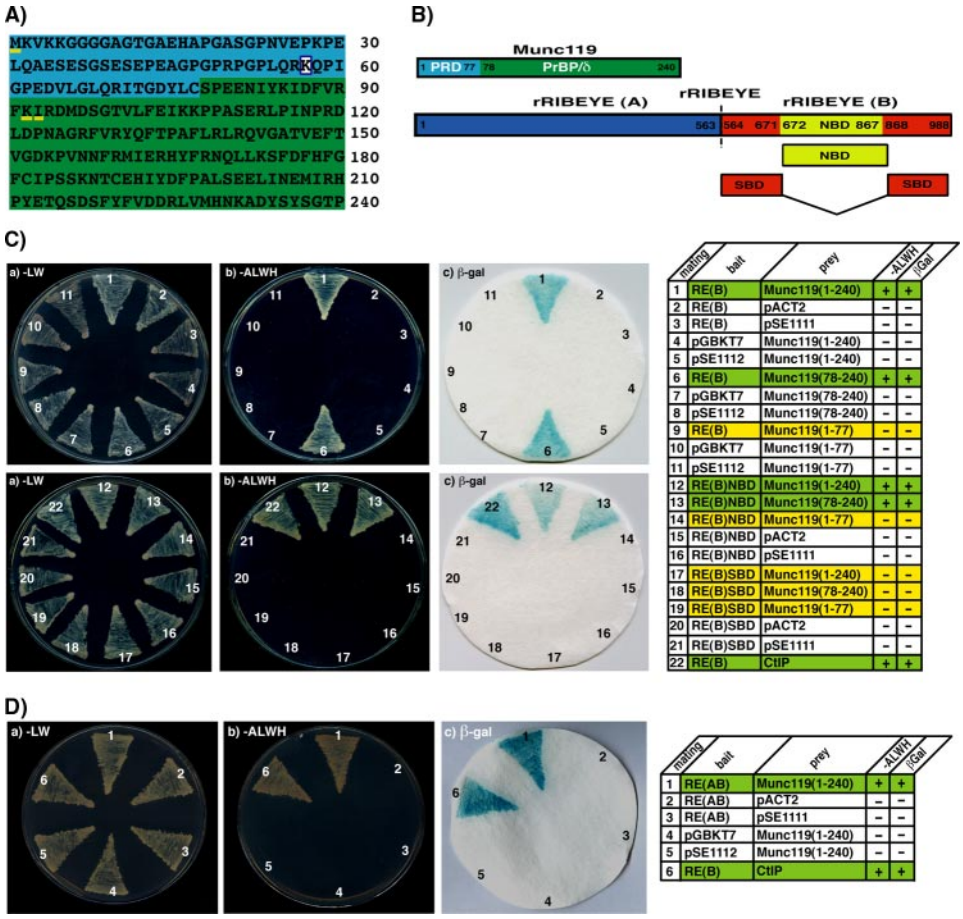

mating	bait	prey	-ALWH	βGal
1	RE(B)	Munc119(1-240)	+	+
2	RE(B)	pACT2	–	–
3	RE(B)	pSE1111	–	–
4	pGBKT7	Munc119(1-240)	–	–
5	pSE1112	Munc119(1-240)	–	–
6	RE(B)	Munc119(78-240)	+	+
7	pGBKT7	Munc119(78-240)	–	–
8	pSE1112	Munc119(78-240)	–	–
9	RE(B)	Munc119(1-77)	–	–
10	pGBKT7	Munc119(1-77)	–	–
11	pSE1112	Munc119(1-77)	–	–
12	RE(B)NBD	Munc119(1-240)	+	+
13	RE(B)NBD	Munc119(78-240)	+	+
14	RE(B)NBD	Munc119(1-77)	–	–
15	RE(B)NBD	pACT2	–	–
16	RE(B)NBD	pSE1111	–	–
17	RE(B)SBD	Munc119(1-240)	–	–
18	RE(B)SBD	Munc119(78-240)	–	–
19	RE(B)SBD	Munc119(1-77)	–	–
20	RE(B)SBD	pACT2	–	–
21	RE(B)SBD	pSE1111	–	–
22	RE(B)	CtIP	+	+

mating	bait	prey	-ALWH	βGal
1	RE(AB)	Munc119(1-240)	+	+
2	RE(AB)	pACT2	–	–
3	RE(AB)	pSE1111	–	–
4	pGBKT7	Munc119(1-240)	–	–
5	pSE1112	Munc119(1-240)	–	–
6	RE(B)	CtIP	+	+

FIGURE 1. **Interaction of RIBEYE(B) and RIBEYE(AB) with Munc119 in the YTH system.** *A*, amino acid sequence of bovine Munc119. The proline-rich domain (*PRD*, aa1–77) is colored in *blue*, the PrBP/δ-homology domain of Munc119 (aa78–240) colored in *green*. The *boxed lysine* indicates the site of a premature stop mutation that causes cone rod dystrophy in a human patient (5). The amino acids methionine 1 (*M1*), lysine 92 (*K92*), and isoleucine 93 (*I93*), which are underlined in *yellow* indicate the beginning of the reading frames of three independently obtained Munc119 YTH prey clones. The amino acid sequence of Munc119 obtained in our YTH screen is identical to the Munc119 sequence deposited at GenBank™ (accession BC103449.1). *B*, schematic domain structures of RIBEYE and Munc119. RIBEYE contains of a large N-terminal A-domain and a C-terminal B-domain. The B-domain of RIBEYE contains the NAD(H) binding subdomain (NBD, depicted in *yellow*) and the substrate binding subdomain (SBD, depicted in *red*). *C*, RIBEYE(B) interacts with the PrBP/δ-homology domain of Munc119 in YTH. Summary plates of YTH analyses obtained with the indicated bait and prey plasmids. For convenience, experimental bait-prey pairs are underlayered in color (*green* in the case of interacting bait-prey pairs; *yellow* in the case of non-interacting bait-prey-pairs; control matings are *non-colored*). *D*, RIBEYE(B) and also full-length RIBEYE (RIBEYE(AB) interact with Munc119. The interaction is mediated via the NBD of RIBEYE and the PrBP/δ homology domain of Munc119, Munc119(78–240) (*C*; matings 6,12–13). Mating 22 in *C* and mating 6 in *D* denote an unrelated positive control mating (CtIP). pSE1111 is an irrelevant prey vector, and pSE1112 an irrelevant bait vector (22).

3,000 rpm (2 min) to pellet the protein A-Sepharose beads. The pellet was washed three times with 1 ml of lysis buffer. The final pellet was boiled with SDS loading buffer and subjected to SDS-PAGE followed by Western blotting with the indicated antibodies.

Antibodies—The following antibodies were used in the present study: mouse monoclonal anti-GST (Sigma), mouse monoclonal anti-MBP (New England Biolabs), anti-RIBEYE(B) domain (U2656, 12), mouse monoclonal anti-CtBP2 (BD Biosciences), and polyclonal anti-EGFP (T3743; gift of Dr. Thomas C. Südhof, Dallas, TX). Full-length bovine Munc119-GST was used as an antigen to generate the immune serum Munc119 V2T2. For the experiments, immune serum at the 120th day after immunization was used. The antibody specifically detects Munc119 (supplemental Fig. S6). In extracts of R28 cells and bovine retina the Munc119 immune serum V2T2.120 specifically detected Munc119 at the expected running position at 35 kDa (Figs. 4 and 5 and supplemental Fig. S6).

Miscellaneous Methods—SDS-PAGE and Western blotting was performed as previously described (12). The fusion protein was expressed in BL21(DE3) as previously described (12, see also supplemental materials). Synaptic ribbons were purified as previously described (12, 27). Immunofluorescence microscopy was performed as previously described (28) using a Zeiss Axiovert 200M equipped with the respective filter sets.

RESULTS

Identification of Munc119 as a RIBEYE-interacting Protein—Using RIBEYE(B) as bait, we obtained three independent clones of Munc119 from the retinal YTH cDNA library as potential interaction partners of RIBEYE. One clone encoded full-length Munc119, the two other clones encoded truncated Munc119 proteins that started at lysine 92 (Lys-92) and isoleucine 93 (Ile-93), shortly after the beginning of the PrBP/δ-homology domain of Munc119 (Fig. 1*A*), suggesting that the PrBP/δ domain of Munc119 is probably responsible for the interaction. Using bait constructs that encoded for the PRD-(aa1–77)- or PrBP/δ-(aa78–240) domain of Munc119 we verified that the PrBP/δ-homology domain of Munc119 is indeed responsible for the interaction with RIBEYE (Fig. 1*C*). The PRD of Munc119 did not interact with RIBEYE in the YTH system. In the case of RIBEYE, the NADH binding subdomain of RIBEYE(B) domain (NBD) is mediating the interaction with Munc119. Munc119 also interacted with full-length RIBEYE indicating that the A-domain of RIBEYE is not inhibiting the interaction of the RIBEYE(B) domain with Munc119 (Fig. 1*D*). The interactions in the YTH were assayed by the growth of the respective mated yeast on −ALWH selective plates, indicating protein-protein interaction, as well as by qualitative and quantitative assessment of the β-galactosidase marker gene expression (Fig. 1, *C* and *D* and supplemental Fig. S1).

Munc119 Interacts with RIBEYE in GST Pull-down Assays—We used various independent approaches to verify the

Downloaded from www.jbc.org at Saarlaendische Univ. u. Landesbibl./Medizinische Abteilung Homburg/Saar on September 24, 2008

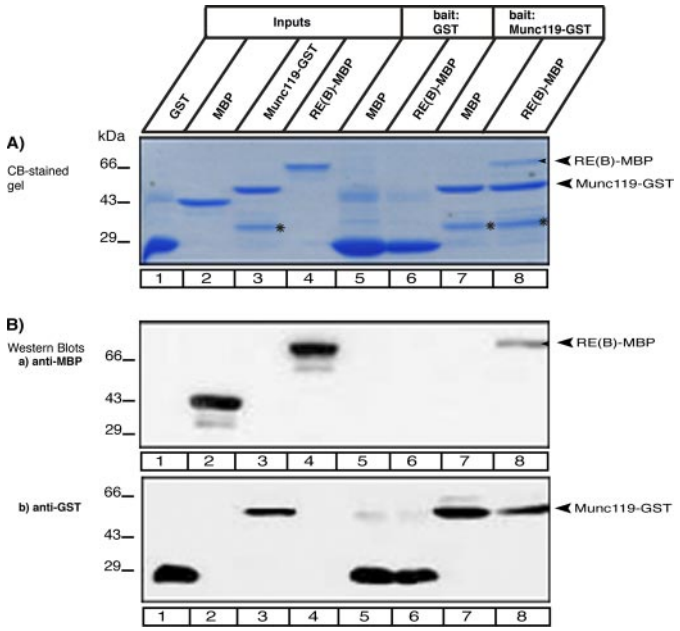

FIGURE 2. **RIBEYE(B) specifically interacts with Munc119 in fusion protein pull-down assays.** Pull-down analyses of RIBEYE(B)/Munc119 complexes using bacterially expressed fusion proteins. In *A*, pull-down experiments were analyzed by Coomassie Blue-stained polyacrylamide gel after SDS-PAGE. In *B*, by Western blot analyses with the indicated antibodies. *A* and *B*, *lanes 1–4* show the indicated purified fusion proteins (input fractions). All input lanes, except for *lane 4*, represent 50% of the input fraction. *Lane 4* represents 25% of the input fraction. In *lanes 5–8*, 100% was loaded. GST-tagged fusion proteins were used as immobilized bait proteins and MBP-tagged proteins as soluble prey proteins. Only Munc119-GST pulled-down RE(B)-MBP (*lane 8*) but not GST alone (*lane 6*). Neither GST alone nor Munc119-GST pulled-down MBP alone (*lanes 5* and *7*). The *asterisks* in *lanes 3*, *7*, and *8* of *A* label a break-down product of Munc119-GST. SDS-PAGE clearly demonstrated that Munc119-GST does not pull-down MBP alone (*A*). To further exclude that any MBP is nonspecifically pulled-down by Munc119-GST, we also analyzed the results of the pull-down assays by Western blotting with anti-MBP antibodies. *B*, Western blot analyses with anti-MBP antibodies (*B*) clearly show that only RE(B)-MBP (*lane 8*) but not MBP alone (*lane 7*) is pulled-down by Munc119-GST. GST alone does not pull-down RE(B)-MBP as well as MBP alone as shown by Western blotting with antibodies against MBP (*Ba*) demonstrating the specificity of the interaction and completely confirming the results in *A*. In *Bb*, the same blot as analyzed in *Ba* was reprobed (after stripping) with antibodies against GST to show equal loading of the bait proteins. Abbreviations: *CB*, Coomassie Blue.

Munc119-RIBEYE(B) interaction. First, we performed pull-down experiments using bacterially expressed and purified fusion protein (Fig. 2). We used GST-tagged proteins (Munc119-GST and GST) as immobilized bait proteins and MBP-tagged proteins (RIBEYE(B)-MBP and MBP) as soluble prey proteins. Munc119-GST (but not GST alone) interacted with RIBEYE(B)-MBP (but not MBP alone) as judged by protein pull-down analyses (Fig. 2). Specificity of interaction in these fusion protein pull-downs was consistently shown by SDS-PAGE and Western blot analyses (Fig. 2, *A* and *B*). Next, we analyzed whether RIBEYE(B) interacts with Munc119 in transfected COS cells. For this purpose, COS cells were co-transfected with eukaryotic expression plasmids that encoded for RIBEYE(B)-EGFP and GST-tagged Munc119 or GST alone (as control protein). Munc119-GST (but not GST alone) pulled-down RIBEYE(B)-EGFP from a crude cell extract of transfected COS cells (Fig. 3), further demonstrating a specific interaction between the RIBEYE(B) domain and Munc119.

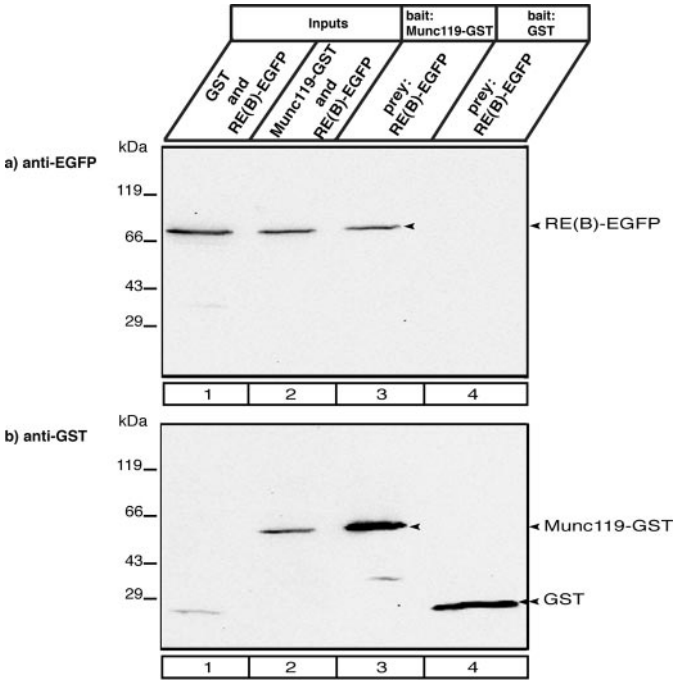

FIGURE 3. **RIBEYE interacts with Munc119 in transfected COS cells.** COS cells were co-transfected either with Munc119-GSTpEBG and RE(B)-EGFP (experimental assays) or with empty GSTpEBG and RE(B)-EGFP (control assays) using lipofection. Glutathione beads were added to the respective cell lysates. Proteins bound to the glutathione beads (*lanes 3* and *4*) were analyzed via Western blotting with antibodies against GST and EGFP. Munc119-GST pulled-down RIBEYE(B)-EGFP (*lane 3*) but not GST alone (*lane 4*) demonstrating the specific interaction between Munc119 and RIBEYE(B). *Lanes 1–2* show the respective input fractions (10% of total input); *Lanes 3* and *4* show 100% of the pulled-down proteins. In *b*, the same blot as shown in *a* was reprobed (after stripping) with antibodies against GST to show equal loading of the samples.

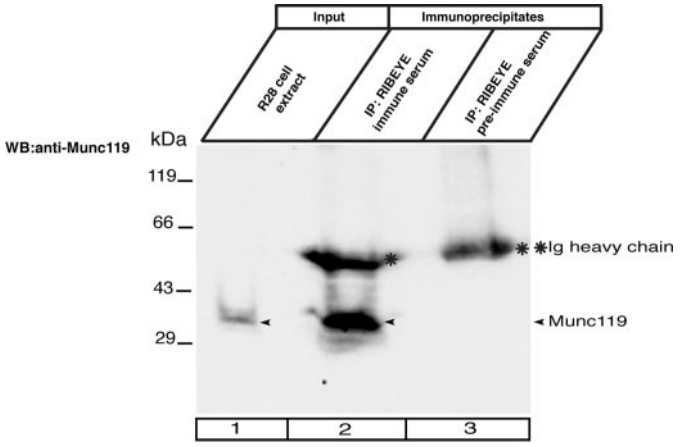

FIGURE 4. **Co-immunoprecipitation of RIBEYE and Munc119 from R28 retinal precursor cells.** R28 retinal progenitor cells endogenously express soluble Munc119 and RIBEYE, which can be readily solubilized from R28 cells by Triton X-100 lysis as described under "Experimental Procedures." Munc119 was co-immunoprecipitated by antibodies against RIBEYE from extracts of R28 retinal progenitor cells (*lane 2*). Immunoprecipitated Munc119 is indicated by an *arrowhead* in *lane 2*. The RIBEYE preimmune serum did not co-immunoprecipitate Munc119 (*lane 3*) demonstrating the specificity of the co-immunoprecipitation. *Lane 1* shows the input fraction (5% of total input); all of the protein A-beads with the immunoprecipitated proteins (100%) were loaded on the gel (*lanes 2* and *3*). *Asterisks* indicate the immunoglobulin heavy chains.

Immunoprecipitation of Endogenous Munc119 and RIBEYE from R28 Retinal Progenitor Cells and Bovine Retina—R28 is an E1A-immortalized retinal precursor cells line (25). These cells are

Downloaded from www.jbc.org at Saarlaendische Univ. u. Landesbibl./Medizinische Abteilung Homburg/Saar on September 24, 2008

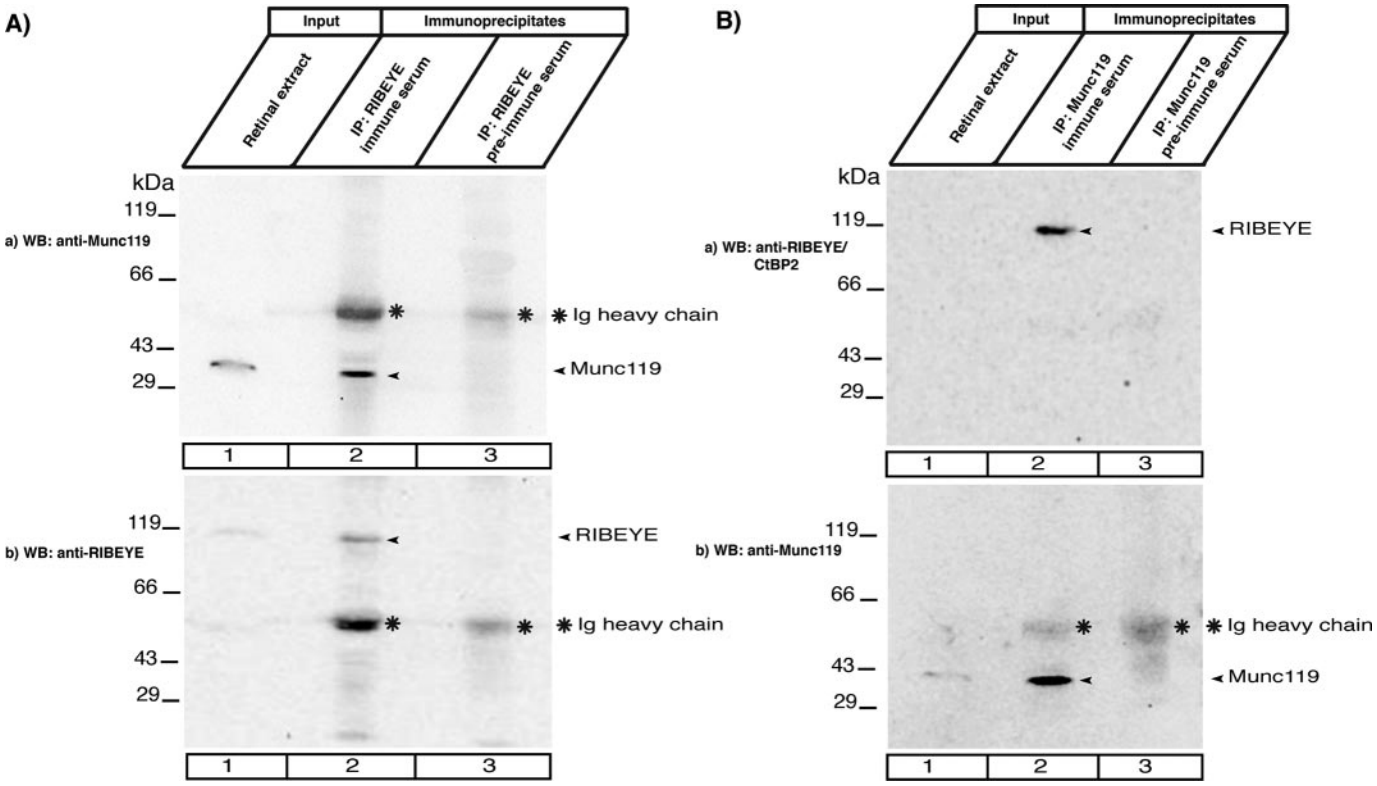

FIGURE 5. **Co-immunoprecipitation of RIBEYE and Munc119 from the bovine retina.** Co-immunoprecipitation of RIBEYE and Munc119 from bovine retina. In *A*, RIBEYE immune serum and RIBEYE preimmune serum were tested for their capability to co-immunoprecipitate Munc119. Munc119 is co-immunoprecipitated by RIBEYE immune serum (*lane 2*, *Aa*) but not by RIBEYE preimmune serum (*lane 3*, *A*). *Ab*, shows the same blot as in *Aa* but reprobed with anti-RIBEYE antibodies. This blot shows the presence of RIBEYE precipitated by the immune serum (*lane 2*) but not by the preimmune serum (*lane 3*). *Asterisks* indicate the immunoglobulin heavy chains. *Lane 1* shows the input fraction (2% of total input). The loaded 2% input fraction corresponds roughly to 200 μg of total proteins (in a volume of $\approx$20 μl). Considerably more input fraction could not be loaded on the gel for volume reasons and also not to overload the gel. Furthermore, synaptic ribbons are mechanically stable, Triton X-100-insoluble structures, which can only be extracted to a certain extent from the bovine retina by the combination of mechanical and chemical lysis. Therefore, the RIBEYE immunosignal is weak in the input fractions. RIBEYE is highly enriched in the experimental immunoprecipitates (*lane 2*) but absent in the control immunoprecipitates (*lane 3*). *Asterisks* indicate the immunoglobulin heavy chains. 100% of the protein A-beads containing the immunoprecipitated proteins were loaded on the gel for experimental and control immunoprecipitations (*lanes 2* and *3*). In *B*, Munc119 immune serum and Munc119 preimmune serum were tested for their capability to co-immunoprecipitate RIBEYE. RIBEYE is co-immunoprecipitated by Munc119 immune serum (*lane 2*, *Ba*) but not by Munc119 preimmune serum (*lane 3*, *Ba*). *Bb* shows the same blot as in *Ba* but reprobed with anti-Munc119. This blot shows the presence of Munc119 immunoprecipitated by the immune serum but not by the preimmune serume. *Asterisks* indicate the immunoglobulin heavy chains.

immature, non-fully differentiated cells that express both neuronal and glial cell markers (26). R28 cells endogenously express Munc119 (Ref. 26, Fig. 4, and supplemental Fig. S6) and RIBEYE in a Triton X-100 soluble fraction (supplemental Fig. S6 and data not shown). Therefore, we used R28 cells for immunoprecipitation experiments and tested whether RIBEYE immune serum could co-immunoprecipitate Munc119 from R28 cell extracts. RIBEYE preimmune serum served as control serum. Indeed, RIBEYE immune serum co-immunoprecipitated endogenous Munc119 whereas RIBEYE preimmune serum did not (Fig. 4).

Next, we prepared extracts from bovine retina as described under "Experimental Procedures" and tested whether antibodies against RIBEYE could co-immunoprecipitate Munc119. RIBEYE immune serum (but not RIBEYE preimmune serum) co-immunoprecipitated Munc119 together with RIBEYE showing a specific interaction of these proteins also in the retina. Similarly, Munc119 immune serum (but not Munc119 preimmune serum) co-immunoprecipitated RIBEYE together with Munc119 (Fig. 5). Because RIBEYE is exclusively present at synaptic ribbons in the mature retina (12) the co-immunoprecipitation experiments suggest that Munc119 may be a component of synaptic ribbons.

Binding of Munc119 to RIBEYE(B) Is Independent of NADH Binding to RIBEYE—Previous YTH analyses demonstrated that the NAD(H) binding subdomain (NBD) of RIBEYE(B) is mediating the interaction with Munc119. Therefore, we generated point mutants of the NBD and analyzed these point mutants of the NBD for their capability to interact with Munc119 in the YTH system to further map the interaction site of Munc119 on RIBEYE(B) domain. RIBEYE(B)G730 is an essential component of the NAD(H) binding motif, and the RIBEYE(B) point mutant RIBEYE(B)G730A does not bind significant levels of NAD(H) (12).[4] In contrast to the NAD(H) binding deficiency, RIBEYE(B)G730A still interacted with Munc119 in YTH analyses indicating that NAD(H) binding is not important for binding of Munc119 to RIBEYE(B) domain (Fig. 6). Similarly, the binding of Munc119 to RIBEYE(B) analyzed by biochemical pull-down analyses was not changed by the addition of either NAD^+ or NADH. Increasing concentrations of both NAD^+ or NADH did not significantly influence the binding of Munc119 to RIBEYE(B) (supplemental Fig. S2).

[4] K. Schwarz and F. Schmitz, unpublished data.

Downloaded from www.jbc.org at Saarlaendische Univ. u. Landesbibl./Medizinische Abteilung Homburg/Saar on September 24, 2008

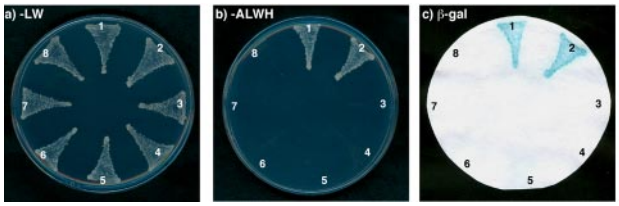

mating	bait	prey	-ALWH	βGal
1	RE(B)	Munc119(1-240)	+	+
2	RE(B)G730A	Munc119(1-240)	+	+
3	pGBKT7	Munc119(1-240)	–	–
4	pSE1112	Munc119(1-240)	–	–
5	RE(B)	pACT2	–	–
6	RE(B)	pSE1111	–	–
7	RE(B)G730A	pACT2	–	–
8	RE(B)G730A	pSE1111	–	–

FIGURE 6. **Binding of Munc119 to RIBEYE(B) is independent of NADH binding.** Summary plates of YTH analyses obtained with the indicated bait and prey plasmids. For convenience, experimental bait-prey pairs are underlayered in color (*green* in the case of interacting bait-prey pairs; control matings are *non-colored*). The NADH binding deficient RIBEYE point mutant RE(B)G730A (mating 2) interacts with Munc119 in YTH indicating that NADH binding to RIBEYE is not essential for the binding of Munc119.

We generated further point mutants located on the NAD(H) binding domain of RIBEYE, namely RE(B)D758N, RE(B)E844Q, RE(B)-F848W, RE(B)K854Q, RE(B)I796A, RE(B)D820N, and RE(B)E790Q, to further map the docking site of Munc119 on the NBD of RIBEYE(B). All of these latter point mutants still interact with Munc119 except for RE(B)E844Q pointing that this amino acid is crucial for the interaction with Munc119 (supplemental Fig. S3). Glutamate E844 is located close to the NADH binding cleft of RIBEYE (12, 16, 17). As judged by NADH-dependent FRET experiments performed as described (29), this mutant still binds NADH (supplemental Fig. S4). Based on these data, the Munc119 binding region of RIBEYE appears to be topographically close to the NADH binding cleft of RIBEYE(B).

Munc119 Is Specifically Recruited to Purified Synaptic Ribbons—The co-immunoprecipitation experiments from bovine retina suggested the presence of Munc119 on synaptic ribbons (Fig. 5). Immunolabeling data clearly showed the presence of Munc119 in the presynaptic terminals at ribbon sites and also at sites close to the synaptic ribbon (Fig. 7*B*). Interestingly, purified synaptic ribbons isolated from bovine retina specifically recruited externally added soluble Munc119-GST fusion protein to synaptic ribbons (Fig. 7*A*). The binding of Munc119 to synaptic ribbons was specific because the control protein GST alone did not bind to synaptic ribbons. Because Munc119 is virtually absent from purified synaptic ribbons (Fig. 7*A*, *lane 3*), Munc119 appears to be a synaptic ribbon-associated component that can relatively easily dissociate from synaptic ribbons (see "Discussion").

The sequence of bovine Munc119 obtained in the present study by YTH screening with RIBEYE(B) as bait protein is identical to the bovine Munc119 sequence previously deposited at GenBank™ (Accession Number BC103449.1).

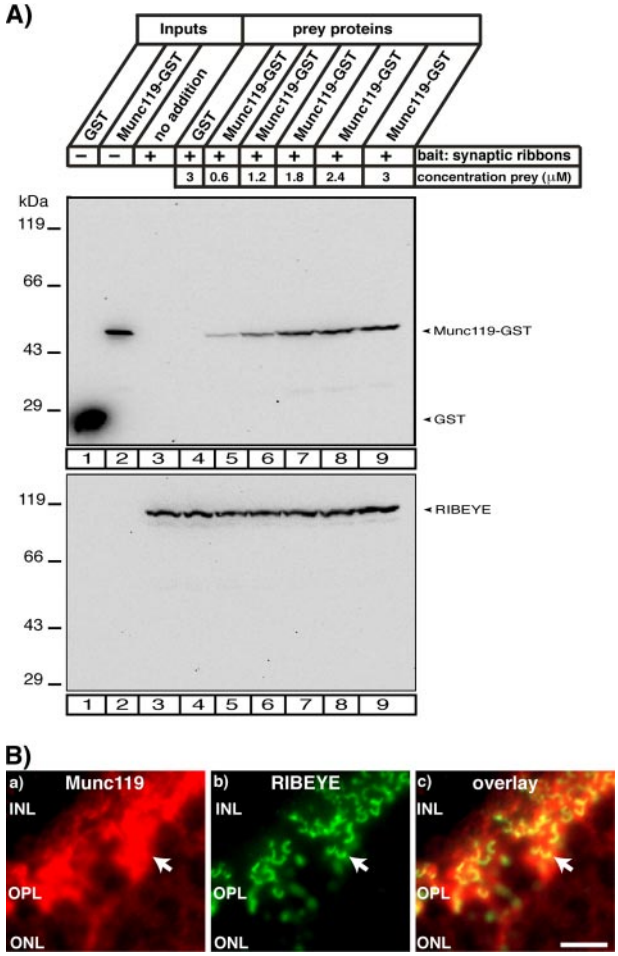

FIGURE 7. **Purified synaptic ribbons specifically recruit Munc119.** *A*, binding of Munc119 fusion protein to synaptic ribbons. 20 μg of purified synaptic ribbons were tested for their capability to bind soluble Munc119 fusion protein at the indicated concentrations. GST alone was used as control protein. Purified ribbons specifically bound Munc119-GST but not GST (*A*). For GST (*lane 1*) and Munc119-GST (*lane 2*) 10% were loaded as input; for the synaptic ribbon (*lane 3*) 100% were loaded as input. The two depicted blots show representative examples of four different experiments, which all showed the same result. The lower blot is stripped and reprobed with antibodies against RIBEYE to show equal loading of ribbons. A quantitative analysis of binding of Munc119 to synaptic ribbons is given in supplemental Fig. S5. *B*, Munc119 co-localizes with synaptic ribbons. Immunolabeling of the outer plexiform layer of the bovine retina that contain photoreceptor ribbon synapses with polyclonal antibodies against Munc119 and monoclonal antibodies against RIBEYE(B)/CtBP2. Strong immunosignals of Munc119 were found at synaptic ribbons and in close vicinity to synaptic ribbons. Abbreviations: *ONL*, outer nuclear layer; *OPL*, outer plexiform layer; *INL*, inner nuclear layer. *Scale bar*: 10 μm.

DISCUSSION

Munc119, a mammalian ortholog of the *C. elegans* protein unc119, is essential for synaptic transmission at the ribbon synapse and for vision (2). In the present study, we demonstrated that Munc119 interacts with the synaptic ribbon protein RIBEYE. The interaction between RIBEYE and Munc119 was consistently shown by five different independent methods, including YTH analyses, fusion protein pull-downs, interaction analyses in transfected COS cells, and immunoprecipitations from R28 retinal precursor cells and from bovine retina. The NADH binding subdomain of RIBEYE was shown to be responsible for the interaction with Munc119. Based on the analyses of RIBEYE(B) point mutants, the binding site of Munc119 appears to be close to the NADH binding site of RIBEYE; but the binding of Munc119 is independent upon NADH binding. In support of this view, RIBEYE(B)G730A that does not bind NADH still interacted with Munc119. Conversely, RIBEYE(B)E844Q that did not interact with Munc119 still bound NADH. Interestingly, the PrBP/δ-homology domain of Munc119 whose

Downloaded from www.jbc.org at Saarlaendische Univ. u. Landesbibl./Medizinische Abteilung Homburg/Saar on September 24, 2008

deletion caused the dramatic defects in vision and synaptic transmission in the respective patients and transgenic mouse model (5) was shown to be responsible for binding to RIBEYE. Therefore, the interaction with RIBEYE could mediate the essential physiological function of Munc119 in synaptic transmission at the photoreceptor ribbon synapse.

Although the physiological importance of Munc119 for synaptic transmission at the photoreceptor ribbon synapse has been well documented it is not yet clear how Munc119 works at the molecular level in the synapse. A key in the understanding of the function of Munc119 is probably its high homology to PrBP/δ. PrBP/δ binds and dissociates prenylated proteins from membranes (6, 30). This enzymatic activity is important for intracellular membrane and protein trafficking (6, 30). In photoreceptors, the trafficking role of PrBP/δ predominantly occurs in the inner and outer segments. We propose that Munc119 fulfills similar functions in the photoreceptor ribbon terminals. Such a trafficking role would be particularly important for the tonically active ribbon synapses, which are characterized by intensive membrane and protein trafficking. The idea that Munc119 supports similar processes as PrBP/δ but at different subcellular locations is further supported by the finding that PrBP/δ and Munc119 share common interaction partners (Arl2/3; 31, 32, 33). Additionally, Munc119 could activate Src-type signaling kinases in the photoreceptor synapse as recently observed for Munc119 in certain cells of the immune system (34, 35). A recent study demonstrated that Munc119 binds to CaBP4 (36) and thus, RIBEYE-Munc119 complexes might also be involved in the regulation of intracellular Ca^{2+} levels in the presynaptic ribbon terminal.

We have shown that purified ribbons could specifically recruit Munc119. Purified synaptic ribbons, which go through stringent washing steps (12, 27), contain little if any Munc119. In conclusion, Munc119 is most likely a peripherally associated component of synaptic ribbons that can relatively easy dissociate from them. In support of this suggestion, a large portion of Munc119 is soluble (Ref. 2 and data not shown). Large amounts of Munc119 are present in the presynaptic terminals in close vicinity to synaptic ribbons as judged by immunolabeling. Munc119 in presynaptic photoreceptor terminals could be recruited to synaptic ribbons. The factors that regulate the association/dissociation of Munc119 with synaptic ribbons *in vivo* remain to be elucidated by future analyses.

The synaptic defects observed in Munc119 transgenic mice and Munc119-deficient patients stress the role of Munc119 for vision and synaptic processing in the visual system. The fact that the PrBP/δ homology domain is crucial for Munc119 function particularly emphasizes the physiological importance of the RIBEYE-Munc119 interaction for synaptic transmission at the photoreceptor ribbon synapse.

Acknowledgment—We thank Conny Franke for excellent technical assistance.

REFERENCES

1. Higashide, T., Murakami, A., McLaren, M. J., and Inana, G. (1996) *J. Biol. Chem.* **271,** 1797–1804
2. Higashide, T., McLaren, M. J., and Inana, G. (1998) *Invest. Ophthalmol. Vis. Sci.* **39,** 690–698
3. Swanson, D. A., Chang, J. T., Campochiara, P. A., Zack, D. J., and Valle, D. (1998) *Investig. Ophthalmol. Vis. Sci.* **39,** 2085–2094
4. Li, L., Florio, S. K., Pettenati, M. J., Rao, N., Beavo, J. A., and Baehr, W. (1998) *Genomics* **49,** 76–82
5. Kobayashi, A., Higashide, T., Hamasaki, D., Kubota, S., Sakuma, H., An, W., Fujimaki, T., McLaren, M. J., Weleber, R. G., and Inana, G. (2000) *Investig. Ophthalmol. Vis. Sci.* **11,** 3268–3277
6. Zhang, H., Liu, X.-H., Zhang, K., Chen, C.-K., Frederick, J. M., Prestwich, G. D., and Baehr, W. (2004) *J. Biol. Chem.* **279,** 407–413
7. Kubota, S., Kobayashi, A., Mori, N., Higashide, T., McLaren, M. J., and Inana, G. (2002) *Investig. Ophthalmol. Vis. Sci.* **43,** 308–313
8. Mori, N., Ishiba, Y., Kubota, S., Kobayashi, A., Higashide, T., McLaren, M. J., and Inana, G. (2006) *Investig. Ophthalmol. Vis. Sci.* **47,** 1281–1292
9. Sterling, P., and Matthews, G. (2005) *Trends Neurosci.* **28,** 20–29
10. Heidelberger, R., Thoreson, W. B., and Witkovsky, P. (2005) *Prog. Ret. Eye Res.* **24,** 682–720
11. tom Dieck, S., and Brandstätter, J. H. (2006) *Cell Tiss. Res.* **326,** 339–346
12. Schmitz, F., Königstorfer, A., and Südhof, T. C. (2000) *Neuron* **28,** 857–872
13. Zenisek, D., Horst, N. K., Merrifield, C., Sterling, P., and Matthews, G. (2004) *J. Neurosci.* **24,** 9752–9759
14. Wan, L., Almers, W., and Chen, W. (2005) *J. Neurosci.* **25,** 941–949
15. Chinnadurai, G. (2002) *Mol. Cell* **9,** 213–224
16. Kumar, V., Carlson, J. E., Ohgi, K. A., Edwards, T. A., Rose, D. W., Escalante, C. R., Rosenfeld, M. G., and Aggarwal, A. K. (2002) *Mol. Cell* **10,** 857–869
17. Nardini, M., Spano, S., Cericola, C., Pesce, A., Massaro, A., Millo, E., Luini, A., Corda, D., and Bolognesi, M. (2003) *EMBO J.* **22,** 3122–3130
18. Tai, A. W., Chuang, J. Z., Wolfrum, U., and Sung C. H. (1999) *Cell* **97,** 877–887
19. James, P., Halladay, J., and Craig, E. A. (1996) *Genetics* **144,** 1425–1436
20. Harper, J. W., Adami, G. R., Wei, N., Keyomarsi, K., and Elledge, S. J. (1993) *Cell* **75,** 805–816
21. Helmuth, M., Altrock, W., Böckers, T. M., Gundelfinger, E. D., and Kreutz, M. R. (2001) *Anal. Biochem.* **293,** 149–152
22. Bai, C., and Elledge, S. J. (1996) *Methods Enzymol.* **273,** 331–347
23. Wang, Y., Okamoto, M., Schmitz, F., Hofmann, K., and Südhof, T. C. (1997) *Nature* **388,** 593–598
24. Stahl, B., Diehlmann, A., and Südhof, T. C. (1999) *J. Biol. Chem.* **14,** 9141–9148
25. Seigel, G. M. (1996) *Dev. Biol. Anim.* **32,** 66–68
26. Seigel, G. M., Sun, W., Wang, J., Hershberger, D. H., Campbell, L. M., and Salvi, R. J. (2004) *Curr. Eye Res.* **28,** 257–269
27. Schmitz, F., Bechmann, M., and Drenckhahn, D. (1996) *J. Neurosci.* **16,** 7109–7116
28. Schmitz, F., Tabares, L., Khimich, D., Strenzke, N., DeLa Villa-Polo, P., Castellano-Munoz, M., Bulankina, A., Moser, T., Fernandez-Chacon, R., and Südhof, T. C. (2006) *Proc. Natl. Acad. Sci. U. S. A.* **103,** 2925–2931
29. Fjeld, C. C., Birdsong, W. T., and Goodman, R. H. (2003) *Proc. Natl. Acad. Sci. U. S. A.* **100,** 9202–9207
30. Zhang, H., Li, A., Doan, T., Rieke, F., Detwiler, P. B., Frederick, J. M., and Baehr, W. (2007) *Proc. Natl. Acad. Sci. U. S. A.* **104,** 8857–8862
31. van Valkenburgh, H., Shern, J. F., Sharer, J. D., Zhu, X., and Kahn, R. A. (2001) *J. Biol. Chem.* **276,** 22826–22837
32. Hanzal-Bayer, M., Renault, R., Roversi, P., Wittinghofer, A., and Hillig, R. C. (2002) *EMBO J.* **21,** 2095–2106
33. Kobayashi, A., Kubota, S., Mori, N., McLaren, M. J., and Inana, G. (2003) *FEBS Lett.* **534,** 26–32
34. Cen, O., Gorska, M. M., Stafford, S. J., Sur, S., and Alam, R. (2003) *J. Biol. Chem.* **278,** 8837–8845
35. Gorska, M. M., Stafford, S. J., Cen, O., Sur, S., and Alam, R. (2004) *J. Exp. Med.* **199,** 369–379
36. Haeseleer, F. (2008) *Investig. Ophthalmol. Vis. Sci.* **49,** 2366–2375

Downloaded from www.jbc.org at Saarlaendische Univ. u. Landesbibl./Medizinische Abteilung Homburg/Saar on September 24, 2008